

Phylogeny and systematic history of early salamanders

Marianne Pearson

University College London

PhD in Palaeobiology

I, Marianne Rose Pearson, confirm that the work presented in this thesis is my own. Where information has been derived from other sources, I confirm that this has been indicated in the thesis

13 July 2016

Abstract

Prevalent paedomorphy and convergence in salamander morphology has made it difficult to resolve relationships using purely morphological characters. However, many new fully articulated fossil salamanders have emerged, especially from China, and it is important to be able to place them within a phylogenetic framework to better understand the origin and radiation patterns of early salamanders.

This study looks at the phylogeny of extant taxa using both molecular and morphological datasets. In deciphering the phylogeny of modern day taxa the limitations and caveats of the data were explored. The extent of the influence homoplasy and convergence have on the phylogenetic topology has been assessed using methods designed to identify and/or down-weight homoplasy in morphological characters. Once characters had been identified as potentially homoplasious and removed from the dataset, further analyses were performed on reduced datasets.

Fossils were simulated by creating subsets of characters (those commonly found in the fossil record) for extant taxa. Analyses using parsimony and Bayesian inference were performed to test the robustness of the placements of these simulated fossils. The impact of missing data caused by poor preservation and incomplete specimens was tested by simulating reduced/limited character scores for living taxa, and then comparing the phylogenetic placement of these artificially degraded taxa with their 'true' position based on complete data. This paves the way for the inclusion of the fossils.

While this study has not resolved the relationships between salamander families it has allowed a deeper understanding of the data, and assesses the confidence with which the placement of key fossils can be made in a new way. This novel method has further implications for the fitting of fossils within a phylogenetic framework in other problem clades. Biogeographic hypotheses can then be tested.

Contents

1.1 Project Aims	11
1.2 Introduction to Salamanders	12
1.2.1 <i>Is it possible to correct for the signal caused by convergence in the morphological data?</i>	13
1.3 The Origins of Salamanders	14
1.4 Previous Phylogenies	18
1.4.1 <i>Do soft body characters give a more reliable and congruent signal relative to molecular results than the signal from the osteological data?</i>	30
1.5 The Mesozoic Fossil Record	30
1.6 Biogeography 1.6.1 Introduction to biogeography	37
1.6.2 <i>Salamander geographic distribution</i>	37
1.6.2.1 Gondwana	38
1.6.2.2 Laurasia.....	38
1.6.2.3 <i>What is the position of Sirenidae in relation to other salamanders? Are the enigmatic Gondwanan fossils (Kababisha and Noterpeton) related to Sirenidae?</i>	40
1.6.2.4 <i>Can fossils be placed robustly at a Family and/or Salamandroidea/Cryptobranchoidea level?</i>	41
2.1 Introduction:	43
2.2 Materials and Methods	44
2.2.1 <i>Molecular data</i>	44
2.2.2 <i>Morphological data</i>	48
2.2.3 <i>Combined Molecular and Morphological data</i>	53
2.2.4 <i>Tree comparisons</i>	53
2.2.5 <i>Character mapping</i>	53
2.3 Results	54
2.3.1.2 <i>Nuclear DNA phylogeny</i>	55
2.3.1.3 <i>Mitochondrial DNA phylogeny</i>	56
2.3.2 <i>Morphological Results</i> 2.3.2.1 <i>Full Morphological dataset with extant outgroups</i>	57
2.3.3 <i>Full Morphological dataset with fossil outgroups</i>	59
2.3.2.2 <i>Morphological phylogeny (osteological)</i>	62
2.3.2.3 <i>Morphological phylogeny (soft body)</i>	64
2.3.3 <i>Molecular and Morphological data</i> 2.3.3.1 <i>Combined molecular data with all morphological data</i>	67
2.4 Discussion 2.4.1 Molecular discussion	67
2.4.2 <i>Morphological discussion</i>	69
2.4.3 <i>Total evidence discussion</i>	71

2.5 Conclusions	71
3.1 Introduction	74
3.1.1 <i>Homology within the dataset.....</i>	74
3.1.2 <i>Problems with fitting fossils</i>	74
3.2 Material and Methods.....	75
3.2.1 <i>Tree dependent character evaluation.....</i>	75
3.2.1.1 Retention Index	75
3.2.1.2 RI dataset.....	76
3.2.2 <i>Tree independent character evaluation.....</i>	77
3.2.2.1 <i>Le Quesne Probability randomisation test.....</i>	77
3.2.2.2 <i>The Le Quesne dataset.....</i>	78
3.2.2.3 <i>Tree comparison statistics</i>	78
3.2.2.4 <i>Simulating fossils</i>	79
3.3 Results.....	79
3.3.1 <i>Tree dependent phylogeny results</i>	79
3.3.2 <i>Tree independent results.....</i>	82
3.3.3 <i>Tree comparison results</i>	86
3.3.4 <i>Simulated fossils using RI subset.....</i>	87
3.3.4.1 Bayesian analysis results:	87
3.3.4.2 Parsimony analysis results:.....	87
3.3.5 <i>Simulated fossils using the Le Quesne subset</i>	89
3.3.6 <i>Stem-ward slippage results of the Bayesian and Parsimony analysis of the RI dataset</i>	95
3.4 Discussion	98
3.5 Conclusions	101
4.1 Introduction	104
4.2 Material and Methods.....	105
4.3 Phylogenetic results of Bayesian analysis of the RI dataset	106
4.3.1 <i>Stem-group fossils.....</i>	106
4.3.2 <i>Scapherpetontidae.....</i>	107
4.3.3. <i>Batrachosauroididae.....</i>	108
4.3.4. <i>Sirenidae-like fossils</i>	110
4.3.5 <i>Fossil salamanders that have previously been placed outside of Salamandroidea</i>	111
4.3.6 <i>Fossils previously assigned to Salamandroidea</i>	118
4.4 Discussion	124

4.5	Conclusions	128
5.1	Discussion	130
5.1.1	<i>What is the position of Sirenidae in relation to other salamanders?.....</i>	130
5.1.2	<i>Do soft body characters give a more reliable and congruent signal relative to molecular results then the signal from the osteological data? Does soft body data show any difference in levels of convergence than the osteological data?.....</i>	130
5.1.3	<i>Is it possible to correct for the signal caused by convergence in the morphological data?.....</i>	131
5.1.4	<i>Can fossils be placed robustly at a family and/or salamandroidea/cryptobranchoidea level? ..</i>	131
5.2	Conclusions	133
5.3	Further Work:.....	135
5.3.1	<i>New Data</i>	135
5.3.2	<i>New Analyses.....</i>	135
5.3.3	<i>Time calibrated phylogeny.....</i>	136
References:	138
Appendix:	152
	<i>Appendix A – Genetic Species List (on CD attached).....</i>	152
	<i>Appendix B - Full morphological character set (also on CD attached).....</i>	152
	<i>Appendix C – Morphological Datasheet (on CD attached)</i>	162
	<i>Appendix D – Species list (on CD attached).....</i>	162
	<i>Appendix E – RI Dataset (on CD attached).....</i>	162
	<i>Appendix F – LQ Dataset (on CD attached).....</i>	162
	<i>Appendix G – Comparison between RI and Le Quesne datasets (also on CD attached)</i>	162

Table of Figures:

Figure 1.3.1 Tetrapod phylogeny according to the temnospondyl ancestor relationship (Anderson 2008)	15
Figure 1.3.2 Tetrapod phylogeny with the ancestors of Lissamphibia originating within the Lepospondyli (Anderson 2008)	15
Figure 1.3.3 Lissamphibia's polyphyletic origins (Anderson 2008)	16
Figure 1.4.1 The Urodela family level phylogeny (Duellman and Trueb 1994)	18
Figure 1.4.2: Lissamphibian relationships based on analysis of combined mitochondrial 12S and 16S rRNA gene sequence (Hay <i>et al.</i> 1995)	20
Figure 1.4.3 The relationships among the three amphibian orders according to Hay <i>et al.</i> 1995	21
Figure 1.4.4: A strict consensus of 40 MPTs generated from 10 heuristic searches from the complete character matrix for extant salamanders (Larson and Dimmick, 1993)	22
Figure 1.4.5: One of 60 most parsimonious trees used to track character changes in salamander characters (Larson and Dimmick, 1993)	23
Figures 1.4.6 Parsimony trees using all morphological data (Wiens <i>et al.</i> 2005)	24
Figures 1.4.7 Parsimony trees with 30 putative pedomorphic characters excluded (Wiens <i>et al.</i> 2005)	25
Figure 1.4.10: The total evidence results using Parsimony analyses (Wiens <i>et al.</i> 2005)	26
Figure 1.4.11: The total evidence results using Bayesian analyses (Wiens <i>et al.</i> 2005)	26
Figure 1.4.12: Phylogeny produced using the complete mitochondrial DNA (Zhang and Wake 2009)	27
Figure 1.4.13 Phylogenetic results of Zhang and Wake (2009). Analysis of the full mitochondrial genome sequence	29
Figure 1.5.1 Calibrated cladogram showing the relationships of <i>Beiyanerpeton</i> to other fossil and extant salamander clades (Gao and Shubin 2012)	35
Figure 2.1 The proposed relationships of the outgroups used in this study (Maddin <i>et al.</i> 2012)	50
Figure 2.2 The constraint placed on the outgroup taxa on the morphological data used in the parsimony analysis in TNT	52
Figure 2.3.1 Result of the Bayesian analysis of eleven genes	54
Figure 2.3.2 Result of a Bayesian analysis of eight nuclear genes	55
Figure 2.3.3 Bayesian analysis of the three mitochondrial genes	56
Figure 2.3.4 Bayesian analysis of the full morphological dataset with extant outgroups	57
Figure 2.3.5 Parsimony agreement subtree of full morphological dataset with extant outgroups	58

Figure 2.3.6 GC bootstrap tree (1000 replicates) of the full morphological dataset with extant outgroups	58
Figure 2.3.7 Bayesian analysis of the full morphological dataset including fossil outgroups	59
Figure 2.3.8: Agreement subtree made from the parsimony analysis of the full morphological dataset including fossil outgroups	60
Figure 2.3.9 GC bootstrap tree of the parsimony results using the full morphological dataset including fossil outgroups	60
Figure 2.3.10 Bayesian analysis of the osteological characters including fossil outgroups	62
Figure 2.3.11: Agreement subtree resulting from a parsimony analysis of the osteological characters	63
Figure 2.3.12 GC bootstrap value tree resulting from a parsimony analysis of the osteological characters	64
Figure 2.3.13 Bayesian analysis of the soft body characters with a hypothetical all zero outgroup	65
Figure 2.3.14: The most parsimonious tree resulting from parsimony analysis of the soft body characters	65
Figure 2.3.15: GC bootstrap tree of the soft body characters	66
Figure 2.3.16 Bayesian analysis of the full molecular and morphological datasets	67
Figure 3.1: The constrained tree reflecting the uncertain relationships between the salamander families, used to find the retention index for the tree dependant character evaluation analysis	76
Figure 3.3: Bayesian result of the RI morphological dataset	80
Figure 3.4: Parsimony result of the RI morphological dataset	81
Figure 3.5: GC bootstrap values for the Parsimony analysis of the RI morphological dataset	82
Figure 3.6: Bayesian analysis of the Le Quesne morphological dataset	83
Figure 3.7: Agreement subtree of the Parsimony analysis of the Le Quesne morphological dataset	84
Figure 3.8: Strict consensus from the Parsimony analysis of the Le Quesne morphological dataset	85
Figure 3.9: GC bootstrap values for the Parsimony analysis of the Le Quesne morphological dataset	86
Figure 3.10: Consensus tree from a Bayesian analysis including all the simulated fossils using the RI dataset	89
Figure 3.11: Consensus tree from a Bayesian analysis of the Le Quesne dataset including all simulated fossils	92
Figure 3.12: The agreement subtree created from the Parsimony analysis of the Le Quesne dataset that included all the simulated fossils	93
Figure 3.13: Strict consensus tree resulting from the Parsimony analysis of the Le Quesne dataset including all the simulated fossils	94

Figure 3.14: GC Bootstrap values from the Parsimony analysis of the Le Quesne dataset that included all the simulated fossils	94
Figure 4.1: Consensus tree from a Bayesian analysis of the RI dataset with extant taxa and the stem-group fossils	106
Figure 4.2: Consensus tree from a Bayesian analysis of the RI dataset with extant taxa and all Scapherpetontidae	108
Figure 4.3: Consensus tree from a Bayesian analysis of the RI dataset with extant taxa and all Batrachosauroididae	109
Figure 4.4: Consensus tree from a Bayesian analysis of the RI dataset with extant taxa, <i>Habrosaurus</i> , <i>Kababisha</i> and <i>Noterpeton</i>	110
Figure 4.5: Consensus tree from a Bayesian analysis of the RI dataset with extant taxa and <i>Regalerpeton</i>	111
Figure 4.6: Consensus tree from a Bayesian analysis of the RI dataset with extant taxa and <i>Pangerpeton</i>	112
Figure 4.7: Consensus tree from a Bayesian analysis of the RI dataset with extant taxa and <i>Chunerpeton</i>	113
Figure 4.8: Consensus tree from a Bayesian analysis of the RI dataset with extant taxa and <i>Jeholotriton</i>	113
Figure 4.9: Consensus tree from a Bayesian analysis of the RI dataset with extant taxa and <i>Liaoxitriton</i>	114
Figure 4.10: Consensus tree from a Bayesian analysis of the RI dataset with extant taxa and <i>Nesovtriton</i>	115
Figure 4.11: Consensus tree from a Bayesian analysis of the RI dataset with extant taxa and <i>Iridotriton</i>	116
Figure 4.12: Consensus tree from a Bayesian analysis of the RI dataset with extant taxa and all fossils previously placed outside of Salamandroidea	117
Figure 4.13: Consensus tree from a Bayesian analysis of the RI dataset with extant taxa and <i>Valdotriton</i>	118
Figure 4.14: Consensus tree from a Bayesian analysis of the RI dataset with extant taxa and <i>Proamphiuma</i>	119
Figure 4.15: Consensus tree from a Bayesian analysis of the RI dataset with extant taxa and <i>Paranecturus</i>	120
Figure 4.16: Consensus tree from a Bayesian analysis of the RI dataset with extant taxa and <i>Beiyanerpeton</i>	121
Figure 4.17: Consensus tree from a Bayesian analysis of the RI dataset with extant taxa and <i>Galverpeton</i>	122
Figure 4.18: Consensus tree from a Bayesian analysis of the RI dataset with extant taxa and fossils previously attributed to Salamandroidea	123

List of Tables:

Table 1.1 The current affinities of the fossil taxa and the morphology they have in common with their proposed clade	33
Table 2.1 Breakdown of the 11 genes in the combined molecular dataset	45
Table 2.2 Results of Partitionfinder assigning best fit model of rate of evolution to each gene/codon region	48
Table 2.3.1 The agreement subtree and symmetric differences results	61
Table 2.3.2 The agreement subtree and symmetric differences (Robinson–Foulds metric) between the combined molecular tree and osteological and soft body trees	66
Table 3.1 Example of binary recoding of one ordered multistate character consisting of one characters with four states between four taxa that share this character	78
Table 3.2 Agreement subtree and Symmetric difference values when the RI and Le Quesne trees are compared to the full molecular tree found in this study	89
Table 3.3 Summary of results of the placement of the simulated fossils using the RI dataset	88
Table 3.4 Summary of results of the placement of the simulated fossils using the Le Quesne dataset	91
Table 3.8: Number of simulated fossils placed correctly to Family level within a Bayesian or Parsimony framework using the RI or Le Quesne datasets	95
Table 3.9: Number of simulated fossils placed correctly to cryptobranchoid/salamandroid level within a Bayesian or Parsimony framework using the RI or Le Quesne datasets	95
Table 3.10: Number of simulated fossils placed in the same place within the topology as in the results of the Bayesian and Parsimony analysis of the RI dataset and the number of simulated fossils placed correctly within either a monophyletic Cryptobranchoidea or Salamandroidea within a Bayesian or Parsimony framework.	97

1. Introduction

1.1 Project Aims

This chapter outlines the background and current questions regarding the phylogeny of salamanders and the impact the inclusion of fossils might have on this group's biodistribution and early radiation patterns. The aims of this study are to investigate the biological signal in the data commonly used to reconstruct salamander phylogeny. This study incorporates both nuclear and mitochondrial DNA within a Bayesian framework, and osteological and soft body characters within both a Parsimony and Bayesian framework. Comparisons between the phylogenies created by nuclear and mitochondrial DNA were drawn and congruence between the morphological and molecular phylogenies was assessed using symmetric differences and agreement subtree values. The difference in signal emerging from the osteological and soft body characters was investigated by comparing their phylogenies to the molecular tree.

The issue of convergence in the morphological dataset was addressed by evaluating each character using two different methods for detecting homoplasy. Once the character set had been reduced, in a bid to remove convergent characters, they (Le Quesne dataset – Appendix A and RI dataset – Appendix B) were tested for the robustness of fitting fossils within both a Parsimony and Bayesian framework by simulating fossils and observing their position within a phylogeny relative to its expected known position (according to molecular evidence). Tracing synapomorphies within a phylogeny gives insight into the support for each clade. Using the results from these analyses, the RI dataset was used to fit the Mesozoic fossils in a Bayesian framework. The results of which might shed some more light on biogeographical hypotheses proposed by Milner (1983).

1.2 Introduction to Salamanders

Living salamanders (crown-group Urodela) form part of the Lissamphibia together with modern frogs (Anura) and extant caecilians (Gymnophiona). Urodela are a diverse group with around 66 genera within ten families. The number of extant species is currently about 668, but new taxa are frequently discovered and described and others become extinct (Duellman and Trueb, 1986; AmphibiaWeb 2012). Salamanders are distinguished from other lissamphibian clades (frogs and caecilians) by the possession of a suite of morphological characters. They possess an open temporal region which lacks postparietals, postorbital, jugals, quadratojugal, tabulars, supraoccipital, basioccipital, ectopterygoids and supratemporals (Duellman and Trueb 1986; AmphibiaWeb, 2012). Spinal nerve cord support projections occur in the neural canal of the vertebrae in urodelans and not in anurans, or gymnophonia (Wake and Lawson 1973; Anderson *et al.* 2007). Almost all salamanders possess ribs, and teeth in both jaws (where maxillae and mandibles are present), and the adductor mandibulae internus superficialis muscle originates on the top and back of the skull (Duellman and Trueb 1986). The ten currently recognised extant monophyletic families are: Cryptobranchidae (Fitzinger, 1826), Hynobiidae (Cope, 1859), Proteidae (Gray, 1825), Sirenidae (Gray, 1825), Dicamptodontidae (Tihen, 1958), Ambystomatidae (Hallowell, 1856), Salamandridae (Gray, 1825), Plethodontidae (Gray, 1850), Amphiumidae (Gray, 1825) and Rhyacotritonidae (Tihen 1958).

Salamanders generally have a biphasic life cycle characteristic of modern amphibians. Hatching as aquatic larvae they grow and metamorphose into an adult terrestrial form. The larval traits that are most common are the retention of external gills, gill slits and the lack of eyelids; others include retention of the aquatic body plan and small or absent limbs (Zug *et al.* 2001). Some species undergo complete metamorphosis, changing from an aquatic larva to a fully terrestrial adult (e.g. some salamandrids, *Rhyacotriton*, *Dicamptodon*, and some ambystomatids) while others lack metamorphosis altogether (e.g. some plethodontids) or only change minimally from aquatic larvae to aquatic adults which retain some larval characteristics such as external gills or general morphological adaptations to an aquatic lifestyle like dorsoventrally flattened tails (e.g. cryptobranchids, proteids, sirenids, and some salamandrids and *Dicamptodon*). Other species are facultatively metamorphic (e.g. some ambystomatids) and change to a terrestrial adult form only under certain environmental conditions, but retaining the ability to live and breed in their aquatic adult form until then. A change in environmental conditions triggers metamorphosis thus allowing the organism to invade a new and usually more favourable niche (usually terrestrial) (Whiteman 1994). Most of the plethodontid salamanders lack a larval stage altogether and hatch on land as miniature

versions of the adult. These are especially common in terrestrial forms which, as adults, usually lack lungs and respire through their skin. Adult amphiumids, seemingly counter-intuitively, lack gills, and breathe using lungs even though their adult forms are aquatic.

Heterochrony which is the change of timing in the development of an animal, has occurred many times in salamander history through paedomorphosis (interspecific retention of larval traits) and paedogenesis (intraspecific) (Gould 1977; Alberch *et al.* 1979; McKinney and McNamara 1991; Gould 1992; Klingenberg 1998; De Beer 2008). The monophyly of crown-group Urodela (Milner 2000; Zhang *et al.* 2005; Roelants *et al.* 2007; Vieites *et al.* 2009; Zhang and Wake 2009) and the monophyly of each of the ten families of living genera within Urodela has, through recent molecular and combined analysis, been supported (Larson and Dimmick 1993; Duellman and Trueb 1994; Gao and Shubin 2001; Mueller *et al.* 2004; Weisrock *et al.* 2005; Wiens *et al.* 2005; Roelants *et al.* 2007; Vieites *et al.* 2009). The interrelationships of these families are not yet well resolved (Wiens *et al.* 2005; Frost *et al.* 2006; Zhang and Wake 2009). Early phylogenetic analyses using purely morphological characters obtained little consensus because of the number of convergent paedomorphic adult forms (Larson and Dimmick 1993; Duellman and Trueb 1994; Wiens *et al.* 2005).

Apart from common possession of derived characters due to descent from a common ancestor, similarity in morphology between species occurs in one of several ways; through lack of change, and so the similarities in structures indicate a plesiomorphic state, or through parallel evolution, convergence or reversal of derived features back to the ancestral condition. Homoplasy was found to be hugely prevalent in modern salamander families (Wake 1991).

1.2.1 Is it possible to correct for the signal caused by convergence in the morphological data?

The suspected homoplasy in salamanders has been the subject of previous phylogenetic studies (i.e. Wiens *et al.* 2005) which have been unable to fully correct for the convergence signal in the data. The methods for evaluating the characters for signs of homoplasy used in this study employed tree dependent and tree independent tests to create a new morphological dataset that would reflect true biological phylogenetic signal and avoid bias from convergence.

1.3 The Origins of Salamanders

Crown-group salamanders (Urodela) and their stem taxa form a total group called Caudata, while the crown-group frogs (Anura) and their stem fossils form Salientia (Zardoya and Meyer 2001; Meyer and Zardoya 2003). *Albanerpetontidae*, a group of extinct salamander-like animals, previously assigned to the Caudata is now thought to represent a fourth lissamphibian group (Fox and Naylor 1982; McGowan and Evans 1995; Evans and Milner 1996; McGowan 2002) which might form the sister clade to Salientia and Caudata (Gardner 2001) or to Gymnophonia (Ruta and Coates 2007; Anderson *et al.* 2007; Anderson *et al.* 2008).

The origins and monophyly of the Lissamphibia are still debated. Three main hypotheses have been proposed regarding the Palaeozoic origins of modern lissamphibians. The first of these proposes Lissamphibia is monophyletic within Temnospondyli (see figure 1.3.1) (Bolt 1977; Milner 1988; Trueb and Cloutier 1991; Milner 1993; Gardner 2001; Ruta *et al.* 2003; Zhang *et al.* 2005; Anderson *et al.* 2007; Anderson *et al.* 2008). Several different taxa emerge as the sister-group to temnospondyls in separate studies using morphology to create phylogenies. *Doleserpeton* (Bolt 1969) *Doleserpeton* and *Amphibamus* (Ruta *et al.* 2003) or the Branchiosauridae (Milner 1993) have all been suggested as sister taxa to salamanders as well as salamanders being a sub-group of the Branchiosauridae (Trueb and Cloutier 1991). This view has recently been supported by the discovery of *Gerobatrachus* (Anderson *et al.* 2007), which is an amphibamid temnospondyl fossil, and has morphological features in common with crown group salamanders, stem salamanders such as *Karaurus*, *Triadobatrachus* (a stem group frog) and crown group frogs (Anderson *et al.* 2007; Anderson *et al.* 2008). This apparent stem batrachian from the Early Permian, with characters that are so similar to both frogs and salamanders, is purported to lie on the stem of Batrachia, after their divergence from Gymnophonia ancestors (Anderson *et al.* 2007; Anderson *et al.* 2008).

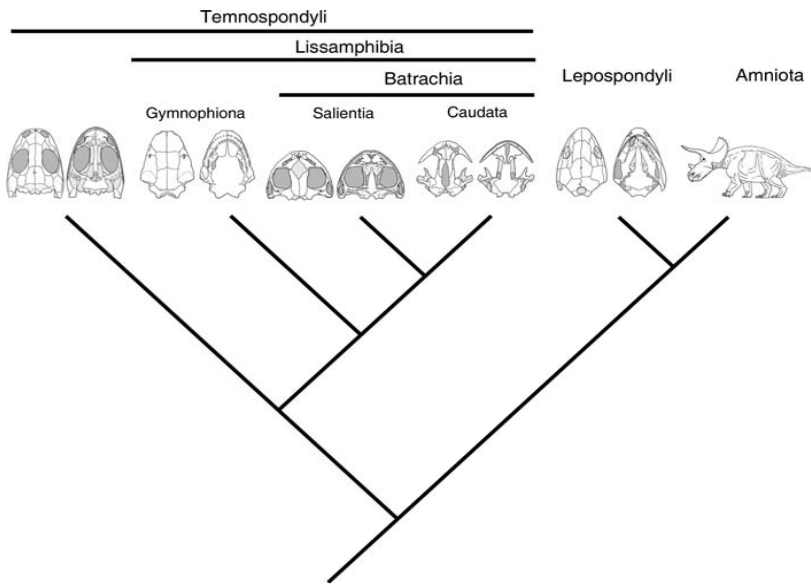


Figure 1.3.1 Tetrapod phylogeny according to the temnospondyl ancestor relationship (Bolt 1977; Milner 1988; 1993; Anderson 2008; Gardner 2001)

A second hypothesis, that Lissamphibia are monophyletic and derived from Lepospondyli rather than temnospondyls, is shown in Fig. 1.3.2 (Laurin 1998; Vallin and Laurin 2004). This hypothesis was put forward based on morphological characters. The hypothesis gained support recently from both molecular analyses and morphological phylogenies in which the divergence dates of the amphibian groups and morphological similarity between amphibians and lepospondyls purportedly matched with an origin from the ‘microsaurian’ lepospondyls (Laurin and Reisz 1997; Marjanovic and Laurin 2007; Marjanović 2008; San Mauro 2010).

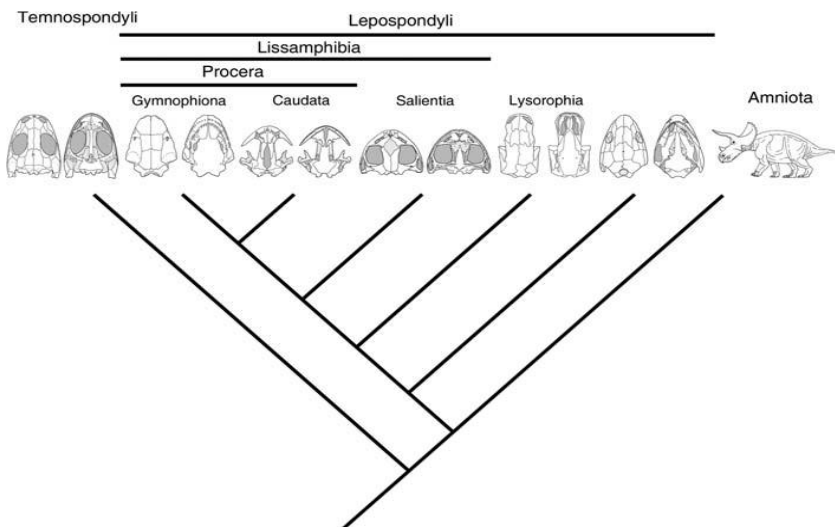


Figure 1.3.2 Tetrapod phylogeny with the ancestors of Lissamphibia originating within the Lepospondyli (Laurin and Reisz 1995, 1997; Marjanovic and Laurin 2007; Marjanovic 2008; San Mauro 2010)

A third hypothesis posits that Lissamphibia are polyphyletic (not sharing the same ancestor) with the origins of Salientia (sometimes with Caudata) occurring within the temnospondyls and the origins of Gymnophiona (sometimes with the Caudata) occurring within lepospondyls (Fig. 1.3.3) (Carroll and Currie 1975; Schoch and Carroll 2003; Carroll 2004; Lee and Anderson 2006; Carroll 2007; Skutschas and Martin 2011). This hypothesis has been suggested to account for the differences in morphology between batrachians (frogs + salamanders) and caecilians, and also the differing opinions on the divergence dates between these clades. The earlier divergence of the caecilians from the Batrachia and the characteristics of the skull and elongate body have been suggested to indicate more affinity with the Permian microsauro *Rhynchonkos* rather than any of the temnospondyls (Carroll 2007).

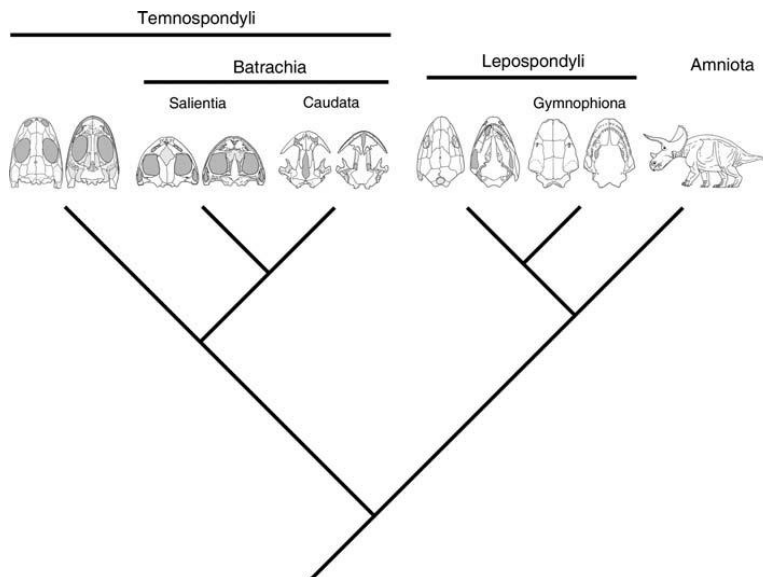


Figure 1.3.3 Lissamphibia have a polyphyletic origin within the Tetrapod phylogeny, with frogs and salamanders clustering together under Batrachia order originating within the temnospondyli and the caecilians originating from within the Lepospondyli (Lee and Anderson 2006).

There has been much support over the years for the monophyly of Lissamphibia (Parker 1956; Lombard and Bolt 1979; Gardiner 1982; Gardiner 1983; Milner 1988; Bolt 1991; Roelants *et al.* 2007). Recent analyses using nuclear or mitochondrial genes or a combination of both have been employed to create large data sets to reach consensus on the monophyly of the Lissamphibia and the clades within it (Hedges *et al.* 1990; Hedges and Maxson 1993; Hay *et al.* 1995; Feller and Hedges 1998; Zardoya and Meyer 2001; Zhang *et al.* 2005). The support for a polyphyletic ancestry of Lissamphibia seems to be based heavily on morphological characters. It is known that homoplasy is common in modern amphibians, and so the

polyphyletic origin for Lissamphibia is less well supported in recent literature with most workers supporting a monophyletic origin for modern amphibians.

However recent studies using molecular evidence have yet to reach agreement on the divergence dates within the lissamphibian clade and between the modern lissamphibians and their as yet unresolved ancestral relatives (Zhang *et al.* 2005; Roelants *et al.* 2007; Zhang and Wake 2009; San Mauro 2010; Pyron 2011).

While results of the molecular studies are dependent on the methods used and choice of DNA, the fossil evidence suggests that the Caudata must have diverged from Salientia at least by the Early Triassic. If Caudata are the sister clade to Salientia, as the molecular evidence suggests (see below), then the presence of the very earliest stem-frogs (*Triadobatrachus* from Madagascar and *Czatkobatrachus polonicus* from Poland) in the Early Triassic (Evans and Borsuk-Białynicka 1998; Borsuk-Białynicka and Evans 2002) implies Caudata must also have existed at this time. This predates the break-up of Pangea (San Mauro *et al.* 2005; San Mauro 2010) when salientians were already evidently widespread globally.

Recent molecular and combined evidence analyses have placed the Caudata as the sister taxon to Salientia (forming the Batrachia), with Gymnophiona as their sister clade (Benton 1990; San Mauro *et al.* 2005; Zhang *et al.* 2005; Roelants *et al.* 2007; Zhang and Wake 2009; San Mauro 2010; Pyron 2011; Skutschas and Martin 2011). However this was not always the consensus with previous analysis of mitochondrial and nuclear ribosomal DNA (Hedges *et al.* 1990; Hedges and Maxson 1993; Feller and Hedges 1998) placing Caudata as sister clade to Gymnophiona in what is known as the Procera hypothesis (Lee and Anderson 2006). This hypothesis was based on the geographic distribution and fossil record of the three living lissamphibian clades. Frogs and their fossils are found world-wide while salamanders are mainly restricted to Laurasia while caecilians have a distinct Gondwanan distribution pattern (Hedges *et al.* 1993; San Mauro *et al.* 2005). However modern day distribution patterns do not always reflect past biodistributions. Early studies lacked extensive taxon and data sampling, and recent molecular and morphological studies, some of which have included fossil taxa, seem to be reaching a consensus that the batrachian clade hypothesis is increasingly well supported (Milner 1988; Trueb and Cloutier 1991; Milner 1993; Duellman and Trueb 1994; Zardoya and Meyer 2001; Ruta *et al.* 2003; Zhang *et al.* 2005; Roelants *et al.* 2007; Ruta and Coates 2007).

1.4 Previous Phylogenies

Early phylogenetic analyses using morphological characters attempted to correct for the extensive convergent evolution in this group and focused on characters less likely to be biased by convergence resulting from paedomorphosis (Edwards 1976; Estes 1981; Milner 1983; Duellman and Trueb 1994). However, the range of phylogenetic results produced using both Parsimony and Bayesian methods of phylogenetic analyses, with purely morphological character matrices, still reflected convergence. (Duellman and Trueb 1994; Wiens *et al.* 2005; Wang and Evans 2006; Zhang *et al.* 2009; Gao and Shubin 2012). Systematic problems are also caused when species within a family display different life histories thus contributing to very different morphological information to phylogenetic analyses. The plethodontids, dicamptodontids and amphiumids have species which are paedomorphic and aquatic as adults and others that are fully terrestrial. Despite convergence biasing phylogenetic relationships, a stable position for Cryptobranchoidea emerged early on (Milner 1988; Duellman and Trueb 1994). Cryptobranchoidea (Cryptobranchidae + Hynobiidae) are usually placed as the sister taxon to all the other crown group salamanders (Estes 1981; Wiens *et al.* 2005; Frost *et al.* 2006; Wang and Evans 2006; Roelants *et al.* 2007; Vieites *et al.* 2009; Zhang *et al.* 2009; Gao and Shubin 2012) or all other crown group salamanders without Sirenidae (Larson and Dimmick 1993; Duellman and Trueb 1994; Zhang and Wake 2009).

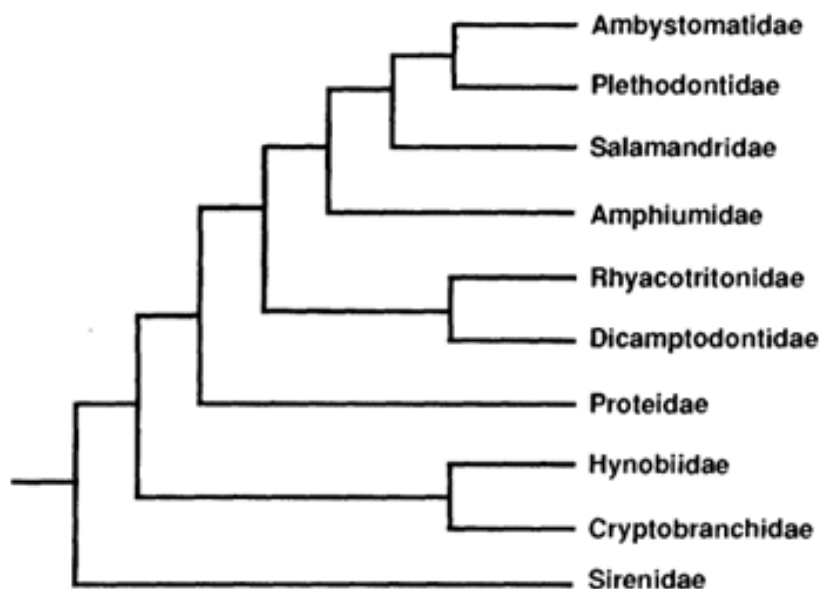


Figure 1.4.1 The Urodela family level phylogeny based on morphological characters only, taken from the *Biology of Amphibians* (Duellman and Trueb 1994).

With the inclusion of molecular data, the family-level relationships within the Urodela began to become clearer. Molecular phylogenies created for salamanders have included Mitochondrial (Zhang and Wake 2009), Nuclear (Wiens *et al.* 2005; Vieites *et al.* 2009), and a combination of both kinds of DNA information over the years (Chippindale *et al.* 2004; Pyron and Wiens 2011). Mitochondrial DNA is thought to be less able to resolve deep nodes and rapidly diversifying clades because of its high saturation potential for mutations (Weisrock *et al.* 2005). Mitochondrial genes have been prone to introgression and ancient lineage sorting in other studies (Krystyna Nadachowska and Wiesaw Babik 2009) and some salamander species are known to hybridise (Majtánová *et al.* 2016). This study aims to address the relationships between families of salamanders only. While mitochondrial DNA is easier to sequence in its entirety because it is shorter than nuclear DNA it has a limited potential for base pair mutations. Nuclear DNA is longer and thus contains potentially more informative base pairs but it is often not all sequenced because of its length.

An early study by Hay *et al.* (1995) used mitochondrial fragments of both 12S and 16S to shed light on amphibian relationships. They used neighbour-joining analysis (Jukes-Cantor distance with pairwise deletion) and included similar outgroups to the study presented here: amniotes including mammal (human), bird (domestic fowl) and *Sphenodon* (tuatara). Their results (Fig. 1.4.2) supported monophyly of frogs, salamanders and caecilians. Within salamanders they found support for sirenids as sister clade to all other salamanders, but they did not find any support for the monophyly of either the Salamandroidea or the Cryptobranchoidea. While Hay *et al.* found salamanders and frogs to be more closely related than either were to caecilians, using the 12S and 16S combined dataset, statistical support was very low.

They further investigated the hypotheses for amphibian relationships by adding 18S and 28S rRNA genes. This extra analysis comprised only a single representative species from each amphibian clade (i.e., one salamander: *Siren intermedia*; one frog: *Xenopus laevis* and one caecilian: *Typhlonectes natans*; together with a rat outgroup: *Rattus rattus*). They were not looking at internal branching relationships and so used only representative taxa for the increased gene dataset. The result of this analysis (Fig. 1.4.3) placed salamanders as more closely related to caecilians than to frogs, although again the statistical support for this relationship was not strong.

A study by Larson and Dimmick (1993) used both mitochondrial DNA and morphological characters combined to create a total evidence tree. This analysis supported the monophyly of the internally fertilising salamanders which was found by Duellman and Trueb

(1986) by using comparative morphology, but still only used small amounts of DNA material. More recent studies using more complete mitochondrial genomes have since found support for the Batrachia clade of frogs + salamanders (Zardoya and Meyer 2001; San Mauro *et al.* 2004; Zhang and Wake 2009) using purely molecular data.

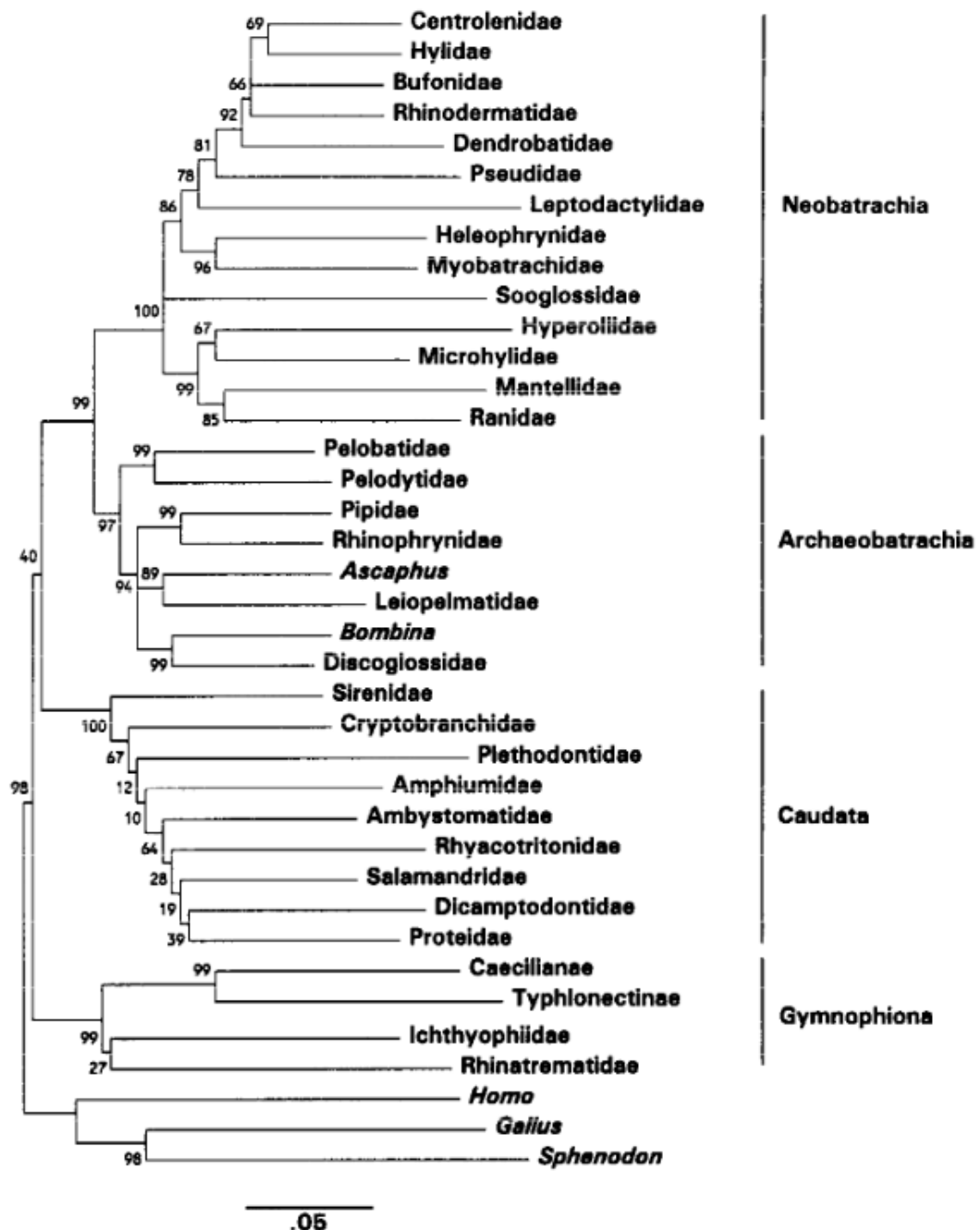


Figure 1.4.2: Lissamphibian relationships based on analysis of combined mitochondrial 12S and 16S rRNA gene sequence (Hay *et al.* 1995). The node numbers are confidence values from an interior-branch test.

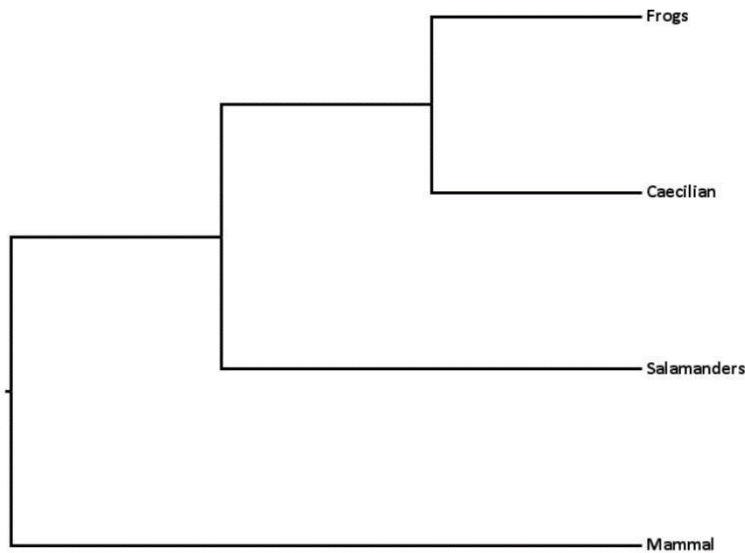


Figure 1.4.3 The relationships among the three amphibian orders, using a combined dataset of 12S, 16S, 18S and 28S genes. The numbers at the nodes represent the confidence values from the interior-branch test (Hay *et al.* 1995).

Weisrock *et al.* (2005) compared the signal between mitochondrial DNA (2100 base pairs from the genes encoding ND1, ND2, COI, and the intervening tRNA genes) and one nuclear gene (RAG-1) and concluded that the mitochondrial results were probably erroneous. However, Weisrock *et al.* (2005) based this assessment on their view that the ‘right’ tree was one that correctly separated internally and externally fertilising salamanders into the ‘correct’ clades. The study presented here instead looked at the hypothesised relationships of the outgroups as a guide to the reliability of ingroup relationships. It expanded on Weisrock *et al.*’s finding by using mtDNA genes (genes used in previously published analyses of salamander phylogeny e.g., Hay *et al.* 1995, Zhang *et al.* 2009, Pyron and Wiens 2011) compared to the results of those of an analysis using nDNA genes (also genes previously used in salamander phylogenies e.g., Pyron and Wiens 2011 and Frost *et al.* 2006) without an a priori agenda for the topology. These results suggest that differing types of DNA produces different results with the nuclear DNA supporting a Salamandroidea affiliation of Sirenidae while mtDNA supports Sirenidae as the sister clade to all other salamanders.

One of the early analyses including molecular data (Larson and Dimmick 1993) based on total evidence analysis using 32 morphological characters and 177 rRNA molecular characters obtained a family level phylogeny with 40 equally most parsimonious trees (MPT) through 10 heuristic searches. Each tree was 460 steps in length for a total character matrix of 209 characters. A strict consensus tree of the 40 MPTs is shown in Fig. 1.4.4.

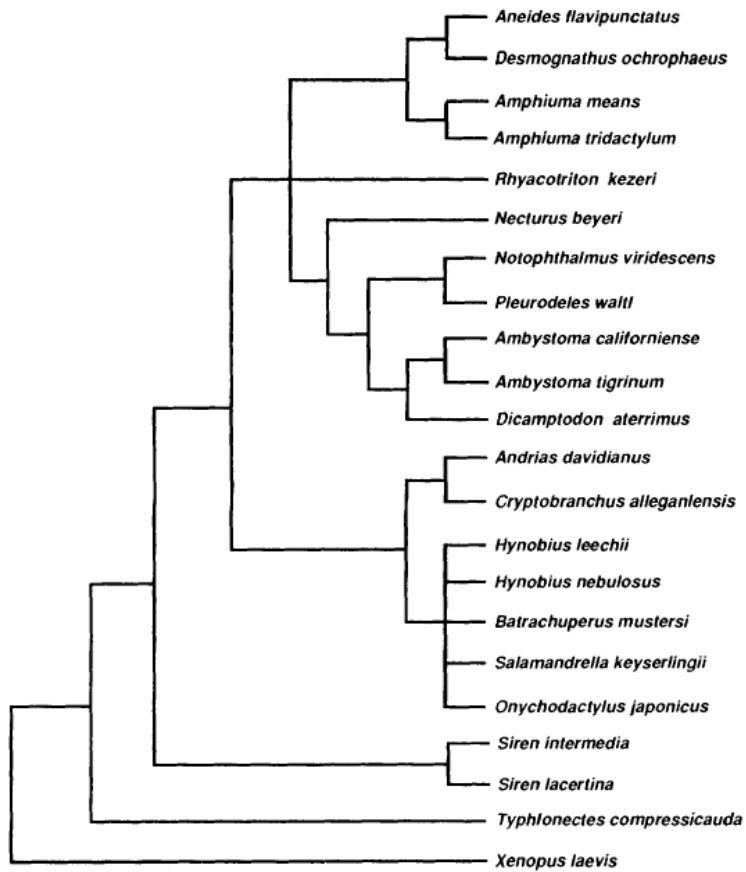


Figure 1.4.4: A strict consensus of 40 MPTs generated from 10 heuristic searches from the complete character matrix for extant salamanders (Larson and Dimmick, 1993)

After excluding 28 characters that displayed evidence for homoplasy the heuristic searches then found 60 MPTs, the one analysed by Larson and Dimmick for morphological changes is displayed below (Fig. 1.4.5). Larson and Dimmick (1993) then followed the character performances and calculated the strength of the characters to determine which were significant in influencing the phylogeny.

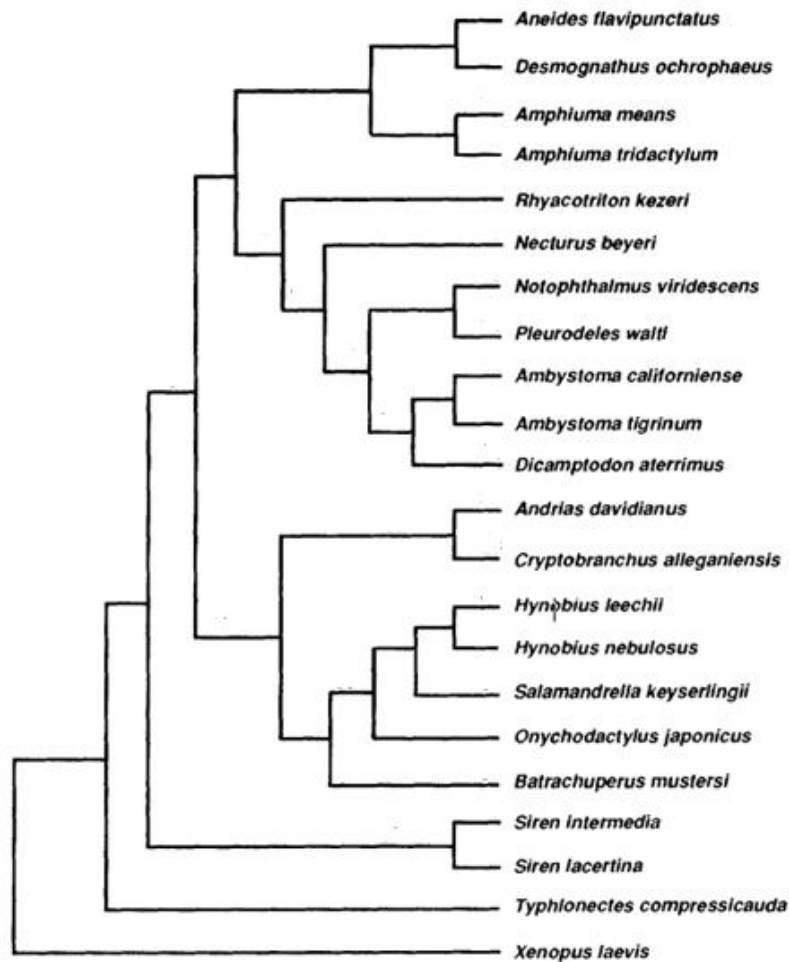
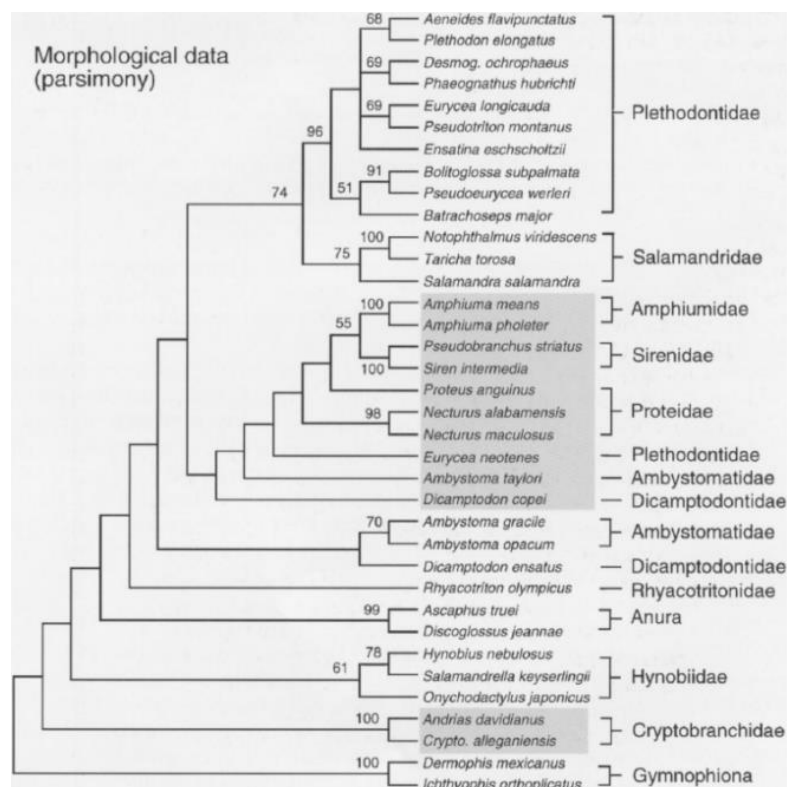


Figure 1.4.5: One of 60 most parsimonious trees used to track character changes in salamander characters (Larson and Dimmick, 1993).

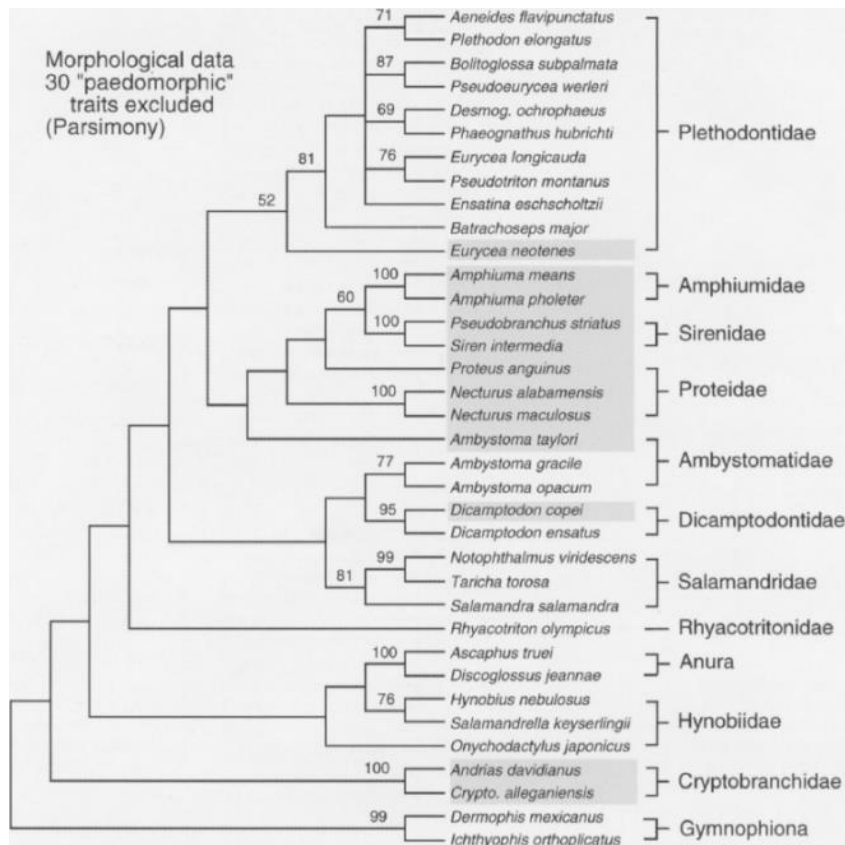
The characters used were divided into fourteen categories consisting of: cloacal anatomy; head and trunk morphology; small subunit rRNA; ten divergent domains of large subunit rRNA; and interdomain regions of large subunit rRNA. Using ACCTRAN character optimisation (the acceleration of the evolutionary transformation of a character), character changes were counted for all of the regions (351 in total). While each character on average underwent 0.5 more changes than the minimum number of changes required if there was a single origin for each derived character state, some required more changes than others. The characters of the head and trunk morphology (1.2 changes more than the minimum required for a single origin of the derived state) and the small D10 domain of the rRNA large subunits (1.5 changes more than the minimum required for a single origin of the derived state) had the highest number of extra changes per character. In this way Larson and Dimmick (1993) were able to identify characters which were highly homoplastic.

In a later study Wiens et al. (2005) tried to make comparisons between phylogenies that used a morphological character matrix and those that used molecular data. The resultant phylogenies showed disparate results. The results of the parsimony analyses using the morphological dataset resulted in the anuran “outgroup” emerging within the urodelan tree between Cryptobranchoidea and all other salamanders. Wiens et al. (2005) drew attention to the importance of species selection for inclusion in an analysis.

The species they highlight in grey in Figs. 1.4.6 and 1.4.7 also 1.4.8 and 1.4.9 below, are aquatic, paedomorphic species. They cluster together in a paraphyletic group (a group not sharing a single common ancestor). The problems caused by convergent characters are most obvious in these clades and the selection of the representatives of these clades is important. However, when Wiens et al. (2005) included molecular characters to create a phylogeny using a purely molecular dataset, the paedomorphic species cluster within their respective family clades regardless of their body plan or mode of life.



Figures 1.4.6 Wiens et al.'s Parsimony trees using all morphological data (Wiens et al. 2005). The paedomorphic salamander taxa are shaded and the numbers above the nodes indicate bootstrap values >50%.



Figures 1.4.7 Wiens *et al.*'s Parsimony trees with 30 putative pedomorphic characters excluded (Wiens *et al.* 2005). The pedomorphic salamander taxa are shaded and the numbers above the nodes indicate bootstrap values >50%.

Wiens *et al.* (2005) ran their combined evidence phylogeny using both morphological and nuclear ribosomal data from previous analyses (Larson and Dimmick 1993; Duellman and Trueb 1994; Gao and Shubin 2001) and also included new data from RAG-1. They used model-based methods for both molecular and morphological data and removed misleading "pedomorphic" characters from the dataset. The results (Figs 1.4.10 and 1.4.11) were similar to the results of Larson and Dimmick (1993).

The results of the combined evidence analyses do not agree on the position of Sirenidae but other clades are supported with high bootstrap values. Although the monophyly of Cryptobranchoidea is supported, its position in the Bayesian analysis differs from that of Larson and Dimmick (1993). Wiens *et al.* (2005) placed Sirenidae as the sister group to the internally fertilising Salamandroidea and the Cryptobranchoidea as the sister group to all other salamanders. Wiens *et al.* (2005) considered the Bayesian analyses to be less sensitive to long-branch attraction which may bias the results somewhat in salamanders; and other studies using nuclear genes have also found Cryptobranchoidea to be the sister group of all other living salamanders including Sirenidae (Frost *et al.* 2006; Roelants *et al.* 2007). The monophyly

of the Salamandroidea was supported. Plethodontidae is more closely related to Amphiumidae in both analyses, which supports the earlier findings of Larson and Dimmick (1993). They further agreed that Rhyacotritonidae is the sister clade to Amphiumidae + Plethodontidae (Wiens *et al.* 2005). The monophyly of the Salamandroidea is supported. Proteidae is confirmed as monophyletic but its relationships within the Salamandroidea are unclear. However, there is some support in the Bayesian analysis for Proteidae as the sister taxon to the highly stable Dicamptodontidae + Ambystomatidae.

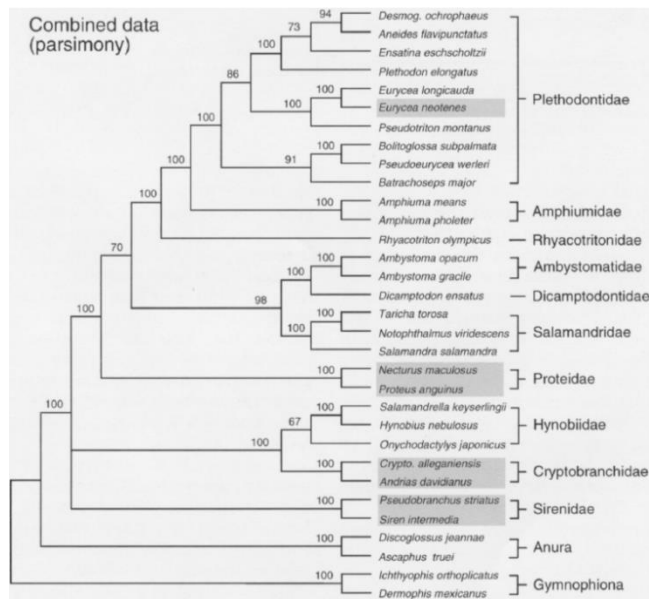


Figure 1.4.10: The total evidence results of Wiens *et al.* (2005) study using Parsimony analyses (Wiens *et al.* 2005). The pedomorphic salamander taxa are shaded and the numbers above the nodes indicate bootstrap values >50%.

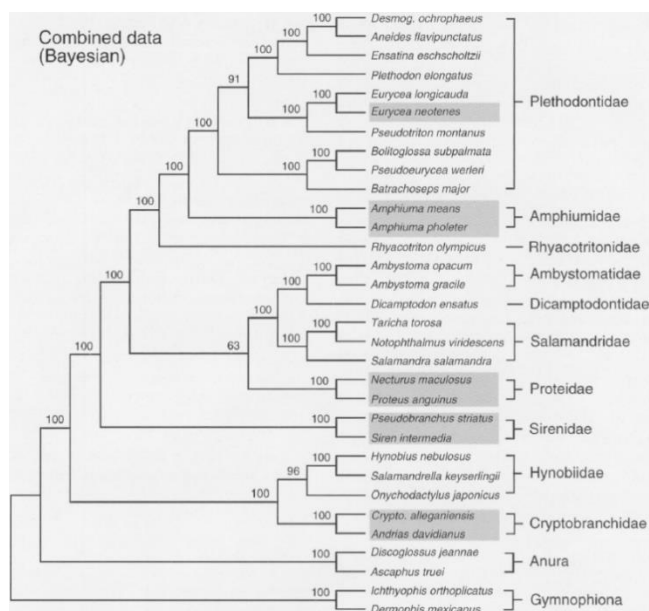


Figure 1.4.11: The total evidence results of Wiens *et al.* (2005) study using Bayesian analyses (Wiens *et al.* 2005). The pedomorphic salamander taxa are shaded and the numbers above the nodes indicate bootstrap values >50%.

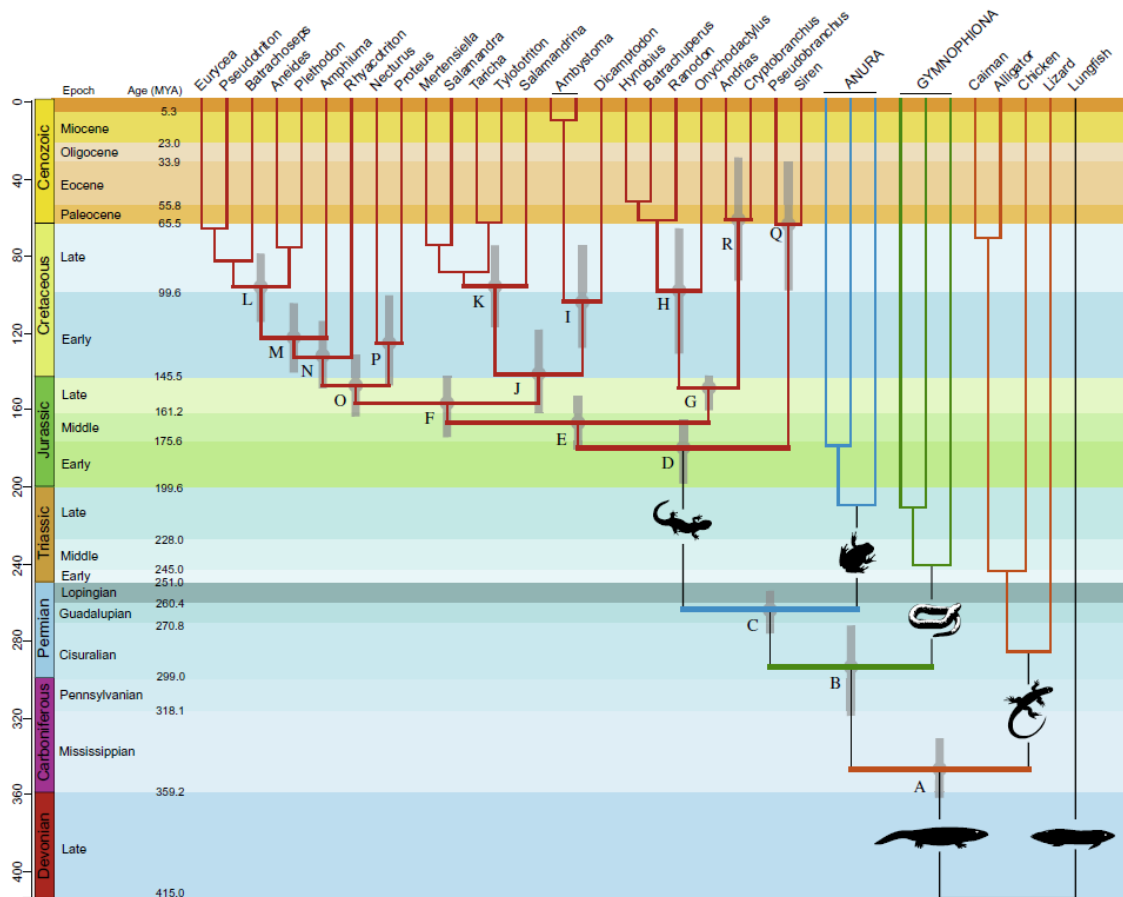


Figure 1.4.12: Phylogeny produced by Zhang and Wake (2009) using the complete mitochondrial DNA suggesting an Early Jurassic origin for salamanders and a Late Permian origin for Lissamphibia.

One of the most recent phylogenetic studies was that of Zhang and Wake (2009) using the complete mitochondrial genome (Fig. 1.4.12). Mitochondrial DNA (mtDNA) is relatively easier to sequence compared to nuclear DNA, thus providing substantial amounts of DNA data for the analysis. Zhang and Wake (2009) followed previous studies and recovered robust phylogenies using mtDNA (Mueller *et al.* 2004; Zhang *et al.* 2005; Zhang *et al.* 2006). They found support for the monophyly of the internally fertilising salamanders (Salamandroidea) and the externally fertilising salamanders (Cryptobranchoidea) and Sirenidae. This phylogeny supports the Plethodontidae + Amphiumidae relationship in agreement with previous molecular studies (Larson and Dimmick 1993; Chippindale *et al.* 2004; Wiens *et al.* 2005; Roelants *et al.* 2007; Cannatella *et al.* 2009) as well as the (Ambystomatidae + Dicamptodontidae) + Salamandridae clade recovered by both molecular and morphological analysis (Larson and Dimmick 1993; Chippindale *et al.* 2004; Wiens *et al.* 2005; Cannatella *et al.* 2009).

There thus seems to be some stability emerging due, in part, to the addition of molecular, soft body and behavioural characters to the previously established morphological data sets (Larson 1991; Zhang and Wake 2009). Previous studies have suggested that the signal

produced by soft body characters are more congruent with molecular results than results produced using osteology or teeth characters as it may contain more variations to measure, thus providing more characters to score for a phylogenetic analysis (Gibbs *et al.* 2000). This might be the case for salamanders. The monophyly of Salamandroidea, including Plethodontidae, Amphiumidae, Rhyacotritonidae, Ambystomatidae, Dicamptodontidae and Proteidae is supported (Larson and Dimmick 1993; Duellman and Trueb 1994; Hay *et al.* 1995; Wiens *et al.* 2005; Roelants *et al.* 2007; Zhang and Wake 2009; Gao and Shubin 2012). Salamandroidea is sometimes split up into: Plethodontoidea (Plethodontidae, Amphiumidae and Rhyacotritonidae), Proteoidea (Proteidae) and Salamandroidea (Ambystomatidae, Dicamptodontidae and Salamandridae) (Cannatella *et al.* 2009).

(Plethodontidae + Amphiumidae) is strongly supported with, usually (but not always), Rhyacotritonidae as their sister taxon. (Ambystomatidae + Dicamptodontidae) is another strongly supported clade, usually (but not always) with Salamandridae as the sister taxon. The monophyly of Proteidae is supported, and most analyses have placed it within the Salamandroidea (Frost *et al.* 2006).

The externally fertilising families consist of the Sirenidae (although reproductive behaviour has not yet been directly observed) and the Cryptobranchoidea (Cryptobranchidae + Hynobiidae) (Duellman and Trueb 1994). There is no strong consensus for the position of the sirenids, with studies (using molecular, morphological or combined evidence character matrices) placing them as sister group to all other salamanders (Milner 1983, 1988; Larson and Dimmick 1993; Duellman and Trueb 1994; Milner 2000; Zhang and Wake 2009) or (mainly using morphological characters) within the salamanders as sister-clade to the salamandroids (Wiens *et al.* 2005; Wang and Evans 2006; Roelants *et al.* 2007; Vieites *et al.* 2009; Zhang *et al.* 2009; Gao and Shubin 2012). Previous studies have failed to reach agreement on the position of Sirenidae within the Salamander phylogeny with some results from molecular analyses supporting Sirenidae as the sister clade to all other salamanders (Larson and Dimmick 1993; Chippindale *et al.* 2004; Zhang and Wake 2009), while others support the placement of Sirenidae within Salamandroidea, or as its sister clade (Wiens *et al.* 2005; Frost *et al.* 2006; Roelants *et al.* 2007; Vieites *et al.* 2009). The result of the molecular analyses in this thesis using both nDNA and mtDNA, supports the placement of Sirenidae within Salamandroidea (Fig. 3.5). However, the analyses were unable to resolve the relationships within Salamandroidea and so determining the position of Sirenidae within Salamandroidea needs further work.

More recent studies collated yet larger molecular datasets by collecting both mitochondrial and nuclear DNA which showed better resolution in the resulting trees and

more congruence with morphological studies (Roelants *et al.* 2007). This led to studies using complete mitochondrial genomes (Zhang and Wake 2009) and large-scale analyses using both nuclear and mitochondrial genes and a very large number of amphibian taxa (Frost *et al.* 2006; Pyron and Wiens 2011).

The results of these large scale studies show incongruence between datasets that has yet to be explored, and a lack of agreement between the molecular data based phylogenies. The complete mitochondrial genome produced a phylogeny that placed Sirenidae as the sister taxa to all other salamanders (Zhang and Wake 2009) (Fig. 1.4.13) whereas in both Frost *et al.* (2006) and Pyron and Wiens (2011) the phylogenies place Cryptobranchoidea (Cryptobranchidae + Hynobiidae) as the sister clade to all other salamanders.

The work presented in this thesis will seek to uncover the origins of the signals being expressed by the data, both molecular and morphological, for extant salamanders. An understanding of the data might elucidate the reasons differing salamander phylogenies have been produced by different authors over the years.

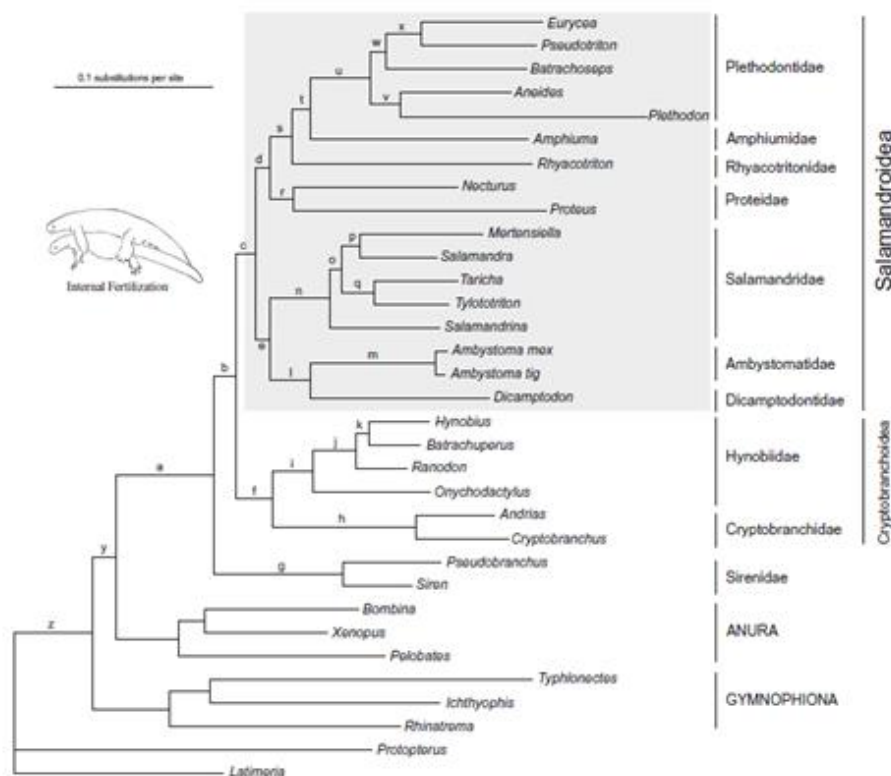


Figure 1.4.13 Phylogenetic results of Zhang and Wake (2009). Analysis of the full mitochondrial genome sequence. The branch support values are given below the phylogeny using (ALL) codon positions or (E3) without the third codon position. ML BS – Maximum likelihood bootstrapping; aLRT – aLRT test values; BI PP – Bayesian posterior probabilities.

1.4.1 Do soft body characters give a more reliable and congruent signal relative to molecular results than the signal from the osteological data?

Early morphological phylogenies displayed convergence by placing aquatic paedomorphic taxa together in paraphyletic groupings (Duellman and Trueb 1986; Wiens *et al.* 2005). It is interesting to investigate the origin of this signal and determine if this is reflected in the osteological or soft body data because of the implication this has in fitting fossils within a phylogeny. If the osteological data shows better congruence with molecular data, then fitting fossils (with incomplete osteological datasets) within phylogenies will give a higher confidence in the resulting topology than if the dataset is inherently compromised by convergent signal.

1.5 The Mesozoic Fossil Record

The Mesozoic fossil record of salamanders has had many new exciting additions in recent years. The earliest caudate fossils are possibly as old as the Early Jurassic of North America (Curtis and Padian 1999) although these are isolated elements and unfortunately unidentifiable to a family level. Further Jurassic material has been recovered from North America, Europe and Asia with some of the Late Jurassic fossils showing remarkable preservation. Many new fully articulated fossils have been found in recently discovered localities in China and these finds have particularly enriched the caudate fossil record in the last ten years.

Salamanders have a variety of life histories and this is often evident in the fossil record of adult specimens. Tooth-bearing vomers may be present in adult paedomorphic fossils as well as in larval forms as they are important for feeding in early life stages. Similarly, reduced, obsolete or absent maxillae is another larval trait that can be retained by sexually mature paedomorphic adults often in conjunction with the presence of vomers. Many features found in fossil specimens may also allow habitat reconstruction. The aquatic species often retain external gills, long haemal arches on the caudal vertebrae denoting a transversely flattened tail. Alternatively, well ossified scapula and coracoid together with a robust skeleton and ossified carpals and tarsals might indicate it had a more terrestrial habitat.

Much of the material found in the USA and Europe consists of isolated elements, usually vertebrae, atlantes, dentaries and other skull fragments (Gardner 2003, Gao and Shubin 2003; Skutschas 2009). Rarer, fully or partially articulated material is known from the

Late Jurassic of Kazakhstan and North America, the Late Jurassic/Early Cretaceous of China, and the Early Cretaceous of Spain (Estes and Sanchíz 1982, Shubin and Gao 2003, Wang and Rose 2005; Carroll and Zheng 2012, Demar 2013).

Current hypotheses of phylogenetic affinity:

Genus	Family/clade affinities	Morphology in common with the affiliated clade	Author(s)
<i>Marmorerpeton</i>	Sister taxon to Urodela	- Absence of spinal nerve notch or foramen in the atlas	(Evans <i>et al.</i> 1988; Skutschas and Martin 2011)
<i>Eoscapherpeton</i>	Scapherpetontidae Cryptobranchoidea	- Midline contact along the dorsal processes of the premaxillae - Frontal-maxillary contact - Parietals strongly overlapped by frontals - No distinct medial process on the pterygoid - Pterygoid-parasphenoid contact	(Gao and Shubin 2003; Skutschas 2009)
<i>Chunerpeton</i>	Cryptobranchidae	- Unicapitate ribs - Number of rib-bearing anterior caudal vertebrae reduced to two or three - Nasal narrower than interorbital width - Nasal-prefrontal contact absent - Lacrimal absent - Frontal extends anteriorly to lateral border of nasal - Anterior process of parietal extends along lateral border of frontal - Internal carotid foramina penetrate palatal surface of parasphenoid	(Shubin and Gao 2003)
<i>Urupia</i>	Outside of crown group Urodela	- Lacks spinal nerve foramina in the atlas - Presence of atlantal transverse processes - Vertebral sculpture present	(Skutschas and Martin 2011; Skutschas and Krasnolutski 2011)
<i>Kokartus</i>	Karauridae	- Monocuspoid teeth - Dermal sculpturing on skull - Squamosal fused to supratemporal	(Skutschas and Martin 2011)
<i>Karaurus</i>	Karauridae Sister taxon to crown-group salamanders	- Monocuspoid teeth - Dermal sculpturing on skull - Squamosal fused to supratemporal	(Skutschas and Martin 2011; Maddin <i>et al.</i> 2012)
<i>Liaoxitriton</i>	Hynobiidae	- Ossified hypobranchial II - Ossified ceratobranchial II	(Wang 2004)
<i>Jeholotriton</i>	Urodela Cryptobranchoidea	- Dentition present on the vomer, palatine and pterygoid - Unicapitate postatlantal ribs - Squamosal contact with the parietal or other roofing elements present - Maximum skull length/width greater than 1.2 - Longitudinal vomerine tooth row	(Wang and Rose 2005; Carroll and Zheng 2012)
<i>Pangerpeton</i>	- Placed close to the base of the crown group Urodela - Sister taxon to <i>Jeholotriton</i>	- Unicapitate ribs	(Wang and Evans 2006)
<i>Beiyangerpeton</i>	- Sister taxon to Salamandroidea	- Nasals separated by anterodorsal fenestra without a midline contact - Angular fused to prearticular - Articular absent by fusion to prearticular	(Gao and Shubin 2012)

		<ul style="list-style-type: none"> - Double-headed ribs associated with dorsal vertebrae - Anterior of parietal extending to midlevel of orbit - Parietal-prefrontal contact medially above orbit 	
<i>Iridotriton</i>	Salamandroidea Stem Salamandroidea/ Cryptobrachoidea	<ul style="list-style-type: none"> - Spinal nerve foramen in caudal vertebrae - Imperforate parasphenoid - Fused ulnare + intermedium - Gracile skull bones without sculpture - Triangular squamosal - Quadratojugal absent - Notochordal ectochordal vertebrae - Unicapitate ribs 	(Evans <i>et al.</i> 2005) (Gao and Shubin 2012)
<i>Paranecturus</i>	Stem-Proteidae/ <i>Necturus</i>	<ul style="list-style-type: none"> - Atlas with shallowly concave anterior cotyles - Alar-like process of the atlas - Solid dorsal rib-bearers - Mediolateral groove on the posterior face of the neural arch spanning between the neural spine and postzygapophyses present on the trunk vertebrae - trunk vertebrae with unicipitate neural spines and divergent rib-bearers 	(Demar 2013)
<i>Proamphiuma</i>	Amphiumidae	<ul style="list-style-type: none"> - Postzygapophyseal crests on the trunk vertebrae - Prominent or flattened anterior basapophyses - Spinal nerve foramen present on the caudal vertebra 	(Estes 1981; Gardner 2003)
<i>Scapherpeton</i>	Cryptobranchidae/ Scapherpetontidae	<ul style="list-style-type: none"> - Angular and prearticular separate - Anterior cotyles of atlas slightly oval - Strong subcentral keel - Prominent neural spines 	(Estes 1981)
<i>Prodesmodon</i>	Batrachosauroididae	<ul style="list-style-type: none"> - opisthocoelous trunk vertebrae - elongate body shape 	(Estes 1964; Naylor 1979; Estes 1981)
<i>Galverpeton</i>	Salamandridae or Plethodontidae	<ul style="list-style-type: none"> - Opisthocoelous vertebrae - At least some of its spinal nerves intravertebral 	(Estes and Sanchíz 1982)
<i>Kababisha</i>	Sirenidae	<ul style="list-style-type: none"> - non-pedicellate teeth - dentaries lacking lateral sensory foramina - highly reduced odontoid process - vertebrae with vertebrarterial canals including a dorsoventral passage - accessory anterior and posterior crests and deep anterior fossae on the vertebrae - strong ventral keels on trunk vertebrae - transverse processes not rib-bearing on most trunk vertebrae - caudal transverse processes with faceted tips - paired tall crests on ventral surface of caudal vertebrae - caudal vertebrae small in relation to trunk vertebrae - in some vertebrae the neural spine is weakly bifurcated 	(Evans <i>et al.</i> 1996) (Rage <i>et al.</i> 1993; Evans <i>et al.</i> 1996; Rage and Dutheil 2008)
<i>Noterpeton</i>	<i>Kababisha</i> Sirenidae	<ul style="list-style-type: none"> - sculpture on the neural arches - continuous surface joining the two cotyles - Procoely of vertebrae 	(Rage <i>et al.</i> 1993) (Evans <i>et al.</i> 1996)

<i>Piceoerpeton</i>	Scapherpetontidae	<ul style="list-style-type: none"> - bicipital rib-bearers - deeply amphicoelous cotyles - anterior position on neural spine - enlarged anterior vertebrarterial fossa 	(Estes 1969)
<i>Valdotriton</i>	Within the Salamandroidea	<ul style="list-style-type: none"> - Derived spinal foramina condition - Single prearticular-angular ossification - Double-headed rib-bearers 	(Evans and Milner 1996; Wang and Evans 2006; Gao and Shubin 2012)
<i>Opisthotriton</i>	Batrachosauroididae	<ul style="list-style-type: none"> - atlas has deeply concave anterior cotyles - atlas has a weak odontoid process 	(Estes 1981)
<i>Lisserpeton</i>	Scapherpetontidae	<ul style="list-style-type: none"> - Anterior cotyles of atlas slightly oval - Strong subcentral keel - Prominent neural spines 	(Estes 1981)
<i>Nesovtriton</i>	Cryptobranchoidea	<ul style="list-style-type: none"> - fully enclosed spinal nerve foramina in the atlas - vertebrae lack any sculpture - unicapitate transverse processes - lack of spinal nerve foramina in the trunk and anterior caudal vertebrae 	(Nesov 1981; Skutschas 2009)
<i>Parrisia</i>	Batrachosauroides	<ul style="list-style-type: none"> - Pterygophyseal process - Ventral keel present on trunk vertebrae - Closely approximated rib bearers and ventral laminae of the transverse process - anterior cotyles of the atlas which are deeply concave - reduced odontoid process - opisthocoelus vertebral condyles bearing a notochordal pit 	(Milner 1983; Denton and O'Neill 1998)
<i>Regalerpeton</i>	Sister taxon to Cryptobranchidae	<ul style="list-style-type: none"> - Absence of lacrimal - Pterygoid process with an additional distinct anteromedial process - Anterolateral process of parietal present and makes up less than 50% of the total length of the parietal - Nasal-prefrontal contact absent - Vomerine dentition marginal 	(Zhang <i>et al.</i> 2009)
<i>Habrosaurus</i>	Stem Sirenidae	<ul style="list-style-type: none"> - The marginal teeth are lost and replaced with a horny beak - The dorsal part of the premaxilla arises laterally and articulates along the lateral edge of the nasal - The parasphenoid projects anteriorly between the paired vomers and the dorsal part of both premaxillae 	(Gardner 2003)

Table 1.1 The current affinities of the fossil taxa and the morphology they have in common with their proposed clade.

Morphological characters are still the only way to incorporate fossils into phylogenies. Placing these fossils has many pitfalls. The degradation of morphological characters in fossils creates difficulties especially when comparing them to extant relatives. Placement of taxa on

the stem of extant clades often reflects the absence of certain derived features (Briggs 2010; Sansom *et al.* 2010). There is a history of palaeontologists studying the decay of living organisms and using their observations to understand fossil preservation better (Briggs and Kear 1993; Hellawell and Orr 2012). The sequence of character loss is thought to be non-random, at least in chordates, which will create a bias in fossil interpretation (Sansom *et al.* 2010).

The effect data paucity has on the placement of taxa and topology of other more data rich taxa has been discussed in the past (Donoghue *et al.* 1989; Huelsenbeck 1991; Anderson 2001). Briggs (2010) studied how decay might distort true ancestry signal. He found (by looking at the decay of extant forms that were similar to early chordates) that the attributes tended to decay in the opposite order to that in which they evolved so that the more ancestral morphology remained. He suggests that stem-ward slippage is widespread as fossil animals with a high proportion of missing information tend to fall out near the base of the evolutionary tree (Briggs 2010).

A recent study by Sansom *et al.* (2010) looked at the non-random decay of characters in chordates and how this non-random loss of data affected the taxon's position in a phylogeny. Later Sansom and Wills (2013) specifically set out to measure the stem-ward slippage of simulated fossils. Their simulated fossils were composed of osteological characters only, to mimic the commonly fossilised parts of a chordate. The results were compared to those of the combined dataset of osteological and soft body characters. They found that while missing data in itself should not present a problem for reconstructing phylogeny, the incompleteness, i.e., the absence of soft tissue, might cause systematic errors. This deletion of soft body characters causes significantly more loss of phylogenetic signal than deleting characters at random (Sansom and Wills 2013).

There have been a few studies that have included a selection of fossil salamanders together with extant taxa (Shubin and Gao 2003; Evans *et al.* 2005; Wang and Evans 2006; Zhang *et al.* 2009; Gao and Shubin 2012). *Karaurus* is usually designated as the outgroup, although sometimes *Marmorerpeton* is included. Recently a study including eight Mesozoic fossil salamanders in a phylogeny of extant taxa was published (Gao and Shubin 2012). This paper describes a new taxon, *Beiyanerpeton*, and places it in a phylogenetic context. The authors used 105 morphological characters and 26 taxa with *Karaurus* as the outgroup. They reweighted characters by using the maximum value of the rescaled consistency indices (Farris

1989) and ran the Parsimony analysis in PAUP 4.0. Their results are shown in the time-calibrated cladogram Fig 1.5.1.

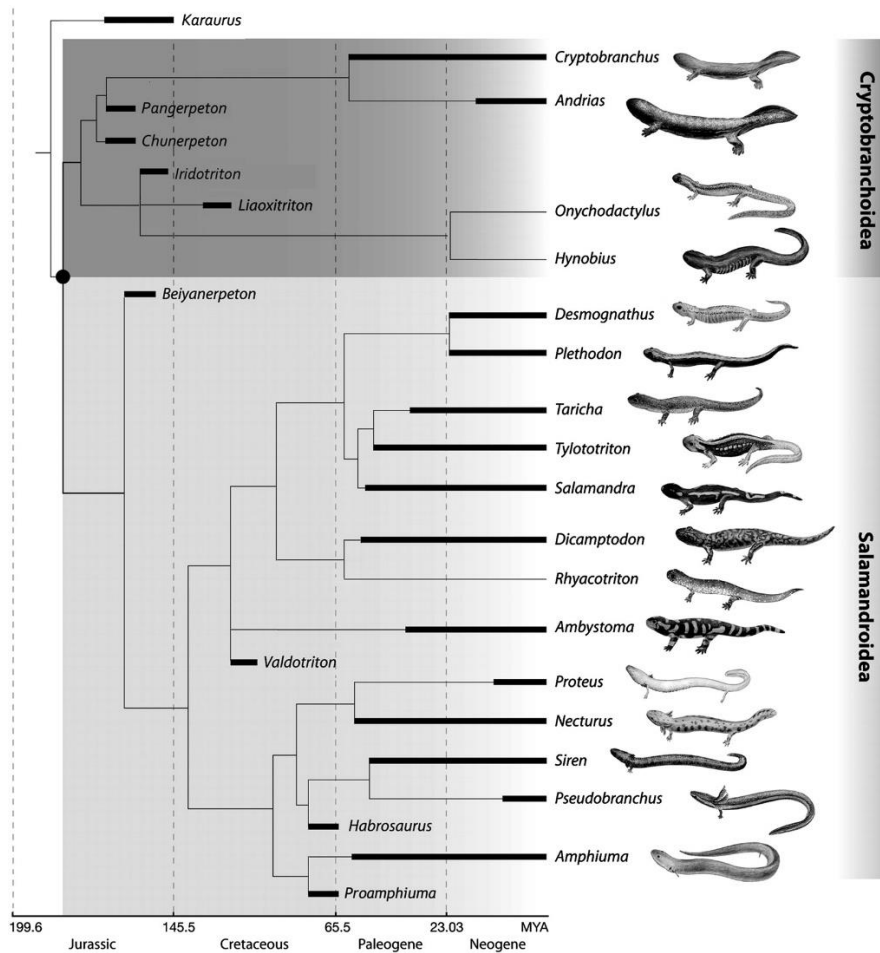


Figure 1.5.1 Calibrated cladogram showing the relationships of *Beiyanerpeton* to other fossil and extant salamander clades, and the timing of the Salamandroidea splitting from Cryptobranchoidea (solid dot) as indicated by the fossil record (Gao and Shubin 2012).

The taxon of focus, *Beiyanerpeton*, was placed on the stem of Salamandroidea. *Pangerpeton*, *Chunerpeton*, *Iridotriton*, and *Liaoxitriton* were placed within Cryptobranchoidea and *Valdotriton* was included within Salamandroidea. These taxa (excluding *Beiyanerpeton*) had previously been included in other phylogenetic analyses (Wang and Evans 2006; Zhang *et al.* 2009) but their relative positions differ slightly. Other fossil salamanders had usually either been assigned to one of the extinct families i.e., Scapherpetontidae and Batrachosauroidae, or to the Cryptobranchoidea and Salamandroidea based on shared characteristics.

The Scapherpetontidae (Estes 1981) is a ‘family’ of fossil salamanders from the Cretaceous of North America and Uzbekistan and includes *Eoscapherpeton*, *Lisserpeton*, *Piceoerpeton*, and *Scapherpeton* (see Table 5.1). This extinct family has historically been hard to diagnose because many of their distinctive features are linked with neoteny. No uniquely

derived features are known that unambiguously differentiate scapherpetontids from all other salamanders (Gardner 2012). They are similar to living Cryptobranchoidea in that their angular is separate from the prearticular, and have previously been assigned to Dicamptodontidae because of the similarity in spinal nerve foramina (Edwards 1976). The assignment of *Piceoerpeton* to Scapherpetontidae is problematic because of the similarity in morphology to Batrachosauroididae (Milner 2002). Although the trunk vertebrae of *Piceoerpeton* are typical for Scapherpetontidae (Estes and Hutchison 1980; Estes 1981; Naylor and Krause 1981) the reduced odontoid process and deeply concave anterior cotyles of the atlas are more similar to the batrachosauroidid condition such as in *Opisthotriton* (Gardner 2012). However the latest results place *Piceoerpeton* as part of Scapherpetontidae (Demar 2013) with a suggestion that it might even be a descendant of *Lissotriton* (Naylor and Krause 1981).

Batrachosauroididae (Auffenberg 1958) is a family of fossil salamanders from the Cretaceous and Cenozoic of North America and the Cenozoic of Europe. It includes *Opisthotriton*, *Parrisia*, and *Prodesmodon*. Batrachosauroididae has been referred to the Salamandroidea (Noble 1931; Taylor and Hesse 1943) and there have been suggestions that they are related to the family Proteidae (Estes 1975; Naylor 1979; Estes 1981; Naylor 1981; Milner 1983; Skutschas and Gubin 2012) although a recent phylogenetic analysis of vertebral characters only has placed Proteidae as more closely related to Scapherpetontidae than Batrachosauroididae (Demar 2013). Batrachosauroididae is characterised by an atlas with large, deeply concave anterior cotyles but a weak or absent odontoid process. They also have presacral vertebrae that are either opisthocoelous (in early forms) or amphicoelous (in later forms); the skull is paedomorphic with long posterior processes of the premaxillae, broad vomers, a broad parasphenoid, and retention of maxillae. Their bodies are often elongated with reduced limbs (Estes 1981).

There are several enigmatic fossils from the southern hemisphere which have been identified as salamanders. *Kababisha sudanensis*, *Kababisha humarensis* from North and Eastern Africa and *Noterpeton bolivianum* from Bolivia and Niger share sculpture on the neural arches and a continuous surface joining the two cotyles (Evans *et al.* 1996). Their similarity with Sirenidae has been noted (Rage *et al.* 1993; Evans *et al.* 1996; Rage and Dutheil 2008) though others disagreed (Gardner 2003), but so far they have not been included in a phylogenetic analysis.

1.6 Biogeography

1.6.1 Introduction to biogeography

The study of the distribution and evolution of organisms through space and time is at the heart of biogeographic studies (Ball 1975). The creation of geographical barriers causing speciation is called vicariant speciation (Rosen 1975; Rosen 1978; Ronquist 1997; Sanmartín and Ronquist 2004; Upchurch 2008). The creation of this geographical barrier may affect more than one organismal lineage. The patterns of distributions of sister species may be seen in multiple lineages and could mirror the history of the formation of the barrier. Conversely dispersal is the expansion of a species range as a geographical barrier is removed and this may distort the vicariance pattern (Upchurch *et al.* 2002; Lieberman 2003). Although geodispersal can overprint the vicariance signal, it is also an important prerequisite for vicariance. Taxa need to have a wide geographic distribution in order to be affected by barriers that form later. Other phenomena such as: post speciation dispersal, allopatric speciation by dispersal (dispersal of the species to such an extent that there is disrupted gene flow causing speciation), phylogenetic errors and extinction events could all distort a vicariance signal but would most likely be clade specific as they would affect each clade in a different manner. The inclusion of fossils to form ancestral area cladograms somewhat dampens the distortion created by extinction in the vicariance signal but only if there is no missing information caused by rock preservation potential bias (Barrett *et al.* 2009; Butler *et al.* 2009; Crisp *et al.* 2011; Upchurch *et al.* 2011). There is also a chance that an area cladogram (a cladogram that depicts the relationships of different areas instead of organisms) formed from a phylogeny could mirror biogeographical history by chance (pseudo-congruence) (Page 1991; Hunn and Upchurch 2001).

Some dichotomies (sister taxa relationships) are not easily explained by geographic events and so cannot reasonably be attributed to vicariance. However with the knowledge that facultative and permanent paedomorphosis occur within living ambystomatids, *Dicamptodon* and plethodontids it is reasonable to assume that dichotomies that occur between paedomorphic urodeles and their terrestrial sister clade may be because of heterochrony (Milner 1983).

1.6.2 Salamander geographic distribution

Apart from two recent southward migrations to northern South America by plethodontids (Hanken and Wake 1982) and Northern Africa by salamandrids (Veith *et al.*

1998; Steinfartz *et al.* 2000) all living salamanders and most fossil taxa are found in previously Laurasian continents (Davic and Welsh 2004). This distribution pattern suggests all modern salamander lineages arose in Laurasia (Savage 1973) with diversification occurring through continental break up (vicariance theory) or range disruptions (Milner 1983)

The salamander stem ancestor may have been cosmopolitan throughout Laurasia by the Middle Jurassic. If salamanders were globally distributed before the break up of Pangaea, why do they not currently have a wider geographical distribution? It may be because of range restriction, to the northern parts of Pangaea, during initial divergence and radiation. If stem salamanders were aquatic they may have been restricted to a specific habitat and favourable climate zones (Romer 1968).

1.6.2.1 Gondwana

There are currently five records of fossil material found in what were once Gondwanan continents. The status of *Ramonellus* (Lower Cretaceous, Israel) remains uncertain pending restudy (Nevo and Estes 1969). There is then the enigmatic material from Bolivia, Niger, Morocco, and Sudan, represented, so far, by isolated atlantes, vertebrae and skull bones. (Rage *et al.* 1993; Evans *et al.* 1996; Rage and Dutheil 2008). Evans *et al.* (1996) suggested these salamanders might be closely related to the Sirenidae. Their position in the phylogenetic tree could shed light on the origins and early radiation of early salamanders. If these Late Cretaceous taxa lie towards the base of the tree, their position may suggest that salamanders once had a more global distribution but were later restricted to the Northern continents (San Mauro *et al.* 2005). However, if these fossils nest amongst recent groups it would suggest that salamanders could have dispersed, in limited numbers, from Laurasia to Gondwana, before or during the Cretaceous, as some modern plethodontid forms have done one or more times within the last 3-5 million years (Hanken and Wake 1982). Milner (1983) noted that, during the late Jurassic, Laurasia may have been in contact with northern Gondwana. If correct, it may account for the presence of the enigmatic fossil salamanders in the southern hemisphere during the Cretaceous if the phylogeny supports the dispersal theory (Ezcurra and Agnolin 2012).

1.6.2.2 Laurasia

By the Upper Jurassic the Turgai Sea had divided Laurasia into east and west landmasses with Cryptobranchoidea on the Asian landmass in the east, and sirenids, proteids, plethodontids and salamandrids on the western Euramerican landmass. Marine barriers formed at least four times with the potential to result in phylogenetic dichotomies (Hallam

1981). However, there are three proposed mechanisms by which dichotomies are formed: geographical events leading to endemism through vicariance, ontogenetic dichotomy between terrestrial and paedomorphic groups, and ecological divergence (Upchurch, 2008). Milner proposed that the split between the Cryptobranchoidea and Salamandroidea occurred because of the formation of the Turgai Sea approximately 150 million years ago. Although some aspects of Milner's (1983) phylogeny are now out of date his hypothesis concerning the impact of certain continental movements on the radiation patterns of early salamanders can still be tested.

Zhang and Wake (2009) found that sirenids diverged from all other living salamanders at around 183 million years ago just as the North Atlantic started to open (Hallam 1994). This would have restricted sirenids to the small land margins along eastern North America, South America and Africa. However if Cryptobranchoidea are placed as the sister taxon to all other salamanders it would suggest an Asian origin for Urodela as *Chunerpeton* (a cryptobranchoid) is proposed as the oldest crown group salamander (Shubin and Gao 2003). Several inconsistencies cast doubt on this Asian origin theory. The date estimates of the *Chunerpeton* fossil horizon have been fiercely contested with age estimates spanning the Middle Jurassic to the Early Cretaceous (Gradstein *et al.* 2004; He *et al.* 2004; Liu *et al.* 2006; Yanxue *et al.* 2006; Ren and Oswald 2002; Zhang *et al.* 2006; Wang *et al.* 2005). Apart from other fossil Caudata found in Europe and North America that may prove inconsistent with an Asian origin until placed in a phylogeny, molecular studies have recently supported the divergence of Sirenidae from the other Urodela before the Cryptobranchoidea diverges from Salamandroidea, but these differing phylogenetic signals are based on the analysis of different types of molecular data.

Several further dispersal events might also account for modern day distribution patterns. Naylor (1981) proposed that cryptobranchoids originated in North America while Milner (1983) suggested it was more parsimonious to hypothesise that the clade originated in Asia with subsequent dispersal to North America via a land bridge. *Chunerpeton* in China and other possible cryptobranchoid salamanders from the Jurassic/Cretaceous supports the theory of an Asian origin for the Cryptobranchoidea clade (Gao and Shubin 2001, 2003; Wang 2004) although there are few Jurassic deposits and only very rare Jurassic salamander fossil material from North America available to challenge this hypothesis. The current distribution of cryptobranchoids in North America might be because of a dispersal event across the Bering land bridge (Milner 1983; Zhang and Wake 2009).

The common ancestor of the Salamandroidea may have been distributed through Euramerica by the Mid-Jurassic according to a recent molecular clock analysis (Zhang and Wake 2009). This is at odds with the fossil calibrated supertree produced by Marjanović and Laurin (2007) which suggests that Salamandroidea originated only 80 million years ago, but in Appendix 1 of their supplementary information they do allow that the fossils they have used, and the uncertain phylogenetic placement of the species, means that their divergence estimation may be too young. In contrast, Zhang and Wake (2009) suggest that their older date of 160mya is consistent with the earliest representatives of Late Jurassic salamandroid-related fossils such as *Iridotriton* (Evans *et al.* 2005).

Zhang and Wake (2009) found that the three most speciose salamander clades (Plethodontidae, Salamandridae and Hynobiidae) initially diversified at nearly the same time approximately 96-100 million years ago. At this time in the Late Cretaceous, the climate was very warm with significantly higher temperatures in northern latitudes (Zachos *et al.* 2001; Jenkyns *et al.* 2004). This may have caused previously continuous clades to split into geographically fragmented groups through shrinking habitats and extinctions, perhaps resulting in the diversification of plethodontids in America, salamandrids in Europe and hynobiids in Asia (Vieites *et al.* 2007).

1.6.2.3 What is the position of Sirenidae in relation to other salamanders? Are the enigmatic Gondwanan fossils (*Kababisha* and *Noterpeton*) related to Sirenidae?

Previous studies have failed to reach agreement on the position of Sirenidae within the Salamander phylogeny with some results from molecular analyses supporting Sirenidae as the sister clade to all other salamanders (Larson and Dimmick 1993; Chippindale *et al.* 2004; Zhang and Wake 2009), while others support the placement of Sirenidae within Salamandroidea, or as its sister clade (Wiens *et al.* 2005; Frost *et al.* 2006; Roelants *et al.* 2007; Vieites *et al.* 2009). Within the phylogeny the position of Sirenidae will help to clarify the possible place of origin for crown group Urodela. With the robust placement of Sirenidae and its purported relatives (*Habrosaurus* from North America and *Kababisha* and *Noterpeton* from Africa and South America respectively) at the base of the salamander phylogeny, the Pangea-wide origin of Salamanders can be supported. If it turns out Cryptobranchoidea is the sister clade to all other salamanders, then a Laurasian origin and diversification/distribution pattern for salamanders is more likely.

Rage (1993) suggested that together the *Kababisha* and *Noterpeton* might form a sister group to salamanders that was caused by a vicariant event. The Late Cretaceous age of this clade and the presence of earlier crown group salamanders found in previously Laurasian continents

precludes this hypothesis. *Kababisha* + *Noterpeton* material of an older age would need to be found for this hypothesis to merit a review. The affinities of this clade in relation to other salamanders remain problematic. However, the result has interesting implications on the distribution potential between the Gondwanan continents (Africa + South America) as *Noterpeton* has been discovered in both Bolivia and Niger in Late Cretaceous age sediments (Rage *et al.* 1993; Rage and Dutheil 2008). Its possible relationship with Caudata also highlights interesting questions about the origins and diversification of Lissamphibia.

1.6.2.4 Can fossils be placed robustly at a Family and/or Salamandroidea/Cryptobranchoidea level?

Although there is some consensus of internal relationships of salamanders emerging (e.g. Ambystomatidae + *Dicamptodon*, and Cryptobranchidae + Hynobiidae), there are still other families, apart from Sirenidae, that are not consistently placed in the same location on the tree (e.g. Proteidae). This uncertainty of the internal relationships of salamander families makes it difficult to place fossils with confidence. The ability to be able to distinguish between the Salamandroidea and Cryptobranchoidea in morphological data would allow for the placement of fossil taxa at this level. This important distinction could lead to a phylogeny that would allow for the hypothesised split between these two main clades due to vicariance to be addressed. The ability to place fossils even at a higher level is significant in salamanders because it will help gain a more complete view of salamander radiation through time.

This thesis will use molecular and morphological data to unravel the phylogenetic signal in chapter 2. Chapter 3 shows the results of the tree dependent and tree independent character evaluation and uncover evidence of stem-ward slippage when phylogenetic analysis uses morphological data. Finally, chapter 4 will show how robustly fossils can be placed in a phylogeny using morphological data.

2. Phylogenetic relationships of extant salamanders using molecular and morphological characters

2.1 Introduction:

The increased use of molecular data has shed new light on many phylogenies because molecular data are thought to be influenced less by convergence and homoplasy than morphological data (Lee 2005, Wiens 2005). Molecular methods have an advantage over morphological methods as there is often far more data available and so more characters to use to evaluate the relationships of different taxa. However morphological methods are capable of including both fossils and museum specimens that are unable to yield DNA material for analysis. It has been noted that perhaps a more biologically reasonable phylogeny can be produced by including fossils (Lee 2005) and this can only occur with the inclusion of morphological data.

Many studies are thought to have benefitted from the inclusion of molecular data in resolving previously controversial phylogenies (e.g. Teeling *et al.* 2005; Wiegmann *et al.* 2009). However, creating new phylogenies that conflict with morphological phylogenies does not bring resolution, just a different result based on an alternative form of data (Patterson *et al.* 1993). Often congruence between different molecular analyses is as elusive as congruence between different morphological studies and again between molecules and morphology (Patterson *et al.* 1993).

There are problems associated with both molecular and morphological data and each analytical method should be carefully considered (See Chapter 1.4). Certain types of DNA e.g., mitochondrial DNA (mtDNA), are thought to evolve rapidly and so run the risk of reaching saturation and might be unable to resolve deep nodes or short branches (Weisrock *et al.* 2005). Furthermore, the inclusion of too many distant outgroups could promote long branch attraction (Lukoschek *et al.* 2011).

Here representative salamander taxa are used in both molecular and morphological datasets that are then compared, not only to each other but also in a combined total evidence approach. The possible cause of the different phylogenetic signals seen in both the results of the study presented here and published phylogenies are then explored. The placement of Sirenidae is examined, and the relationship between the phylogenetic results of soft body and also osteological characters are compared to the phylogenetic results of molecular data.

2.2 Materials and Methods

2.2.1 Molecular data

A reduced version of the Pyron and Wiens (2011) genetic dataset was used as a base to which extra outgroups were added. A reduced version was necessary because the genes chosen by Pyron and Wiens covered all amphibian groups which included hundreds of taxa. Therefore, once most of the frogs and caecilians had been removed there were some gaps in the data where many of the salamander taxa had not been sequenced for every gene. However, the number of genes was reduced from 12 to 11 based on the completeness of data for the selected taxa. Three mitochondrial genes were included: cytochrome *b* (cyt-*b*), and the large and small subunits of the mitochondrial ribosome genes (12S/16S; omitting the adjacent tRNAs as they were difficult to align and represented only a small amount of data), and the nuclear genes, sodium–calcium exchanger (NCX1), solute-carrier family 8 (SLC8A3), C-X-C chemokine receptor type 4 (CXCR4), pro-opiomelanocortin (POMC), seventh-in-absentia (SIA), rhodopsin (RHOD), histone 3a (H3A) and recombination-activating gene 1 (RAG1) were selected to include both mitochondrial and nuclear DNA. (The species that had been coded for the morphological dataset were almost all represented in the molecular dataset.) Salamanders are represented by 26 extant species from all ten of the living families (Appendix A).

As the closest living clade to salamanders, frogs were chosen as one of the outgroup clades. Representative taxa were selected from the sister group to all other frogs, *Ascaphus* and *Leiopelma* and also a more derived frog, *Bombina*. Caecilians, as sister taxa to Batrachia were also included as outgroups and representative taxa were chosen based on the Zhang et al. (2009) study which included; *Ichthyophis bannanicus*, *Ichthyophis tricolor*, *Rhinatrema bivittatum*, and *Typhlonectes natans*. A range of further outgroups were chosen for the molecular analysis from clades less closely related to salamanders such as representatives from Rhynchocephalia, Squamata, Crocodylia, Aves, Dipnoi, Mammalia, and Actinistia.

The available genes for *Sphenodon punctatus*, *Takydromus tachydromoides*, *Caiman crocodilus*, *Alligator mississippiensis*, *Gallus gallus*, *Protopterus dolloi*, *Homo sapiens*, and *Latimeria chalumnae* were downloaded from GenBank to add to the Urodela dataset, together with the selected frog and caecilian sequences. Alignment was carried out using the clustal function in Jalview and then the multiple alignment tool in Geneious using the default Blosum62 model with gap open penalty of 12 and gap penalty of 3. Each alignment was then manually checked and trimmed with the hair-pin bends removed from the 12S and 16S genes.

The final dataset consisted of a total of 45 species with 10085 base pairs. The mean length per species is 4485 bp (44.5% of the total length of the matrix, 10085 bp), with a range from 869 to 9744 bp (8.6–96.6%) (See Table 2.1).

Gene	Gene Length (b.p)	Number of species	Coverage of dataset
16S	1880	41	91%
12S	971	39	87%
Cvt-b	1096	42	93%
RHOD1	315	9	20%
SIA	315	9	20%
POMC	553	13	29%
H3A	332	15	33%
CXCR4	714	13	29%
NCX1	278	16	36%
SLC8A3	1132	21	47%

Table 2.1 – Breakdown of the 11 genes in the combined molecular dataset

Molecular substitution models were selected for each gene individually using partitionfinder (Lanfear 2012). The nuclear genes were split into codons and individual models were assigned to their relevant codon using Bayesian Inference Criterion (BIC) (Schwarz 1978) (Table 2.2).

The molecular dataset was analysed using MrBayes version 3.2 (Ronquist and Huelsenbeck 2003; Ronquist *et al.* 2009). MrBayes is a program that uses a Bayesian method for calculating the best topology for a given dataset using the Markov chain Monte Carlo (MCMC) method for predicting the posterior probability. The Bayesian method was used (rather than Parsimony) on the molecular dataset because Bayesian analysis incorporates explicit models of DNA sequence evolution and so may give a more accurate estimate of phylogeny than parsimony (Weisrock *et al.* 2005). Bayesian analysis may also be less prone to long branch attraction (Alfaro *et al.* 2003). However Alfaro *et al.* (2003) also suggested that Bayesian analysis may sometimes produce unduly high support for questionable branch nodes.

Each gene was unlinked from the other genes in each analysis so the rate of evolution of one gene did not influence or impact on the rate of evolution of any other gene in the dataset. Full constraints (i.e., no other taxa can intrude on the monophyly of the specified clade constraints) and partial constraints (i.e., floating taxa, not specified in the constraint, are allowed to intrude on the specified constrained clades) were utilised in different analyses to

group together taxa with well-supported phylogenetic positions according to previously published studies.

Two runs were used as recommended by the algorithm authors because the program is designed to recognise that a good posterior probability has been reached by comparing the similarity of trees in each run. Each run had six mcmc chains in every Bayesian analysis of this study (this means there were five hot chains and one cold chain in each run). A swap frequency of 1 was also used for each Bayesian analysis and was chosen to compliment the Temp setting. In this study a temp setting of 0.1 was used throughout all analyses. The temperature of the hot chains is an indication of the tree space sampled. The higher the Temp setting the “hotter” the chain and the further the chain samples the available tree space, but this is often off-set with the ability of the hot chains to swap with the cold chains. Through the failure of run convergence of early analyses an optimal value of 0.1 was found that allowed the convergence of the runs without taking an impractical amount of time to complete. The swap setting has to change in conjunction with the Temp setting so that the chains swap information to allow them to converge towards a statistically significant consensus tree.

The sample and print frequencies were set at 100 each. These settings control how many times the trees generated in the search were sampled, in this case once every 100th generation. This setting was optimised to be the highest number of times the trees could be sampled without creating unmanageably large tree files. Each sampled tree topology and branch length is written to the tree file and simultaneously printed to the output screen. The percentage of trees removed from the cold chain tree file before all the trees are combined into a consensus tree was set at the recommended default setting of 25%. This was not changed in any of the analyses.

Several criteria were used to assess whether the chains had converged on a statistically significant tree topology. The average standard deviation of split frequencies value had to be below 0.01, the average Estimated Sample Size (ESS) must be above 100 (otherwise it may indicate that the parameter is under-sampled), and the Potential Scale Reduction Factor (PSRF) should approach 1.000 as the runs converge (Gelman and Rubin 1992). Posterior probability values are used to infer robustness of nodes in the Bayesian phylogenies.

Constraints were applied to the data restricting the following outgroup taxa to fall outside of salamanders: *Protopterus dolloi*, *Latimeria chalumnae*, *Alligator mississippiensis*, *Caiman crocodilus*, *Takydromus tachydromoides*, *Sphenodon punctatus*, *Homo sapiens*, and *Gallus gallus*. Frogs and caecilians were similarly constrained each to form a monophyletic group consisting of *Ascaphus montanus*, *Ascaphus truei*, *Bombina bombina*, *Bombina*

variegata, *Leiopelma hamiltoni*, *Pelobates cultripes* and *Pelobates fuscus*, also *Ichthyophis bannanicus*, *Ichthyophis tricolor*, *Rhinatrema bivittatum* and *Typhlonectes natans* respectively. No constraint was applied to the relationships between the various outgroup clades. No other constraint was applied to force the salamander species to cluster together and they were free to fall outside of the crown group Caudata if need be. Although they could not breach the constraints mentioned above, they could form sister taxa to any of the outgroups. The rooted outgroup taxon was assigned to *Latimeria* by putting it as the first species listed in the MrBayes script.

A MrBayes analysis was run with a temperature setting of 0.1 for the hot chain and both the print frequency and the sample frequency were set to one every 100. There were two runs, each with six chains, and after a burnin fraction of 25% a majority rule consensus tree was obtained (using the sump and sumt commands). To check that the resultant tree topology in each run, of each chain, were converging on the same result (with an acceptably low level of variation), the average standard deviation of split frequencies values was calculated to indicate the level to which the two runs have converged. An optimum level of 0.01 was used to indicate that the runs had converged sufficiently. ESS and PSRF scores were also used to further assess whether the individual runs in each chain had sampled enough of the data to form robust posterior probabilities at each node. An ESS value had to be over 100 to represent adequate posterior sampling and the PSRF value should approach 1.000 as the runs converge. All node values are posterior probability percentage values. Further analyses were completed using subsets of the molecular data. The three mitochondrial genes were analysed separately from the eight nuclear genes. This was done to test the hypothesis that the disparity in placement of Sirenidae was due to the type of genetic material sampled (e.g., mitochondrial v nuclear genes). The same MrBayes settings that were applied to the total molecular dataset were used again in each of the analyses using the nuclear and mitochondrial dataset.

<u>Gene</u>	<u>Model</u>
12S	GTR+I+G
16S	GTR+I+G
cytb	GTR+I+G
NCX1	Codon 1+2 – GTR+I+G Codon 3 – SYM+I+G
SIA	Codon 1 – K80+g Codon 2+3 – GTR+I+T
SLC8A3	Codon 1 – SYM+I+G Codon 2+3 – GTR+I+G
POMC	HKY+G
RHOD	Codon 1 – K80+G Codon 2 – GTR+I+G Codon 3 – GTR+G
CXCR4	Codon 1 – K80+G Codon 2 – GTR+I+G Codon 3 – GTR+G
H3A	Codon 1 – GTR+G Codon 2 – GTR+I+G Codon 3 – JC+I
RAG1	Codon 1 – GTR+I+G Codon 2 – SYM+I+G Codon 3 – GTR+I+G

Table 2.2 – Results of Partitionfinder assigning best fit model of rate of evolution to each gene/codon region.

2.2.2 Morphological data

A comprehensive literature review was undertaken to collect morphological characters and data used in previous salamander phylogenies (Edwards 1976; Sever and Trauth 1990; Hanken and Hall 1993; Larson and Dimmick 1993; Duellman and Trueb 1994; Gao and Shubin 2001; Wiens *et al.* 2005; Wang and Evans 2006; Zhang *et al.* 2009). The list of morphological

characters was edited to exclude overlapping characters and states and also modified by expanding character states to encompass all taxa and outgroups. Twenty new osteological characters were also created through personal specimen observation. The final character matrix consists of 249 discrete characters (19 were ordered multistate characters, the rest were unordered), made up of 197 osteological, and 52 soft-body and behavioural characters (see Appendix B). The osteological characters cover the entire skeleton but especially focusing on parts that are commonly preserved in the fossil record. These characters were scored for 27 extant taxa, 6 outgroups, and 34 fossil taxa and the matrix is stored in an excel spreadsheet (Microsoft Excel 2010) (see Appendix C). The extant taxa were scored for a combination of computerised tomography (CT) images [3D images were created from micro-CT scans of specimens at the NHM using the free software Spiers (Sutton *et al.* 2012)], whole specimens donated by the NHM to Evans Lab and 3D scans from Digimorph.org (Appendix D). The fossil taxa were scored from specimens where possible (as they are kept in museums around the world) and from the available literature where not. Notable exclusions to the fossil taxa list include *Ramonellus* (Early Cretaceous, Israel), *Sinerpeton* and *Laccotriton* (Jurassic/Cretaceous, China) that are genera that need further work on their descriptions and interpretations before being included in phylogenetic analyses. *Kiyatriton* (Early Cretaceous, Siberia) was scored using the available literature, however the final reduced dataset did not include enough scored characters to be included in a phylogenetic analysis at this time (see Further Work section in Chapter 5).

Taxa were selected to match those used in previous studies and were further influenced by the availability of molecular data and of osteological specimens for examination. Each family is represented by at least two species except for Sirenidae and *Dicamptodon*, each of which are represented by only one species (Sirenidae has only four species within two genera, and *Dicamptodon* is a single genus). The larger, more speciose families, such as Salamandridae and Plethodontidae, have had species selected from across as many subfamilies as possible (See Appendix D).

Outgroups were chosen from a wide range of taxa starting at the closest living relative to the salamanders, frogs. The morphological outgroups include *Rana* as a representative of a common frog used in previous studies and the fossil *Triadobatrachus massinoti* as one of the earliest representatives of fossil frogs. Caecilian representatives were chosen based on the Zhang *et al.* (2009) study and include *Typhlonectes natans* which is nested high in the caecilian phylogeny and also *Eocaecillia micropodia* representing the earliest fossil caecilian. They were chosen to represent the whole Caecilian clade from the most basal to the clades nested higher in the group.

Further outgroups were chosen from among Temnospondyli (Schultze and Trueb 1991): *Gerobatrachus hottoni* (Anderson *et al.* 2007; Anderson *et al.* 2008) and *Doleserpeton annectens* (Sigurdson and Bolt 2010). They were chosen because their placement relative to salamanders is well known and it is likely that they are ancestral to salamanders (Maddin *et al.* 2012).

The phylogenetic program used for all parsimony analyses is the Willi Hennig Society edition of TNT (Tree analysis using New Technology) (Goloboff *et al.* 2008; Goloboff *et al.* 2008) version 1.1 (published July, 2011). TNT is a free software tool used to create and analyse phylogenetic relationships using Parsimony. Constraints were applied to the outgroups to follow the relationships shown below in Fig. 2.1. A strict constraint was placed on these relationships so that they fell outside the crown group Urodela. The designated outgroup taxon in each script was *Doleserpeton* as it is the sister taxon to all other outgroups + salamanders. *Gerobatrachus* forms the sister taxon to frogs and salamanders according to previous published phylogenies (Anderson *et al.* 2007; Anderson *et al.* 2008; Maddin *et al.* 2012).

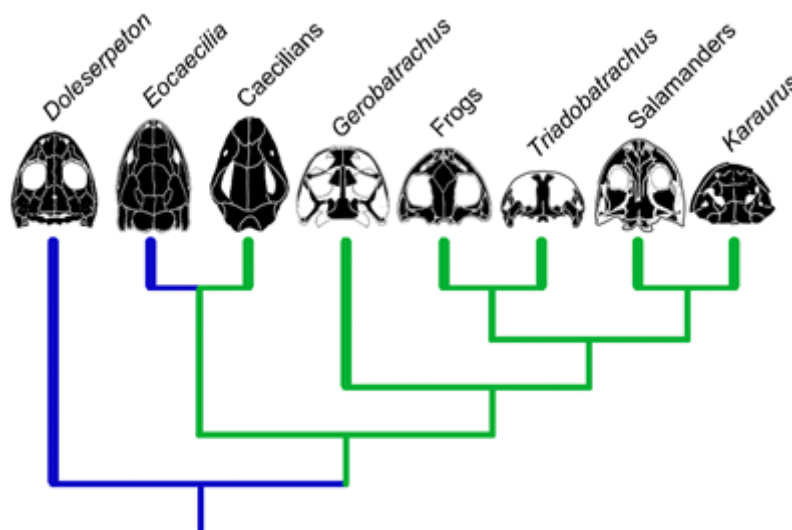


Figure 2.1 The proposed relationships of the outgroups used in this study as suggested by a parsimony analyses Maddin *et al.* 2012. (Figure after Maddin *et al.* 2012)

MrBayes (version 3.2) was used for the Bayesian analysis of the morphological data and the combined data analysis. Both ordered and unordered characters were used (19 ordered and 230 unordered) as was the default rate of evolution in MrBayes which is similar to a homogeneous rate of evolution such as the Jukes Cantor model (Jukes and Cantor 1969). Constraints were applied to the frog and caecilian taxa so that they each formed a monophyletic group, but the frog and caecilian clades were not restricted in their relationships

to any of the other outgroups. No other inter-relationship constraints were applied to any of the other outgroups on MrBayes, but they were constrained to be outside Urodela.

All TNT analyses used 20 random seed starts in the 'New Technology Search' option (Goloboff *et al.* 2008) as this is a large enough number to get a random sample of tree space for the start of the tree search. The New Technology searches used drift, sectorial searches and Tree Fusing options which are three different algorithms for searching for the optimal trees which gives an increased chance for success. Stabilising consensus value of five was used in each analysis which was three more than the default setting. This ensures that a minimum tree length is hit upon at least 5 times in the search. In order to search for additional topologies, the trees from the New Technology were stored in RAM and used as the starting trees in a Traditional search using tree bisection-reconstruction (TBR). The constraints were enforced in the Traditional Search. Agreement subtrees were calculated in each case where more than one most parsimonious tree (MPT) was found. If, for some reason, the taxon (or taxa) under scrutiny in an analysis was not included in the agreement subtree a strict consensus tree was produced. Once the most parsimonious trees had been found, subsampling was used in each analysis to provide relative support values allowing an assessment of relationship robustness. GC bootstrap values were calculated (1000 replicates) using the Traditional Search option in TNT. The New Technology Search option was not used in the bootstrap analyses as it crashed every time. The resultant tree topology was sometimes slightly different to the results of the New Technology Search because the different search methods found different topologies for their MPTs. The New Technology Search + Traditional Search combination always found shorter MPTs than the Traditional Search option alone, and so it was used in each parsimony analysis within this study.

The full morphological dataset was analysed using an extant frog (*Rana catesbeiana*) and an extant caecilian (*Typhlonectes natans*) as outgroups to provide a comparison with a phylogeny that was produced using morphological data that also includes fossil outgroups. In MrBayes this initial morphological analysis had a partial constraint applied where the frog and caecilian species were constrained to fall outside of the salamander clade. The caecilian species was designated as the root because earlier results from the molecular analysis and previous studies placed caecilians as sister clade to Batrachia (frogs + salamanders).

However further analyses were conducted on the morphological dataset using more extensive outgroups including Temnospondylii, *Gerobatrachus hottoni* and *Doleserpeton annectens*, and also the stem frog (*Triadobatrachus massinoti*) and stem caecilian (*Eocaecillia micropodia*), as well as the extant *Rana catesbeiana* and *Typhlonectes natans*. This was done

to test the resolution of the phylogenies when more outgroups are included. Also as fossils are introduced, more appropriate outgroups had to be included in the matrix. In all analyses of the morphological data the settings in MrBayes remained the same. The 19 ordered characters were included using the 'ctype ordered' function and the print frequency and sample frequency were both set to one in every 100. The burnin rate and temperature for the hot chains were the same as the molecular analysis settings i.e. 25% and 0.1 respectively. The analyses consisted of two runs each with three chains. In both TNT and MrBayes, constraints were in place to force the outgroup taxa to fall outside of salamanders. A hard constraint was applied in TNT to the outgroup taxa so that their internal relationships were unmovable with *Doleseperpeton annectens* as the ultimate outgroup with the other taxa constrained as depicted in Figure 2.2.

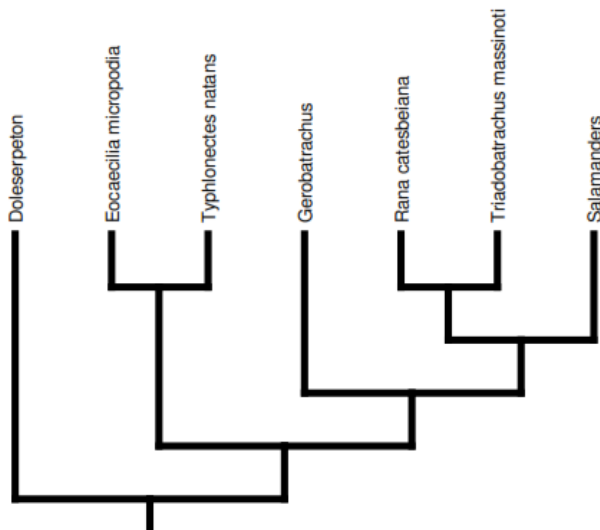


Figure 2.2 The constraint placed on the outgroup taxa on the morphological data used in the parsimony analysis in TNT

In the analyses designed to look at the signal in different parts of the anatomy, the same additional outgroups were kept. It has previously been suggested that molecular phylogenies reflect the topology resulting from the soft body anatomy of some clades better than the osteological data (Gibbs *et al.* 2000) and so this was tested by dividing the morphological data into skeletal characters and soft body and behavioural characters. However, because the soft body dataset had to be scored from literature sources, a hypothetical all zero outgroup had to be included as specific data for the outgroup taxa was not available to allow for the scoring of the characters.

2.2.3 Combined Molecular and Morphological data

The molecular data comprising the full eleven genes plus the full 249 morphological characters was analysed using MrBayes. The outgroups used included both the outgroups used in the first molecular dataset and a reduced set from the morphological analysis (just the representative for frogs and caecilians). The settings are consistent with the previous analyses. The constraints include restricting the outgroups to fall outside of the salamander clade.

2.2.4 Tree comparisons

Several methods for comparing trees are implemented within PAUP (Phylogenetic Analysis Using Parsimony) version 4.0 (Swofford 2003). Comparisons between trees using agreement subtrees, and Symmetric differences (Robinson folds) show the similarity of topology between the resultant trees. Tree results from morphological datasets and molecular datasets were compared to see the level of congruence in the results. The hypothesis that soft body characters produce a tree more similar in topology to the molecular results, compared to osteological results, is tested by comparing the results of the parsimony and Bayesian analyses of the soft body characters and the results of the parsimony and Bayesian analyses of the osteological results to the full molecular tree.

The outgroups were removed and the datasets reduced to their lowest common taxa set before being imported into PAUP. Rooted trees were used in every case and similarity in topology of just the common taxa in each tree, were assessed.

2.2.5 Character mapping

Characters were mapped onto a strict consensus tree to detect synapomorphies that support clades. The dataset was imported into Mesquite (version 3.0) and the MPT(s) or Bayesian consensus tree was attached to the data file using the 'included' function in the File menu. Once the trees had been linked to the dataset, a strict consensus tree was created for the TNT results (as the Bayesian results already consisted of a consensus tree). Character histories were traced onto the consensus tree using a parsimony framework. Synapomorphies were then noted by manually searching character by character.

2.3 Results

2.3.1 Molecular results

2.3.1.1 Combined mtDNA and nuDNA molecular phylogeny

The analysis of the full molecular dataset comprising eleven genes and 44 taxa resulted in a phylogeny that supports the monophyly of Batrachia with caecilians as their sister clade. All currently recognised salamander families are monophyletic. This analysis places the cryptobranchid and hynobiid taxa together in a monophyletic group (the Cryptobranchidae) which is sister to all other salamanders (Fig. 2.3.1). All the remaining salamanders are placed within Salamandroidea. Sirenid is placed as the sister taxon to all other Salamandroidea. *Dicamptodon* is more closely related to *Ambystoma* than to any other salamander family but support is poor. *Amphiuma* is placed as more closely related to plethodontids than to any other salamanders but support is again poor.

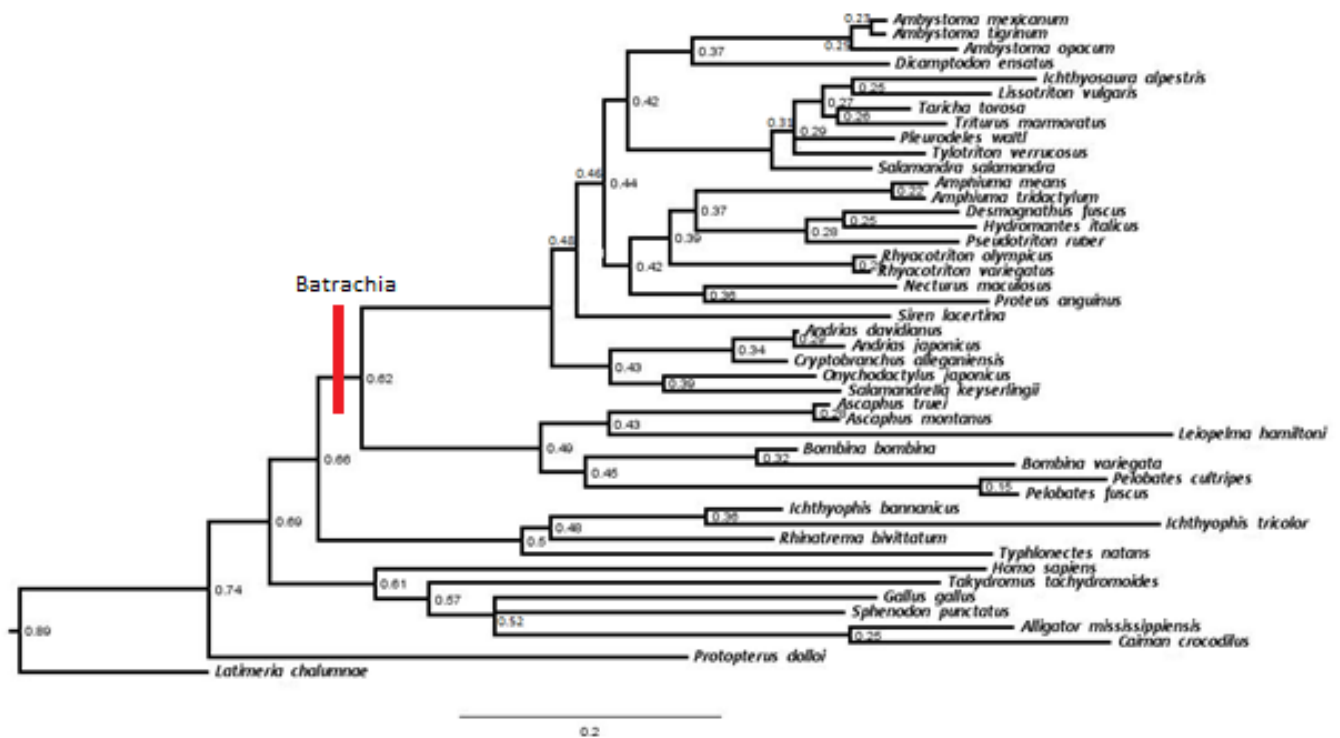


Figure 2.3.1 Result of the Bayesian analysis of eleven genes. Average standard deviation of split frequency value 0.005357. The average ESS for each partition was over 1000 and every partition's PSRF+ = 1.000 All Bayesian node values are posterior probability values

2.3.1.2 Nuclear DNA phylogeny

The nuclear tree is less resolved than the previous full molecular tree. The phylogeny result supports the monophyly of the Batrachia clade (61 BPP) (Fig. 2.3.2) but salamanders are not resolved as monophyletic. Caecilians are placed as the sister clade to Batrachia with moderate support. None of the salamander families are confirmed to be monophyletic except for *Amphiura* and *Ambystoma* but only with poor support. The phylogeny does not show any clear distinction between the Cryptobranchoidea and the Salamandroidea + Sirenidae. But in this tree *Amphiura* and Sirenidae are more closely related and *Dicamptodon* is most closely related to ambystomatids, which is consistent with the previous combined genetic dataset result.

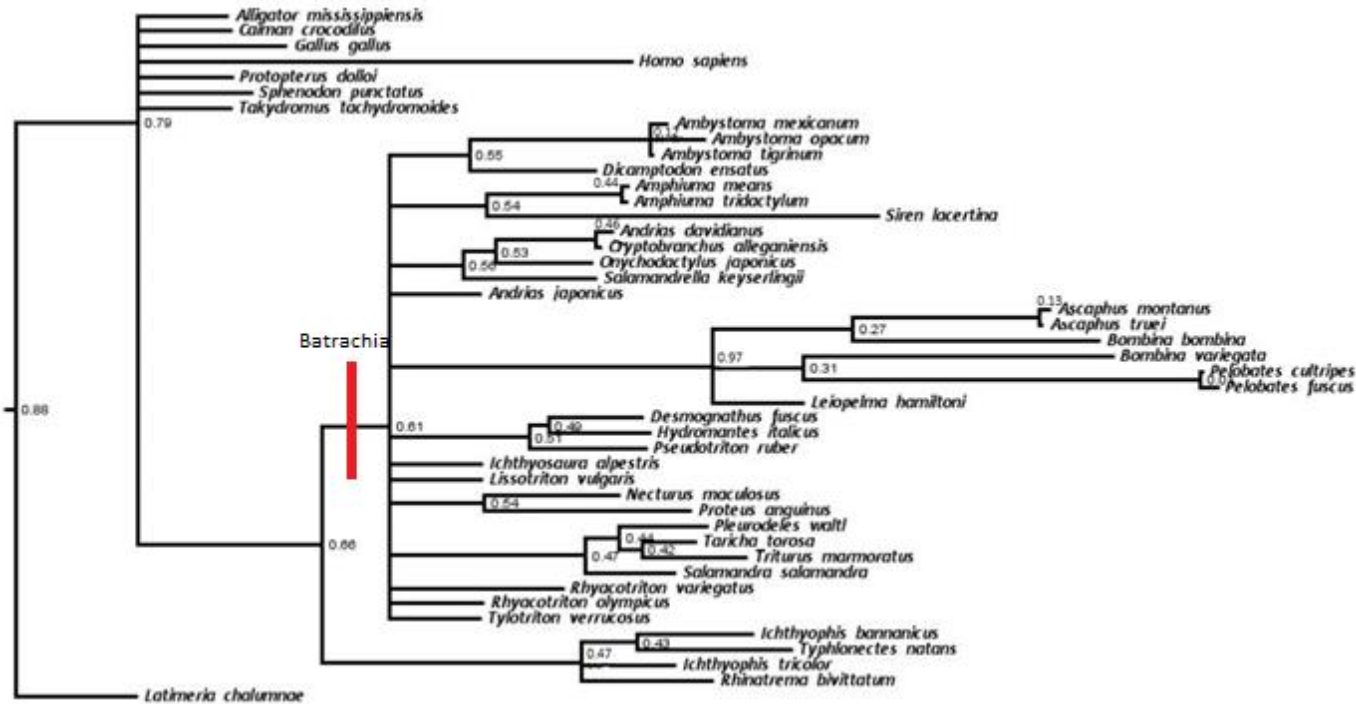


Figure 2.3.2 Result of a Bayesian analysis of eight nuclear genes in MrBayes version 3.2, with an average standard deviation of split frequency value of 0.009838. Bayesian posterior probability values at the nodes

2.3.1.3 Mitochondrial DNA phylogeny

This analysis of the mitochondrial DNA still supports the monophyly of Lissamphibia. The tree shows that salamanders and caecilians are more closely related, with frogs forming their sister clade with moderate support. All salamander families have been resolved as monophyletic, however support is low. Cryptobranchoidea is monophyletic, but Salamandroidea is paraphyletic. Siren is placed as the sister taxa to Cryptobranchoidea.

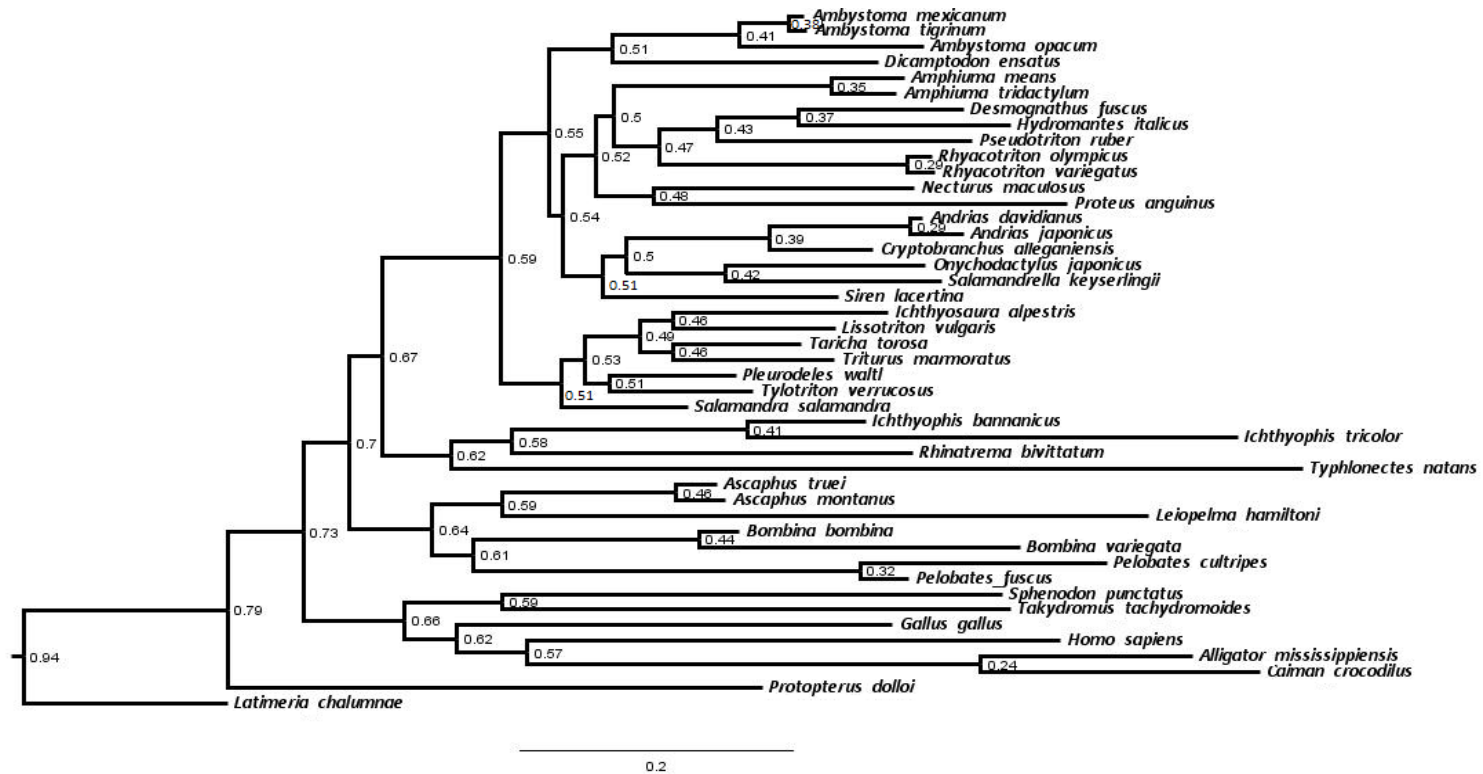


Figure 2.3.3 Bayesian analysis of the three mitochondrial genes. The analysis resulted in an average standard deviation of split frequency value of 0.004379. Bayesian posterior probability values at the nodes

2.3.2 Morphological Results

2.3.2.1 Full Morphological dataset with extant outgroups

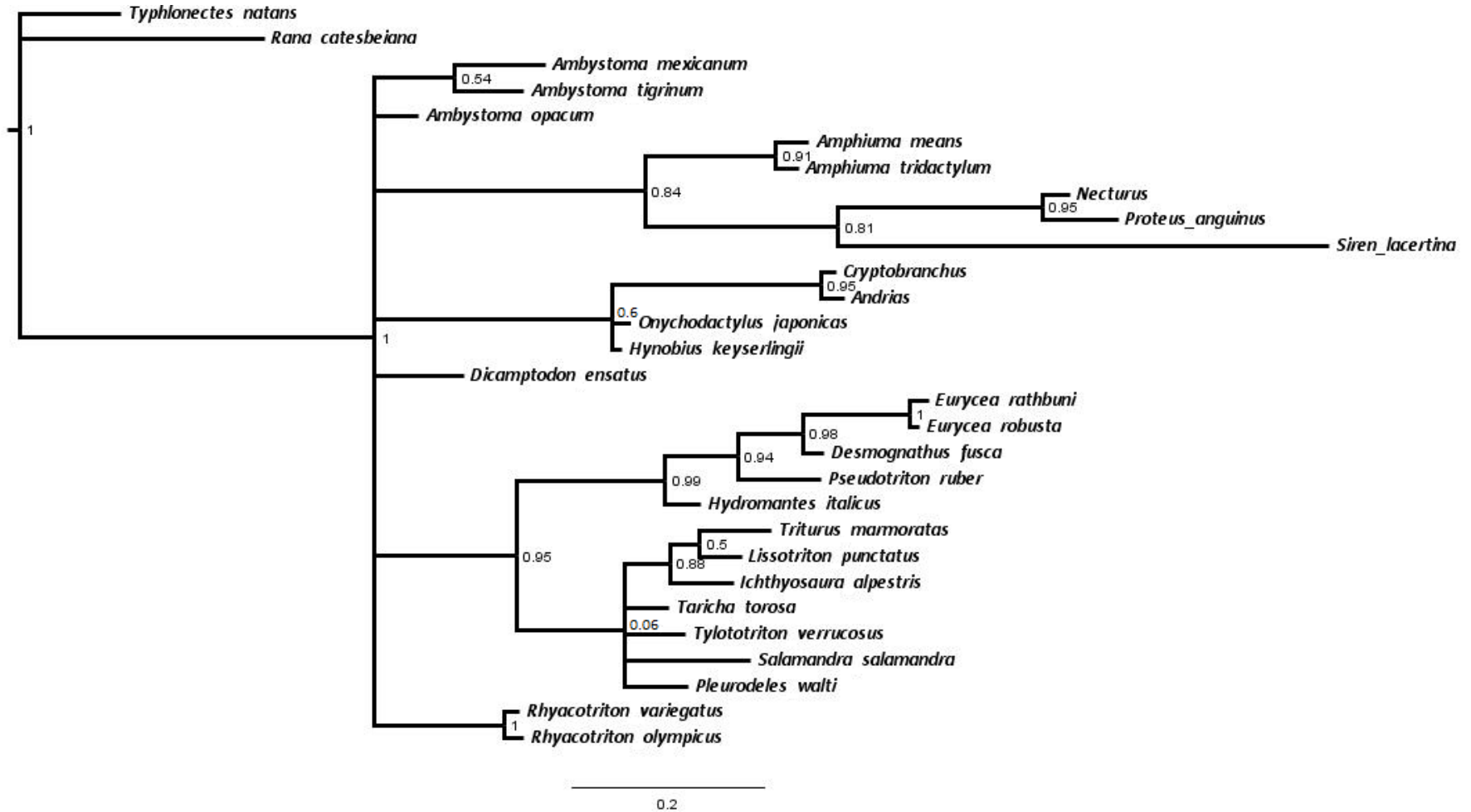


Figure 2.3.4 Bayesian analysis of the full morphological dataset with extant outgroups. This reached an average standard deviation of the split frequency value of 0.005371. Values at the nodes are Bayesian posterior probabilities.

This phylogeny (Fig. 2.3.4) comprises a polytomy of Rhyacotritonidae, (Salamandridae + Plethodontidae), *Dicamptodon*, Cryptobranchidae, (Amphiumidae + Proteidae + Sirenidae), *Ambystoma opacum* and (*Ambystoma tigrinum* + *Ambystoma mexicanum*). Sirenidae is grouped with Proteidae and Amphiumidae, and is not placed as the sister group to all other salamanders. Similarly, Cryptobranchoidea and Salamandroidea do not form monophyletic groups.

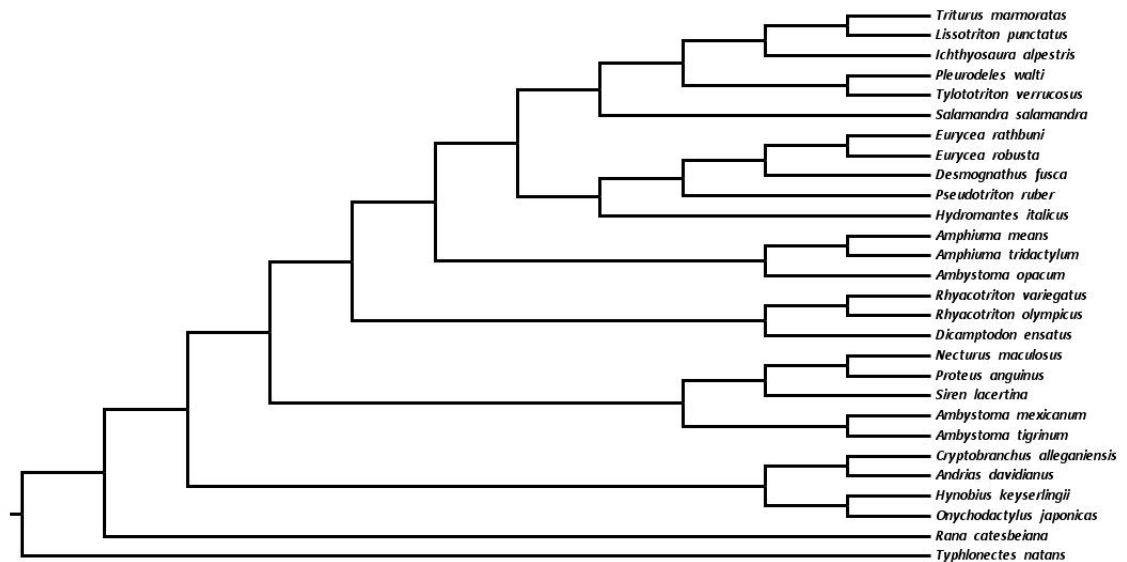


Figure 2.3.5 Parsimony agreement subtree of full morphological dataset with extant outgroups made from three MPTs each 660 in length in TNT. CI = 2.74, RI = 0.322

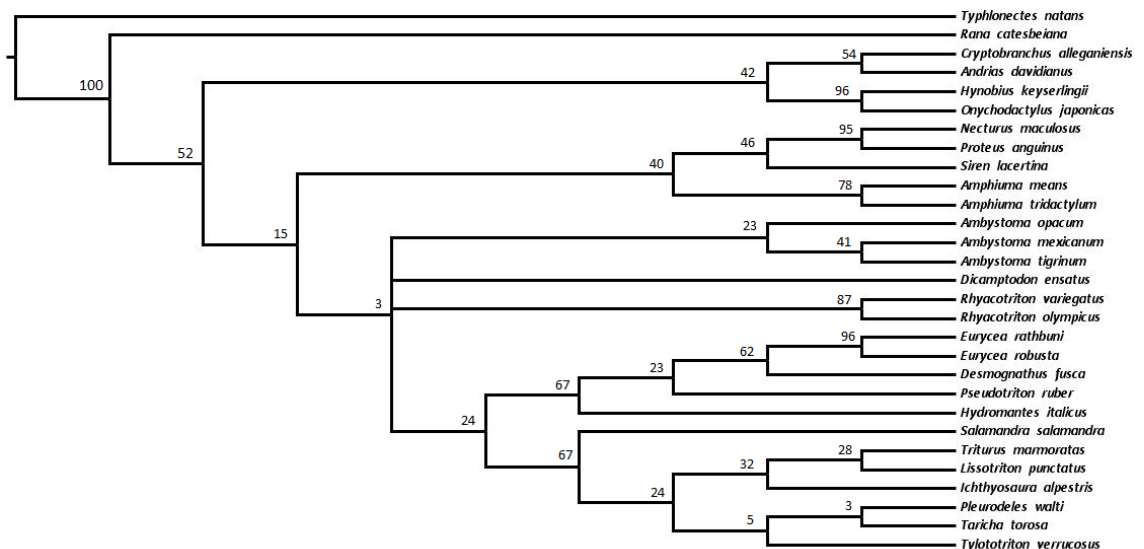


Figure 2.3.6 GC bootstrap tree (1000 replicates) of the full morphological dataset with extant outgroups generated in TNT (Traditional search).

In contrast to the Bayesian analysis of the full set of morphological characters, the parsimony analysis supports a monophyletic Cryptobranchoidea and places it as sister clade to all other salamanders, although the support values are relatively low (Fig 2.3.6). The support

values throughout the Salamandroidea are extremely low but it is monophyletic. Amphiumidae + Sirenidae + Proteidae form a sister clade, with relatively high bootstrap support.

2.3.3 Full Morphological dataset with fossil outgroups

The resulting Bayesian topology does not support the monophyly of Hynobiidae nor, therefore, of Cryptobranchoidea. The other family which does not emerge as monophyletic is Ambystomatidae as *Ambystoma opacum* forms part of a polyphyletic group comprised of (Sirenidae + Proteidae + Amphiumidae), (Plethodontidae + Salamandridae) and (*Ambystoma mexicanum* + *Ambystoma tigrinum*). *Dicamptodon* forms the sister clade to the aforementioned polytomy and *Rhyacotriton* is placed as the sister taxon to all other salamanders excluding Cryptobranchidae and the Hynobiidae. In this tree the outgroup taxon *Gerobatrachus* is placed as the sister group to salamanders, but caecilians are the sister clade to (salamanders + *Gerobatrachus*) and frogs.

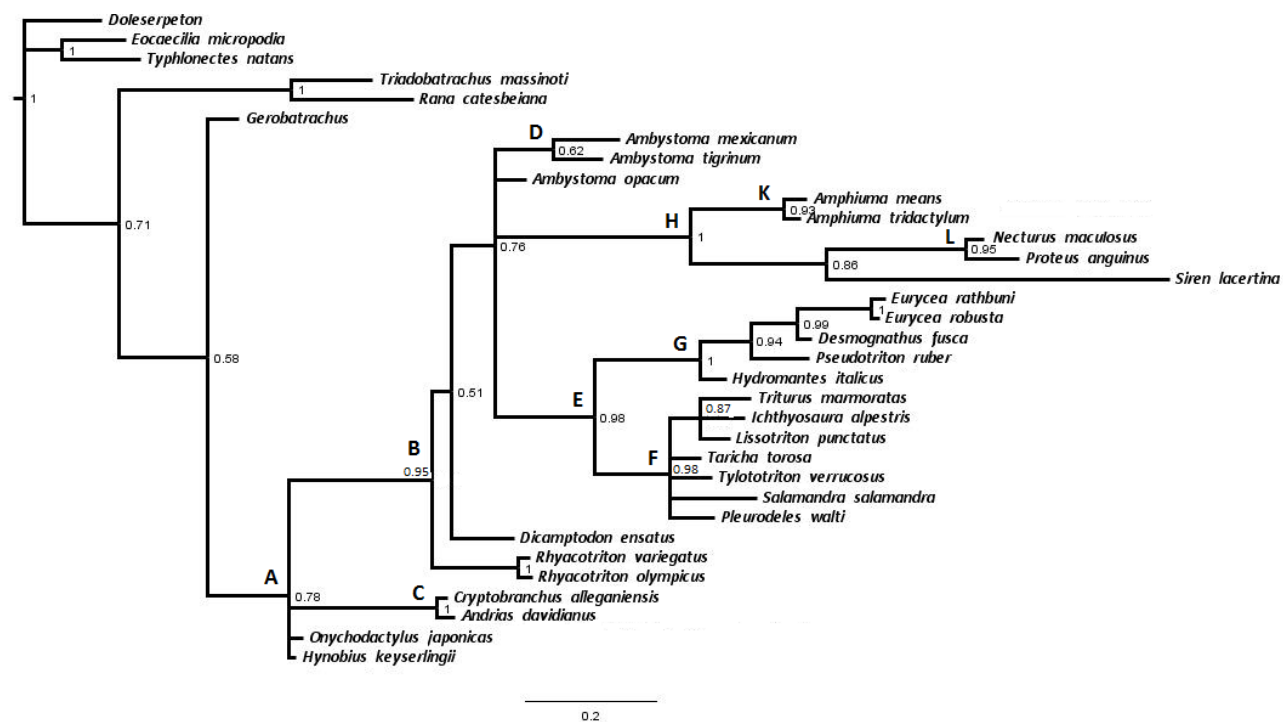


Figure 2.3.7 Bayesian analysis of the full morphological dataset including fossil outgroups. Average deviation of the split frequencies value of 0.006565 with an average ESS of 500.87 and a PSRF value of 1.001 Node values are Bayesian posterior probability percentages

The synapomorphies supporting the lettered nodes follow the format of character number (from Appendix B) followed by state A- 116:2, 117:2, 174:1; B - 153:2, 181:1, 202:1, 242:1, C - 50:1, D - 169:1, 171:1; E - 199:2, 211:1, 212:1; F - 122:2, 214:3; G - 50:3, 165:1, 214:2, 230:1, 238:1; H - 50:2, 244:1; J - 62:1, 104:3, 203:2, 223:1, 248:1; K - 232:1, 240:1

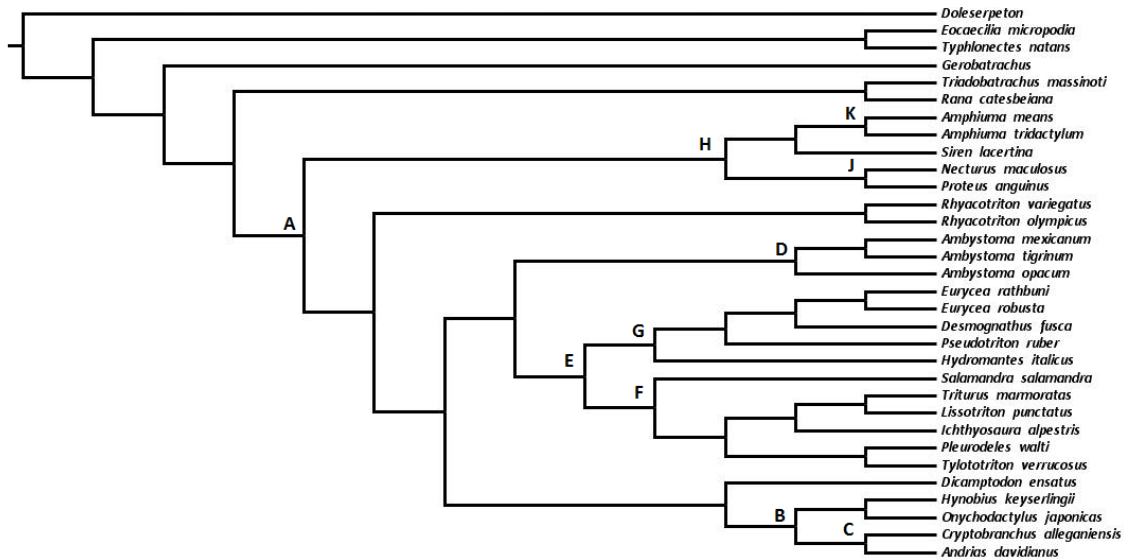


Figure 2.3.8: Agreement subtree made from the parsimony analysis of the full morphological dataset including fossil outgroups made from three MPTs, 699 steps in length CI = 0.376, RI = 0.587

The synapomorphies supporting the lettered nodes follow the format of character number (from Appendix B) followed by state A- 116:2, 117:2, 174:1; B - 153:1, 206:1; C - 50:1, D - 166:1; E - 199:2, 211:1, 212:1; F - 122:2, 214:3; G - 50:3, 165:1, 214:2, 230:1, 238:1; H - 50:2, 244:1; J - 62:1, 104:3, 203:2, 223:1, 248:1; K - 232:1, 240:1

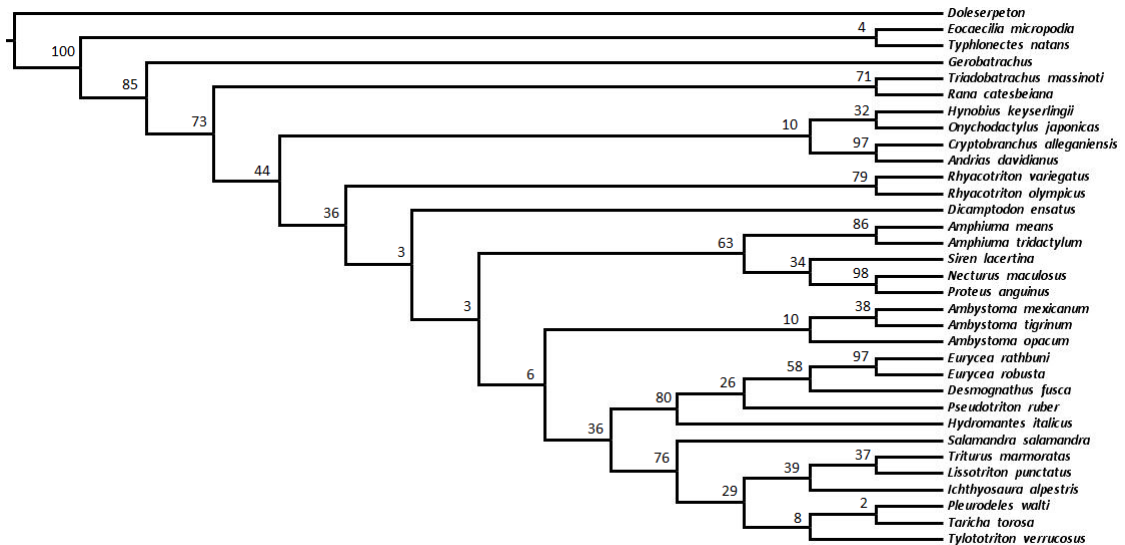


Figure 2.3.9 GC bootstrap tree of the parsimony results using the full morphological dataset including fossil outgroups (Traditional search in TNT).

The parsimony analysis resulted in a different topology to the Bayesian analysis, with the major difference is that the Cryptobranchoidea is monophyletic, but Salamandroidea is not. The Salamandridae and Plethodontidae cluster together with Ambystomatidae as their sister clade. Although Ambystomatidae is monophyletic in this tree the bootstrap support values are extremely low. *Dicamptodon* is the sister taxon to Cryptobranchoidea. The clade

formed by Amphiumidae, *Siren* and Proteidae is the same as in the Bayesian analysis the support values are far lower. The only taxon missing from the agreement subtree is one of the Salamandridae (*Taricha torosa*).

In both the Bayesian and parsimony results it is clear that there are no synapomorphies for *Rhyacotriton* or Hynobiidae. The other families (represented by more than one taxon) form monophyletic groups Figs. 2.3.7 and 2.3.8.

Combined Molecular tree vs combined Morphological tree (temnospondyl OG or ExtantOG)	Bayesian		Parsimony	
	Extant outgroups	Temnospondyl outgroups	Extant outgroups	Temnospondyl outgroups
Agreement sub-trees	7/24	8/24	9/24	8/24
Symmetric diff	29	30	37	30

Table 2.3.1: The agreement subtree and symmetric differences (Robinson–Foulds metric) results of the comparison between the full molecular tree and the morphological tree using either extant outgroups or fossil outgroups.

The Molecular tree topology was compared to the results of the Bayesian and parsimony analyses of the full morphological dataset using just extant outgroups and then also the parsimony and Bayesian trees with temnospondyl outgroups. The results show that the molecular tree (Fig. 2.3.1) shared more clades in common according to the agreement subtrees values with the parsimony morphological tree with just extant outgroups (Fig. 2.3.5) and differs the least (according to the symmetric differences test) when compared to the Bayesian results of the morphological data with just extant outgroups (Fig. 2.3.4).

2.3.2.2 Morphological phylogeny (osteological)

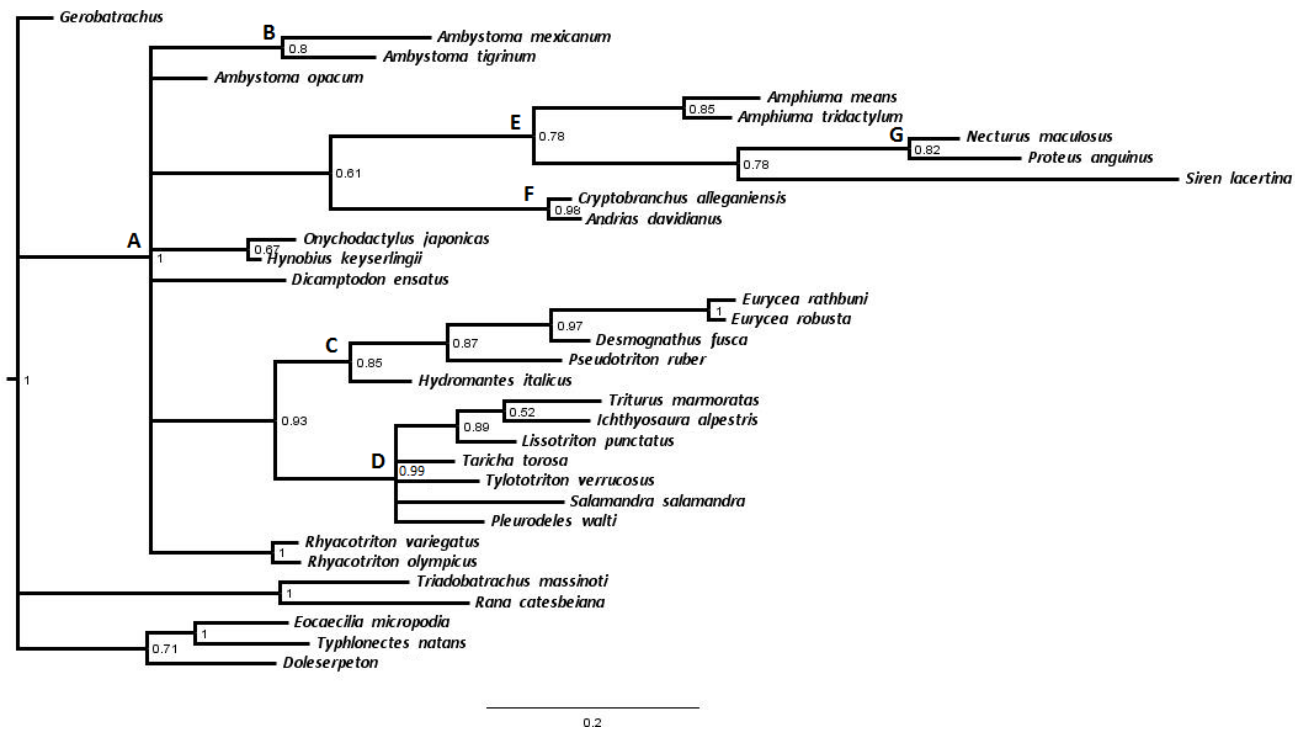


Figure 2.3.10 Bayesian analysis of the osteological characters including fossil outgroups. Average standard of split frequency value 0.004453. The average ESS value equalled 530.09 and the PSRF was 1.000. Values at the nodes are Bayesian posterior probability

The synapomorphies supporting the lettered nodes follow the format of character number (from Appendix B) followed by state: A – 30:1, 116:2, 117:2, 174:1, 174:1; B – 171:1, C – 50:3, 165:1; D – 122:2; E – 50:2; F – 50:1; G – 62:1

The tree in Fig. 2.3.10 is the result of the Bayesian analysis of the osteological characters and is less resolved than the full morphological result (Fig. 2.3.1) because it has a very large polytomy consisting of *Rhyacotriton*, (Salamandridae + Plethodontidae), *Dicamptodon*, Hynobiidae, (Cryptobranchidae + Amphiumidae + Proteidae + Sirenidae), *Ambystoma opacum*, (*Ambystoma tigrinum* + *Ambystoma mexicanum*). Sirenidae is not placed as the sister clade to all other salamanders. Cryptobranchoidea (cryptobranchids + hynobiids) is not monophyletic. *Ambystoma* is not monophyletic and there are no osteological synapomorphies for *Amphiuma* or Hynobiidae.

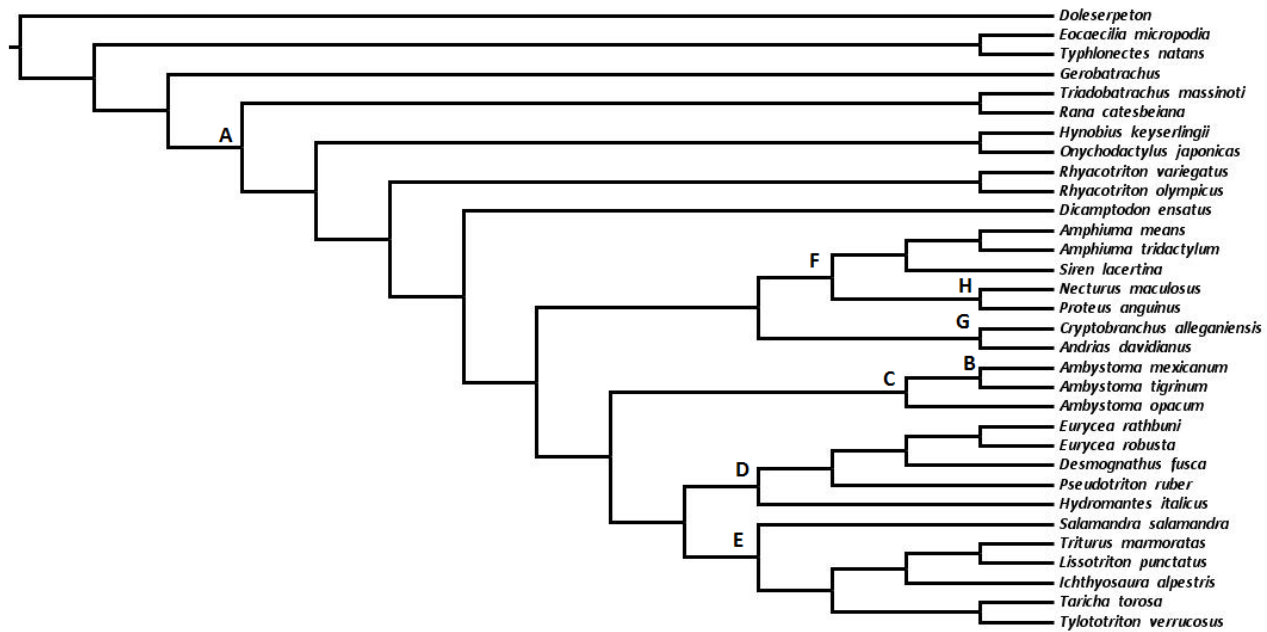


Figure 2.3.11: Agreement subtree resulting from a parsimony analysis of the osteological characters – based on two MPT both 610 steps in length CI = 0.351, RI = 0.513

The synapomorphies supporting the lettered nodes follow the format of character number (from Appendix B) followed by state: A – 30:1, 116:2, 117:2, 174:1, 174:1; B – 171:1, 169:1; C – 166:1; D – 50:3, 165:1; E – 122:2; F – 50:2; G – 50:1; H – 62:1

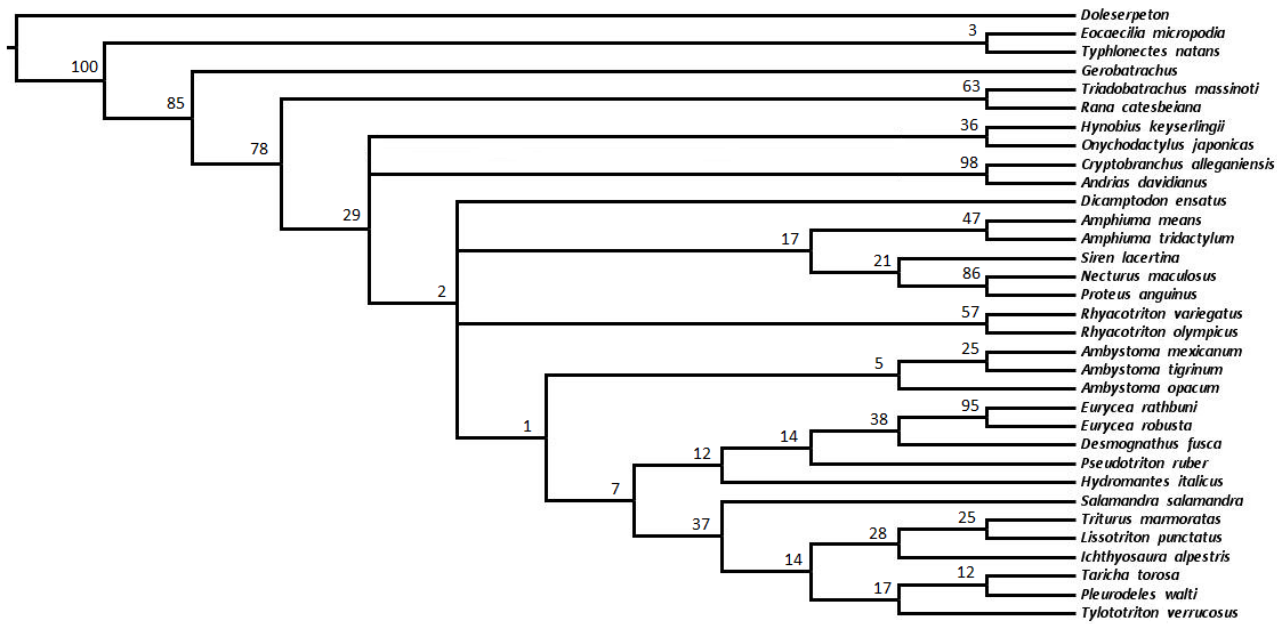


Figure 2.3.12 GC bootstrap value tree resulting from a parsimony analysis of the osteological characters (Traditional search in TNT).

The phylogeny resulting from the parsimony analysis of the osteological characters shows that Cryptobranchoidea no longer forms a clade and Hynobiidae forms the sister clade to all other salamanders. However, the bootstrap support values are extremely low throughout the tree. The only taxon missing from this agreement subtree is one of the Salamandridae (*Pleurodeles waltii*). The characters supporting the nodes are almost exactly the same as in the Bayesian results except *Ambystoma* is monophyletic and supported by common possession of spinal nerves that exit intravertebrally in some presacral vertebrae (node C, Fig. 2.3.11).

2.3.2.3 Morphological phylogeny (soft body)

The outgroup (and root) for both the Bayesian and parsimony analyses is a hypothetical all zero species. The bayesian analysis places Sirenidae in an unresolved relationship with the hypothetical outgroup and all other salamanders. The cryptobranchids and hynobiids form a monophyletic Cryptobranchoidea. Within the monophyletic Salamandroidea (excluding *Siren*), Plethodontidae forms a clade with Proteidae and *Rhyacotriton* and together they provide one branch in a polytomy with *Dicamptodon* and Ambystomatidae. Salamandridae forms the sister clade to this polytomy and Amphiumidae forms the sister clade to all other Salamandroidea.

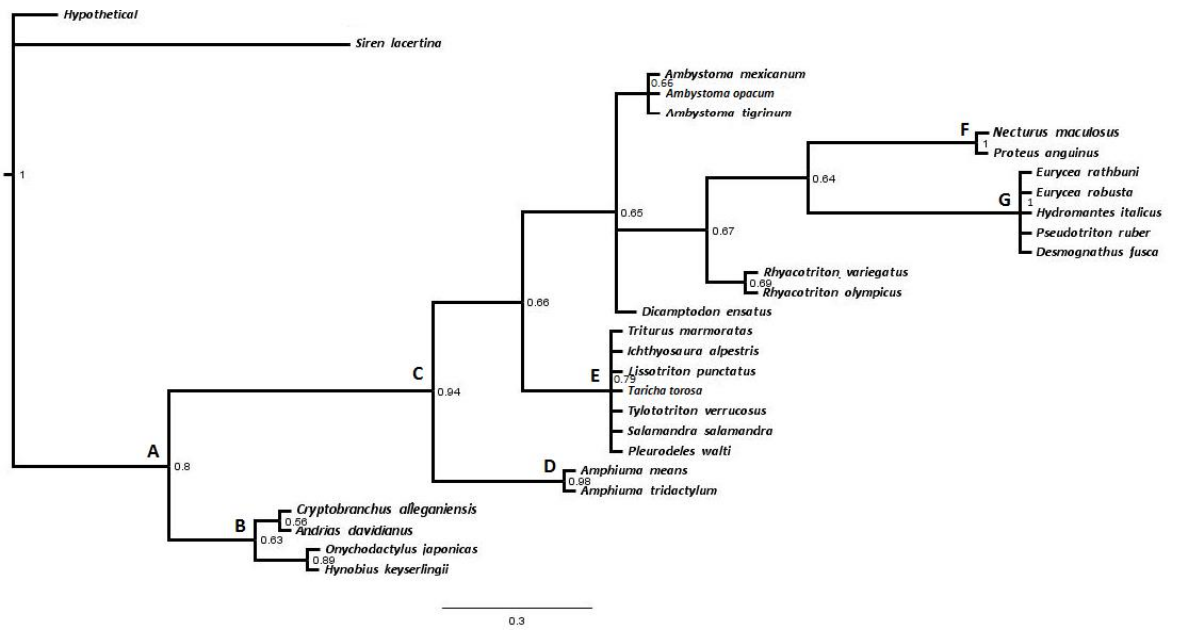


Figure 2.3.13 Bayesian analysis of the soft body characters with a hypothetical all zero outgroup. This analysis ran for 1000000 generations and reached an average standard deviation value of 0.008918. Values at the nodes are Bayesian posterior probability percentages. The synapomorphies supporting the lettered nodes follow the format of character number (from Appendix B) followed by state: A – 205:2, 207:1, 247:1; B – 201:1; C – 208:1, 235:1; 236:1, 239:1, 249:2; D – 232:1, 240:1; E – 214:3, 233:1; F – 203:2, 223:1, 248:1; G – 214:2, 230:1, 238:1

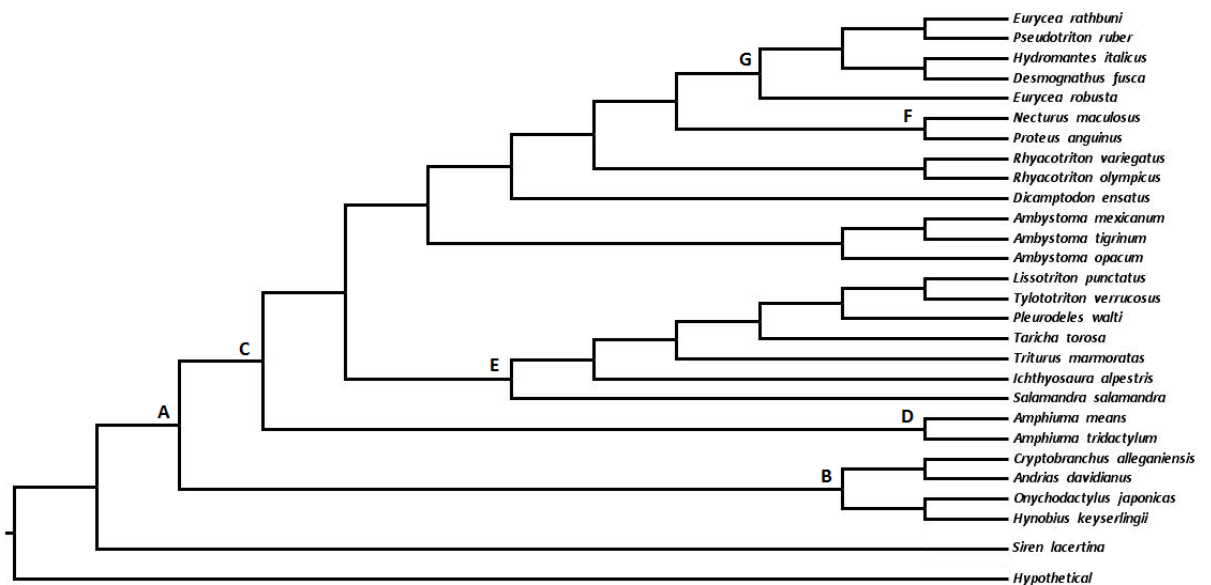


Figure 2.3.14: The most parsimonious tree resulting from parsimony analysis of the soft body characters. It is 82 steps in length CI = 0.646, RI = 0.894. The synapomorphies supporting the lettered nodes follow the format of character number (from Appendix B) followed by state: A – 205:2, 207:1, 247:1; B – 201:1; C – 208:1, 235:1; 236:1, 239:1, 249:2; D – 232:1, 240:1; E – 214:3, 233:1; F – 203:2, 223:1, 248:1; G – 214:2, 230:1, 238:1

The parsimony analysis places Sirenidae as the sister clade to all other salamanders whereas the (traditional search) bootstrap tree placed Cryptobranchioidea as the sister clade of Salamandroidea (excluding *Siren*).

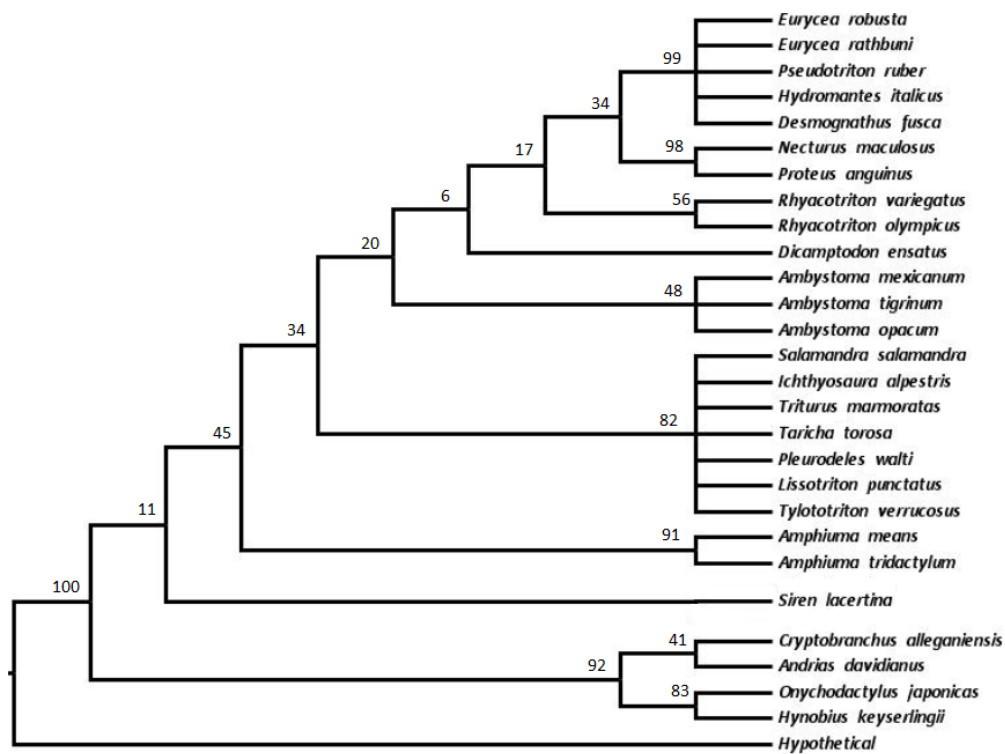


Figure 2.3.15: GC bootstrap tree of the soft body characters (Traditional search in TNT).

Molecular tree vs Osteological or Soft Body datasets	Bayesian		Parsimony	
	Osteological	Soft Body	Osteological	Soft Body
Agreement sub-trees	7/24	11/24	15/24	11/24
Symmetric diff	21	17	20	17

Table 2.3.2 The agreement subtree and symmetric differences (Robinson–Foulds metric) between the combined molecular tree and osteological and soft body trees.

The molecular tree topology (Fig. 2.3.1) was compared to the results of the Bayesian and parsimony analyses of the osteological and soft body morphological datasets. The results show that the molecular tree shared more clades in common according to the agreement subtree when compared to the parsimony result of the osteological only data (Figs. 2.3.11) than the Bayesian and parsimony soft body morphological trees and the Bayesian Osteological tree (Figs. 2.3.13, 2.3.14, and 2.3.10). The molecular tree differs less (according to the symmetric differences test) with the soft body trees in both the parsimony and Bayesian results (Figs. 2.3.13 and 2.3.14) when compared to the osteological results.

2.3.3 Molecular and Morphological data

2.3.3.1 Combined molecular data with all morphological data

This total evidence analysis places salamanders, frogs and caecilians each as monophyletic. However, the relationship between the amphibian clades places the frogs as sister clade to all other taxa except *Latimeria* (which was constrained as the root taxa). Caecilians are more closely related to all the other outgroup taxa than with the other amphibian groups. The relationships between the salamander families in the combined data results exactly matches the relationships in the molecular tree (Fig 2.3.1).

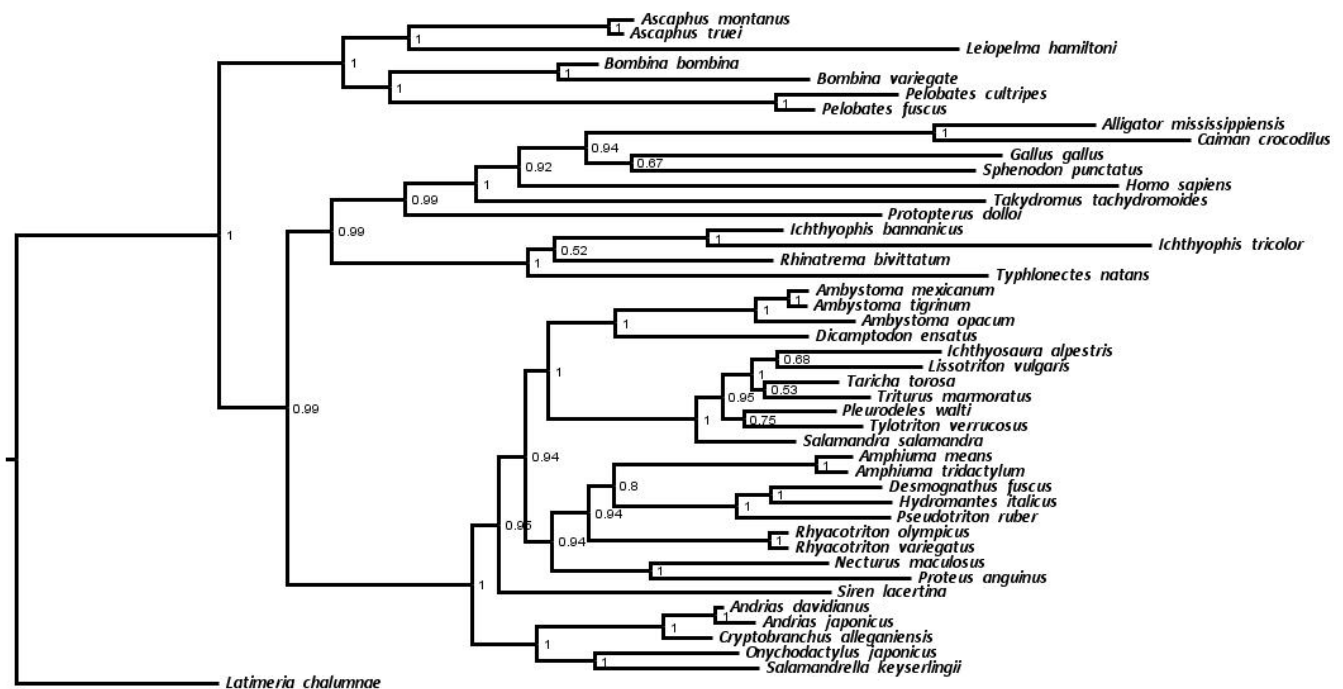


Figure 2.3.16 Bayesian analysis of the combined molecular and morphological datasets. Both extant and fossil outgroups were included. This analysis ran for 1468000 generations and reached an average standard deviation of the split frequencies value of 0.007414. Values at the nodes are Bayesian posterior probability percentage.

2.4 Discussion

2.4.1 Molecular discussion

The analysis presented here resulted in a molecular phylogeny, using eleven genes, which (Fig. 2.3.1) places salamanders, frogs and caecilians as more closely to one another than any one of them is to either fish or amniotes supporting previous studies (e.g. Parker 1956;

Lombard and Bolt 1979; Gardiner 1982; Gardiner 1983; Milner 1988; Bolt 1991; Roelants *et al.* (2007). This study also finds support for the Batrachia clade of salamanders plus frogs with caecilians as the sister clade to Batrachia in agreement with Benton (1990), San Mauro *et al.* (2010), Zhang *et al.* (2005), Roelants *et al.* (2007), Zhang and Wake (2009), San Mauro (2010), Pyron (2011) and Skutschas and Martin (2011).

This study's molecular results placed Cryptobranchidae and Hynobiidae together to form a monophyletic Cryptobranchoidea which agrees with previously published topologies such as Estes (1981), Frost *et al.* (2006), Wang and Evans (2006), Roelants *et al.* (2007), Vieites *et al.* (2009), Zhang *et al.* (2009) and Gao and Shubin (2012). The rest of the salamander families in this study form a monophyletic Salamandroidea clade which includes Sirenidae as found in Wiens *et al.* (2005), Frost *et al.* (2006), Roelants *et al.* (2007), Vieites *et al.* (2009), Pyron and Wiens (2011) and Gao and Shubin (2012).

Within the Salamandroidea there seems to be evidence supporting the stable relationship between Ambystomatidae + Dicamptodontidae as seen in previous studies such as Larson and Dimmick (1993), Chippindale *et al.* (2004), Wiens *et al.* (2005), Cannatella *et al.* (2009), Pyron and Wiens (2011). Plethodontidae is more closely related to *Amphiuma* with *Rhyacotriton* as their sister taxon which is consistent with the findings of Wiens *et al.* (2005), Frost *et al.* (2006), Roelants *et al.* (2007) and Pyron and Wiens (2011). Sirenidae is placed as the sister taxon to the internally fertilising Salamandroidea. (Hay *et al.* 1995; Wiens *et al.* 2005; Wang and Evans 2006; Roelants *et al.* 2007; Vieites *et al.* 2009; Zhang *et al.* 2009; Gao and Shubin 2012)

To further test the origins of the molecular phylogenetic signal, the molecular data were divided up and analysed to obtain a phylogeny made from nuclear genes and a separate phylogeny derived from mitochondrial genes. The results showed that there is a different signal from each of the different types of molecular data.

The nuclear DNA phylogeny still supports Batrachia with Caecilia as its sister clade, however there is no resolution that places salamanders as monophyletic. Cryptobranchoidea is not supported and neither is Salamandroidea, which is contrary to previous studies that have supported the monophyly of salamanders and frogs within Batrachia. The nodes in this phylogeny have low support values, and there is very little internal resolution of familial relationships.

The mitochondrial DNA generates a phylogeny that has the internal familial salamander relationships that resemble the full molecular result in this study and agrees with

early studies by e.g., Hay *et al.* in 1995 which placed frogs as the sister clade to salamanders + caecilians. Both the monophyly of Cryptobranchoidea and Salamandroidea are supported in this phylogeny.

It seems that the mitochondrial DNA results give a more resolved internal phylogeny with fewer polytomies than the tree produced by the nuclear DNA. This is in line with Zhang *et al.* (2009) as they posited that mitochondrial DNA would be able to resolve phylogenies with deep nodes despite saturation issues. However, the Batrachia clade is unsupported which reflects earlier studies (Hay *et al.* 1995) but is contrary to later studies which find support for Batrachia (Benton, 1990, San Mauro *et al.* 2010, Zhang *et al.* 2005, Roelants *et al.* 2007, Zhang and Wake 2009, San Mauro 2010, Pyron 2011 and Skutschas and Martin 2011).

2.4.2 Morphological discussion

The initial analysis using just the extant outgroup taxa produced an unresolved salamander phylogeny in MrBayes with neither Cryptobranchidae nor Sirenidae forming the sister clade to all other salamanders contrary to the molecular results. The only family that does not emerge as monophyletic is Ambystomatidae, however *Ambystoma opacum* has a completely different life history to other *Ambystoma* species and lays its eggs on dry land as opposed to laying eggs in water like the other members of that Family (Nussbaum 1985). This difference in habitat might produce varying superficial morphological characters from the other taxa in the genus. Both *Ambystoma tigrinum* and *Ambystoma mexicanum* share an overlapping procoracoid and coracoid and a suprascapula that is not expanded in width (characters 169 and 171 in Appendix B) however all the *Ambystoma* species in this study share spinal nerves that exit intravertebrally in some presacral vertebrae. This suggests that vertebral characters (specifically spinal nerve foramina characters) are especially useful in supporting monophyletic groups using purely morphological data in salamanders. *Ambystoma opacum* was included in this study to provide additional congruence with the taxon lists of previous studies. Cryptobranchidae emerges as monophyletic but with very poor posterior probability support whereas the plethodontid + salamandrid sister group relationship receives high support.

In order to include fossils in the morphological data analysis, additional fossil outgroups had to be incorporated so that the fossils could fall on the stem of salamanders. The resultant phylogenies which include two temnospondyls, *Gerobatrachus hottoni* and *Doleserpeton annectens* (Figs 2.3.7 and 2.3.8), show better resolution within salamanders as

there are fewer polytomies. However, cryptobranchids and hynobiids no longer group within a monophyletic Cryptobranchoidea in the Bayesian result, and Cryptobranchoidea was weakly supported in the parsimony analysis but no longer forms the sister clade to all other salamanders. The agreement subtree and symmetric difference analyses suggest that there are fewer clades in common (and more differences) between the morphological tree using fossil outgroups than there are with the tree using just extant outgroups in both the parsimony and Bayesian results respectively. However, in order to incorporate fossil taxa, which may fall outside of the salamander crown clade (Urodela), these fossil outgroups will be used in further analysis.

It has been proposed that phylogenies based on soft part characters are more accurate (i.e. are more congruent with molecular phylogenies) than are those based on osteological data (Gibbs *et al.* 2000). This was tested here by examining the phylogenetic signal of the two different morphological datasets independently.

The osteological dataset resulted in a Bayesian tree topology that somewhat resembles the total morphological dataset. The monophyly of Cryptobranchoidea is not supported, and the monophyly of Hynobiidae has low support from Bayesian posterior probability. Salamandridae and Plethodontidae are still placed as sister taxa in the total morphological dataset. The monophyly of the Amphiumidae + Sirenidae + Proteidae clade is also still well supported. The parsimony analysis shows a similar result to the Bayesian tree, with Cryptobranchidae as the sister clade to Proteidae + Sirenidae + Amphiumidae. However, Hynobiidae is placed as the sister clade to all other salamanders.

In contrast the soft body topology of the Bayesian analysis (with a hypothetical all zero outgroup) shows a very different result (Fig. 2.3.13). Sirenidae is placed as the sister clade to all other salamanders and Cryptobranchoidea and Salamandroidea are found to be monophyletic, although the monophyly of Cryptobranchidae does not have very strong support. This is the case in both the Bayesian and parsimony results.

The results of the agreement subtree analysis show there is less congruence between the molecular tree (Fig. 2.3.1) and the soft body trees (Fig. 2.3.14 and 2.3.13) than between the molecular tree and the osteological tree (Fig. 2.3.11). However, the results of the symmetric differences analyses shows there is more congruence between the molecular tree and the soft body trees in both the parsimony and Bayesian results when compared to the osteological results. The soft body phylogeny is more resolved with fewer polytomies than the osteological tree even though there are only 52 characters in the soft body dataset and 197 characters in the osteological dataset. This might mean that the osteological dataset is more

prone to homoplasy. The next results chapter will investigate homoplasy in the morphological characters and what this might mean for fitting fossils into a phylogeny.

2.4.3 Total evidence discussion

The total evidence analysis, with the fossil outgroups included, resulted in less resolution of the relationships between the outgroup taxa. Both the frog and caecilian clades were placed in positions not supported by previous studies (Fig. 2.3.16). However, the internal familial relationship of the salamanders reflects the relationships exhibited in the full molecular results. It was shown in the earlier morphological analysis that the use of molecular data was sufficient to produce a consensus tree that found support for the monophyly of both the Batrachia and Amphibia. However, it is clear that the inclusion of morphological data had decreased resolution of amphibian relationships. Thus it is the total evidence consensus tree that shows that further work is needed to dissect the signal within the morphological data so that fossils can be included with confidence.

2.5 Conclusions

A monophyletic Batrachia (salamanders + frogs) is supported as is a monophyletic Lissamphibian (with caecilians placed as the sister taxon to Batrachia) within the molecular results. Within salamanders some consensus has been reached with the externally fertilising salamanders (i.e., Cryptobranchoidea) generally supported as monophyletic and as the sister clade to all other salamanders. Salamandroidea, including Sirenidae, is also found to be monophyletic. It is clear that there are many different signals emerging from different data types i.e., molecular vs morphological but also from within each data type i.e., mitochondrial DNA vs nuclear DNA and osteological characters vs soft body characters. The analysis using the nuclear dataset seemed to yield a more coherent tree that was consistent with the results produced by previous studies i.e a monophyletic Batrachia (Larson and Dimmick 1993; Chippindale *et al.* 2004; Wiens *et al.* 2005; Frost *et al.* 2006; Zhang and Wake 2009). The results presented in this study highlights that caution should be taken when selecting genes and choosing just mitochondrial or just nuclear genes in future molecular analyses of salamanders.

There is still little congruence between the molecular and morphological results except for the monophyly of Cryptobranchoidea which can be seen in both the molecular and some of the morphological trees. The soft body characters did not produce a tree that was significantly more similar to the molecular tree (in this study) than the osteological tree was to the molecular tree.

In conclusion, there are still issues with the morphological data as the characters do not yet resolve the interfamilial relationships as well as the molecular data. There are also inconsistencies between the parsimony and Bayesian analyses. This may be due to convergence in morphological data influencing the parsimony analyses more than the Bayesian analyses. In order to place fossils within this morphological framework, with confidence, further investigation into the morphological dataset is required, specifically the robustness of characters (a topic covered in Chapter 3).

3. Testing a morphological dataset – a new method for estimating confidence in fossil placement within a phylogeny

3.1 Introduction

3.1.1 Homology within the dataset

It has long been known that data are particularly susceptible to convergent evolution and with morphology, it really depends on character atomisation, sample size, and other factors that might create errors in phylogenetic analysis (Hedges and Sibley 1994; McCracken *et al.* 1999). Parsimony analyses assume that convergence is not an issue a priori (Wiley and Lieberman 2011), but in many cases (including salamanders) convergence has a strong influence on phylogenetic analysis that needs to be taken into account. Wiens *et al.* (2003) suggested that certain criteria need to be taken into account to establish if a phylogenetic analysis has been compromised by convergent characters.

These criteria are; characters that support the membership of the convergent clade are associated with the selective pressures of the shared environment, and a convergent clade which is supported with morphological characters but are unsupported in two or more unlinked molecular analyses.

A test of the robustness of the salamander morphological data was published by Wiens *et al.* (2005) which made it clear that there are issues of convergence associated with the salamander dataset. However, despite the possibility of convergence influencing the resultant phylogeny, morphological characters are still the only way to incorporate fossil salamanders. This study will try to identify the convergent characters that support relationships and then test the accuracy of the placement of simulated fossils using characters that display the least homoplasy.

3.1.2 Problems with fitting fossils

The identification of shared characters (synapomorphies) is the basis on which evolutionary analysis ultimately rests. Our view of the fossil record is obscured by the fact that most organisms are not preserved and those few that are fossilised are never complete (Sansom *et al.* 2010). The information used to facilitate a fossil's incorporation into any matrix depends on the amount of decay it underwent and speed of fossilisation. The process of decay and preservation might distort characteristics and the results of subsequent phylogenetic analyses (Donoghue and Purnell 2009).

Many fossil salamanders are known only from isolated vertebral elements. The earliest known salamanders, the Middle Jurassic *Marmorerpeton* and *Kokartus* are known mostly from atlantal and vertebral elements (Evans *et al.* 1988). In the Cretaceous record of North America salamander fossil record consists for the most part of fragmentary vertebral elements from *Habrosaurus*, *Lisserpeton*, *Opisthotriton*, *Proamphiuma*, and *Piceoerpeton*. The vertebral structure is thought to be constant within families and therefore it may help decipher relationships between families (Naylor 1979). This might be enough to place a fossil if extant salamander representatives are included. Simulating fossils that reflect the paucity of the actual salamander fossil record and including them in the analyses allows assessment of the confidence with which we can place real fossils.

The main aims of this study are to identify the convergent characters in the morphological dataset by using both tree dependent and tree independent methods of character evaluation. Once the highly convergent characters are removed, the resulting reduced character set will be analysed by including simulated fossils into the matrix and observing their placement relative to the known placement of the simulated fossil taxa.

3.2 Material and Methods

3.2.1 Tree dependent character evaluation

3.2.1.1 Retention Index

The Retention Index (ri) is a tree-dependent method of character evaluation and gives an indication of how well synapomorphies explain the given phylogenetic tree. By comparing the observed and expected number of changes for each character in a tree an ri value can be calculated. If the minimum amount of changes observed in a character is the minimum amount possible for the given tree then $ri = 1$, indicating that it is a perfect synapomorphy (Farris 1989; Egan 2006).

A starting tree was constrained to reflect the results of previous analysis of the full morphological dataset in this study (Fig 2.3.4, see also Fig. 3.1) and was then exported together with the data matrix to Mesquite (version 3.0) (Maddison 2008). The *Cryptobranchoidea* was placed as sister taxon to all other salamanders to reflect the growing consensus mentioned in Chapter 1. The internal family relationships remain largely unresolved as this study is interested in assessing the inter-clade relationships. The retention index for each character was calculated using the 'Parsimony Statistics' function. With the starting tree

open in the viewing window, the 'Values for Current Tree' option was used. As the ri value increases towards one, the better the character fits the tree. The characters with an ri of 0.5 or higher were kept in the matrix and those that did not reach this threshold were discarded as homoplasious. This resulted in a dataset consisting of 122 characters which will hereafter be referred to as the RI dataset (Appendix E).

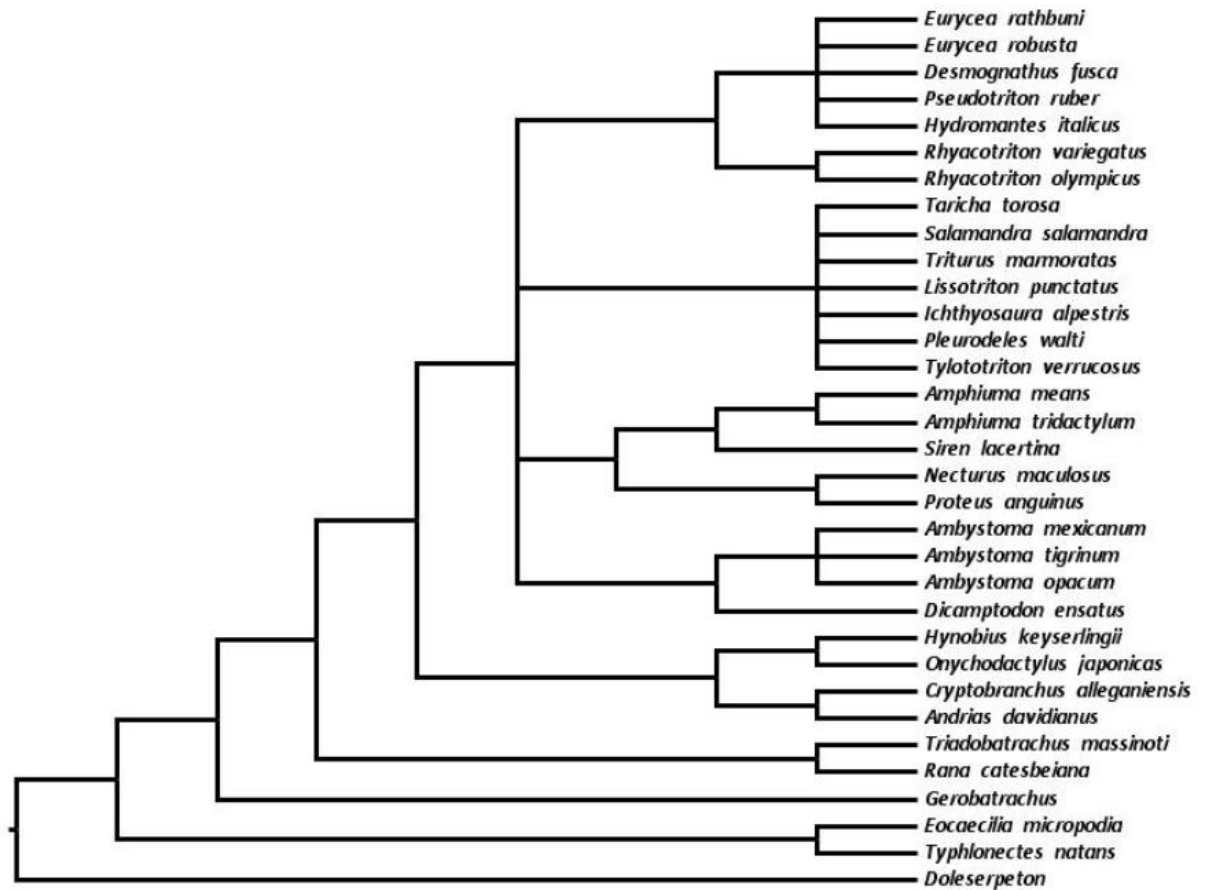


Figure 3.1: The constrained tree reflecting the uncertain relationships between the salamander families, used to find the retention index for the tree dependant character evaluation analysis

3.2.1.2 RI dataset

After the tree-dependent character evaluation methods was applied to the full morphological dataset (Appendix B) the reduced RI character set (Appendix E) retained 42 out of 99 skull characters, 9 out of 22 atlantal characters, 12 out of the 20 presacral vertebrae characters, 5 out of 11 caudal vertebrae characters, 3 out of 10 rib characters, all 4 spinal nerve characters, 8 out of 17 pectoral girdle characters, only 1 of the 14 pelvic girdle characters and 38 of the 52 soft body characters.

3.2.2 Tree independent character evaluation

3.2.2.1 Le Quesne Probability randomisation test

Le Quesne (1969) proposed a method for finding the probability that a character's features were distributed independently, and at random, among taxa of a given data matrix (Lequesne 1969, 1972; Sober 1994). The Le Quesne probability randomisation test was applied to the data in this study, to test that the characters were no less incompatible with the other characters in the data than a random character (Wilkinson 1997, 2001). This is a tree independent method that assesses character fit in comparison with the other characters, and compared to the fit of a random character. The analysis was performed using the free software PICA version 4.0 (Wilkinson 2001). All the ordered multistate characters (16 characters) were recoded into binary states and linked using the 'codes' function in each analysis. This was done by breaking down each multistate ordered character into multiple individual characters so that the sum of the new states in binary characters equal the original multistate character (Table 3.1 below). Polymorphic characters were recoded as unknown (i.e. ?). The data included 33 taxa with six of those designated as outgroup taxa (*Doleserpeton*, *Triadobatrachus*, *Eocaecilia*, *Gerobatrachus*, *Rana* and *Typhlonectes*). 265 Characters were included (the original 249 characters inflated to 265 as a result of the binary recoding) and 999 random character permutations were run.

A lack of compatibility i.e. the actual number of steps per character being greater than expected, may indicate homoplasy. So a "boil down" method of character assessment and removal was implemented. In the first round all the characters that had a higher number of incompatibilities observed relative to the number that were expected were removed from the analysis. The reduced dataset (173 characters) was run through PICA again and the results were filtered to remove all characters that had a Le Quesne probability higher than 0.1. A Le Quesne probability of 0.1 was recommended by the author as a threshold to remove characters that were demonstrating convergence but not the characters that might show true biological relationships. The result was a dataset with 105 characters which, after a final run through PICA, and a further removal of four more characters, identified a final list of 101 characters used in the analyses. This reduced dataset was analysed in exactly the same way as the full morphological dataset was in the previous chapter 2. GC bootstrap support values were calculated with TNT using 1000 replicates in a Traditional Search framework.

	Original multistate coding	=	New binary character state 1	New binary character state 2	New binary character state 3	Sum of character states of new binary characters
Species A	0	=	0	0	0	0
Species B	1	=	1	0	0	1
Species C	2	=	1	1	0	2
Species D	3	=	1	1	1	3

Table 3.1: Example of binary recoding of one ordered multistate character consisting of one characters with four states between four taxa that share this character.

3.2.2.2 The Le Quesne dataset

The Le Quesne character set (Appendix F) is made up of 31 out of 99 skull characters, five out of 22 atlas characters, six out of the 20 presacral vertebrae, two out of 11 caudal vertebrae characters, three out of 10 rib characters, all four spinal nerve characters, six out of 17 pectoral girdle characters, only one of the 14 pelvic girdle characters and 38 of the 52 soft body characters.

3.2.2.3 Tree comparison statistics

Trees were compared in a number of ways. Agreement subtrees test the similarity of topology by depicting relationships among groups of taxa that branch identically in two or more trees. Paup version 4.0 (Swofford 2003) returns a ratio for the similarity as it counts the number of similar nodes in each tree compared to the total number of nodes. Robinson-Foulds (RF) metric (symmetric differences) (Robinson and Foulds 1981) calculates the sum of the number of partitions of data implied by the first tree but not the second tree and the number of partitions of data implied by the second tree but not the first tree. This additional measure of the differences in topology of two trees was used to further test the similarity of different phylogenetic results. Outgroups were removed and the datasets reduced to their lowest common taxa set before being imported into PAUP.

3.2.2.4 Simulating fossils

The full morphological dataset of 249 characters is made up of 197 skeletal and 52 soft body and behavioural characters (as described in the Materials and Methods section of chapter 2). Fossils rarely have soft body parts preserved and therefore only have a chance to score up to about 80% of the characters due to preservational bias (Sansom *et al.* 2010 and Sansom and Wills 2013). However, in real life this is rarely the case as the entire skeleton is not always preserved. Even fully articulated skeletons lose some information because the internal structure of the vertebral centrum and braincase, and articulation surfaces are usually unavailable for study.

For this study simulated fossils were made up using just characters of the presacral vertebrae and atlas. These are characters commonly found in fragmentary, disarticulated specimens and provide a realistic simulation of the completeness of character scoring available in typical fossil deposits. This simulation was applied to selected extant taxa, each with a known place in the salamander phylogeny, based on molecular data. Then the morphological dataset was analysed using both Parsimony and Bayesian methods to observe the placement of the artificially reduced character set of the “fossil” taxa. If the simulated fossils were placed in their expected position within the phylogeny, then we can be reasonably confident in the placement of actual fossils. In this way the robustness of the morphological dataset can be explored and its strengths and weaknesses assessed.

Further tests of the reduced RI dataset were performed with a reduced taxic selection. The study presented here also considers the result of the stem-ward slippage effect on salamander data. As in the previous analyses, the placement of simulated fossils is tested, but this time no extant relatives of the simulated fossil were included. This might shed light on the placement of fossils that have no obvious affinities to modern salamander families.

3.3 Results

3.3.1 Tree dependent phylogeny results

Bayesian result:

The tree (Fig. 3.3) shows the results of the Bayesian analysis of the reduced morphological dataset, once the characters with an RI value below 0.5 were removed. Cryptobranchoidea and Salamandroidea are both monophyletic. Amphiumidae is

monophyletic but Hynobiidae is not. Sirenidae is more closely related to Amphiumidae than either is to Proteidae but together they still form a monophyletic group.

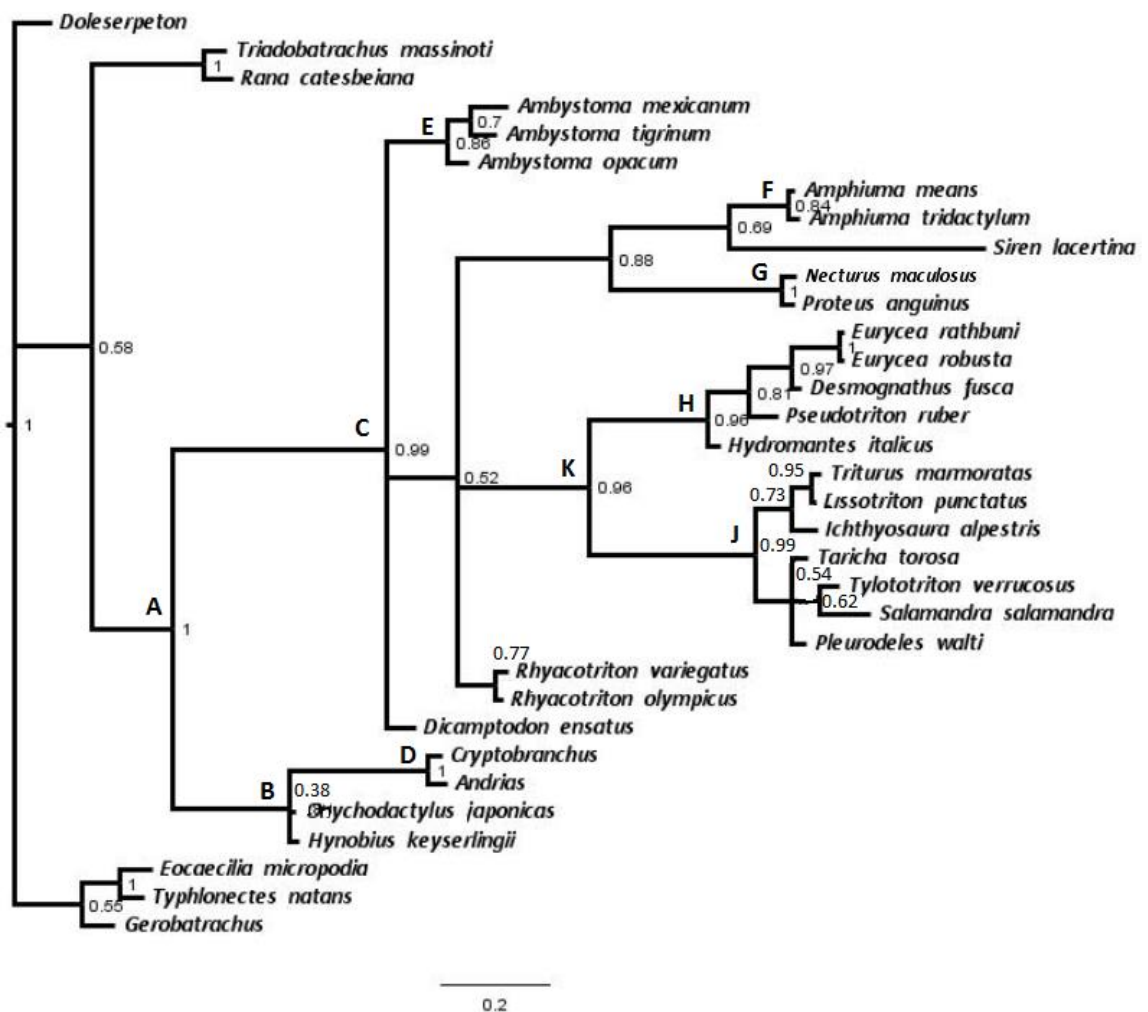


Figure 3.3: Bayesian analysis of the RI morphological dataset. Consensus tree from a Bayesian analysis that ran for 2000000 generations; Average standard deviation of the split frequency value: 0.004980; av ESS: 636.05; PSRF+: 1.000

The following synapomorphies support the following clades:

A - Urodela is characterised by possessing a fully enclosed atlantal spinal nerve foramen, four faceted articulation of exoccipital and atlas present, and loss of quadratojugal.

B - Cryptobranchoidea all share 2-3 pairs of ribs on anterior caudal vertebrae, and uncapitate ribs (Including 1 of characters 111, 112, 92, and 88 – See Appendix E)

C - Salamandroidea in this study share one central element in manus, and free ribs absent on anterior caudal vertebrae (in addition to sharing state 1 of character 89, and 117 - See Appendix E)

D - Cryptobranchidae in this study share no derived features.

Sirenidae differ from all other Urodela by possessing between 40 and 55 diploid chromosomes

E - *Ambystoma* have a Meckel's cartilage that extends to the mandibular symphysis, spinal nerve exits intravertebrally in some presacral vertebrae, and *Ambystoma mexicanum* and *Ambystoma tigrinum* share a suprascapula that is not expanded.

F - *Amphiuma* are characterised by presence of amphiumid pit glands and the presence of additional female cloacal glands.

G - Proteidae is characterised by having 19 haploid chromosomes, more than ten pairs of rugae in the male cloaca, two pairs of larval gill slits, and prootic-exoccipital fused, separate opisthotic.

H - Plethodontidae all share the presence of caudal pelvic glands, presence of a common tube to the spermathecae, laterally and posteriorly replacement pattern of vomerine teeth, dorsal and ventral roots of presacral vertebrae that exit through separate foramina, and loss of pterygoid.

J - Salamandridae all share medial pattern of vomerine teeth replacement.

K - Plethodontidae and Salamandridae are placed together because they share a small periotic cistern, presence of fibrous connective tissue around amphibian periotic canal, and periotic canal with one or more flexures.

Parsimony result:

The Parsimony analysis of the RI dataset results in a similar topology to the Bayesian analysis. Cryptobranchoidea and Salamandroidea are both monophyletic. Within the first, both Hynobiidae and Cryptobranchidae are monophyletic. Salamandroidea is made up of (Sirenidae + Amphiumidae + Proteidae + *Rhyacotriton*), (Ambystomatidae + *Dicamptodon*), and (Plethodontidae + Salamandridae) in an unresolved trichotomy. The only taxa not included in the agreement subtree are two of the Salamandridae (*Taricha torosa* and *Tylotriton verrucosus*).

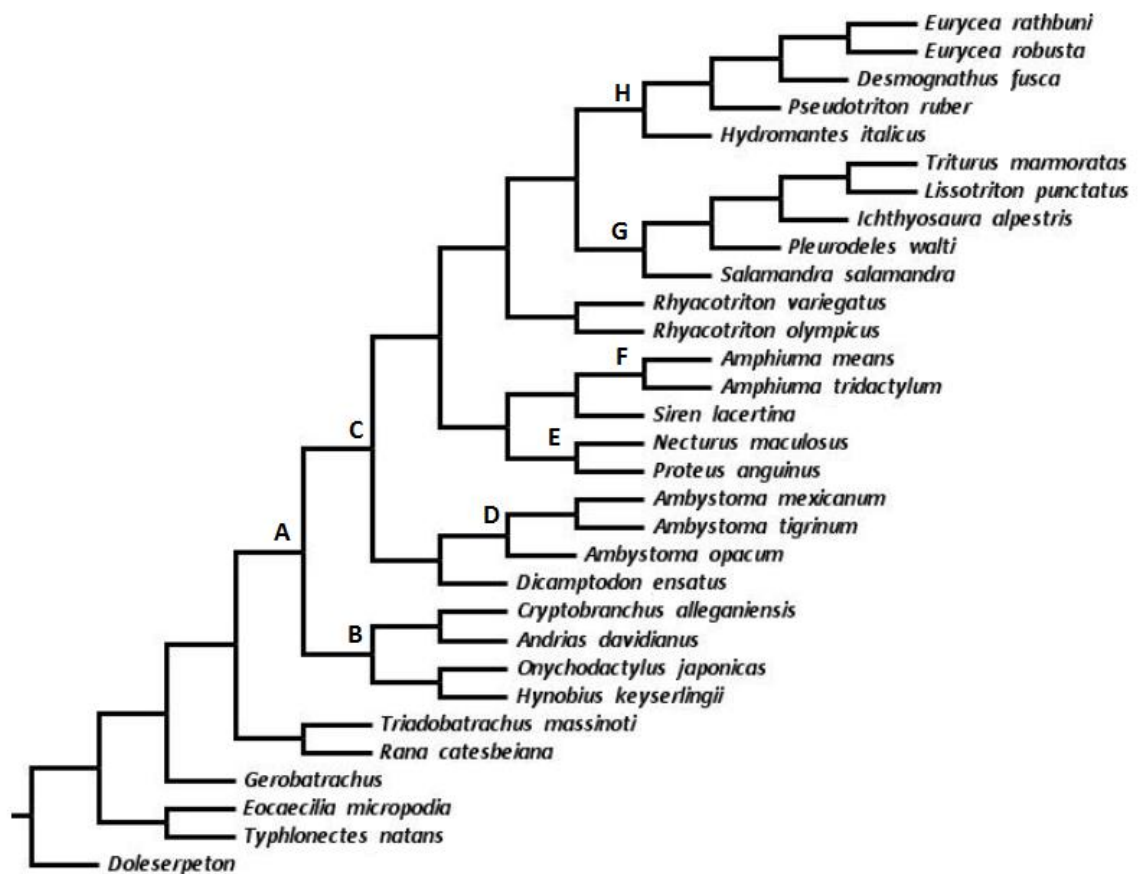


Figure 3.4: Parsimony analysis of the RI morphological dataset. Agreement sub-tree made of two MPT each 338 steps in length CI = 0.44, RI = 0.74

The following synapomorphies support the following clades (Appendix F):

- A** - Urodela have four-faceted articulation of the exoccipital and atlas, and fully enclosed spinal nerve foramen in atlas.
- B** - Cryptobranchoidea have two to three pairs of ribs on anterior caudal vertebrae, and fusion of first hypobranchial and first ceratobranchial.
- C** - Salamandroidea have free ribs absent on anterior caudal vertebrae, one central element in manus, first hypobranchial and first ceratobranchial separate, absence of second ceratobranchial, pubotibialis and puboischiotibialis as separate muscles, less than 40 diploid chromosomes, and an incomplete lateral wall of nasal capsule.
- D** - *Ambystoma* all share spinal nerves that exit intravertebrally in some presacral vertebrae, but *Ambystoma tigrinum* and *Ambystoma mexicanum* share a suprascapula which is expanded, about same width as dorsal width of scapula to the exclusion of *Ambystoma opacum*.
- E** - Proteidae share two pairs of larval gill slits, more than ten pairs of rugae in the male cloaca, and 19 haploid chromosomes.
- F** - *Amphiuma* share presence of amphiumid pit glands and the presence of additional female cloacal glands.
- G** - Salamandridae share medial vomerine dentition pattern
- H** - Plethodontidae share dorsal and ventral roots of presacral vertebrae exit through separate foramina, both laterally and posterior vomerine dentition, presence of caudal pelvic glands, presence of a common tube to the spermathecae.

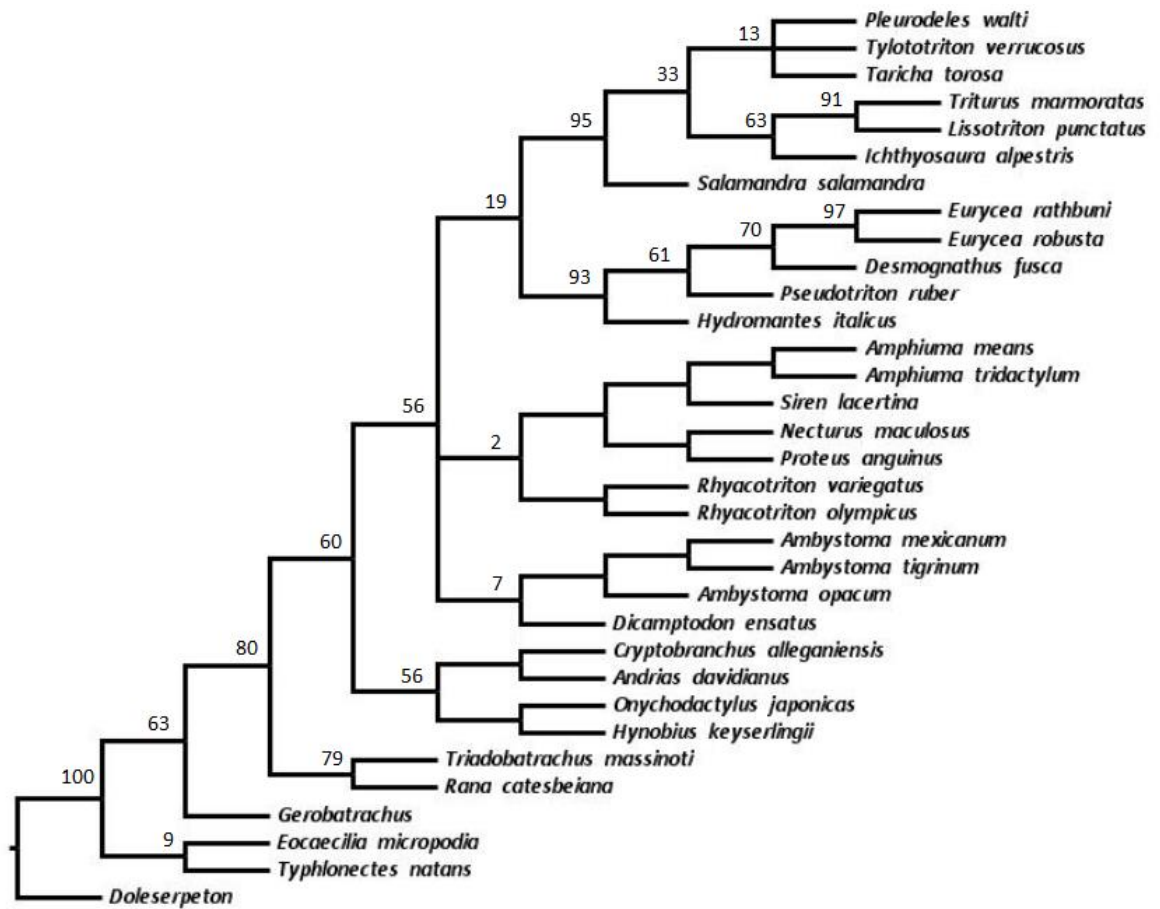


Figure 3.5: GC bootstrap values for the Parsimony analysis of the RI morphological dataset with traditional search option.

The Parsimony analysis of the RI dataset results in a similar topology to the Bayesian analysis. Cryptobranchoidea and Salamandroidea are both monophyletic. Within the first, both Hynobiidae and Cryptobranchidae are monophyletic. Salamandroidea is made up of (Sirenidae + Amphiumidae + Proteidae + *Rhyacotriton*), (Ambystomatidae + *Dicamptodon*), and (Plethodontidae + Salamandridae) in an unresolved trichotomy. The only taxa not included in the agreement subtree are two of the Salamandridae (*Taricha torosa* and *Tylostrotion verrucosus*).

3.3.2 Tree independent results

Bayesian Result:

The Bayesian analysis of the Le Quesne morphological dataset (Fig. 3.6) results in a tree that looks similar to the full morphological tree (Fig. 2.3.7). The Cryptobranchoidea and Salamandroidea are both monophyletic with the Cryptobranchoidea as the sister clade to other salamanders (Salamandroidea). The other families are all monophyletic except for

Ambystomatidae where the position of *Ambystoma opacum* is unresolved in relation to Salamandridae + Plethodontidae and the other two *Ambystoma* species, and Hynobiidae which forms part of an unresolved relationship with Cryptobranchidae.

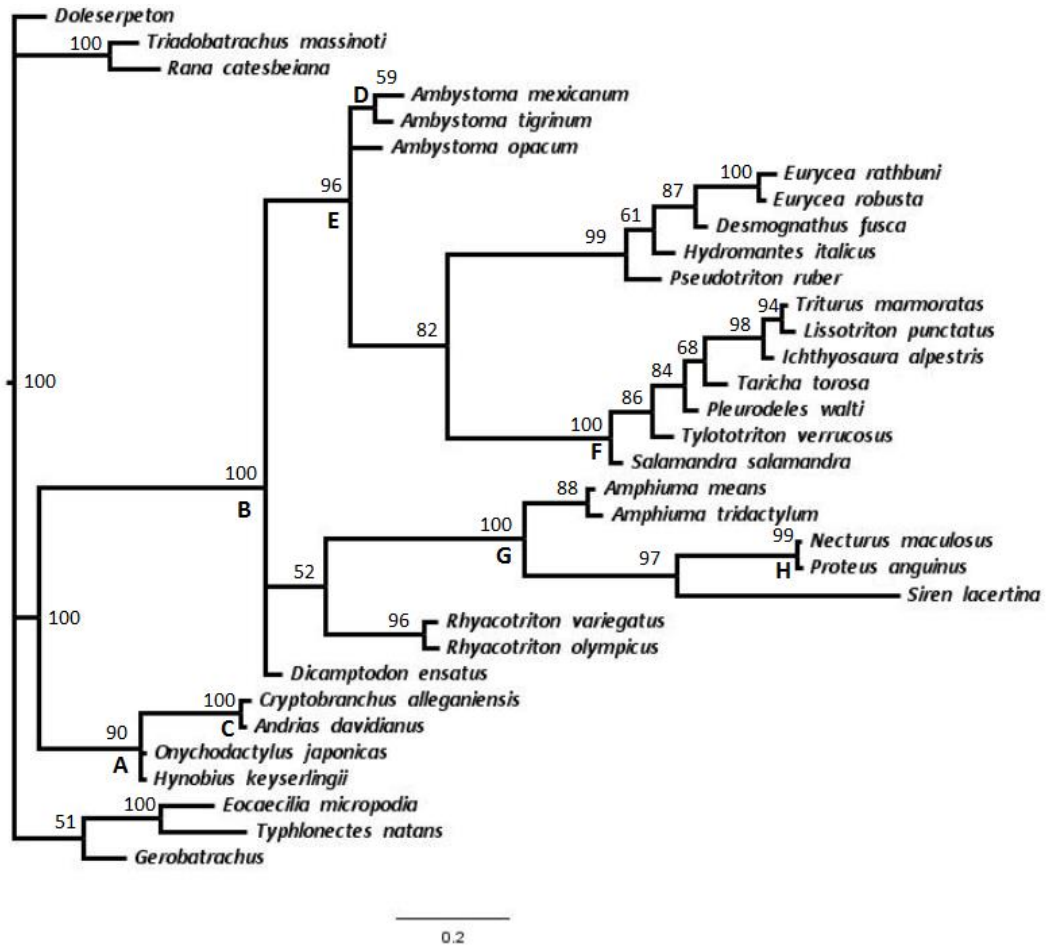


Figure 3.6: Bayesian analysis of the Le Quesne morphological dataset. Consensus tree from a Bayesian analysis that ran for 2000000 generations, resulting in an average standard deviation of split frequency value of 0.003710; av ESS: 743.1; PSRF+: 1.001

The following synapomorphies support the following clades:

- A – Cryptobranchioidea share unicapitate postatlantal ribs, fusion of the first hypobranchial and first ceratobranchial, fusion of the pubotibialis and puboischiotibialis muscles.
- B - Salamandroidea share no distinct angular in adults, free ribs absent on anterior caudal vertebrae, one central element in the manus, absence of second ceratobranchial, incomplete lateral wall of nasal capsule.
- C - Cryptobranchidae and Hynobiidae have no synapomorphies.
- D - *Ambystoma tigrinum* and *Ambystoma mexicanum* share a suprascapula that is about the same width as the dorsal width of the scapula.
- E - Plethodontidae have all lost their pterygoid, dorsal and ventral roots of their presacral vertebrae exit through separate foramina, a vomerina teeth replacement pattern that starts from the posterior of the vomer, presence of a common tube to the spermathecae, and presence of caudal pelvic glands.
- F - Salamandridae lack vomerine teeth on the postchoanal process.
- G - Amphiumidae share three pairs of larval gill slits, presence of additional female cloacal glands, and amphiumid pit glands.
- H - Proteidae all share a highly reduced odontoid process, two pairs of larval gill slits, more than ten pairs of rugae in the male cloaca, and haploid chromosome numbers reduced to 19.

Parsimony result:

The Parsimony results look slightly different to the Bayesian analysis of the same Le Quesne morphological dataset. Salamanders are not monophyletic as Cryptobranchoidea and Salamandroidea are placed in an unresolved relationship with frogs. The Le Quesne dataset is missing two atlantal characters that were retained in the RI dataset that are common in Urodela (Character 116 and 117 Appendix B). Salamandroidea form a clade but the internal relationships differ from the Bayesian analysis. Ambystomatidae is not monophyletic and *Dicamptodon* is part of an unresolved polytomy including *Rhyacotriton* and Ambystomatidae + (Salamandridae + Plethodontidae). The agreement subtree excluded *Dicamptodon*, *A. opacum*, *Hydromantes italicus*, and *Taricha torosa* from the phylogeny as they did not occur in the same place in the topology of all 24 MPTs.

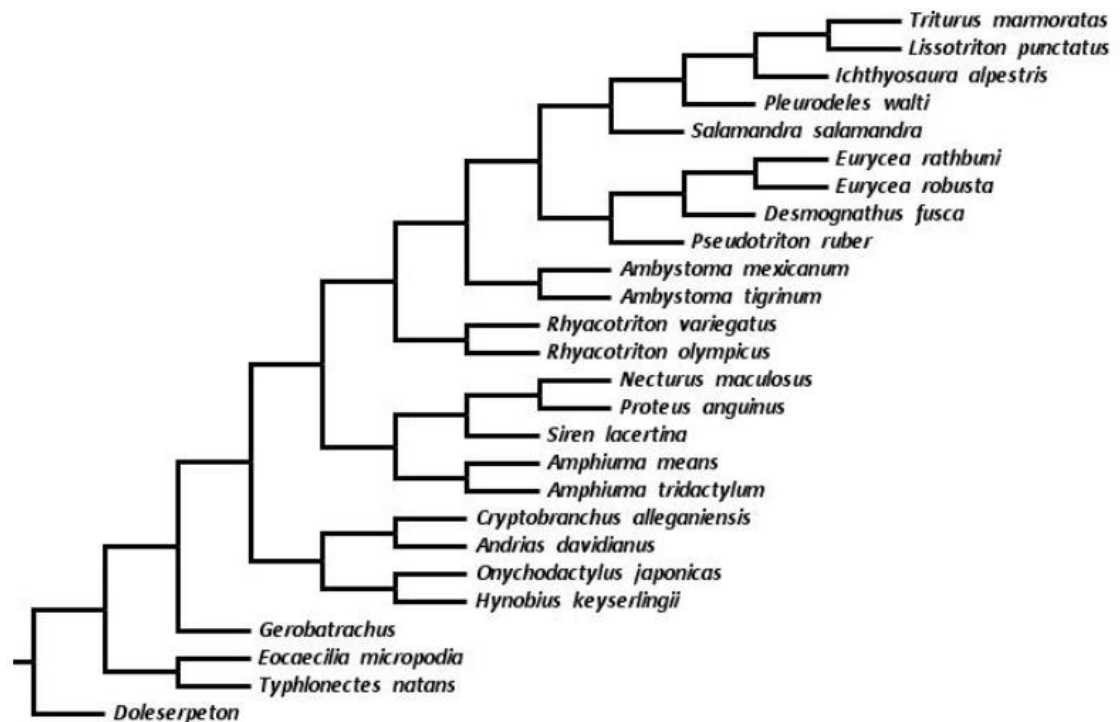


Figure 3.7: Agreement subtree of the Parsimony analysis of the Le Quesne morphological dataset made from 24 MPTs trees each 289 steps in length CI = 0.429, RI = 0.751

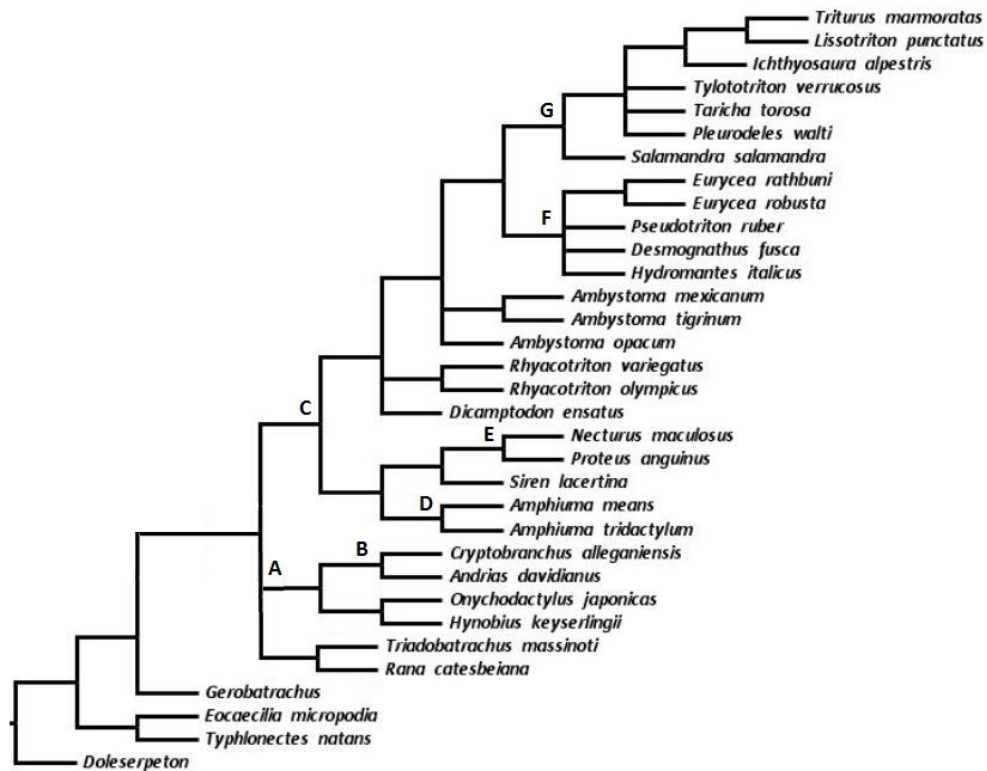


Figure 3.8: Strict consensus from the Parsimony analysis of the Le Quesne morphological dataset made from 24 MPTs trees each 289 steps in length.

The following synapomorphies support the following clades:

A - Cryptobranchoidea share pubotibialis and puboischiotibialis muscles that are fused, and the first hypobranchial and first ceratobranchial fused.

B - Cryptobranchidae share the following character: vomer articulates with pterygoid.

C - Salamandroidea share two to three pairs of ribs on anterior caudal vertebrae, one central element in the manus, loss of second ceratobranchial, and incomplete lateral wall of nasal capsule.

D - *Amphiuma* share three pairs of larval gill slits, presence of additional female cloacal glands, and presence of amphiumid pits.

E - Proteidae share 19 haploid chromosomes, greater than ten pairs of rugae in the male cloaca, and two pairs of larval gill slits.

F - Plethodontidae share the loss of Pterygoid, dorsal and ventral roots of presacral vertebrae exit through separate foramina, both laterally and posteriorly pattern of vomerine teeth replacement, common tube to the spermathecae present, and caudal pelvic glands present.

G - Salamandridae share a medial pattern of vomerine teeth replacement.

Ambystoma share a suprascapula about same width as dorsal width of scapula

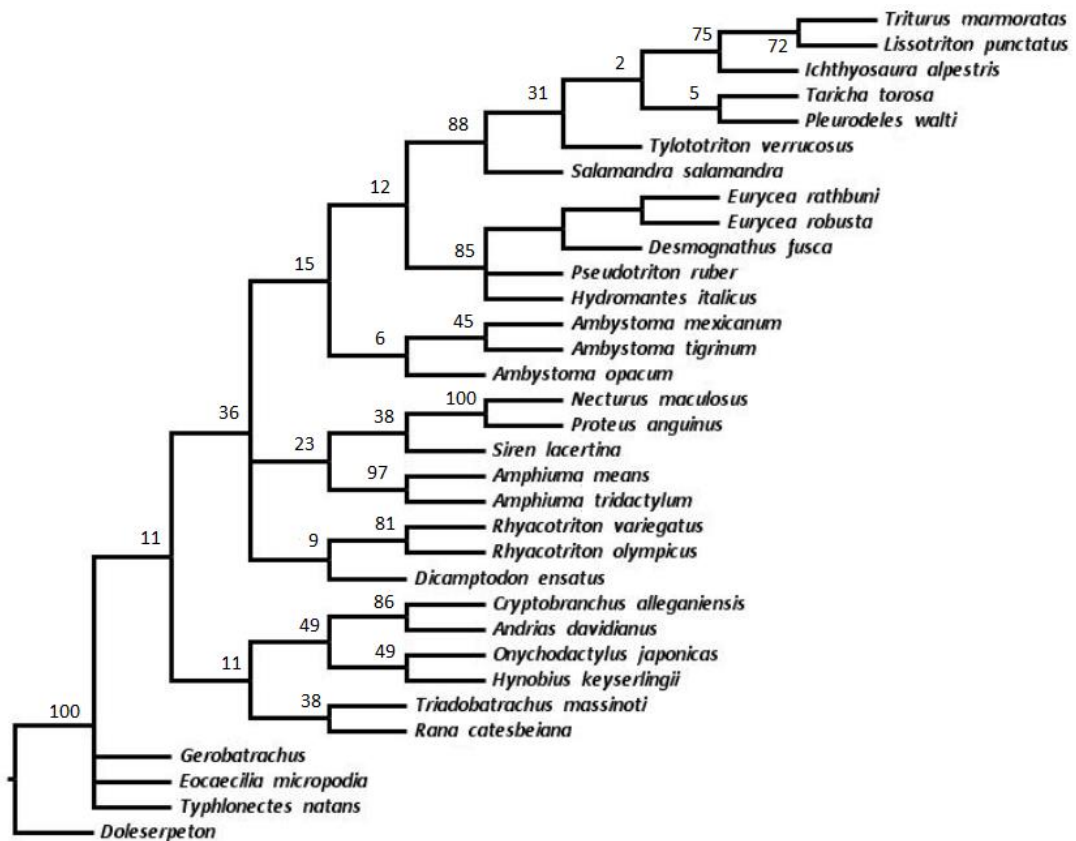


Figure 3.9: GC bootstrap values for the Parsimony analysis of the Le Quesne morphological dataset with traditional search option

3.3.3 Tree comparison results

The results of the agreement subtrees show the number of shared nodes between the molecular tree (fig 2.3.1) and the ri tree (fig. 3.3 and 3.4) and the molecular tree and the Le Quesne tree (fig. 3.6 and 3.7) (Table 3.2). The results of the Symmetric difference test show the number of differences in taxa placement between the molecular tree (fig. 2.3.1) and the ri tree (fig. 3.3 and 3.4) and the molecular tree and the Le Quesne tree (fig.3.6 and 3.7).

Tree comparison method	Bayesian		Parsimony	
	RI	Le Quesne	RI	Le Quesne
Agreement sub-trees	10/25	11/25	14/23	15/25
Symmetric diff	33	34	14	18

Table 3.2 Agreement subtree and Symmetric difference values when the RI and Le Quesne trees are compared to the full molecular tree found in this study

3.3.4 Simulated fossils using RI subset

3.3.4.1 Bayesian analysis results:

The simulated *Hynobius* fossil species does not form a monophyletic group with the other Hynobiidae taxon but it does fall within a monophyletic Cryptobranchoidea. The Bayesian posterior probability value supporting this clade is low. The simulated *Hynobius* fossil shares unicapitate ribs with the other Cryptobranchoidea but lacks mid-dorsal keel on the presacral vertebrae like *Onychodactylus*. It differs from the other Cryptobranchoidea by possessing anterior basapophyses on the presacrals.

Although *Desmognathus* was placed correctly as a simulated fossil (it shared dorsal and ventral roots of spinal nerves that exit through separate foramina in presacral vertebrae, with all other Plethodontidae), not all Plethodontidae are placed as accurately when they are converted to “fossils”. The simulated *Pseudotriton* fossil relationship is unresolved as it forms a polytomy with the other Plethodontidae and Salamandridae species, but it is at least in the correct part of the tree topology. The simulated *Pseudotriton* fossil shares dorsal and ventral roots that exit through separate foramina of the presacral vertebrae with the other plethodontids, but it is still placed in an unresolved position. Both *Pseudotriton* and *Desmognathus* share spinal nerves that exit intravertebrally in some vertebrae with Salamandridae, Sirenidae, and Plethodontidae.

The Bayesian analysis does not place the simulated *Amphiuma* fossil in the same clade as the other *Amphiuma* species but places it in an unresolved relationship with *Amphiuma means* and *Siren lacertina*. The simulated *Amphiuma* fossil shares a pointed dorsal outline of posterior margin of the atlas neural arch roof, and intravertebral spinal nerve exits in some or all caudal vertebrae with *Amphiuma means*.

3.3.4.2 Parsimony analysis results:

The simulated *Proteus* fossil was not included in the agreement subtree and the strict consensus result did not place the simulated *Proteus* fossil in a monophyletic group with *Necturus*. Instead it joins *Necturus* in an unresolved relationship with *Rhyacotriton*, *Siren* + *Amphiuma* and Salamandridae + Plethodontidae in the strict consensus tree. The simulated *Proteus* fossil only shares a highly reduced odontoid process with *Necturus*. The lack of data for some of the other taxa has allowed the possibility that this is not a synapomorphy for this clade.

The simulated *Hynobius* fossil's placement is very unstable as it is not included in the agreement subtree. The strict consensus places the simulated *Hynobius* fossil into an

unresolved relationship with *Onychodactylus japonicus*, Cryptobranchoidea, and Salamandroidea. Not only is Hynobiidae not monophyletic, Cryptobranchoidea is not monophyletic either. The bootstrap support values are extremely low. The simulated *Hynobius* fossil shares no vertebral characters exclusively with the other members of the Cryptobranchoidea in this phylogeny however the ancestral state reconstruction has hypothesised that it probably had unicapitate ribs.

Simulated salamander	Bayesian placement	Parsimony placement
<i>Ambystoma</i>	correct	correct
<i>Amphiuma</i>	incorrect	correct
<i>Rhyacotriton</i>	correct	correct
<i>Andrias</i>	correct	correct
<i>Hynobius</i>	incorrect	incorrect
<i>Salamandra</i>	correct	correct
<i>Pseudotriton</i>	Incorrect	correct
<i>Desmognathus</i>	correct	correct
<i>Proteidae</i>	correct	incorrect

Table 3.3 Summary of results of the placement of the simulated fossils using the RI dataset

Bayesian analysis using all simulated fossils:

The Bayesian analysis has placed the simulated fossils in similar positions to those in which they were placed when they were run individually. The simulated *Andrias*, *Proteus*, *Amphiuma* and *Desmognathus* fossils were placed in their respective families. *Dicamptodon* was placed in the same position as in the tree using the RI subset of data. The simulated *Ambystoma* and *Hynobius* fossils were both placed in unresolved positions. The simulated *Siren* fossil was not placed in the same place as when it was run in the analysis individually, it is now in an unresolved relationship with the Salamandridae species and the simulated *Salamandra* fossil. The results of the Parsimony analysis were very similar, with low bootstrap support for most clades.

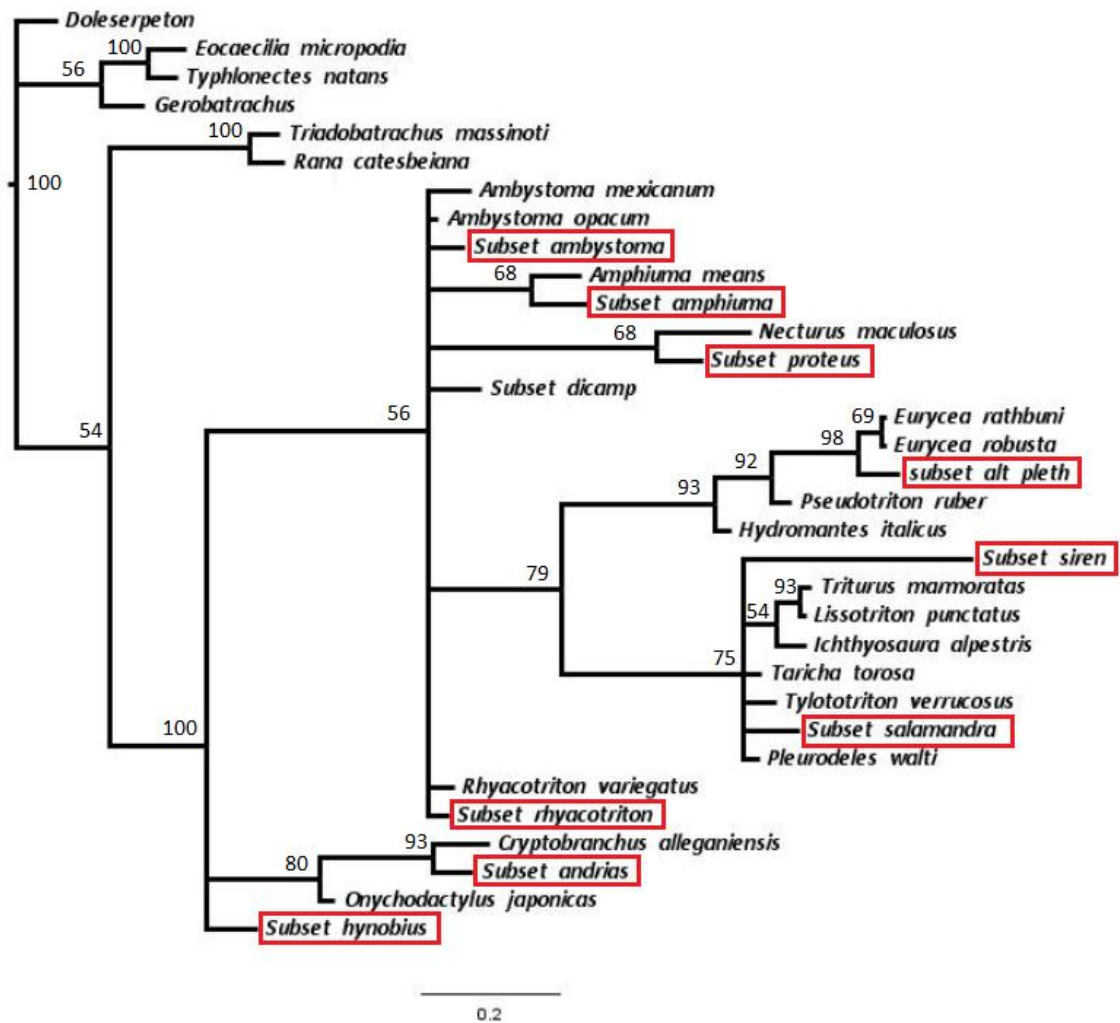


Figure 3.10: Consensus tree from a Bayesian analysis including all the simulated fossils using the RI dataset (in red outline) that ran for 2000000 generations, resulting in an average standard deviation of split frequency value of 0.005134; av ESS: 653.09; PSRF+: 1.000 Node values are Bayesian posterior probability values

3.3.5 Simulated fossils using the Le Quesne subset

Bayesian analysis results:

The simulated *Ambystoma* fossil is placed as the sister taxon to *Ambystoma mexicanum* but does not form part of a monophyletic Ambystomatidae. *Ambystoma opacum*'s position is unresolved as it forms part of a polytomy together with Plethodontidae + Salamandridae and the simulated *Ambystoma* fossil + *Ambystoma mexicanum*. The simulated *Ambystoma* fossil shares presence of basapophyses on the atlas with *Ambystoma mexicanum*, while *Ambystoma opacum* lacks them. The simulated *Ambystoma* fossil also shares presence of a partial bony lamina between diapophyses and parapophyses with *Ambystoma mexicanum* while it is absent in *Ambystoma opacum*.

The simulated *Hynobius* fossil forms a trichotomy with other cryptobranchoids and a monophyletic Salamandroidea. Unicapitate rib morphology is a character that has been reconstructed as shared with the other Cryptobranchoidea.

Although the simulated *Desmognathus* fossil was placed correctly, the *Pseudotriton* fossil is placed as the sister taxon to Salamandridae. The simulated *Pseudotriton* fossil shares a separate form of the odontoid process with all Salamandridae, except *T. verucosus*, while all the other Plethodontidae species in this study have dorsoventrally flattened odontoid process. The simulated fossil differs from Salamandridae by the presence of posterior basapophyses on the presacral vertebrae. The presacral spinal nerves exit intravertebrally in both the Salamandridae and Plethodontidae in this study. The presacral vertebrae have dorsal and ventral roots of the spinal nerves exiting through separate foramina of both the simulated plethodontid fossil, and the other plethodontid taxa.

The simulated *Amphiuma* fossil is placed in a trichotomy with *Amphiuma means* and Proteidae + Sirenidae. The simulated *Amphiuma* fossil shares an odontoid process which is partially separate in the middle, and a pointed dorsal outline of posterior margin of the atlas neural arch roof with *Amphiuma means*. It differs from *A. means* by having a smaller neural canal relative to the anterior cotyle of the atlas.

Parsimony analysis results:

The simulated *Ambystoma* fossil is placed as the sister taxon to *Ambystoma mexicanum* but not within a monophyletic Ambystomatidae family, as the position of *Ambystoma opacum* is as sister taxon to Salamandridae + Plethodontidae. The simulated *Ambystoma* fossil is placed as sister taxon to *Ambystoma mexicanum* because they both share basapophyses present on the atlas, and a bony lamina between the diapophyses and parapophyses of the presacral vertebrae, however *Ambystoma opacum* differs from *A. mexicanum* and the simulated *Ambystoma* fossil because it does not possess either of these traits.

The simulated *Pseudotriton* fossil is placed in a large polytomy that includes frogs. Whereas the simulated *Rhyacotriton* fossil is placed in a polytomy together with *Rhyacotriton variegatus*, *Dicamptodon*, (*Amphiuma* + *Siren* + Proteidae), and (*A. opacum*, + [*A. tigrinum* + *A. mexicanum*], + [Plethodontidae + Salamandridae]). The simulated *Rhyacotriton* shares odontoid process that is slightly separate with *Amphiuma*, posterior basapophyses with *Rhyacotriton variegatus*, *A. mexicanum*, *Desmognathus* and *Pseudotriton*. The simulated fossil

also shares intravertebral spinal nerve exits in some or all caudal vertebrae with *Dicamptodon*, *Rhyacotriton variegatus*, and *Amphiuma*.

The simulated *Salamandra* fossil is placed in a polytomy with the other Salamandridae species and Plethodontidae. The simulated fossil shares opisthocoelous presacral vertebrae with both the other Salamandridae and Plethodontidae.

The simulated *Hynobius* fossil is not included in the agreement subtree and is placed in an unresolved relationship with *Dicamptodon*, *Onychodactylus*, frogs, *Rhyacotriton*, Cryptobranchidae, (*Amphiuma* + *Siren* + Proteidae), and (*Ambystoma* + Salamandridae + Plethodontidae) in the strict consensus tree. There are no synapomorphies that the simulated *Hynobius* fossil shares with either *Onychodactylus* or with either of the Cryptobranchidae. The simulated fossil shares spinal nerves that exit intervertebrally in the presacral vertebrae with other taxa in the polytomy.

The simulated *Proteus* fossil is not placed in the agreement subtree and is positioned in an unresolved relationship with *Siren*, *Necturus*, and *Amphiuma* in the strict consensus tree. The simulated *Proteus* fossil only shares a highly reduced odontoid process with *Necturus*. The results of all the simulated fossils are summarised in Table 3.4.

Simulated salamander	Parsimony placement	Bayesian placement
<i>Ambystoma</i>	incorrect	incorrect
<i>Amphiuma</i>	correct	incorrect
<i>Rhyacotriton</i>	incorrect	correct
<i>Andrias</i>	correct	correct
<i>Hynobius</i>	incorrect	incorrect
<i>Salamandra</i>	incorrect	correct
<i>Pseudotriton</i>	incorrect	incorrect
<i>Desmognathus</i>	correct	correct
<i>Proteidae</i>	incorrect	correct

Table 3.4 Summary of results of the placement of the simulated fossils using the Le Quesne dataset

Bayesian analyses including all simulated fossils:

The Bayesian analysis has resulted in a tree that is poorly resolved, but Cryptobranchoidea and Salamandroidea are both monophyletic as are *Rhyacotriton*, Proteidae, Plethodontidae, Salamandridae and Cryptobranchidea, whereas Ambystomatidae, Amphiumidae, and Hynobiidae are unresolved.

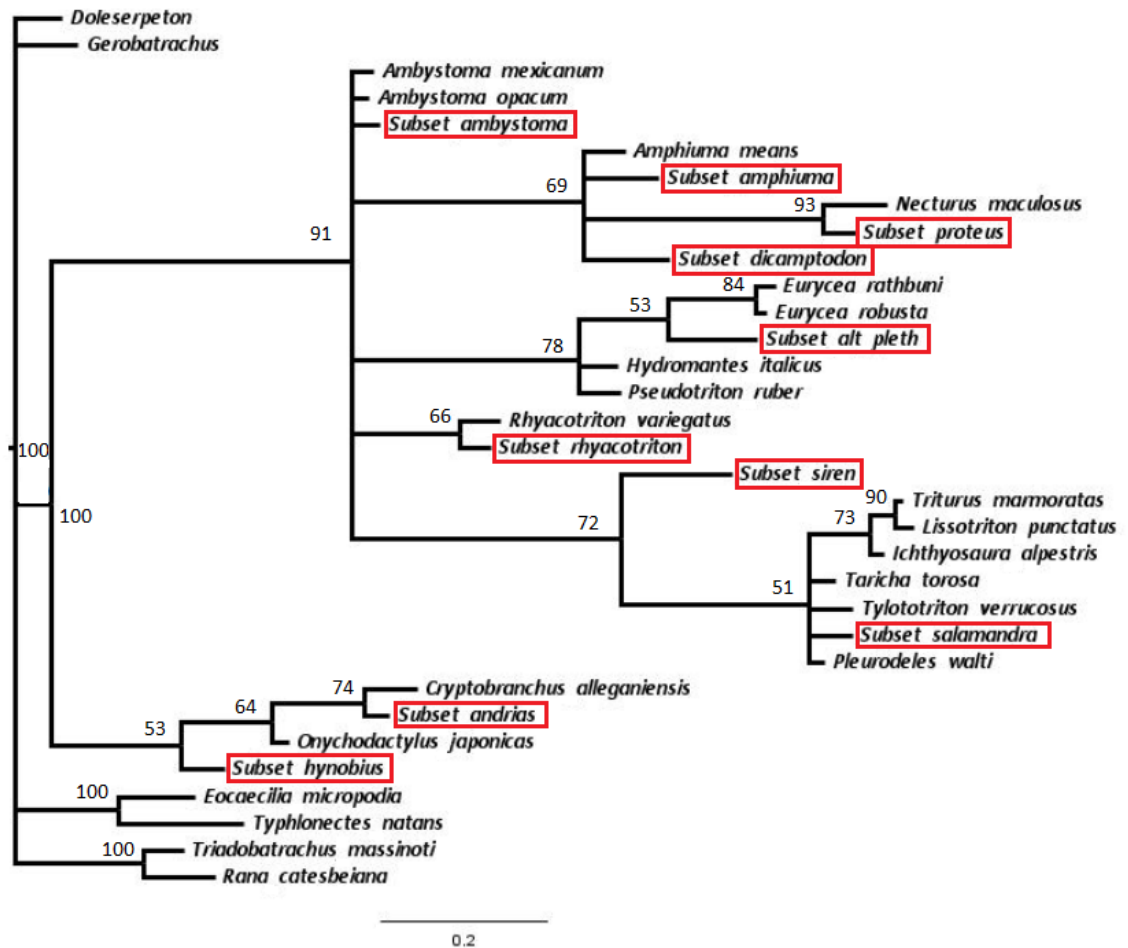


Figure 3.11: Consensus tree from a Bayesian analysis of the Le Quesne dataset including all simulated fossils that ran for 2000000 generations, resulting in an average standard deviation of split frequency value of 0.007661; av ESS: 681.17; PSRF+: 1.000 Node values are Bayesian posterior probability percentage

Parsimony analyses including all simulated fossils:

The parsimony analysis (fig. 3.22) has resulted in a tree that places frogs in an unresolved relationship with the taxa typically comprising the Cryptobranchoidea and *Dicamptodon*. Neither Cryptobranchoidea nor Salamandroidea are monophyletic, nor are Ambystomatidae, Cryptobranchidae or Hynobiidae. The bootstrap support throughout the tree is extremely low.

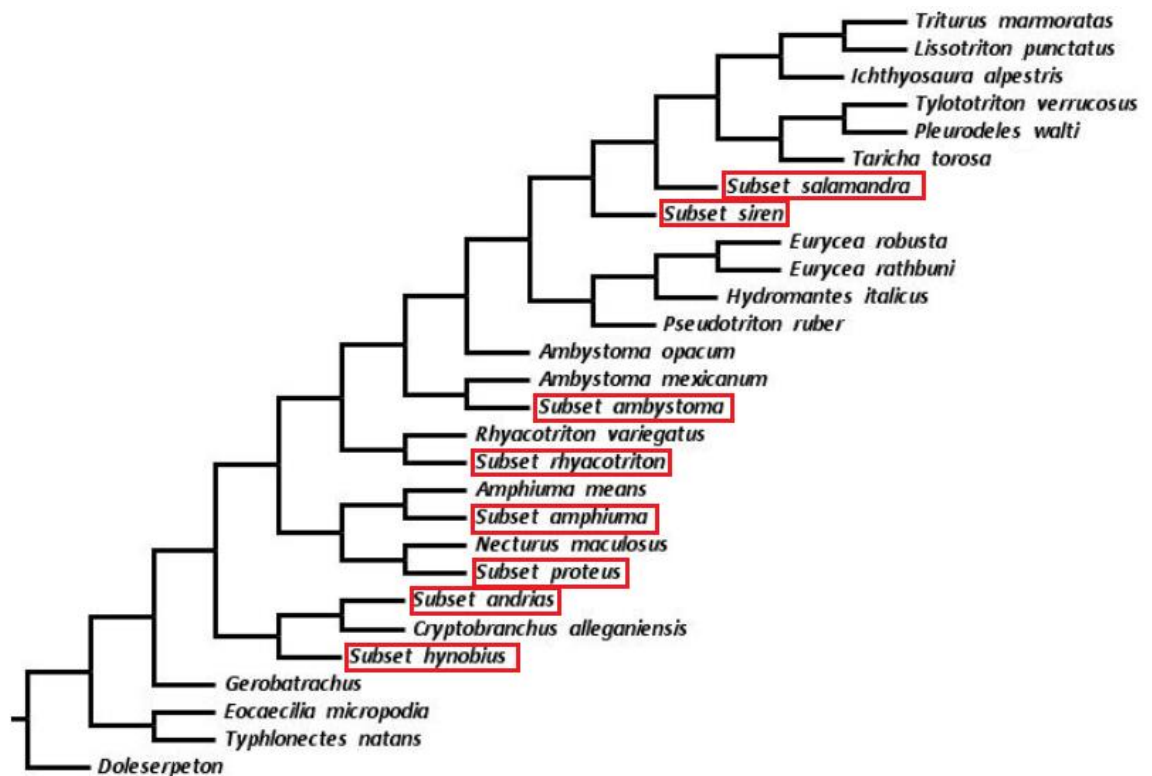


Figure 3.12: The agreement subtree created from the Parsimony analysis of the Le Quesne dataset that included all the simulated fossils, made from 24 MPTs each 235 steps in length.

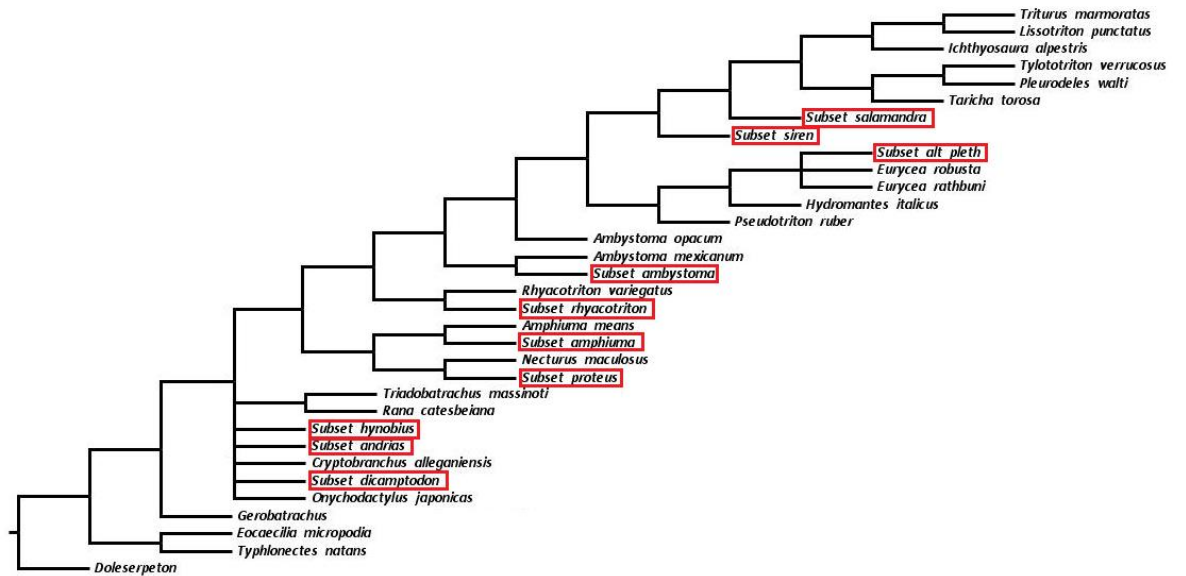


Figure 3.13: Strict consensus tree resulting from the Parsimony analysis of the Le Quesne dataset including all the simulated fossils, made from 24 MPTs each 235 steps in length.

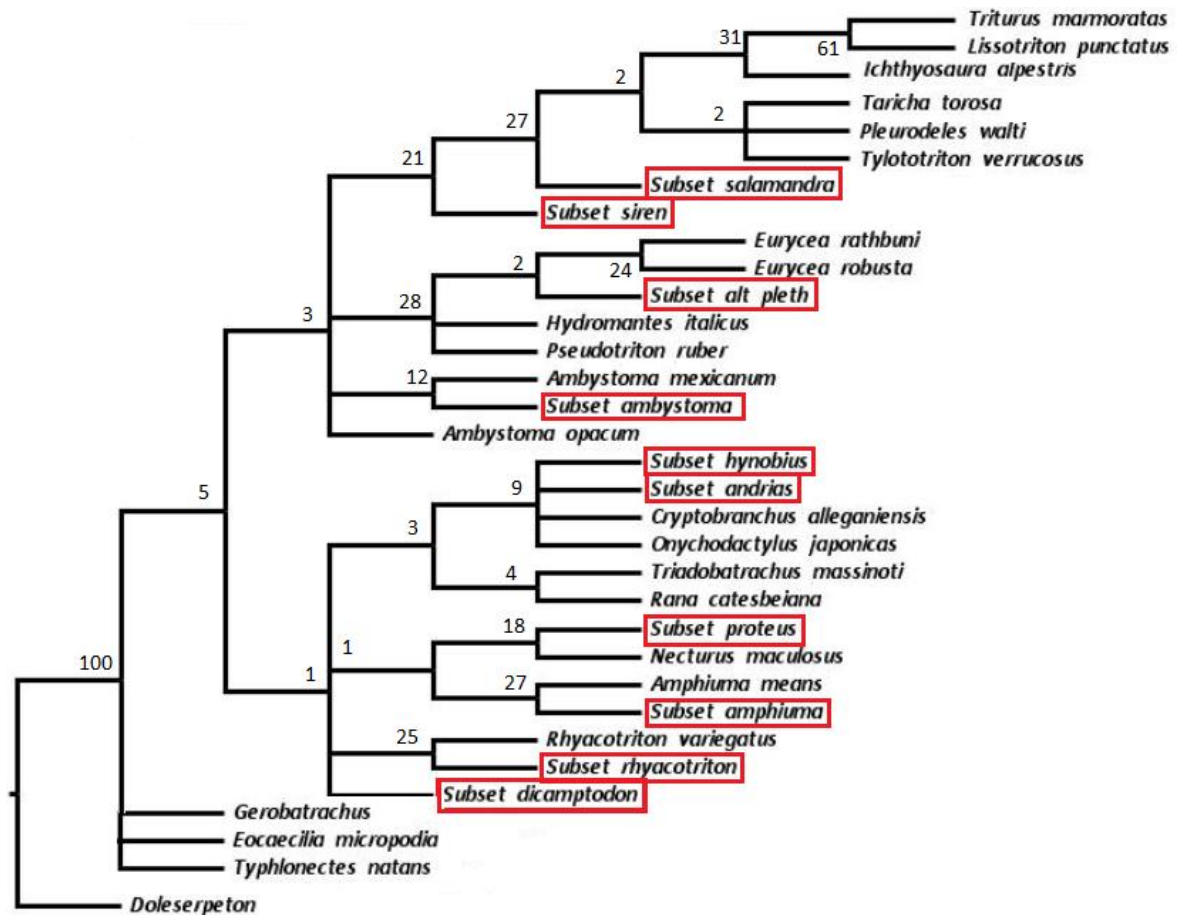


Figure 3.14: GC Bootstrap values from the Parsimony analysis of the Le Quesne dataset that included all the simulated fossils in TNT

Tree comparison summary:

The results of the placements of the simulated fossils are summarised below in tables 3.8 and 3.9. The number of simulated fossils placed correctly either to family (table 3.8) level is higher when the RI dataset is used within a Parsimony framework. And both the Bayesian results and the Parsimony results placed the simulated fossils correctly to Cryptobranchoidea/Salamandroidea level when the RI dataset was used.

	Bayesian	Parsimony
RI	6 of 9	7 of 9
Le Quesne	5 of 9	3 of 9

Table 3.8: Number of simulated fossils placed correctly to Family level within a Bayesian or Parsimony framework using the RI or Le Quesne datasets

	Bayesian	Parsimony
RI	9 of 9	9 of 9
Le Quesne	8 of 9	7 of 9

Table 3.9: Number of simulated fossils placed correctly to cryptobranchoid/salamandroid level within a Bayesian or Parsimony framework using the RI or Le Quesne datasets

3.3.6 Stem-ward slippage results of the Bayesian and Parsimony analysis of the RI dataset

Simulated fossils (*Hynobius*, *Dicamptodon*, *Desmognathus* and *Pseudotriton*) are placed in exactly the same place in the Bayesian analysis as in the results of the analysis of the full RI dataset, once their living relatives had been excluded from the dataset. In the Parsimony analysis only the Plethodontidae simulated fossils were positioned in the same place as in the phylogeny resulting from the analysis of the full RI dataset. Some of the other simulated fossils were not placed as accurately.

Rhyacotritonidae

Rhyacotriton is placed as the sister taxon to all other salamandroids in both the Bayesian and Parsimony analyses, which is the same placement as in the results of the

Bayesian analysis of the full morphological dataset (Chapter 2, Fig. 2.13). However, it has slipped stem-ward in placement compared to the Bayesian analysis of just the RI data (Fig. 3.3).

Proteidae

In the Bayesian analysis the simulated fossil *Proteus* has changed position in the phylogeny and is no longer sister taxon to *Amphiuma* + *Siren*. However, it still falls in the same place as in the Bayesian analysis of the RI dataset (Fig. 3.3). It is rather *Amphiuma* + *Siren* that have moved stem-ward to form an unresolved relationship with *Ambystoma*, *Dicamptodon* and a *Rhyacotriton* + *Proteus* + Plethodontidae + Salamandridae clade. The Parsimony analysis has placed the simulated *Proteus* fossil as the sister taxon to *Rhyacotriton* with the lowest Bootstrap support possible. *Proteus* + *Rhyacotriton* form a sister clade to all other Salamandroidea which is a slightly more stem-ward position in the phylogeny than in the Parsimony analysis of the full RI dataset (Fig. 3.4).

Amphiumidae

The simulated *Amphiuma* fossil has moved from being a sister taxon to *Siren* to an unresolved relationship with Proteidae + Sirenidae, Plethodontidae + Salamandridae, and *Rhyacotriton* in the Bayesian analysis. The simulated *Amphiuma* fossil is placed as the sister taxon to *Ambystoma* + *Dicamptodon* in the Parsimony analysis. This is a change in position from the results of the Parsimony analysis of the whole RI dataset, where *Amphiuma* is placed as the sister clade to *Siren*, but not a slip stem-ward.

Ambystomatidae

The simulated *Ambystoma* fossil is placed in a similar place to that of the Bayesian analysis of the RI data but its position is less resolved. The Parsimony analysis placed the simulated fossil in the same position (sister taxon to *Dicamptodon*) as in the Parsimony analysis of the RI dataset.

Cryptobranchidae

The simulated *Andrias* fossil is placed as the sister taxon to all other Salamandridae in the Bayesian analyses, but it is no longer part of a monophyletic Cryptobranchoidea. In the parsimony analysis the simulated *Andrias* fossil is not included in the agreement subtree but is rather placed in an unresolved position including the Hynobiidae and Salamandroidea in the strict consensus.

Sirenidae:

This study included only one species of *Siren*, but this changes position when it is in simulated fossil form. Both the Bayesian and Parsimony analysis places the simulated Sirenidae fossil in a monophyletic group including all Salamandridae. The internal relationships within this Salamandridae + Sirenidae clade are mostly unresolved in the Bayesian phylogeny.

Hynobiidae

The Bayesian analysis of the simulated *Hynobius* fossil placed it in the same position as the Bayesian analysis of the full RI dataset, as the sister taxon to Cryptobranchidae within a monophyletic Cryptobranchoidea. However, *Hynobius* is not placed in the agreement subtree and is located within Salamandroidea in the strict consensus tree, in an unresolved relationship.

Dicamptodonidae:

The Bayesian analysis of the simulated *Dicamptodon* fossil placed it in exactly the same position as the Bayesian analysis of the full RI dataset, but the Parsimony analysis of the same simulated fossil places it as sister taxon to *Siren* + *Amphiuma*.

No. of correctly placed simulated fossils:	Bayesian	Parsimony
Relative to the previous position within the phylogeny	5/9	2/9
At Cryptobranchoidea/ Salamandroidea level	8/9	7/9

Table 3.10: Number of simulated fossils placed in the same place within the topology as in the results of the Bayesian and Parsimony analysis of the RI dataset and the number of simulated fossils placed correctly within either a monophyletic Cryptobranchoidea or Salamandroidea within a Bayesian or Parsimony framework.

The simulated fossils were placed more accurately, once their extant relatives were removed from the matrix, using the RI dataset within a Bayesian framework. The Parsimony results were very poor with only two out of the nine simulations placed correctly. The placement of the simulated fossils to Cryptobranchoidea/Salamandroidea level was slightly better using the Bayesian framework.

3.4 Discussion

The lack of congruence between the molecular and morphological trees in the study by Wiens (2005), even after removing putative juvenile characters from the morphological dataset, was attributed to some alternate, as yet unknown biological signal. However, it might be that their method of character exclusion was flawed. One cannot use a priori bias towards character fit as a reason to exclude characters. The fact that some characters are a consequence of the paedomorphic life history of a species does not mean they are not useful when trying to elucidate the relationships of salamander clades. In this study convergent characters (not simply characteristics associated with paedomorphy) were removed using both tree dependent and tree independent methods of character evaluation. An example of a character that was identified as convergent is the presence of dermal sculpture on the skull roof, which occurs in some stem-group salamanders and also in Salamandridae. The resultant reduced character sets showed that there was more agreement between the tree dependent and tree independent method of character evaluation on the soft body characters than the osteological characters. Both the RI and Le Quesne datasets included exactly the same soft body characters. Proportionally more soft body characters were retained in both the RI and Le Quesne datasets with 73% showing no homoplasy. The osteological characters displayed more homoplasy with only 29% and 42% of characters retained in the reduced Le Quesne and RI datasets respectively. This supports the hypothesis that the loss of soft body characters may distort the biological signal more than the loss of osteological data (Sansom *et al.* 2010; Sansom and Wills 2013).

The results, using the reduced datasets, still show some incongruence with the combined morphological and DNA trees from both the study presented in this thesis and previously published studies (Larson and Dimmick 1993; Wiens *et al.* 2005). Both the RI and Le Quesne phylogenies are significantly different from the nDNA phylogeny (Fig. 2.3.2) but the Le Quesne phylogeny shows marginally more similarities to the molecular phylogeny (Fig. 2.3.1) and the nDNA phylogeny (Fig. 2.3.2) than the RI dataset result did. Both the reduced datasets can reliably recover a monophyletic Cryptobranchoidea and monophyletic Salamandroidea as found by many other published phylogenies (Duellman and Trueb 1986; Larson and Dimmick 1993; Wiens *et al.* 2005; Roelants *et al.* 2007). However, in the Parsimony analysis of the Le Quesne dataset, frogs are included in the unresolved relationship with Cryptobranchoidea and Salamandroidea meaning that if any fossils (simulated or real) are included and fall to the base of either Cryptobranchoidea or Salamandroidea the relationship to either might be unresolved. This is most likely a resolution issue with the reduced dataset.

The RI dataset performed better than the Le Quesne dataset in the Parsimony analysis, given that previous analyses of both the full morphological data and the molecular data [both herein and in the work of other authors, (Hay *et al.* 1995)] show that salamanders are monophyletic and frogs form their sister clade. Although the morphological data (reduced through tree dependent or independent methods) still provides little resolution to the interfamilial salamander relationships, it can still allow us to place fossils (even fossils with limited character availability) with some confidence at least within a monophyletic Salamandroidea and Cryptobranchoidea. The RI dataset performed better than the Le Quesne dataset in placing more simulated fossils to family level although their placement was frequently only supported by reconstructed characters.

The family that showed consistent non-monophyly when simulated fossils were included in the matrix was the Hynobiidae. The simulated hynobid fossil was at least placed within Cryptobranchoidea in both the Bayesian and Parsimony analysis using the RI dataset, but it did not form a monophyletic Hynobiidae in any of those results. Hynobiidae has caused problems in previous systematic analyses (Schultze and Trueb 1991). Although Hynobiidae differ from Cryptobranchidae by having more complete metamorphosis they still share a suite of characteristics that have led previous studies to place them within Cryptobranchoidea (Edwards 1976; Estes 1981). Historically it has been suggested that Hynobiidae might be related to the Ambystomatidae due to similarities in feeding mechanisms of metamorphosed forms (Regal 1966). Further analysis of the morphology and genetic information has confirmed Hynobiidae monophyly (Zhang *et al.* 2006) although Hynobiidae morphological characteristics clearly still provide a challenge for accurate placement at family level.

Among the other genera that were misplaced was the plethodontid *Pseudotriton* which displays a superficial resemblance to the salamandrid *Notophthalmus viridescens* (Howard and Brodie 1971) and whose adult forms can be both aquatic and terrestrial. *Pseudotriton* actually forms part of the subfamily Spelerpinae within which previous researchers have recovered substantial cryptic diversity (Chippindale 2000; Hillis *et al.* 2001; Wiens *et al.* 2003; Bonett and Chippindale 2004). This subfamily is made up of species with very different life histories including the traditional biphasic life history, as well as aquatic and the perennibranchiate. Some Spelerpinae are trogloditic (cave-dwelling) and exhibit a range of convergent morphological features that have previously hampered attempts to infer phylogenetic relationships based on morphological data (Sweet 1982; Chippindale 2000; Wiens *et al.* 2003).

The other genera that were occasionally misplaced as simulated fossils were the permanently aquatic *Proteus* and *Amphiura*. Proteidae in the full morphological dataset tree in the previous chapter (Fig. 3.13) were made up of one skull, one atlantal, and two soft body characters. The simulated fossil only has one atlantal character exclusively in common with *Necturus* which was not always enough to place them in a monophyletic Proteidae. *Ambystoma opacum* had previously not been placed in a monophyletic Ambystomatidae however the Le Quesne dataset failed to place *A. opacum* in a monophyletic clade with the two other *Ambystoma* species. One of the characters observed to support the monophyly of *Ambystoma* using the RI dataset was a character relating to spinal nerve foramina, but the recoding of this ordered multistate character in the Le Quesne dataset divided it into two separate characters, neither of which supported a monophyletic *Ambystoma*.

The RI dataset was then used to test for stem-ward slippage by removing the living relatives of the simulated fossil from the dataset. The Bayesian analysis of the RI dataset shows less stem-ward slippage of taxa run as simulated fossils (i.e., reduced to just vertebral and atlantal characters) than the Parsimony analysis. Many of the simulated fossils were placed in very similar positions compared to when the full matrix was analysed with their extant relatives included, although the relationships of *Amphiura*, *Proteus* and *Ambystoma* were less resolved and *Salamandra* was classified as a plethodontid. The only exception was the placement of the simulated *Andrias* fossil, which did not group with Hynobiidae in a monophyletic Cryptobranchoidea (however, it still maintained its place outside of Salamandroidea). This is contrary to the findings of Sansom and Wills (2013) even though they used a more relaxed approach to simulating fossils. Their use of the whole osteological character set to simulate fossils (while removing just the soft body characters) still lead to the apparent stem-ward slippage of 61% of significantly shifting taxa. Although this study presented here did not rigorously test the data by comparing the movement of the simulated fossils to a simulated fossil with randomly deleted characters, the position of the simulated fossil taxa was still observed relative to the position before being “fossilised”. This study did not show quite the same high proportion of simulated fossils that exhibited stem-ward slippage as Sansom and Wills (2013), perhaps because the morphological dataset focused on the elements commonly found in the fossil record (i.e. vertebral characters) and the RI dataset retained a higher proportion of atlantal, presacral and spinal nerve characters relative to the skull and appendicular parts of the body (approx. 54% of vertebral characters were retained which makes up 31% of the RI osteological characters). Stem-ward slippage still occurred in just less than half of simulations in this study and is a phenomenon that needs to be taken into consideration when interpreting results of actual fossil placement.

3.5 Conclusions

The soft body characters showed less homoplasy than osteological characters with 73% of soft body characters remaining after the homologous characters were removed. Compared to 43% of osteological characters that remained, soft body characters may show less homoplasy than osteological characters. The Le Quesne tree showed more symmetric differences with molecular phylogenies (in this study) than the RI phylogeny.

The RI dataset places all the simulated fossils accurately in Cryptobranchoidea and Salamandroidea within both the Bayesian and Parsimony framework. But it was the Parsimony analyses that accurately placed more simulated fossils to a family level than the Bayesian analysis. However, the Bayesian phylogenies exhibited better support values even though many of these simulated fossils often had no synapomorphies supporting their placement.

Simulated fossils (with extant relatives removed) were placed within their respective Cryptobranchoidea and Salamandroidea clade more accurately using the RI dataset within a Bayesian framework (although the resolution of relationships was not high). With the poor performance of the Parsimony analyses of the RI dataset, it was concluded that further analyses in this study, to place actual fossils would use the Bayesian analysis of the RI dataset. Phylogenetic analysis of fragmentary fossils may therefore yield some useful results, (provided there are not too many of them in any one analysis) but stem-ward slippage is still a real concern.

Although the reduced datasets still show some incongruence with the combined morphological and DNA trees, there are still uses for the new morphological datasets. Cryptobranchoidea and Salamandroidea are still monophyletic using both the RI and Le Quesne datasets. And the placement of simulated fossils within Cryptobranchoidea and Salamandroidea is robust and consistent for the Bayesian analysis of the RI and Le Quesne dataset.

The RI dataset performed better than the Le Quesne dataset in the parsimony analysis because we know from our previous analyses of both the full morphological data and the molecular data that Salamanders are monophyletic and frogs form their sister clade. Although the morphological data (reduced through tree dependent or independent methods) still provides little resolution to the interfamilial salamander relationships (except the Bayesian analysis of the RI dataset) it can still allow us to place fossils within an extant framework with

confidence that they will place at least within a monophyletic Salamandroidea and Cryptobranchoidea if not with/within their respective families.

The trees lose resolution as more than one simulated fossil is added to an analysis however in the Bayesian analysis of both the RI and Le Quesne datasets the full set of simulated fossils still placed accurately in Cryptobranchoidea and Salamandroidea. The Bayesian analyses accurately placed more simulated fossils than the parsimony analysis and with higher support. The inclusion of fossils can therefore be done with confidence as long as there are not too many of them in any one analysis.

4. Using a new morphological dataset to test the phylogenetic placement of fossil salamanders

4.1 Introduction

Although the earliest Salientia fossils are known from the Early Triassic, salamanders do not appear in the fossil record until the Middle Jurassic (See Chapter 1 section 1.4). There are several stem-group salamanders: *Karaurus sharovi*, *Kokartus honorarius*, *Urupia monstrosa*, *Marmorerpeton kermacki*, and *Marmorerpeton freemani*, however their position in relation to crown-group salamanders has yet to be tested all together. Skutschas (2011) suggested that *Urupia* could not be placed in a phylogenetic analysis based on the available material (i.e. atlantal centrum, presacral fragments and associated elements of dentaries and broken femur) but the new data set presented in this thesis has demonstrated the potential to place simulated fossils with reduced characters relatively accurately to Cryptobranchoidea and Salamandroidea-level. These early fossils lack key derived characters such as an enclosed nerve foramen in the atlas and so have been placed on the stem of Caudata (see table 1.1).

All stem salamanders used to be attributed to the family Karauridae (Skutschas and Martin 2011) but this is now thought to be a paraphyletic grouping (Evans *et al.* 2005; Averianov *et al.* 2008). *Marmorerpeton* was excluded from Karauridae by Skutschas and Martin (2011) because it had weak or no sculpture on the premaxilla and maxilla and bicuspid teeth, whereas *Karaurus* and *Kokartus* both have monocuspid teeth. *Marmorerpeton* further differs from *Kokartus* by having a circular dentary symphysis (it is rectangular in *Kokartus*) (Skutschas and Martin 2011). All Karauridae and other stem group salamanders are thought to be aquatic, and so this might have been the ancestral life strategy for the Caudata (Skutschas and Martin 2011; Skutschas and Krasnolutskii 2011). The placement of these Middle Jurassic fossils in a phylogeny might lead to the elucidation of early salamander biogeographic and diversification patterns.

Although many of the Late Jurassic and Cretaceous salamanders have been included in phylogenetic analyses, either in matrices which have included other fossil salamanders or exclusively extant taxa, very few of these analyses have used the same character set or phylogenetic method. It has been demonstrated that the inclusion of multiple simulated fossils (chapter 3) results in lower phylogenetic resolution but the analysis of individual taxa results in a high chance of the “correct” placement of the simulated fossil to either Cryptobranchoidea or Salamandroidea. As a result, we can have some confidence when actual fossils are included in a phylogenetic analysis using this dataset, that they will be placed relatively accurately at a high taxonomic level. This study will aim to place Mesozoic fossil salamanders using the tested dataset and the same method as in previous chapters (2 and 3), and compare the results with those of previously published phylogenies or hypothesised affinities.

4.2 Material and Methods

The placement of Mesozoic fossil salamanders is analysed using the newly tested RI dataset within a Bayesian framework. The results of chapter three showed that simulated fossils were placed relatively accurately (although some were based on reconstructed characters) together with their closest relatives according to the molecular evidence and also exhibited the least amount of stem-ward slippage as long as a close relative was included (although the simulated fossils were often placed in unresolved relationships with other clades). The same settings and constraints used in Bayesian analyses of previous chapters (three and four) were applied. These constraints did not apply to the fossils and they were free to fall anywhere except within frogs or caecilians (although they could be placed as the sister taxon to either).

Total evidence analyses were also performed using the nuclear DNA and the RI morphological dataset to test the placement of the fossils as a whole. The settings for MrBayes were exactly the same as in all the previous Bayesian analyses using nDNA but with one addition: a partial constraint was used that separated the outgroups and the extant salamanders while still allowing the fossils to fall anywhere in the topology.

4.3 Phylogenetic results of Bayesian analysis of the RI dataset

4.3.1 Stem-group fossils

When *Karaurus*, *Kokartus*, *Urupia monstrosa*, and *Marmorerpeton* were analysed individually none of them were placed as the sister taxon to all other salamanders (i.e. neither taxon was placed on the stem of Caudata). When all stem-group taxa were analysed together the putative stem-caudate taxa are unresolved within Amphibia, with *Urupia monstrosa* emerging as the sister taxon to frogs. *Kokartus* and *Karaurus* were not placed within a monophyletic Karauridae.

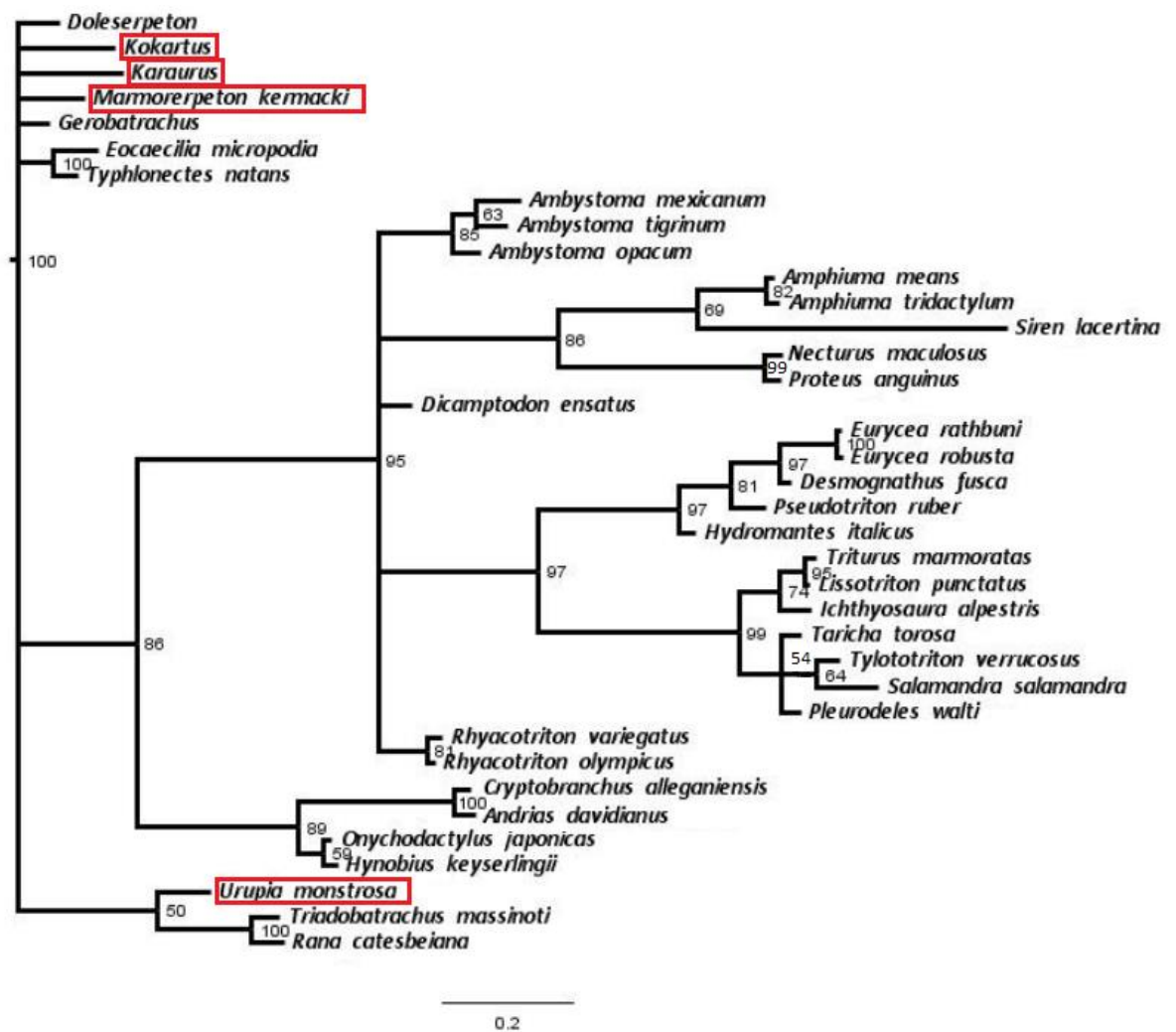


Figure 4.1: Consensus tree from a Bayesian analysis of the RI dataset with extant taxa and the stem-group fossils. The analysis ran for 2000000 generations, resulting in an average standard deviation of split frequency value of 0.005323; av Ess: 749.44; PSRF+: 1.000

4.3.2 Scapherpetontidae:

Scapherpeton is placed in an unresolved relationship with Cryptobranchidae, Hynobiidae, and Salamandroidea. *Scapherpeton* shares a fully enclosed atlantal foramen and four-faceted articulation of exoccipital and atlas with the other Urodela taxa. It also shares bicapitate ribs with Salamandroidea (except *Siren*).

Lisserpeton is placed outside of the crown group Urodela, in an unresolved amphibian position, when analysed without other Scapherpetontidae taxa. *Lisserpeton* does however share a fully enclosed atlantal foramen with Urodela. *Lisserpeton* also shares bicapitate transverse processes with Salamandroidea (except *Siren*), and has a small ventral keel on presacral vertebrae like *Siren* and an anterodorsal keel on the transverse process like Salamandridae and *Siren*.

Eoscapherpeton is placed in an unresolved relationship with *Cryptobranchus* and *Andrias* within Cryptobranchidae. It shares unicapitate ribs with Cryptobranchidae and Hynobiidae.

The *Piceoerpeton* species do not form a monophyletic group and instead *Piceoerpeton naylori* is placed as sister taxon to *Siren lacertina*, while *Piceoerpeton willwoodense* is placed in an unresolved relationship with Proteidae, Amphiumidae and *Piceoerpeton naylori* + *Siren*. Both *Piceoerpeton* species share the presence of a large ventral keel on the presacral vertebrae with *Siren*. *P. naylori* shares a reduced odontoid process with Proteidae (*P. willwoodense* was uncoded for this character).

When all the fossils previously assigned to the Scapherpetontidae were analysed together they do not form a monophyletic group. *Eoscapherpeton* is placed as the sister taxon to Cryptobranchidae and *Scapherpeton* is still placed outside Salamandroidea, in an unresolved relationship with Salamandroidea, Cryptobranchidae + *Eoscapherpeton*, and Hynobiidae. *Lisserpeton* is now placed in an unresolved relationship with Cryptobranchidae + *Eoscapherpeton*, *Scapherpeton*, Hynobiidae, and Salamandroidea, within Urodela. *Piceoerpeton* is placed in exactly the same place as when it was analysed individually and is the only member of the Scapherpetontidae to be placed within Salamandroidea.

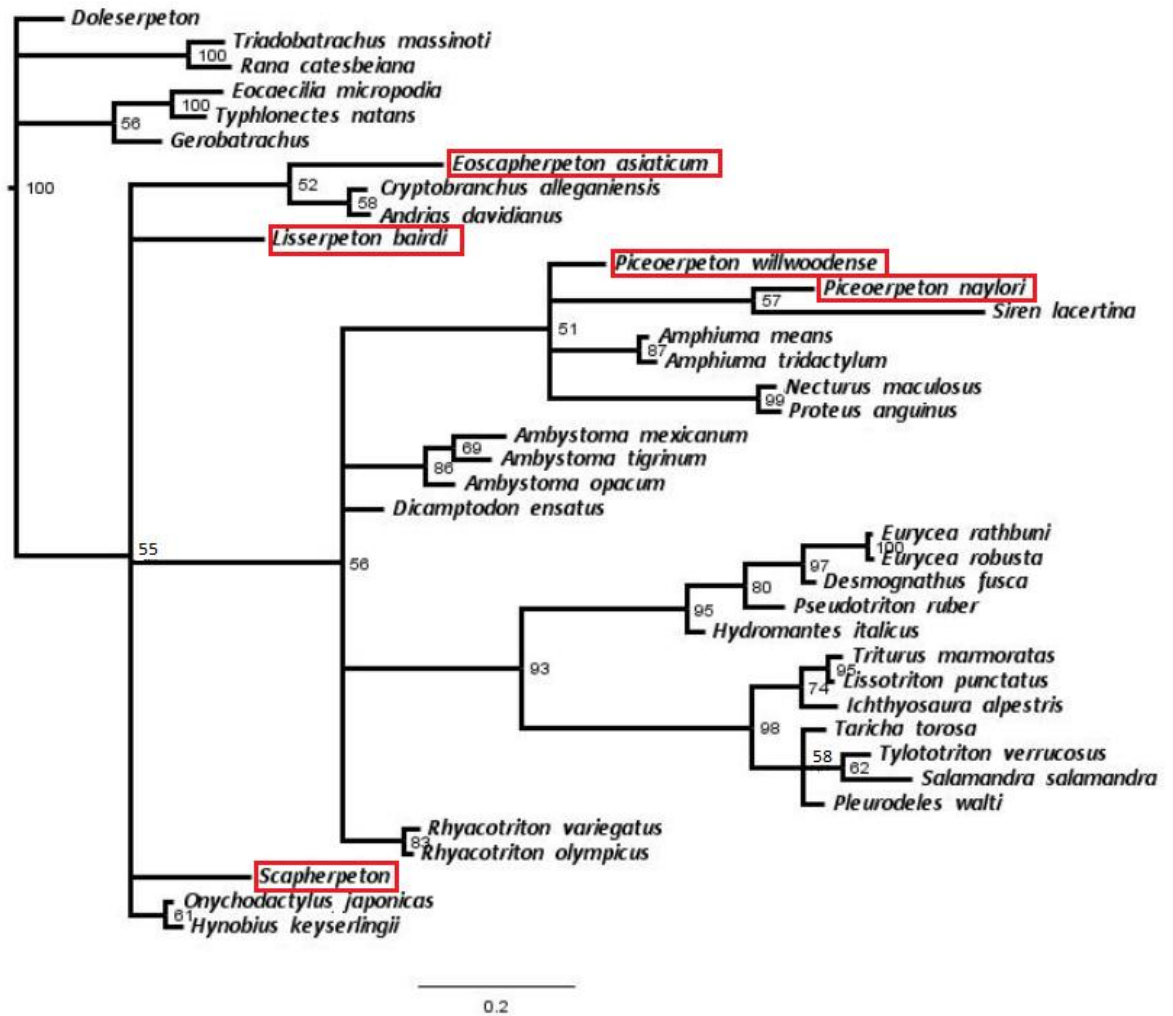


Figure 4.2: Consensus tree from a Bayesian analysis of the RI dataset with extant taxa and all Scapherpetontidae. The analysis ran for 2000000 generations, resulting in an average standard deviation of split frequency value of 0.008791; av Ess: 693.44; PSRF+: 1.000

4.3.3. Batrachosauroididae:

Opisthotriton is placed within Salamandroidea in an unresolved relationship with *Siren*, *Amphiuma*, and Proteidae. It shares an atlas that has an enclosed spinal nerve foramen with Urodela, lacks free ribs on anterior caudal vertebrae like the other Salamandroidea, and shares a reduced odontoid process with Proteidae.

Parrisia is placed in an unresolved relationship with the Salamandridae. It shares an enclosed atlantal spinal nerve foramina with Urodela, bicapitate transverse processes with Salamandroidea (except *Siren*), a reduced odontoid process with Proteidae, opisthocelous presacral centra with Salamandridae, and a subcentral keel on the presacral vertebrae with *Siren*.

Prodesmodon has been placed as the sister taxon to Urodela. It shares unicapitate transverse processes with Cryptobranchoidea, a mid-ventral keel on the presacral vertebrae with *Siren*, opisthocoelous presacral centra with Salamandridae, and a reduced odontoid process with Proteidae and other Batrachosauroidae.

When Mesozoic Batrachosauroididae are analysed together they are all placed within Salamandroidea, although they do not form a monophyletic group. Batrachosauroididae (except *Prodesmodon*) share the presence of an atlantal spinal nerve foramen with Urodela. They all lack four faceted articulations of the exoccipital and atlas due to the reduction of the odontoid process. Batrachosauroididae also shares a massively reduced odontoid process with Proteidae. *Parrisia* and *Prodesmodon* share opisthocoelous presacral centra with Salamandridae, and a large mid-ventral keel on the presacral vertebrae with *Siren*.

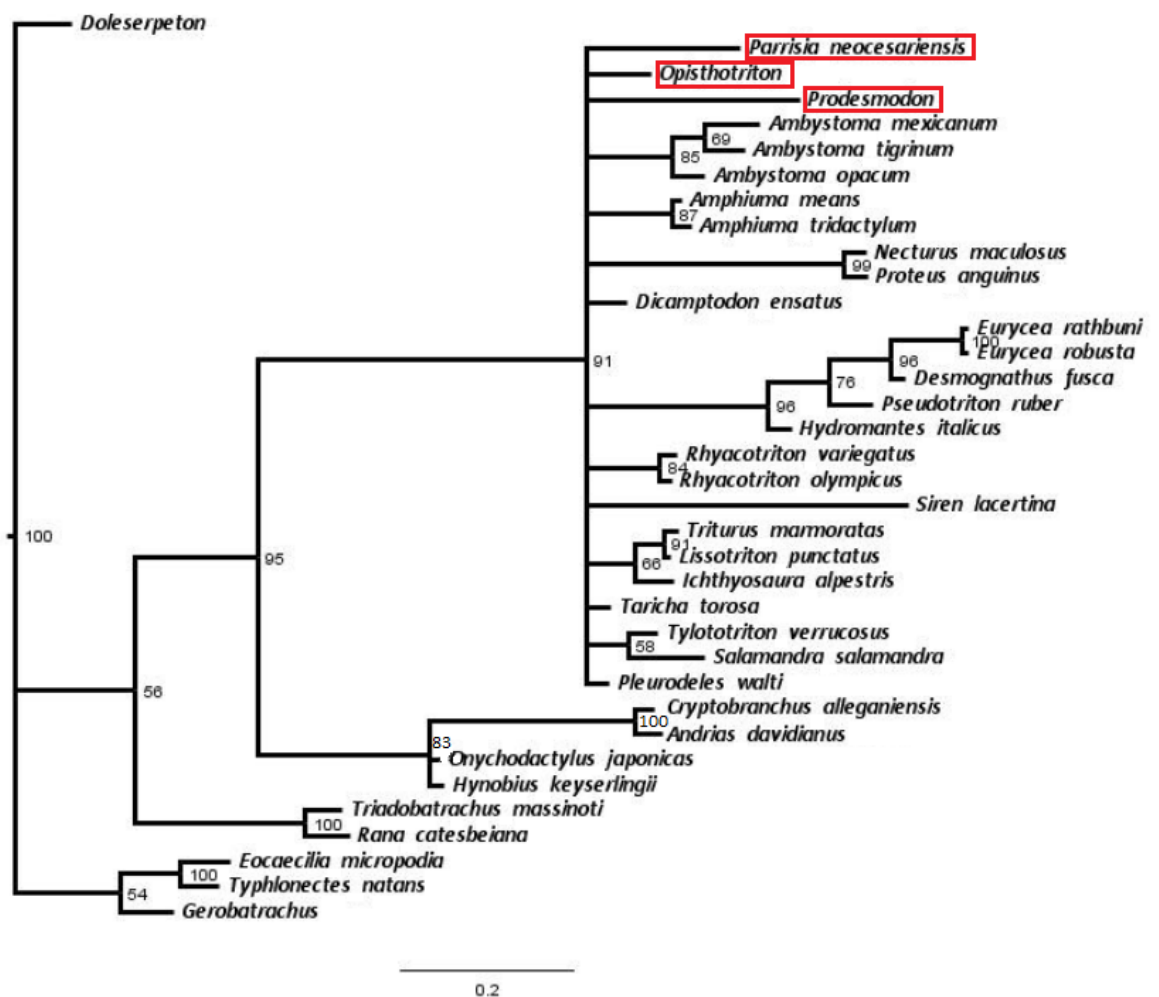


Figure 4.3: Consensus tree from a Bayesian analysis of the RI dataset with extant taxa and all Batrachosauroididae. The analysis ran for 4000000 generations, resulting in an average standard deviation of split frequency value of 0.007779; av Ess: 1470.88; PSRF+: 1.000

4.3.4. Sirenidae-like fossils:

The two *Kababisha* species and *Noterpeton bolivianum* form a monophyletic group which is placed in an unresolved position within Amphibia. *Kababisha* lacks an atlantal spinal nerve foramen and four faceted articulations on the exoccipital and atlas, which are features common to Urodela. However, the absence of the exoccipital-atlantal articulation character may not be significant as both *Kababisha* possess a highly reduced form of the odontoid process, which also occurs in Proteidae and *Siren*. Both *Kababisha* and *Noterpeton* share a lack of postatlantal ribs with *Siren*. They also share the presence of a mid-ventral keel with *Amphiuma means*. *Noterpeton* shares a Meckel's cartilage that extends to the mandibular symphysis with *Ambystoma*. *Kababisha sudanensis* and *Noterpeton* both possess a procoelous presacral centra.

Habrosaurus is placed within Salamandroidea but in an unresolved relationship with *Amphiuma*, Proteidae, (Salamandridae + Plethodontidae), *Rhyacotriton*, and *Siren*. *Habrosaurus* shares a mid-ventral keel on the presacral vertebrae with *Siren*, and a fenestra in the anterior keel of the presacral vertebrae with *Siren* and Salamandridae.

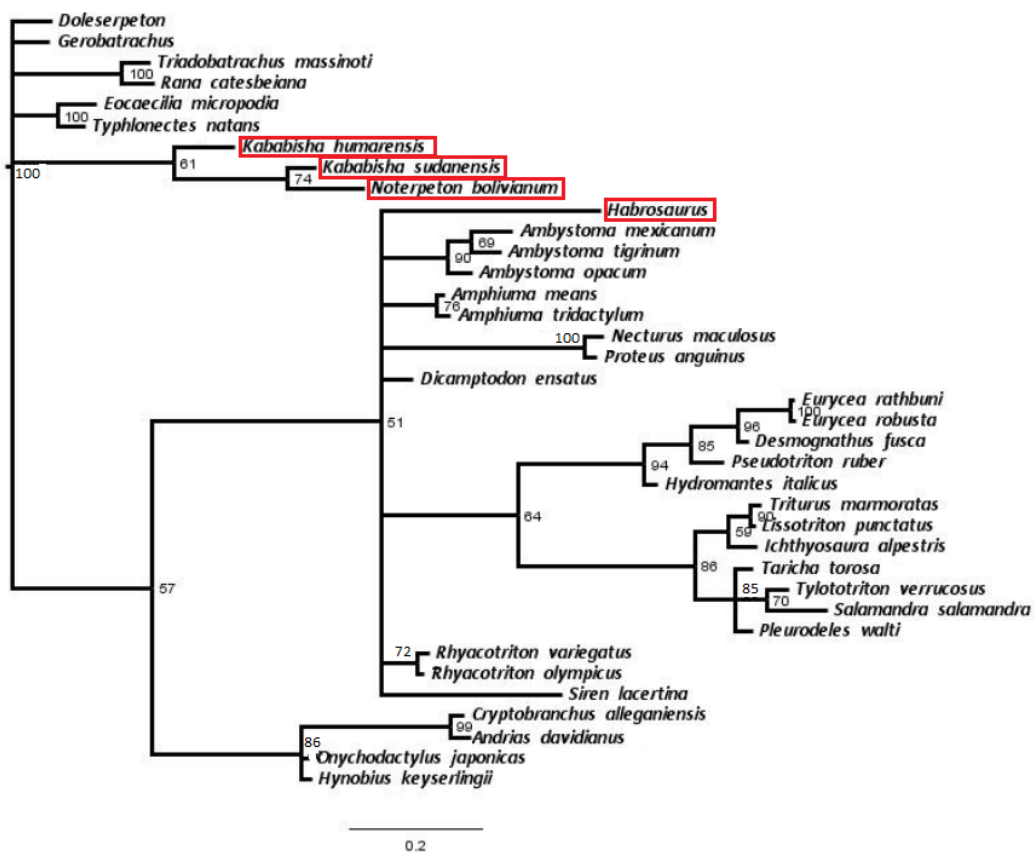


Figure 4.4: Consensus tree from a Bayesian analysis of the RI dataset with extant taxa, *Habrosaurus*, *Kababisha* and *Noterpeton*. It ran for 4000000 generations, resulting in an average standard deviation of split frequency value of 0.007605; av Ess: 1489.21; PSRF+: 1.000

When all the fossils that have previously been associated with Sirenidae are analysed, together they fall in exactly the same place as they did when analysed separately. They do not form a monophyletic group with one another, or with *Siren*.

4.3.5 Fossil salamanders that have previously been placed outside of Salamandroidea:

Regalerpeton is placed as the sister taxon to Cryptobranchoidea, with which it shares unicapitate ribs.

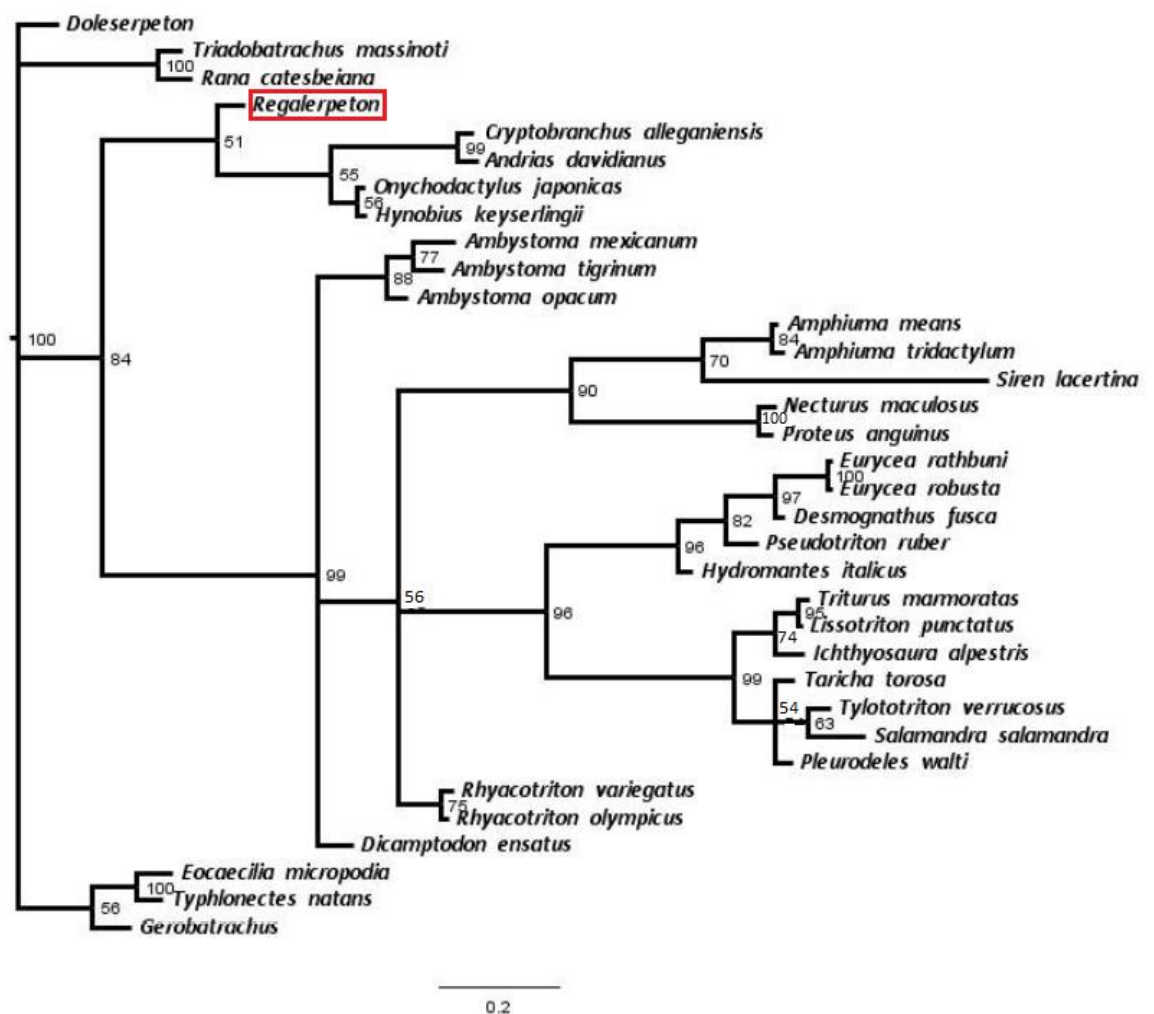


Figure 4.5: Consensus tree from a Bayesian analysis of the RI dataset with extant taxa and *Regalerpeton*. It ran for 2000000 generations, resulting in an average standard deviation of split frequency value of 0.005614; av Ess: 677.21; PSRF+: 1.000

Pangerpeton is placed as the sister taxon to Salamandroidea. It possesses uncapitate ribs which also occurs in Cryptobranchoidea, and the presence of one phalanx on digit one of the pes with Plethodontidae + *Salamandra salamandra*.

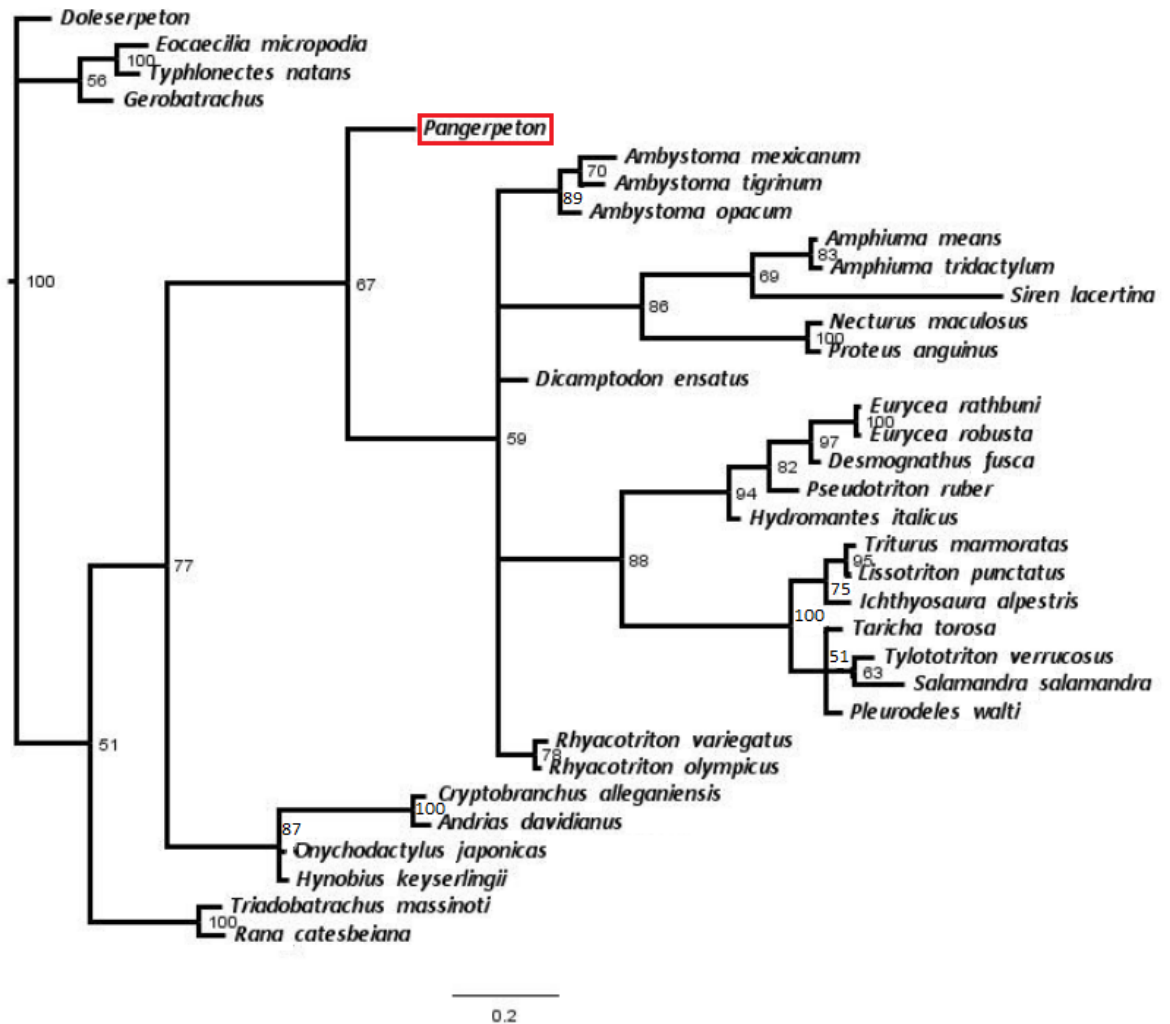


Figure 4.6: Consensus tree from a Bayesian analysis of the RI dataset with extant taxa and *Pangerpeton*. It ran for 2000000 generations, resulting in an average standard deviation of split frequency value of 0.005572; av Ess: 908.26; PSRF+: 1.000

Chunerpeton is placed in an unresolved relationship with Salamandroidea, Cryptobranchidae, and the two Hynobiidae species. It shares a multi-branched, second basibranchial morphology with *Siren*, and uncapitate ribs with Cryptobranchoidea.

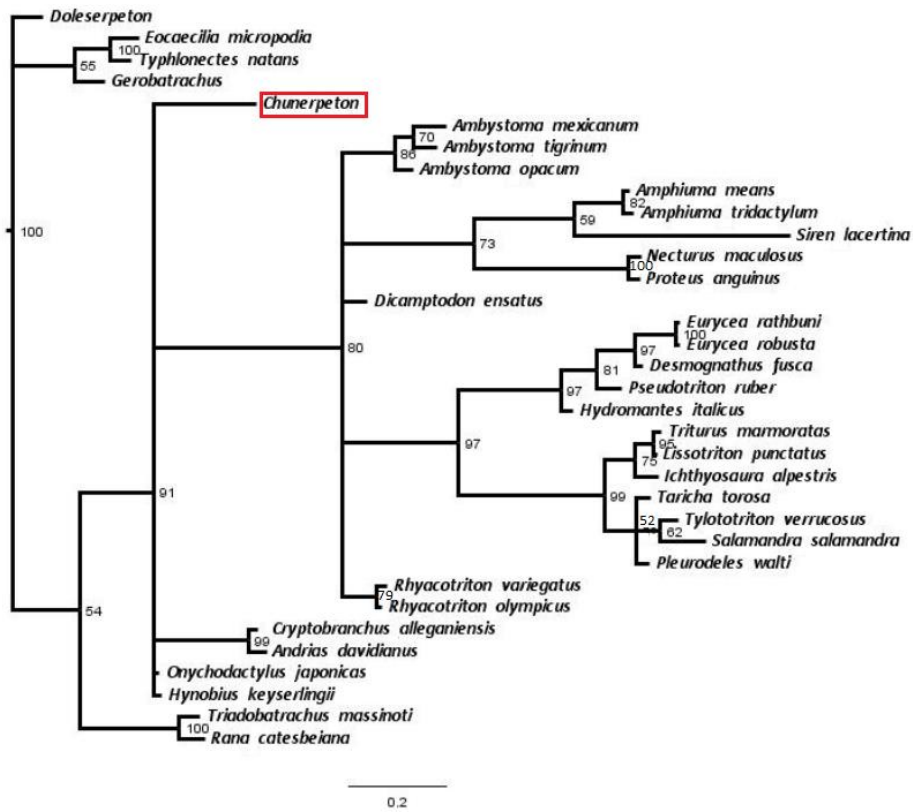


Figure 4.7: Consensus tree from a Bayesian analysis of the RI dataset with extant taxa and *Chunerpeton*. It ran for 2000000 generations, resulting in an average standard deviation of split frequency value of 0.006845; av Ess: 626.98; PSRF+: 1.000

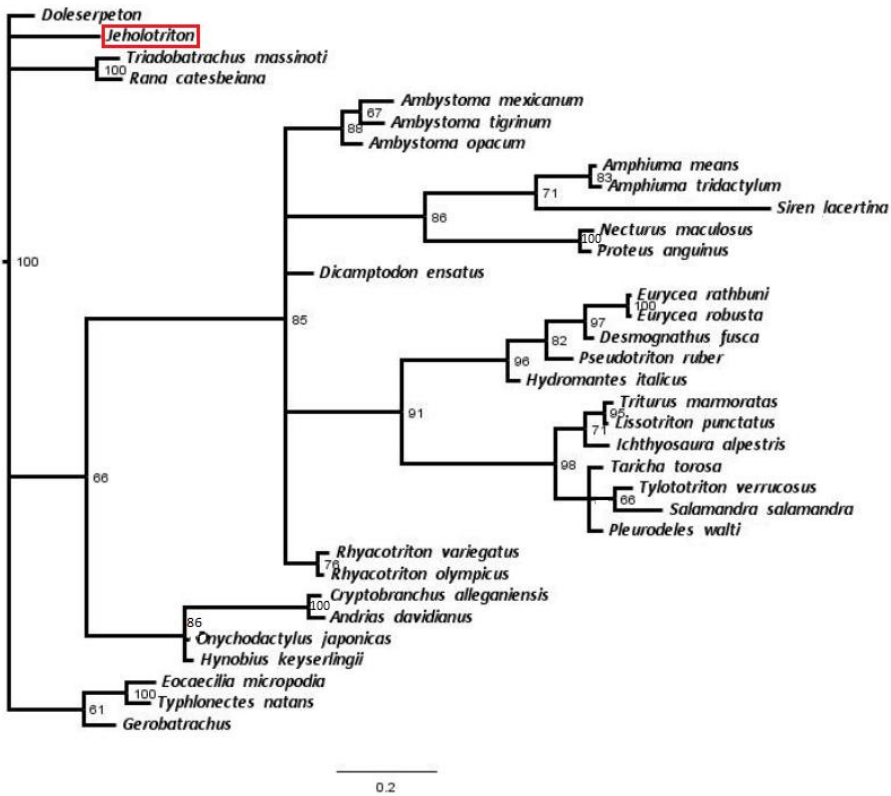


Figure 4.8: Consensus tree from a Bayesian analysis of the RI dataset with extant taxa and *Jeholotriton*. The analysis resulted in an average standard deviation of split frequency value of 0.006984

Jeholotriton is placed outside of Urodela in an unresolved position within Amphibia (Fig. 4.7) *Liaoxitriton zhongjiani* and *Liaoxitriton daohugouensis* do not form a monophyletic group (Fig. 4.8). They are placed separately in an unresolved relationship with Salamandroidea and Cryptobranchoidea. *Liaoxitriton zhongjiani* and *Liaoxitriton daohugouensis* differ in that *L. zhongjiani* has a vomer with a postchoanal process and *L. daohugouensis* lacks the postchoanal process. They both share unicapitate ribs with Cryptobranchoidea.

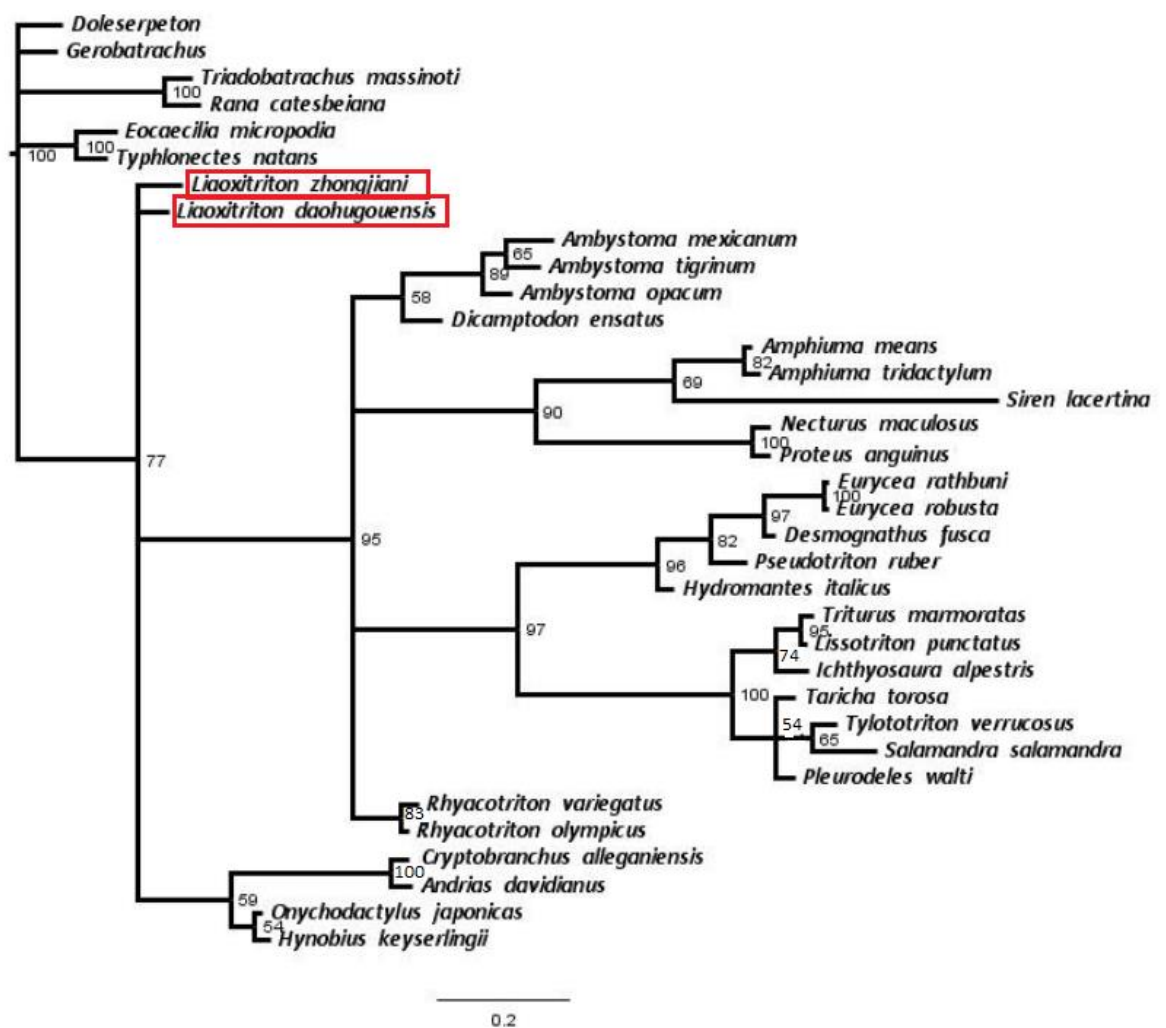


Figure 4.9: Consensus tree from a Bayesian analysis of the RI dataset with extant taxa and *Liaoxitriton*. The analysis ran for 2000000 generations, resulting in an average standard deviation of split frequency value of 0.007875; av Ess: 762.79; PSRF+: 1.000

Nesovtriton is placed in an unresolved relationship with Salamandroidea, Cryptobranchidae, and the two Hynobiidae species. It shares uncapitate transverse processes with Cryptobranchoidea. *Nesovtriton* shares basapophyses on the atlas with *Ambystoma* and *Desmognathus*. It differs from all other Urodela by its lack of a four faceted articulation of exoccipital and atlas.

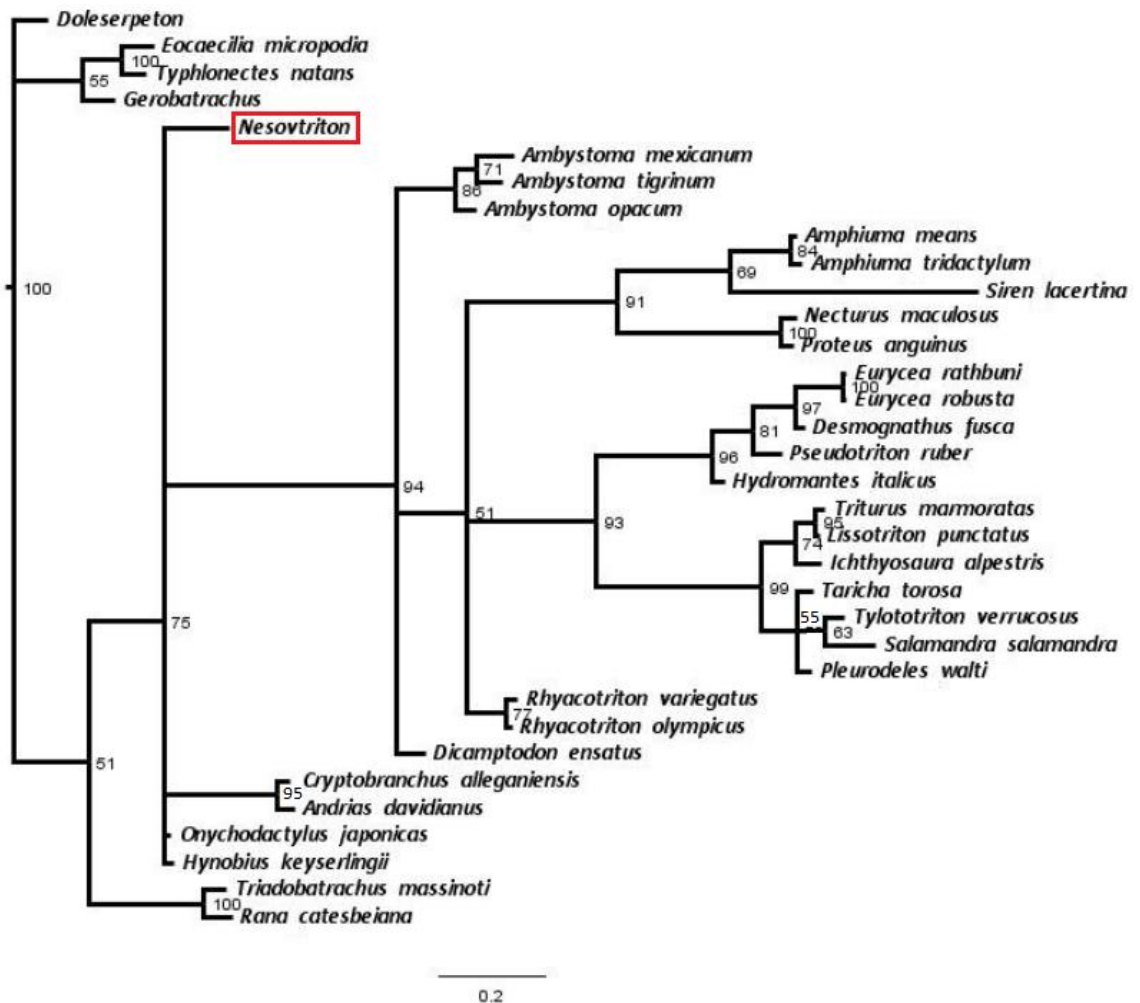


Figure 4.10: Consensus tree from a Bayesian analysis of the RI dataset with extant taxa and *Nesovtriton*. The analysis ran for 2000000 generations, resulting in an average standard deviation of split frequency value of 0.007419; av Ess: 754.71; PSRF+: 1.000

Iridotriton is placed in a trichotomy with Salamandroidea and Cryptobranchoidea. It shares uncapitate ribs with Cryptobranchoidea. *Iridotriton* also possesses a fused prootic-exoccipital with separate opisthotic, as does Proteidae.

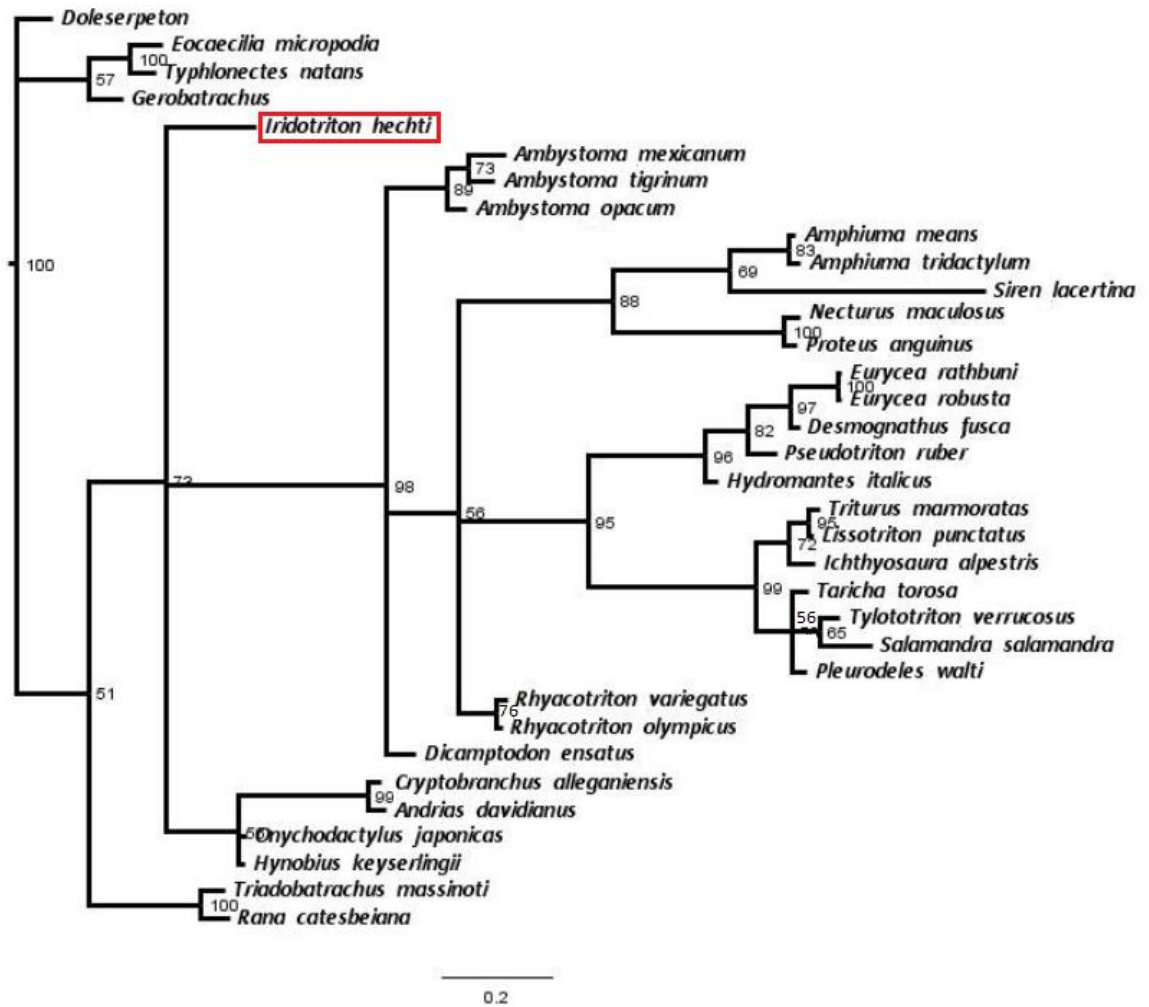


Figure 4.11: Consensus tree from a Bayesian analysis of the RI dataset with extant taxa and *Iridotriton*. The analysis ran for 3673400 generations, resulting in an average standard deviation of split frequency value of 0.007027; av Ess: 1064.52; PSRF+: 1.000

When all of these Mesozoic fossil salamanders that have previously been placed outside of Salamandroidea are analysed together form a polytomy with Salamandroidea, *Doleserpeton*, caecilians + *Gerobatrachus*, frogs, Cryptobranchidae, and Hynobiidae.

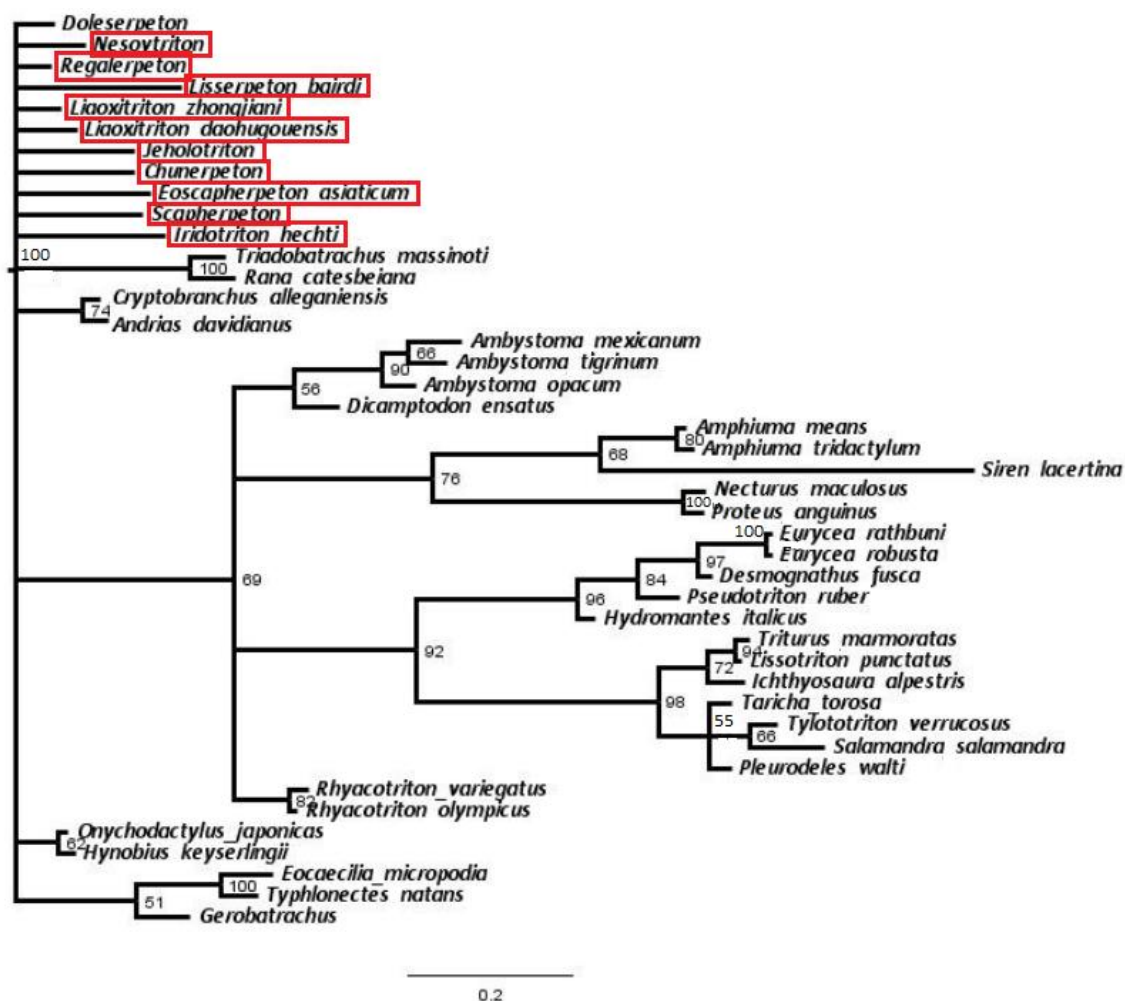


Figure 4.12: Consensus tree from a Bayesian analysis of the RI dataset with extant taxa and all fossils previously placed outside of Salamandroidea (and not assigned to Batrachosauroididae or Scapherpetontidae). The analysis ran for 4000000 generations, resulting in an average standard deviation of split frequency value of 0.005408; av Ess: 1340.54; PSRF+: 1.000

4.3.6 Fossils previously assigned to Salamandroidea:

Valdotriton is placed within Salamandroidea in an unresolved position. It lacks a distinct angular and has no free ribs on anterior caudal vertebrae, which are two characters it has in common with the other taxa in Salamandroidea. *Valdotriton* also shares bicapitate transverse processes with all other Salamandroidea except *Siren*. It possesses spinal nerves that exit intravertebrally in some or all caudal vertebrae, which is a character it has in common with *Amphiuma*, *Dicamptodon*, and *Rhyacotriton*. *Valdotriton* shares a Y-shaped second basibranchial with *Ambystoma tigrinum* and *Dicamptodon*, also basapophyses on the atlas with *Ambystoma* and *Desmognathus*.

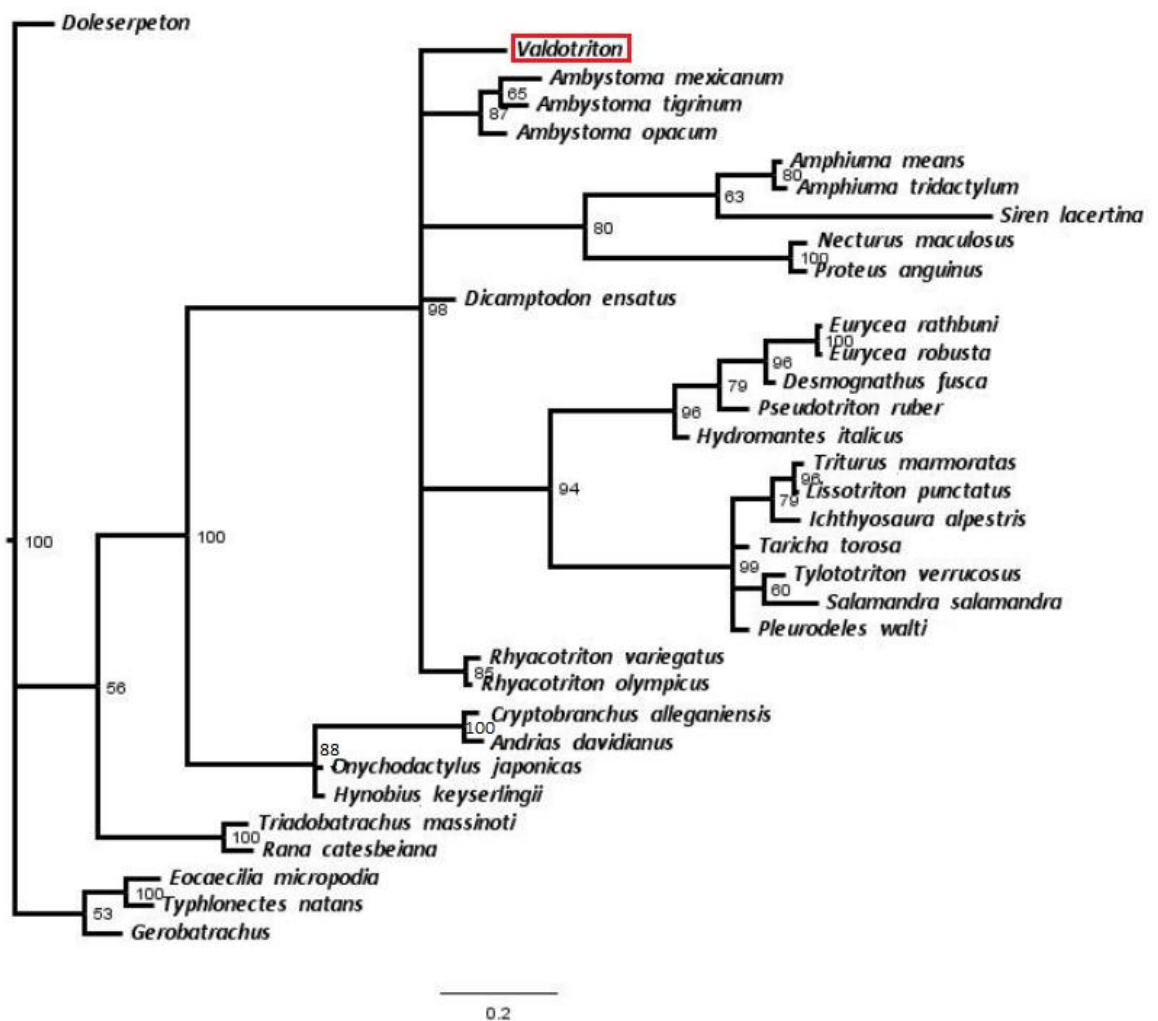


Figure 4.13: Consensus tree from a Bayesian analysis of the RI dataset with extant taxa and *Valdotriton*. The analysis ran for 2000000 generations, resulting in an average standard deviation of split frequency value of 0.005532; av Ess: 716.21; PSRF+: 1.000

Proamphiuma is placed as the sister taxon to *Siren lacertina* with *Amphiuma* forming their sister clade. *Proamphiuma* shares bicapitate transverse processes with the other taxa in Salamandroidea, the presence of a mid-ventral keel on the presacral vertebrae with *Siren*, and intravertebral spinal nerve foramina in some or all caudal vertebrae with *Amphiuma*, *Rhyacotriton*, and *Dicamptodon*.

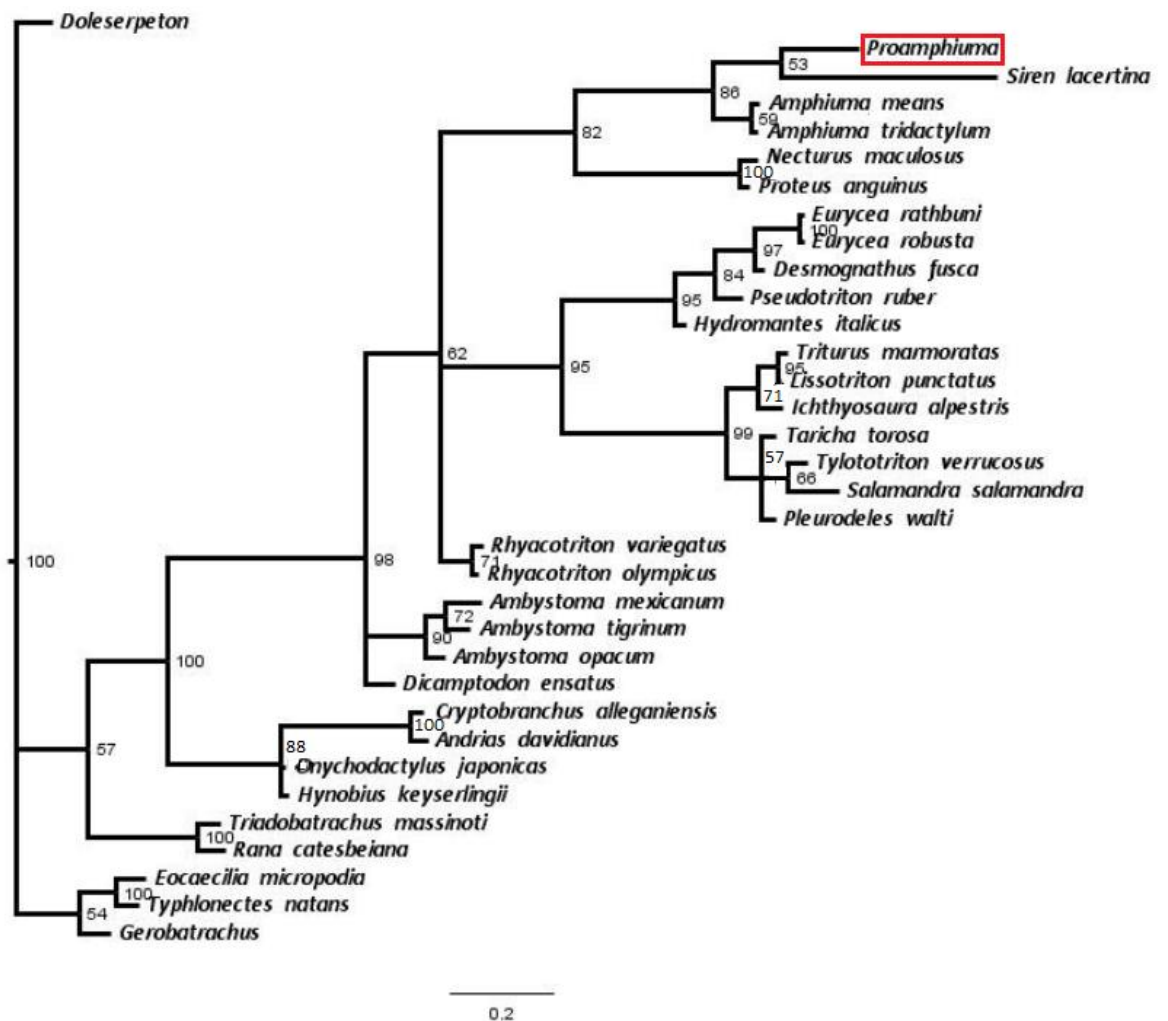


Figure 4.14: Consensus tree from a Bayesian analysis of the RI dataset with extant taxa and *Proamphiuma*. The analysis ran for 2000000 generations, resulting in an average standard deviation of split frequency value of 0.005250; av Ess: 764.13; PSRF+: 1.001

Paranecturus has been placed within Salamandroidea in a polytomy with *Amphiuma*, Proteidae, and *Siren lacertina*. The fossil taxon has a four faceted articulation of the exoccipital and atlas like the other Urodela, and bicapitate transverse processes like all other Salamandroidea except *Siren*. *Paranecturus* shares the presence of a mid-ventral keel on mid-body presacrals with *Siren*.

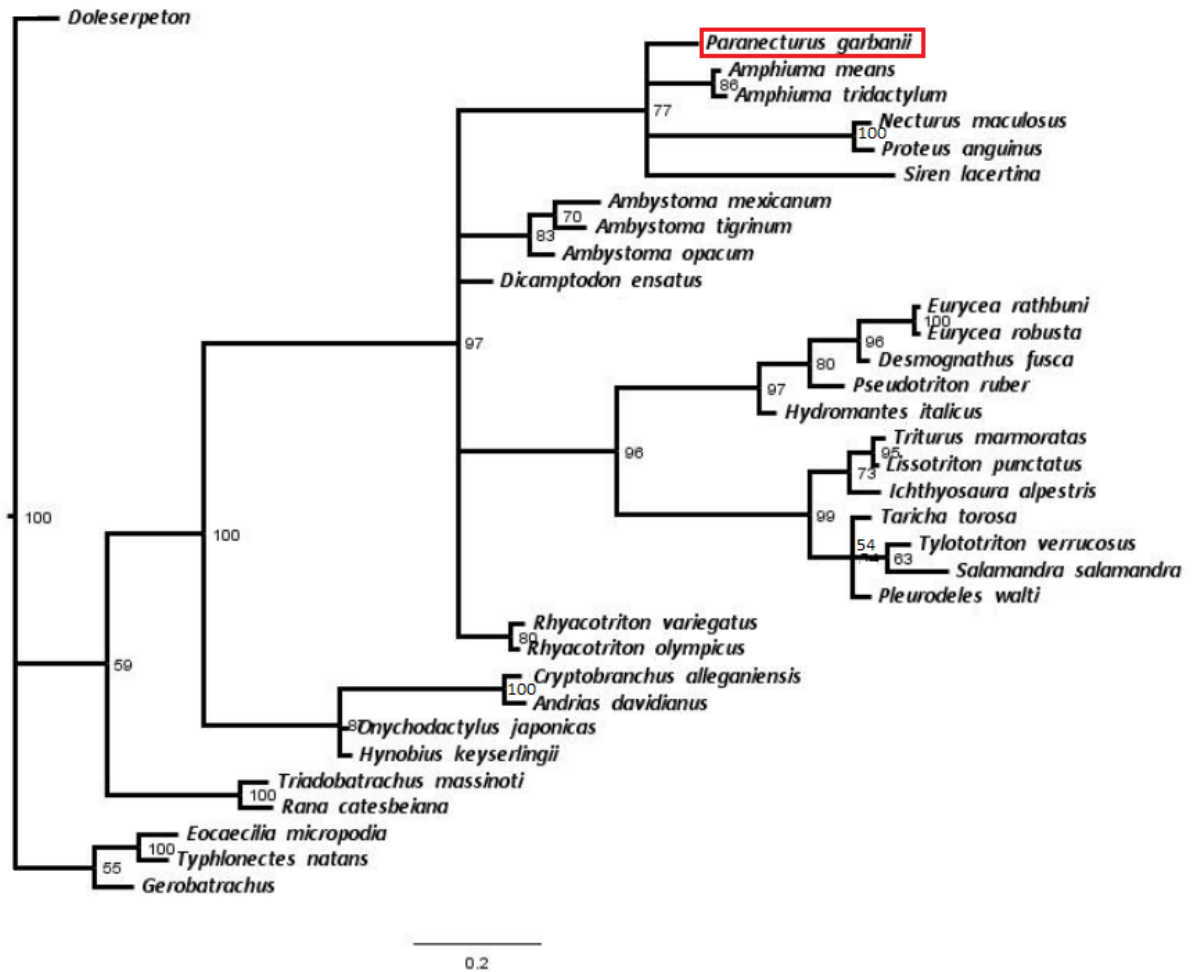


Figure 4.15: Consensus tree from a Bayesian analysis of the RI dataset with extant taxa and *Paranecturus*. The analysis ran for 2000000 generations, resulting in an average standard deviation of split frequency value of 0.003865; av Ess: 721.26; PSRF+: 1.000

Beiyanerpeton is placed as sister taxon to Salamandroidea, in exactly the same place as the results of the study by Gao and Shubin (2012). *Beiyanerpeton* shares a mid-ventral keel on the presacral vertebrae with *Siren*.

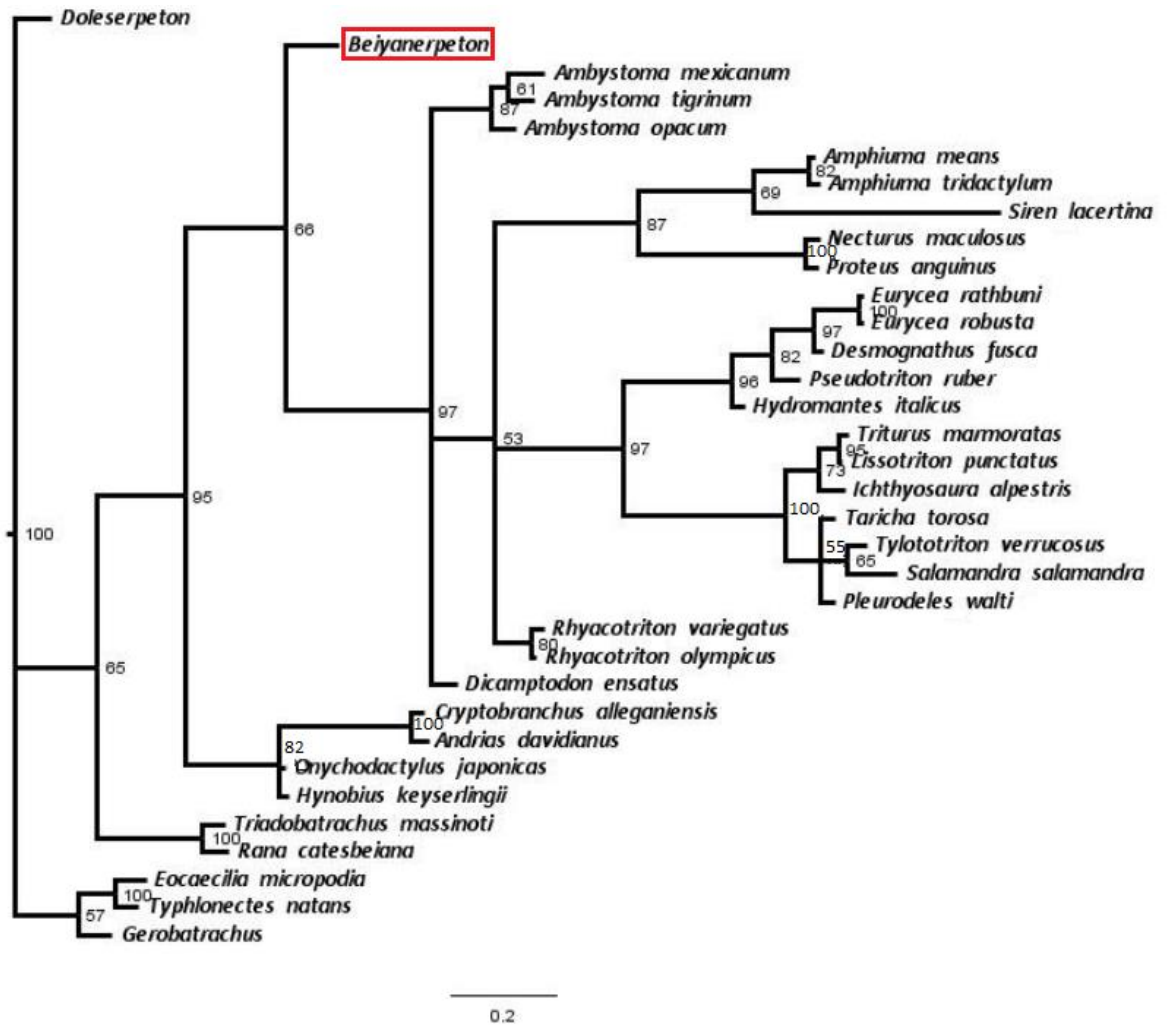


Figure 4.16: Consensus tree from a Bayesian analysis of the RI dataset with extant taxa and *Beiyanerpeton*. The analysis ran for 3000000 generations, resulting in an average standard deviation of split frequency value of 0.004418; av Ess: 1115.71; PSRF+: 1.000

Galverpeton is placed as the sister taxon to Salamandridae + Plethodontidae, within Salamandroidea in exactly the position hypothesised by Estes and Sanchiz (1982). *Galverpeton* shares opisthocoelous vertebrae with Salamandridae, and spinal nerves that exit intravertebrally in some presacral vertebrae with *Ambystoma*.

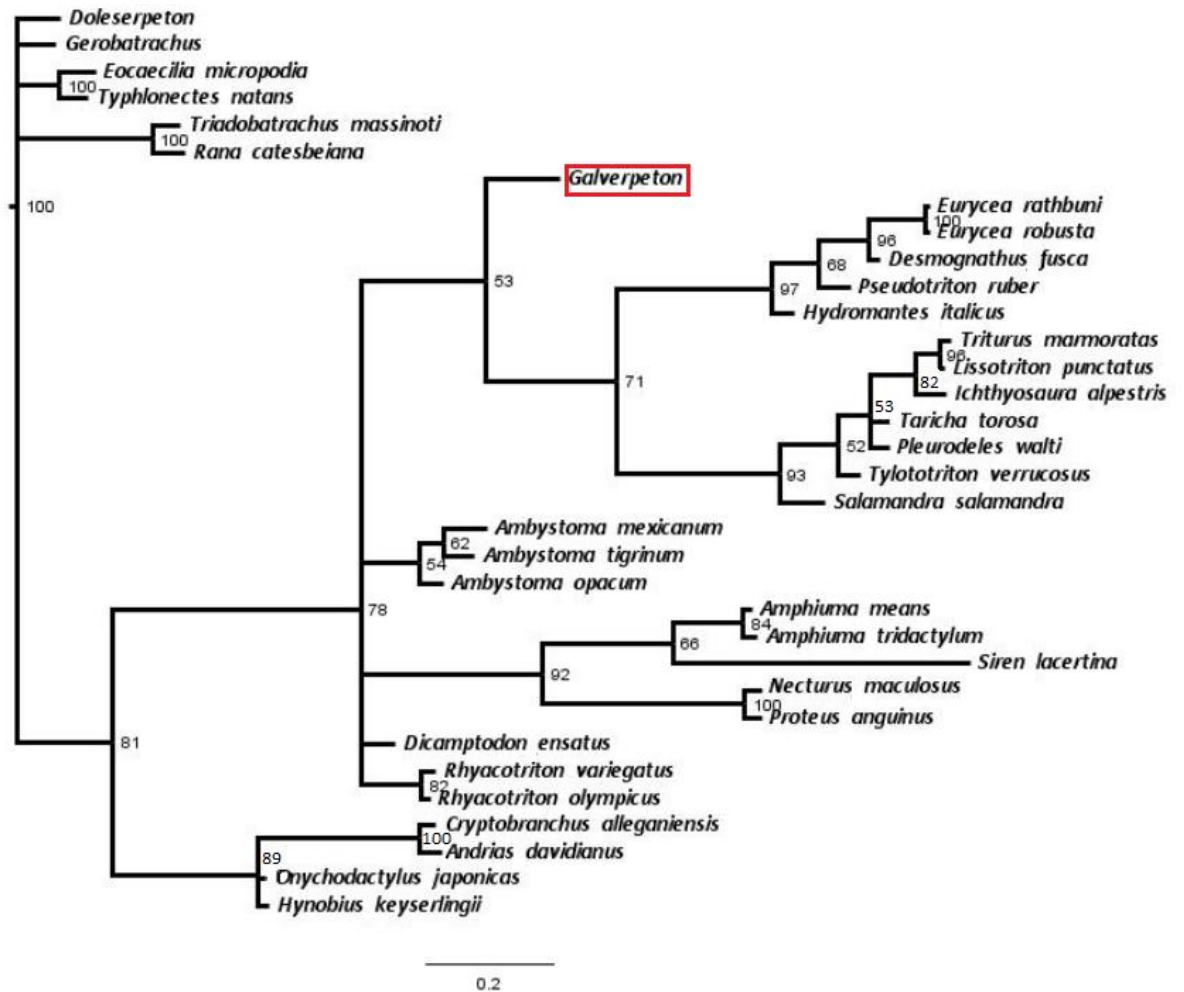


Figure 4.17: Consensus tree from a Bayesian analysis of the RI dataset with extant taxa and *Galverpeton*. The analysis ran for 2000000 generations, resulting in an average standard deviation of split frequency value of 0.006500; av Ess: 622.76; PSRF+: 1.000

Figure 4.18 is a tree with all the Mesozoic salamander fossils that have previously been placed within Salamandroidea (or as a stem Salamandroidea taxon). *Opisthotriton*, both *Piceoerpeton* species, *Parissia*, *Prodesmodon*, *Valdotriton*, *Paranecturus*, *Proamphiuma*, *Habrosaurus* are all placed within Salamandroidea. *Beiyanerpeton* is placed on the stem of Salamandroidea.

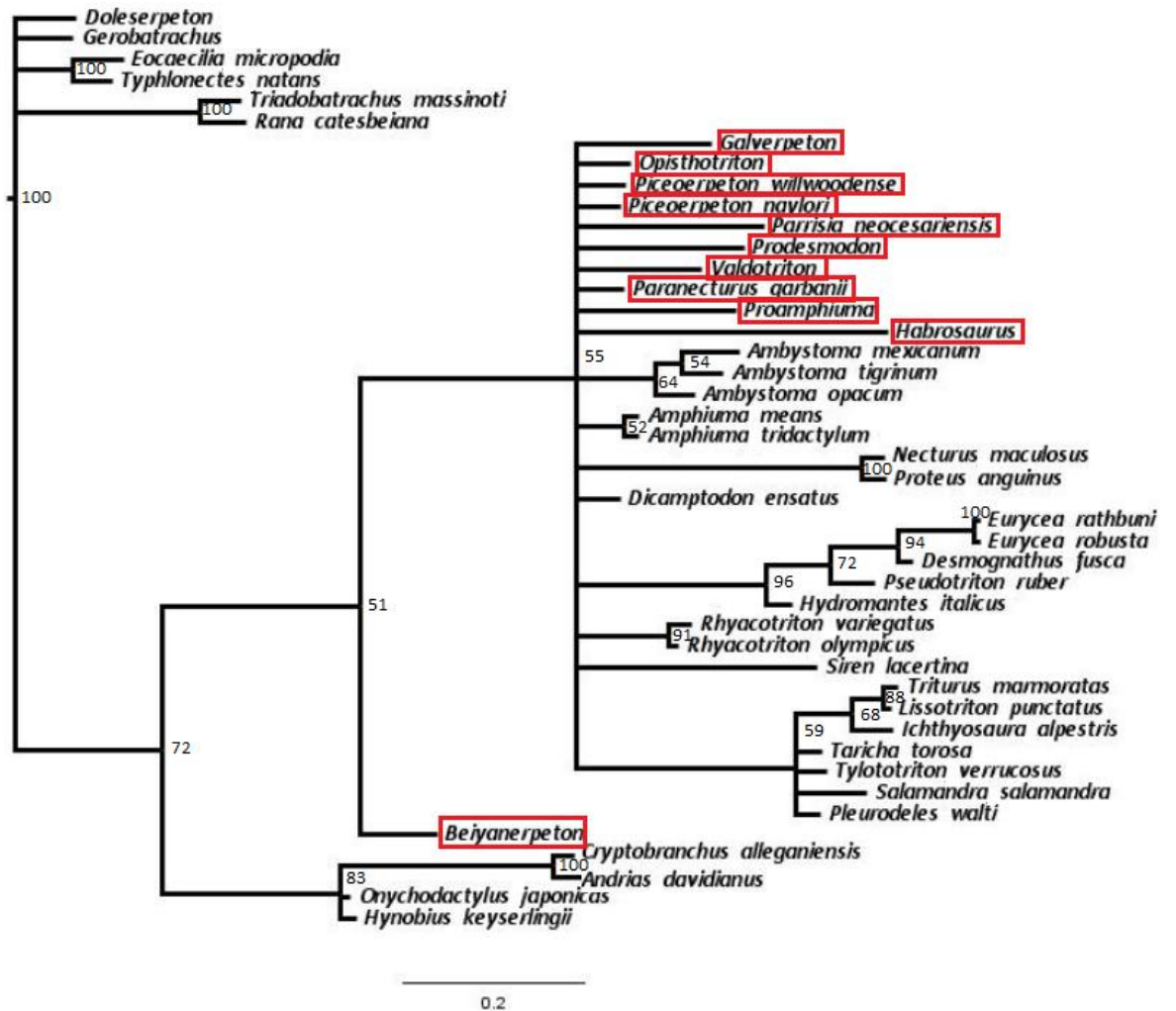


Figure 4.18: Consensus tree from a Bayesian analysis of the RI dataset with extant taxa and fossils previously attributed to Salamandroidea. The analysis ran for 2000000 generations, resulting in an average standard deviation of split frequency value of 0.006500; av Ess: 622.76; PSRF+: 1.000

4.4 Discussion

In this new analysis, many of the Mesozoic fossil salamanders have been placed in relatively unresolved positions. The putative stem-group salamanders (*Karaurus*, *Kokartus*, *Marmorerpeton*, and *Urupia*) have not been placed on the stem of Caudata as was expected based on previously published studies (Evans *et al.* 1988; Ruta *et al.* 2003; Skutschas and Martin 2011). Previous phylogenetic analyses also placed *Karaurus* and *Kokartus* as sister taxa in a monophyletic Karauridae and placed this family as sister to crown group salamanders (Skutschas and Martin 2011). The study presented here does not recover a monophyletic Karauridae or place any of the putative stem group fossils as sister to all salamanders. The dermal sculpture on the skull (Estes 1981) character was removed by the tree dependant and tree independent methods of character evaluation, as it was deemed to display a high level of convergence. This dermal sculpture character needs further evaluation as there is certainly evidence of dermal sculpture on skull bones of some derived Urodela [e.g. *Tylototriton* (Noble 1928)]. However, this is not a suggestion that these taxa (*Karaurus* and *Kokartus*) are not more closely related to salamanders than to other lissamphibians, but alternative characters are needed in the current matrix to determine if these taxa really do lie on the stem of Caudata. The results presented here are almost certainly due to a resolution issue. The results for *Urupia* may also reflect a resolution issue because only 11 characters for this taxon survived the character evaluation process, and only eight of these were vertebral characters. Skutschas and Krasnolutsii (2011) were probably correct in suggesting further phylogenetic analysis wait until more material is found for this taxon.

Most of the taxa previously assigned to Scapherpetontidae have been placed outside of Salamandroidea except for *Piceoerpeton*. *Piceoerpeton* is placed within Salamandroidea making Scapherpetontidae non-monophyletic contrary to Estes (1969; 1981). Similarities in atlas morphology in Batrachosauroididae and *Piceoerpeton* have been noted by Gardner (2012) and others (Estes and Hutchison 1980; Naylor and Krause 1981). This study reveals similarities in presacral ventral keels with *Siren*, and pterygoid morphology with *Siren*, *Amphiurna*, and Proteidae, that may support placement of *Piceoerpeton* within one or other of these clades. The main argument against placing *Piceoerpeton* with the batrachosauroids was that the similarity of the atlantal and vertebral characters was considered as evidence of convergence (Estes 1981). With the removal of convergent characters in this dataset, and subsequent testing, this study supports placement of *Piceoerpeton* within Salamandroidea (Edwards 1976).

Although this study does not support a monophyletic Batrachosauroididae, they were at least all placed within Salamandroidea as expected (Noble 1931; Taylor and Hesse 1943; Auffenberg 1958; Auffenberg 1961; Demar 2013). A sister relationship of Batrachosauroididae with Proteidae was proposed in early studies due to the similarity in odontoid process reduction (Estes 1975; Naylor 1978) but a more recent phylogeny proposed the Proteidae belongs in a sister relationship with 'Scapherpetontidae' (Demar 2013). A highly reduced odontoid process is seen in *Piceoerpeton* (previously attributed to Scapherpetontidae) which is similar to the condition found in Proteidae and may have placed Proteidae closer to Scapherpetontidae than to Batrachosauroididae in Demar's results, especially as he used only vertebral characters. Demar added the caveat that the inclusion of more taxa and characters would resolve the relationship of his taxa at a higher level. The results presented here have placed *Opisthotriton* in an unresolved relationship with Proteidae, *Siren*, and *Amphiuma*. *Parrissia* was placed as closely related to the Salamandridae rather than Proteidae, which is a position that agrees with the proposal of Denton and O'Neill (1998). The shared opisthocoelous condition of the trunk vertebrae influenced the position of *Parrissia* as this is a derived feature present in Salamandridae. *Prodesmodon* was placed as sister taxon to all salamanders when analysed separately, as it possesses uncapitate rib transverse processes, which is often thought to be a diagnostic character for the Cryptobranchoidea (Skutschas and Martin 2011). However, when included in an analysis with the other supposed Batrachosauroidae, *Prodesmodon* moved to within Salamandroidea in an unresolved relationship with the other supposed Batrachosauroididae and Salamandroidea clades.

The sirenid-like fossils (*Habrosaurus*, *Kababisha*, and *Noterpeton*) did not cluster together, or with sirenids, or even within the same higher level clade. *Habrosaurus* was placed within Salamandroidea as proposed by Gardner (2003). Although *Habrosaurus* does share characters with *Siren*, they are apparently not sufficient to place it as sister taxon to *Siren*. Despite the similarity in morphology with Sirenidae noted by Evans *et al.* (1996), *Kababisha* and *Noterpeton* form a clade that is placed in an unresolved position among the sampled amphibian taxa and not within Caudata or even on the Caudata stem. While *Kababisha* and *Noterpeton* share synapomorphies with some of the Salamandroidea clades, they lack the four faceted articulations of exoccipital and atlas and atlantal spinal nerve foramen, which are features common to Urodela. Additionally, the two *Kababisha* species, found in Africa, are not placed as sister taxa, instead *K. sudanensis* is placed as sister taxon to *Noterpeton* because of their shared atlantal centrum morphology. This suggests that *Kababisha sudanensis*, which is found in Sudan, is more closely related to a genus that is found in both Niger and Bolivia, than to *Kababisha humarensis* from the same locality in Sudan. The suggestion that *Kababisha* and

Noterpeton were related was first proposed by Evans *et al.* (1996) based on shared features such as continuous surface joining the two cotyles and procoely of vertebrae.

Pangerpeton was initially placed towards the base of Urodela (Wang and Evans 2006) supported by the presence of uncapitate ribs, vomerine teeth placement, and head measurements. In this study *Pangerpeton* is placed as sister taxon to Salamandroidea. It differs from Salamandroidea in possessing uncapitate ribs but shares the possession of one phalanx on digit one of the pes, with Plethodontidae and *Salamandra salamandra*. However pes morphology may be relatively plastic (Bishop 1947) and uncapitate rib morphology is not diagnostic for Cryptobranchoidea as it is also found in a Salamandroidea taxon, *Prodesmodon*. Continuous measurement characters [such as those used by Wang and Evans (2006)] were not included in this study and so could not influence the placement of *Pangerpeton*, but further morphometric work might help resolve the relationships of fossils (especially those known only from isolated material – see further work Chapter 6).

Regalerpeton was placed in a very similar position (sister taxon to living Cryptobranchoidea + *Chunerpeton*) as in the analysis by Zhang *et al.* (2009). The placement of *Galverpeton* and *Beiyanerpeton* here also agrees with previous studies (Estes and Sanchíz 1982; Gao and Shubin 2012), but this is not the case for some of the full bodied salamander fossils. The positions of *Chunerpeton*, *Nesovtriton*, *Jeholotriton*, and *Liaoxitriton* are unresolved and *Jeholotriton* has slipped stem-ward. Previously *Jeholotriton* was placed as sister taxon to *Pangerpeton* (Wang and Evans 2006), or as the sister taxon to Cryptobranchidae + *Chunerpeton* + *Regalerpeton* supported by synapomorphies that included, lack of contact between squamosal and roofing elements, and dentition present on vomer, palatine, and pterygoid (Zhang *et al.* 2009). However, in my study, the character relating to the contact of squamosal and roofing elements was removed by both methods of character evaluation employed to detect homoplasy. Stem-ward slippage is still an issue which this dataset has yet to resolve, which is likely to be affecting *Jeholotriton* as it apparently has no taxon close enough in the phylogeny to help stabilise its placement.

Valdotriton has previously been placed essentially as a stem-salamandroid (Evans and Milner 1996; Wang and Evans 2006), in an unresolved relationship with Salamandroidea, Cryptobranchidae, and Hynobiidae (Zhang *et al.* 2009) and within Salamandroidea (Gao and Shubin 2012). The study presented here agrees with Gao and Shubin and places *Valdotriton* within Salamandroidea. The result supports the idea that *Valdotriton* is the earliest Salamandroidea fossil in Europe (published so far), although there is some unpublished material from Purbeck that is almost certainly salamandroid (Evans pers. comm. 2012) that

should push this record further back. *Iridotriton* was initially placed on the stem of Salamandroidea based mainly on the presence of spinal nerve foramina in the caudal vertebrae (Evans *et al.* 2005), however subsequent phylogenetic analyses have placed *Iridotriton* within Cryptobranchoidea (Zhang *et al.* 2009; Gao and Shubin 2012). This study did not support either hypothesis as *Iridotriton* was placed in an unresolved relationship with both Cryptobranchoidea and Salamandroidea. The affinities of this Jurassic North American fossil are important to help elucidate the origins of Cryptobranchoidea and Salamandroidea. Milner (1983) proposed that the Turgai Sea had divided Laurasia into east and west landmasses with Cryptobranchoidea on the Asian/Russian landmass in the east, and sirenids, proteids, plethodontids and salamandroids on the western Euramerican landmass by the Upper Jurassic. However, *Iridotriton* in North America raises questions about the origin and dispersal of whichever clade it belongs to.

Proamphiura was not placed together with *Amphiura*, as proposed by Estes (1969; 1981) and suggested by Gardner (2003). Instead it was placed as the sister taxon to *Siren*. *Proamphiura* shares some morphological characters with *Amphiura* in this study's character set but they are characters also shared with other taxa. In this study the synapomorphies supporting *Amphiura* were specialised amphiumid pit glands and female cloacal glands, so the ultimate phylogenetic position of a fossil relative would have to rely on the shared characteristics common to both *Amphiura* and other clades. This study can only support the placement of *Proamphiura* within Salamandroidea.

Paranecturus is also placed within Salamandroidea as suggested by Demar (2013) but does not provide support for a sister group relationship of *Paranecturus* + Proteidae.

4.5 Conclusions

Many fossil taxa cannot be placed within the phylogeny with high resolution. Previous analyses by other authors have made assumptions about the placement of many of the fossil taxa that cannot be supported by this analysis such as the placement of *Jeholotriton*, *Kababisha*, and *Noterpeton*. Furthermore, Scapherpetontidae is not found to be monophyletic and neither is the Batrachosauroididae. Piceoerpeton is placed within Salamandroidea whereas the other Scapherpetontidae are placed outside of the Salamandroidea. The historic view that uncapitate ribs is an exclusively Cryptobranchoidea feature has been confounded by the presence of that character in both *Pangerpeton* and *Prodesmodon* which have been placed within Salamandroidea in this study. The geographic locations of Cryptobranchoidea and Salamandroidea (especially those that possess uncapitate ribs) will be important in helping to understand not only the evolution of that character but also their pattern of dispersal across Laurasia since *Pangerpeton* is found in China and *Prodesmodon* is known from the USA.

Kababisha and *Noterpeton* form a monophyletic group but *Kababisha sudanensis* may be more closely related to *Noterpeton bolivianum* than to *Kababisha humarensis*. The *Kababisha* and *Noterpeton* clade is placed in an unresolved position within Amphibia and its relationship to Caudata remains unclear. This may be an artefact of stem-ward slippage as there is still evidence of this occurring, most notably in the placement of *Jeholotriton*. However, the placement of *Kababisha* and *Noterpeton* in the amphibian phylogeny is significant in determining dispersal patterns of this clade not only from Laurasia to Gondwana (if related to Salamanders) but also from Africa to South America during the Cretaceous.

5. Discussion and Conclusions

5.1 Discussion

5.1.1 What is the position of Sirenidae in relation to other salamanders?

Previous studies have failed to reach agreement on the position of Sirenidae within the Salamander phylogeny (Larson and Dimmick 1993; Chippindale *et al.* 2004; Zhang and Wake 2009; Wiens *et al.* 2005; Frost *et al.* 2006; Roelants *et al.* 2007; Vieites *et al.* 2009). The result of the molecular analyses supports the placement of Sirenidae as sister taxon to all other Salamandroidea (Fig. 3.5). However, the other analyses (using nuclear, mitochondrial, or morphological data) were unable to resolve the relationships of Sirenidae in relation to Salamandroidea and so needs further work.

5.1.2 Do soft body characters give a more reliable and congruent signal relative to molecular results than the signal from the osteological data? Does soft body data show any difference in levels of convergence than the osteological data?

Early morphological phylogenies displayed convergence by placing aquatic taxa together in paraphyletic groupings (Duellman and Trueb 1986; Wiens *et al.* 2005). The morphological phylogeny in this thesis showed some congruence with the molecular results and agrees on the placement of Sirenidae within the Salamandroidea. Previous studies have found that there is more congruence between soft body characters and molecular results (Gibbs *et al.* 2000). The phylogeny from soft body characters in this study showed lower levels of congruence with the combined molecular tree results than the osteological phylogeny according to the agreement subtree and symmetrical differences tests (Table 2.3.2). However, the soft body characters displayed less apparent homoplasy than the osteological data. After both the tree dependant and tree independent methods of character evaluation had been applied to the full morphological dataset, 73% of the soft body characters were retained. The osteological characters fared less well with the RI dataset retaining just 42%, and the Le Quesne dataset containing just 29% of the original 197 osteological characters. This result might support the apparent loss of phylogenetic signal with the removal of soft body characters (Sansom *et al.* 2010; Sansom and Wills 2013) compared to random loss of characters. Many salamander clades in this study, especially *Amphiuma* which was supported by female cloacal gland and amphiumid pit gland characters (Fig. 2.3.7), relied on soft body synapomorphies to support monophyly.

5.1.3 Is it possible to correct for the signal caused by convergence in the morphological data?

The suspected homoplasy in salamanders has been the subject of previous phylogenetic studies [i.e. Wiens *et al.* (2005)] which have been unable to fully correct for the convergence signal in the data. The methods for evaluating the characters for signs of homoplasy in this study used tree dependant and tree independent tests. Both the RI (tree dependant) and the Le Quesne (tree independent) reduced datasets showed little increase in congruence with the molecular tree compared to the full morphological phylogeny. While the Le Quesne tree showed more congruence relative to the RI tree when compared to the molecular phylogeny, there was no significant improvement in the topology compared to molecular data. However, even after rigorous character evaluation and exclusion the RI and Le Quesne data support a monophyletic Cryptobranchoidea and Salamandroidea in both the Bayesian and Parsimony results. The lack of phylogenetic resolution within Cryptobranchoidea and Salamandroidea suggests that a loss of signal, perhaps due to the removal of too many characters, should be addressed in future work.

5.1.4 Can fossils be placed robustly at a family and/or salamandroidea/cryptobranchoidea level?

Although there is some consensus of internal relationships of salamanders emerging, there are still other families, other than Sirenidae, that are not consistently placed in the same location on the tree. This uncertainty of the internal relationships of salamander families makes it difficult to place fossils with confidence. However, the ability to place fossils even at a higher level is significant in salamanders because it will help gain a more complete view of salamander radiation through time. Testing the placement of simulated fossils showed mixed results. The RI dataset outperformed the Le Quesne dataset by placing the simulated fossils more accurately compared to previous placement using molecular data, more often. However, *Andrias*, *Rhyacotriton*, and Hynobiidae were not supported by any unique osteological synapomorphies in either dataset. This is consistent with the findings of other researchers who reported difficulties, especially placing Hynobiidae into a morphology based phylogeny (Schultze and Trueb 1991), as there are no morphological characters exclusive to the clade (AmphibiaWeb 2012).

The Bayesian and Parsimony analyses showed almost equal success in placing simulated fossils to family level until the test for stem-ward slippage. Bayesian results outperformed Parsimony with less stem-ward slippage but even so only managed to place five out of nine simulated fossils relative to their previous position within the phylogeny. At a Cryptobranchoidea/Salamandroidea level Bayesian results fared better but stem-ward slippage is still an issue to be considered when interpreting results. This was apparent in the placement of some of the fossils previously assigned to Cryptobranchoidea by other authors. In my analysis, *Jeholotriton* was placed outside of Caudata unlike the finding of Wang and Evans (2006), who had previously placed it as sister taxon to *Pangerpeton*.

Cryptobranchoidea is often diagnosed by the presence of unicapitate ribs and rib bearers. Similarly, in this study, Salamandroidea are characterised by the possession of bicapitate ribs and rib bearers, even though this study has identified two taxa that have been placed in Salamandroidea that possess unicapitate ribs (*Prodesmodon* and *Pangerpeton*). Milner (1983) proposed that the vicariant event that split Cryptobranchoidea and Salamandroidea was the formation of the Turgai Sea during the Late Jurassic. This Sea divided Laurasia into east and west landmasses with Cryptobranchoidea on the Asian/Russian landmass in the east, and Salamandroidea (sirenids, proteids, plethodontids, and salamandrids) on the western Euramerican landmass. However, there is no clear geographical divide in the fossil taxa that display this unicapitate rib character. Salamander B (Evans and Milner 1994) and *Iridotriton* (Evans *et al.* 2005) are Middle and Late Jurassic respectively and both found on the “Salamandroidea side” of the Turgai Sea. Both taxa possess unicapitate ribs (Evans *et al.* 2005, Evans pers. comm. 2012). Similarly, *Prodesmodon* and *Pangerpeton* are Salamandroidea taxa that possess unicapitate ribs. Either unicapitate ribs, used so often to support the placement of taxa within Cryptobranchoidea, is more plastic than previously thought or the biogeographic history of Salamandroidea and Cryptobranchoidea is less clear cut than the product of a single large vicariant event. If unicapitate ribs are indeed a diagnostic feature of Cryptobranchoidea, the presence of Salamander B in the UK during the Middle Jurassic could possibly be part of a wider distribution of Cryptobranchoidea during this time. *Iridotriton*, found in North America, would have had to disperse from Asia across some sort of land bridge to North America unless it was part of a wider distribution, or the group originated in Euramerica.

5.1.5 Are the enigmatic Gondwanan fossils (*Kababisha* and *Noterpeton*) related to Sirenidae?

Rage (1993) suggested that together the *Kababisha* and *Noterpeton* might form a sister group to salamanders that was caused by a vicariant event. In this thesis' analyses, *Kababisha sudanensis*, *Kababisha humarensis*, and *Noterpeton bolivianum* form a clade with *K. sudanensis* placed as sister taxon to *Noterpeton bolivianum*, with *K. humarensis* as their sister taxon (Evans *et al.* 1996), outside of Caudata. This is in contrast to the sirenid relationship suggested by Evans *et al.* (1996) and more in agreement with the suggestion of Gardner (2003). If this is the correct relationship, then there is a taxonomic issue as the genus *Kababisha* would be a junior synonym of *Noterpeton*. However, the alternative would be to place *K. humarensis* in a separate genus depending on whether the differences between them are at a species or genus level. However new material is emerging from the Sudan and other localities which might shed new light on the relationship of this enigmatic clade either to Sirenidae or to salamanders as a whole. Further work on this group will be conducted by Dr Mueller at the Museum für Naturkunde in Berlin in conjunction with Dr Gardner of the Royal Tyrell Museum in Drumheller.

The placement of these taxa in a fossil amphibian phylogeny has interesting implications on the distribution potential between the Gondwanan continents (Africa + South America) as *Noterpeton* has been discovered in both Bolivia and Niger in Late Cretaceous age sediments (Rage *et al.* 1993; Rage and Dutheil 2008). Its' possible relationship with Caudata also highlights interesting questions about the origins and diversification of Lissamphibia.

5.2 Conclusions

It is clear that there are many different signals emerging from different data types i.e., molecular vs morphological, but also from within each data type i.e., mitochondrial DNA vs nuclear DNA and osteological characters vs soft body characters. The analysis using a combination of mitochondrial and nuclear genes supported a Batrachia (salamanders + frogs) clade with caecilians as their sister taxon. Within salamanders some consensus has been reached with the externally fertilising salamanders (i.e., Cryptobranchoidea) generally supported as monophyletic and as the sister clade to all other salamanders. Salamandroidea, including Sirenidae, is also generally found to be monophyletic.

The morphological phylogenies showed little congruence with the molecular results. However, they agreed on a Salamandroidea placement of Sirenidae, and Cryptobranchoidea as the sister clade to all other salamanders. Suspected homoplasy in salamander morphology has proved difficult to address in many past studies (Wiens *et al.* 2005). The current study has found that soft body characters display less homoplasy than their osteological counterparts. There is still little understanding of the relationship between phenotype and genotype. This makes the identification of morphological characters that offer true phylogenetic signal, difficult without first understanding their developmental history. Of the vertebral characters, the ones relating to spinal nerve foramina seemed to be supporting nodes more often than others. These characters are directly related to soft body anatomy, which could be a criterion to consider when evaluating osteological characters to better enable the successful placement of the taxa, at least at a higher level within salamanders. This study has highlighted the need for a better understanding of the data and the signal it contributes to phylogeny.

Although initially it seemed that vertebral characters were able to place simulated fossils in the 'correct' place in the tree, more detailed examination showed that this was often based on coding reconstructions for missing data. This affected the results when extant relatives of the simulated fossil were removed, the signal for those character reconstructions was removed, resulting in stem-ward slipping on a number of occasions. The reliance on reconstructed characters makes placement of fossils difficult when no obvious relationship with extant families exists. However, the simulated fossils were placed within Cryptobranchoidea and Salamandroidea with a high success rate, supported mainly by the presence of unicapitate or bicapitate ribs and rib bearers. The use of this character to distinguish between the two main clades with salamanders should be reviewed. The developmental history of ribs is so little known in salamanders and the variation of rib-bearer morphology in individuals of other clades [i.e. *Sphenodon* and Crocrodilia (Hoffstetter and Gasc 1969)] is so large, that this should be a site of particular interest as it is relied upon so heavily to support important phylogenetic relationships.

The puzzling Gondwanan salamanders (*Kababisha* and *Noterpeton*) are confirmed as forming a monophyletic group, but the position of that group with respect to caudate remains problematic. The apparent paraphyly of *Kababisha* in relation to *Noterpeton* would have taxonomic implications. Further descriptive work will be carried out on new material that will hopefully reveal further details of the morphology of taxa within this enigmatic clade. Whether these taxa are ultimately placed within Sirenidae, within another urodelan clade, or on the stem of Caudata, their Gondwanan distribution is of interest for lissamphibian biogeography.

5.3 Further Work:

5.3.1 New Data

Kiyatriton leshchinskiyi is an Early Cretaceous salamander from Russia and is purportedly the only Early Cretaceous fossil from Asia, found outside of China (Skutschas 2014). Recently new material attributed to this taxon has been described which might allow for more characters to be scored (Skutschas 2014). This should be included in the new data matrix (Appendix B) and its position within the salamander phylogeny tested. It has provisionally been referred to Cryptobranchoidea as it shares characters such as unicapitate ribs, flattened neural arches, neural spines reduced to a low keel, and reduced subcentral keel (Skutschas 2014). The current study did not include *Kiyatriton* as there were too few characters for evaluation, but the inclusion of these new data should allow for phylogenetic hypothesis testing.

Kababisha and *Noterpeton* are thought to be fossil salamanders however the results of this study placed them outside of salamanders. Further analyses could include a wider range of taxa including temnospondyl, lepospondyl and albanerpedontid to provide more resolution of its affinities. More morphological characters should also be included in future analyses and these could focus on the synapomorphies for stem salamanders. With the re-description of *Kababisha* by Dr Gardner and Dr Muller, new insights into this species might come to light. This clade is especially important due to its location and the biogeographic hypothesis suggesting salamanders dispersed across land bridges during the Cretaceous from Laurasia to Gondwana as proposed Milner in 1983.

5.3.2 New Analyses

Chapter 3 of this study looked at simulating fossils by excluding all characters except the ones commonly found in the salamander fossil record. However, this method can be modified to simulate fossils more closely by replicating the exact characters specific to each fossil taxa. This way even if fossil taxa have characters not commonly found in the fossil record then its' placement can still be tested. This might be a very time consuming task but would simulate the robustness of the phylogenetic relationships and the potential for stem-ward slippage more accurately if you had a small number of fossils.

In fossils that consist of fragmentary or isolated remains, it is often the atlas that has been made the holotype. A pilot study using only atlantal characters to create a phylogeny was

conducted to investigate the diagnostic potential for this element. The results showed little congruence with previously published molecular phylogenies but did suggest subordinal clustering of Cryptobranchoidea. With further character evaluation and assessment, and inclusion in both Bayesian and Parsimony framework analyses, biological signal may be detected. The dataset could be enhanced by including morphometric data. Landmarks or outline data could be collected and analysed in PAST (Hammer *et al.* 2001) and tpsDig2 (Rohlf 2004).

5.3.3 Time calibrated phylogeny

The phylogeny (once fossils have successfully been incorporated) can be time-calibrated using multiple calibration points. Some of the points used by Zhang and Wake (2009) might be incorporated. External calibration points (outside the salamander lineage) such as: the lungfish-Tetrapod split (408-419 mya)(Müller and Reisz 2005); Amphibia-Amniota split (330-360 mya) (Benton and Donoghue 2007; Marjanović and Laurin 2007); bird-lizard split (252-300 mya) (Müller and Reisz 2005; Benton and Donoghue 2007); bird-crocodile split (235-251 mya) (Müller and Reisz 2005; Benton and Donoghue 2007); and the alligator-caiman split (66-75 mya) (Müller and Reisz 2005) might be incorporated to better constrain the phylogeny. Internal as well as external calibration points have been advocated by Brochu (2004) and Marjanovic and Laurin (2007) and so there are five internal calibration points to be included such as: the common ancestor of salamanders and frogs (250 mya) [*Triadobatrachus* Rage and Rocek (1989), *Czatkobatrachus*, Evans and Borsuk-Białynicka (1998)] although this date might be modified with the recent publication of *Geobatrachus* (Anderson *et al.* 2007); cryptobranchid-hynobiid split (145 mya) [this is following Zhang and Wake (2009) more conservative estimate than Gao and Shubin (2003)]; *Ambystoma-Dicamptodon* split (55.8 mya) (Naylor and Fox 1993); and the *Necturus-Proteus* split (55.8 mya) (Estes 1981).

Although some suggest that maximum constraint calibration points are also needed (Marjanović and Laurin 2007) the salamander fossil record is not complete enough to use maximal bounds with confidence. Instead ACCTRAN and DELTRAN character optimisation might be able to better give a maximum and minimum branch length for a phylogeny which will further give upper and lower bound restraints to the molecular phylogeny estimated divergence dates (Agnarsson and Miller 2008).

ACCTRAN and DELTRAN are used in parsimony reconstructions and maximise ambiguous character state change as close to the root (ACCTRAN) or to the tips (DELTRAN) of the branches as possible. Thus ACCTRAN might lead to branch lengths between internal nodes

that are generally greater than those of DELTRAN analyses, which should produce phylogenies with greater terminal branch lengths (Agnarsson and Miller 2008). Therefore ACCTRAN should give older age estimates for nodes while DELTRAN should give younger ages, thus providing the upper and lower limits of the node age (Forest *et al.* 2005).

Salamanders and their fossil relatives have the potential to help elucidate Mesozoic biogeographical patterns. By studying their early evolution and diversification patterns a better understanding of this clade as a whole could support the efforts of conservationists.

Salamanders are important, because they fill diverse ecological roles (Davic and Welsh 2004) and like frogs they can be good indicators of ecosystem stress (Welsh and Ollivier 1998). Many clades are already on the IUCN Red List e.g. *Andrias davidianus*, due to pollution, habitat loss, and over collection (iucnredlist.org, September 2014), and work on taxonomy is important for monitoring their diversity today.

References:

- Agnarsson, I. and J. A. Miller (2008). "Is ACCTRAN better than DELTRAN?" Cladistics **24**(6): 1032-1038.
- Akaike, H. (1980). "Likelihood and the Bayes procedure." Trabajos de Estadística Y de Investigación Operativa **31**(1): 143-166.
- Alberch, P., S. J. Gould, G. F. Oster and D. B. Wake (1979). "Size and shape in ontogeny and phylogeny." Paleobiology **5**(3): 296-317.
- Alfaro, M. E., S. Zoller and F. Lutzoni (2003). "Bayes or bootstrap? A simulation study comparing the performance of Bayesian Markov chain Monte Carlo sampling and bootstrapping in assessing phylogenetic confidence." Molecular Biology and Evolution **20**(2): 255-266.
- Anderson, J. (2008). "Focal Review: The origin(s) of modern amphibians." Evolutionary Biology **35**(4): 231-247.
- Anderson, J., D. Scott, R. Reisz and S. Sumida (2007). "A new stem batrachian (Temnospondyli : Amphibamidae) from the early Permian of Texas." Journal of Vertebrate Paleontology **27**(3): 40a-40a.
- Anderson, J. S. (2001). "The phylogenetic trunk: Maximal inclusion of taxa with missing data in an analysis of the lepospondyli (Vertebrata, Tetrapoda)." Systematic Biology **50**(2): 170-193.
- Anderson, J. S., R. R. Reisz, D. Scott, N. B. Frobisch and S. S. Sumida (2008). "A stem batrachian from the Early Permian of Texas and the origin of frogs and salamanders." Nature **453**(7194): 515-518.
- Auffenberg, W. (1958). "A new family of Miocene salamanders from the Texas coastal plain." Quarterly Journal of The Florida Academy of Sciences **21**.
- Auffenberg, W. (1961). "A new genus of fossil salamander from North America." American Midland Naturalist **66**(2): 456-465.
- Averianov, A. O., T. Martin, P. P. Skutschas, A. S. Rezvyi and A. A. Bakirov (2008). "Amphibians from the Middle Jurassic Balabansai Svita in the Fergana depression, Kyrgyzstan (Central Asia)." Palaeontology **51**(2): 471-485.
- Ball, I. R. (1975). "Nature and Formulation of Biogeographical Hypotheses." Systematic Biology **24**(4): 407-430.
- Barrett, P. M., A. J. McGowan and V. Page (2009). "Dinosaur diversity and the rock record." Proceedings of the Royal Society B-Biological Sciences **276**(1667): 2667-2674.
- Benton, M. J. (1990). "Phylogeny of the major tetrapod groups: Morphological data and divergence dates." Journal of Molecular Evolution **30**(5): 409-424.
- Benton, M. J. and P. C. J. Donoghue (2007). "Paleontological Evidence to Date the Tree of Life." Molecular Biology and Evolution **24**(1): 26-53.
- Bishop, D. W. (1947). "Polydactyly in the Tiger Salamander." Journal of Heredity **38**(10): 291-293.
- Bolt, J. (1991). Lissamphibian origins. Origins of the Higher Groups of Tetrapods: Controversy and Consensus. H. P. Schultze and L. Trueb (eds). London, Comstock Pub. Associates: 194-222.
- Bolt, J. R. (1969). "Lissamphibian Origins: Possible Protolissamphibian from the Lower Permian of Oklahoma." Science **166**(3907): 888-891.
- Bolt, J. R. (1977). "Dissorophoid Relationships and Ontogeny, and the Origin of the Lissamphibia." Journal of Paleontology **51**(2): 235-249.
- Bonett, R. M. and P. T. Chippindale (2004). "Speciation, phylogeography and evolution of life history and morphology in plethodontid salamanders of the Eurycea multiplicata complex." Molecular Ecology **13**(5): 1189-1203.
- Borsuk-Białynicka, M. and S. E. Evans (2002). "The scapulocoracoid of an Early Triassic stem-frog from Poland." Acta Palaeontologica Polonica **47**(1): 79-96.

- Box, G. E. P. (1976). "Science and Statistics." Journal of the American Statistical Association **71**(356): 791-799.
- Briggs, D. E. G. (2010). "Palaeontology: Decay distorts ancestry." Nature **463**(7282): 741-743.
- Briggs, D. E. G. and A. J. Kear (1993). "Decay and Preservation of Polychaetes: Taphonomic Thresholds in Soft-Bodied Organisms." Paleobiology **19**(1): 107-135.
- Brochu, C. (2004). "Patterns of calibration age sensitivity with quartet dating methods." Journal of Paleontology **78**(1): 7-30.
- Butler, R. J., P. M. Barrett, S. Nowbath and P. Upchurch (2009). "Estimating the effects of sampling biases on pterosaur diversity patterns: implications for hypotheses of bird/pterosaur competitive replacement." Paleobiology **35**(3): 432-446.
- Cannatella, D. C., D. R. Vieites, P. Zhang, M. H. Wake and D. B. Wake (2009). Amphibians (Lissamphibia). The Timetree of Life. S. B. Hedges and S. Kumar (eds), OUP Oxford: 353-356.
- Carroll, R. and A. Zheng (2012). "A neotenic salamander, *Jeholotriton paradoxus*, from the Daohugou Beds in Inner Mongolia." Zoological Journal of the Linnean Society **164**(3): 659-668.
- Carroll, R. L. (2004). The importance of branchiosaurs in determining the ancestry of the modern amphibian orders. Studies in lower vertebrate palaeontology. R. R. Schoch, J. Müller and M. Fastnacht (eds). Stuttgart. **232**: 157-180.
- Carroll, R. L. (2007). "The Palaeozoic ancestry of salamanders, frogs and caecilians." Zoological Journal of the Linnean Society **150**: 1-140.
- Carroll, R. L. and P. J. Currie (1975). "Microsaurs as possible apodan ancestors." Zoological Journal of the Linnean Society **57**(3): 229-247.
- Chippindale, P. T. (2000). "Species boundaries and species diversity in the central Texas hemidactyliine plethodontid salamanders, genus *Eurycea*." Biology of Plethodontid Salamanders: 149-165.
- Chippindale, P. T., R. M. Bonett, A. S. Baldwin and J. J. Wiens (2004). "Phylogenetic evidence for a major reversal of life-history evolution in Plethodontid salamanders." Evolution **58**(12): 2809-2822.
- Crisp, M. D., S. A. Trewick and L. G. Cook (2011). "Hypothesis testing in biogeography." Trends in Ecology & Evolution **26**(2): 66-72.
- Curtis, K. and K. Padian (1999). "An Early Jurassic microvertebrate fauna from the Kayenta Formation of northeastern Arizona: Microfaunal change across the Triassic-Jurassic boundary." PaleoBios **19**(2): 19-37.
- Davic, R. D. and H. H. Welsh (2004). "On the ecological roles of salamanders." Annual Review of Ecology Evolution and Systematics **35**: 405-434.
- De Beer, G. (2008). Embryos and ancestors, Caven Press, pp.
- Demar, D. G. (2013). "A New Fossil Salamander (Caudata, Proteidae) from the Upper Cretaceous (Maastrichtian) Hell Creek Formation, Montana, U.S.A." Journal of Vertebrate Paleontology **33**(3): 588-598.
- Denton, R. K. and R. C. O'Neill (1998). "Parrisiana neocesariensis, a new batrachosauroidid salamander and other amphibians from the Campanian of eastern North America." Journal of Vertebrate Paleontology **18**(3): 484-494.
- Donoghue, M. J., J. A. Doyle, J. Gauthier, A. G. Kluge and T. Rowe (1989). "The Importance of Fossils in Phylogeny Reconstruction." Annual Review of Ecology and Systematics **20**: 431-460.
- Donoghue, P. C. J. and M. A. Purnell (2009). "Distinguishing heat from light in debate over controversial fossils." BioEssays **31**(2): 178-189.
- Duellman, W. E. and L. Trueb (1986). Biology of amphibians, McGraw Hill, pp. 461-508.
- Duellman, W. E. and L. Trueb (1994). Biology of Amphibians, Johns Hopkins University Press, pp. 461-508.
- Edwards, A. W. F. (1972). Likelihood. Cambridge, Cambridge University Press, pp.

- Edwards, J. L. (1976). "Spinal nerves and their bearing on salamander phylogeny." Journal of Morphology **148**(3): 305-328.
- Egan, M. G. (2006). "Support versus corroboration." Journal of Biomedical Informatics **39**(1): 72-85.
- Estes, R. (1964). Fossil vertebrates from the Late Cretaceous Lance Formation, Eastern Wyoming. University of California publications in geological sciences(eds), University of California Press. **49**: 186.
- Estes, R. (1965). "A new fossil salamander from Montana and Wyoming." Copeia **1965**(1): 90-95.
- Estes, R. (1969). "The Batrachosauroididae and Scapherpetontidae, Late Cretaceous and Early Cenozoic Salamanders." Copeia **1969**(2): 225-234.
- Estes, R. (1975). "Lower Vertebrates from the Fort Union Formation, Late Paleocene, Big Horn Basin, Wyoming." Herpetologica **31**(4): 365-385.
- Estes, R. (1981). Gymnophiona, Caudata. Pennsylvania State University, G. Fischer, pp. 115.
- Estes, R., P. Berberian and C. Meszoely (1969). "Lower vertebrates from the Late Cretaceous Hell Creek Formation, McCone County, Montana." Breviora **337**: 33.
- Estes, R. and J. H. Hutchison (1980). "Eocene Lower-Vertebrates from Ellesmere Island, Canadian Arctic Archipelago." Palaeogeography Palaeoclimatology Palaeoecology **30**(3-4): 325-347.
- Estes, R. and B. Sanchíz (1982). "Early Cretaceous Lower Vertebrates from Galve (Teruel), Spain." Journal of Vertebrate Paleontology **2**(1): 21-39.
- Evans, S. E. and M. Borsuk-Białynicka (1998). "A stem-group frog from the Early Triassic of Poland." Acta Palaeontologica Polonica **43**(4): 573-580.
- Evans, S. E., C. Lally, D. C. Chure, A. Elder and J. A. Maisano (2005). "A late Jurassic salamander (Amphibia : Caudata) from the Morrison formation of North America." Zoological Journal of the Linnean Society **143**(4): 599-616.
- Evans, S. E. and A. R. Milner (1994). Middle Jurassic microvertebrate assemblages from the British Isles. In the Shadow of the Dinosaurs, Early Mesozoic Tetrapods. N. Fraser, C. and H.-D. Sues (eds). Cambridge, Cambridge University Press: 303-321.
- Evans, S. E. and A. R. Milner (1996). "A metamorphosed salamander from the Early Cretaceous of Las Hoyas, Spain." Philosophical Transactions of the Royal Society of London Series B-Biological Sciences **351**(1340): 627-646.
- Evans, S. E., A. R. Milner and F. Mussett (1988). "The earliest known salamanders (Amphibia, Caudata) - a record from the Middle Jurassic of England." Geobios **21**(5): 539-552.
- Evans, S. E., A. R. Milner and C. Werner (1996). "Sirenid salamanders and gymnophionan amphibian from the Cretaceous of the Sudan." Palaeontology **39**: 77-95.
- Ezcurra, M. D. and F. L. Agnolin (2012). "A New Global Palaeobiogeographical Model for the Late Mesozoic and Early Tertiary." Systematic Biology **61**(4): 553-566.
- Farris, J. S. (1989). "The Retention Index and the Rescaled Consistency Index." Cladistics-the International Journal of the Willi Hennig Society **5**(4): 417-419.
- Feller, A., E. and S. Hedges, B. (1998). "Molecular Evidence for the Early History of Living Amphibians." Molecular Phylogenetics and Evolution **9**(3): 509-516.
- Felsenstein, J. (1981). "Evolutionary Trees from DNA-Sequences - a Maximum-Likelihood Approach." Journal of Molecular Evolution **17**(6): 368-376.
- Forest, F., V. Savolainen, M. W. Chase, R. Lupia, A. Bruneau, P. R. Crane and M. Lavin (2005). "Teasing Apart Molecular- Versus Fossil-based Error Estimates when Dating Phylogenetic Trees: A Case Study in the Birch Family (Betulaceae)." Systematic Botany **30**(1): 118-133.
- Fox, R. C. and B. G. Naylor (1982). "A reconsideration of the relationships of the fossil amphibian Albanerpeton." Canadian Journal of Earth Sciences **19**(1): 118-128.
- Frost, D. R., T. Grant, J. Faivovich, R. H. Bain, A. Haas, C. F. B. Haddad, R. O. De Sa, A. Channing, M. Wilkinson, S. C. Donnellan, C. J. Raxworthy, J. A. Campbell, B. L. Blotto, P. Moler, R. C. Drewes, R. A. Nussbaum, J. D. Lynch, D. M. Green and W. C. Wheeler (2006). "The

- amphibian tree of life." Bulletin of the American Museum of Natural History(297): 8-370.
- Gao, K.-Q. and N. H. Shubin (2012). "Late Jurassic salamandroid from western Liaoning, China." Proceedings of the National Academy of Sciences **109**(15): 5767-5772.
- Gao, K. Q. and D. Ren (2006). "Radiometric dating of ignimbrite from Inner Mongolia provides no indication of a post-Middle Jurassic age for the Daohugou beds." Acta Geologica Sinica-English Edition **80**(1): 42-45.
- Gao, K. Q. and N. H. Shubin (2001). "Late Jurassic salamanders from northern China." Nature **410**(6828): 574-577.
- Gao, K. Q. and N. H. Shubin (2003). "Earliest known crown-group salamanders." Nature **422**(6930): 424-428.
- Gardiner, B. G. (1982). "Tetrapod classification." Zoological Journal of the Linnean Society **74**(3): 207-232.
- Gardiner, B. G. (1983). "Gnathostome vertebrae and the classification of the Amphibia." Zoological Journal of the Linnean Society **79**(1): 1-59.
- Gardner, J. D. (2001). "Monophyly and affinities of albanerpetontid amphibians (Temnospondyli; Lissamphibia)." Zoological Journal of the Linnean Society **131**(3): 309-352.
- Gardner, J. D. (2003). "The fossil salamander *Proamphiuma cretacea* Estes (Caudata ; Amphiumidae) and relationships within the Amphiumidae." Journal of Vertebrate Paleontology **23**(4): 769-782.
- Gardner, J. D. (2003). "Revision of *Habrosaurus gilmore* (Caudata; Sirenidae) and relationships among sirenid salamanders." Palaeontology **46**: 1089-1122.
- Gardner, J. D. (2012). "Revision of *Piceoerpeton Meszoely* (Caudata: Scapherpetontidae) and description of a new species from the late Maastrichtian and early Paleocene of Western North America." Bulletin Soc. geol. France **183**(6): 611-620.
- Gelman, A. and D. B. Rubin (1992). "Inference from Iterative Simulation Using Multiple Sequences." Statistical Science **7**(4): 457-472.
- Gibbs, S., M. Collard and B. Wood (2000). "Soft-tissue characters in higher primate phylogenetics." Proceedings of the National Academy of Sciences **97**(20): 11130-11132.
- Goin, C. J. and O. B. Goin (1962). Introduction to herpetology, W. H. Freeman, pp.
- Goldman, N. (1990). "Maximum likelihood inference of phylogenetic trees, with special reference to a Poisson process model of DNA substitution and to parsimony analyses." Systematic Biology **39**(4): 345-361.
- Goldman, N., J. P. Anderson and A. G. Rodrigo (2000). "Likelihood-Based Tests of Topologies in Phylogenetics." Systematic Biology **49**(4): 652-670.
- Goloboff, P., J. Farris and K. Nixon (2008). "TNT, a free program for phylogenetic analysis." Cladistics **24**: 774-786.
- Goloboff, P. A., J. M. Carpenter, J. S. Arias and D. R. M. Esquivel (2008). "Weighting against homoplasy improves phylogenetic analysis of morphological data sets." Cladistics **24**(5): 758-773.
- Good, D. A. (1989). "Hybridization and cryptic species in *Dicamptodon* (Caudata, *Dicamptodontidae*)." Evolution **43**(4): 728-744.
- Good, D. A., D. B. Wake and B. M. o. V. Z. University of California (1992). Geographic variation and speciation in the Torrent salamanders of the Genus *Rhyacotriton* (Caudata: Rhyacotritonidae), University of California Press, pp.
- Gould, S. J. (1977). Ontogeny and Phylogeny, Belknap Press of Harvard University Press, pp.
- Gould, S. J. (1992). Heterochrony. Keywords in Evolutionary Biology. E. F. Keller and E. A. Lloyd (eds), Harvard University Press: 158-165.
- Gradstein, F. M., J. G. Ogg, A. G. Smith, W. Bleeker and L. J. Lourens (2004). "A new Geologic Time Scale, with special reference to Precambrian and Neogene." Episodes **27**(2): 83-100.

- Hallam, A. (1981). Relative importance of plate movements, eustasy and climate in controlling major biogeographical changes since the early Mesozoic. Vicariance Biogeography: A Critique. G. Nelson and D. E. Rosen (eds), Columbia University Press: 303-340.
- Hallam, A. (1994). An outline of Phanerozoic Biogeography, Oxford University Press, pp. 254.
- Hammer, O., D. Harper and P. Ryan (2001). PAST: Paleontological Statistics software package for education and data analysis. Palaeontologia Electronica.
- Hanken, J. and B. K. Hall (1993). The Skull: Patterns of structural and systematic diversity, University of Chicago Press, pp.
- Hanken, J. and D. B. Wake (1982). "Genetic differentiation among Plethodontid salamanders (Genus *Bolitoglossa*) in Central-America and South-America - Implications for the South-American invasion." Herpetologica **38**(2): 272-287.
- Hay, J. M., I. Ruvinsky, S. Hedges, B. and M. L.R. (1995). "Phylogenetic relationships of amphibian families inferred from DNA sequences of mitochondrial 12S and 16S ribosomal RNA genes." Molecular Biology and Evolution **12**(5): 928.
- He, H. Y., X. L. Wang, Z. H. Zhou, R. X. Zhu, F. Jin, F. Wang, X. Ding and A. Boven (2004). "40Ar/39Ar dating of ignimbrite from Inner Mongolia, northeastern China, indicates a post-Middle Jurassic age for the overlying Daohugou Bed." Geophys. Res. Lett. **31**(20): L20609.
- Hecht, M. K. and J. L. Edwards (1976). "The determination of parallel or monophyletic relationships: The proteid salamanders - A test case." The American Naturalist **110**(974): 653-677.
- Hedges, S. B. and L. R. Maxson (1993). "A Molecular Perspective on Lissamphibian Phylogeny." Herpetological Monographs **7**(ArticleType: research-article / Full publication date: 1993 / Copyright © 1993 Herpetologists' League): 27-42.
- Hedges, S. B., K. D. Moberg and L. R. Maxson (1990). "Tetrapod phylogeny inferred from 18S and 28S ribosomal RNA sequences and a review of the evidence for amniote relationships." Molecular Biology and Evolution **7**(6): 607-633.
- Hedges, S. B., R. A. Nussbaum and L. R. Maxson (1993). "Caecilian Phylogeny and Biogeography Inferred from Mitochondrial DNA Sequences of the 12S rRNA and 16S rRNA Genes (Amphibia: Gymnophiona)." Herpetological Monographs **7**(ArticleType: research-article / Full publication date: 1993 / Copyright © 1993 Herpetologists' League): 64-76.
- Hedges, S. B. and C. G. Sibley (1994). "Molecules Vs Morphology in Avian Evolution - the Case of the Pelecaniform Birds." Proceedings of the National Academy of Sciences of the United States of America **91**(21): 9861-9865.
- Hellawell, J. and P. Orr (2012). "Deciphering taphonomic processes in the Eocene Green River Formation of Wyoming." Palaeobiodiversity and Palaeoenvironments **92**(3): 353-365.
- Hillis, D. M., D. A. Chamberlain, T. P. Wilcox and P. T. Chippindale (2001). "A new species of subterranean blind salamander (Plethodontidae : Hemidactyliini : Eurycea : Typhlomolge) from Austin, Texas, and a systematic revision of central Texas paedomorphic salamanders." Herpetologica **57**(3): 266-280.
- Hoffstetter, R. and J.-P. Gasc (1969). Vertebrae and ribs of modern reptiles. Biology of Reptilia, Volume 1: Morphology. A. C. Gans, A. Bellairs and T. S. Parsons (eds). London, Academic Press: 201-310.
- Holloway, S. (1983). "The shell-detrital calcirudites of the Forest Marble Formation (Bathonian) of southwest England." Proceedings of the Geologists' Association **94**(3): 259-266.
- Howard, R. R. and E. D. Brodie (1971). "Experimental Study of Mimicry in Salamanders Involving *Notophthalmus-Viridescens-Viridescens* and *Pseudotriton-Ruber-Schenski*." Nature **233**(5317): 277-&.
- Huelsenbeck, J. P. (1991). "When Are Fossils Better Than Extant Taxa in Phylogenetic Analysis." Systematic Zoology **40**(4): 458-469.
- Hugall, A. F., R. Foster and M. S. Y. Lee (2007). "Calibration choice, rate smoothing, and the pattern of tetrapod diversification according to the long nuclear gene RAG-1." Systematic Biology **56**(4): 543-563.

- Hunn, C. A. and P. Upchurch (2001). "The importance of time/space in diagnosing the causality of phylogenetic events: Towards a "chronobiogeographical" paradigm?" Systematic Biology **50**(3): 391-407.
- Jenkyns, H. C., A. Forster, S. Schouten and J. S. S. Damste (2004). "High temperatures in the Late Cretaceous Arctic Ocean." Nature **432**(7019): 888-892.
- Jhwueng, D.-C., S. Huzurbazar, B. C. O'Meara and L. Liu (2014). "Investigating the performance of AIC in selecting phylogenetic models." Statistical Applications in Genetics and Molecular Biology **0**(0).
- Jukes, T. H. and Cantor (1969). Evolution of protein molecules. Mammalian Protein Metabolism. H. N. Munro (eds), Elsevier Science: pp. 21-132.
- Keane, T., C. Creevey, M. Pentony, T. Naughton and J. McInerney (2006). "Assessment of methods for amino acid matrix selection and their use on empirical data shows that ad hoc assumptions for choice of matrix are not justified." BMC Evolutionary Biology **6**(1): 29.
- Kishino, H. and M. Hasegawa (1989). "Evaluation of the maximum likelihood estimate of the evolutionary tree topologies from DNA sequence data, and the branching order in hominoidea." Journal of Molecular Evolution **29**(2): 170-179.
- Klingenberg, C. P. (1998). "Heterochrony and allometry: the analysis of evolutionary change in ontogeny." Biological Reviews **73**(1): 79-123.
- Kumar, S. and S. B. Hedges (1998). "A molecular timescale for vertebrate evolution." Nature **392**(6679): 917-920.
- Lanfear R, Calcott B, Ho SYW, Guindon S (2012). "PartitionFinder: combined selection of partitioning schemes and substitution models for phylogenetic analyses" Molecular Biology and Evolution **29**(6):1695–1701
- Larson, A. (1991). "A molecular perspective on the evolutionary relationships of the salamander families." Evolutionary Biology **25**: 211-277.
- Larson, A. and W. W. Dimmick (1993). "Phylogenetic relationships of the salamander families: An analysis of congruence among morphological and molecular characters." Herpetological Monographs **7**(ArticleType: research-article / Full publication date: 1993 / Copyright © 1993 Herpetologists' League): 77-93.
- Laurin, M. (1998). "The importance of global parsimony and historical bias in understanding tetrapod evolution. Part I. Systematics, middle ear evolution and jaw suspension." Annales des sciences naturelles. Zoologie et biologie animale **19**(1): 1.
- Laurin, M. and R. Reisz (1997). A new perspective on tetrapod phylogeny. Amniote Origins: Completing the Transition to Land. S. S. Sumida and K. L. M. Martin (eds). San Diego, Academic Press: 9-59.
- Lee, M. S. Y. (2005). "Squamate phylogeny, taxon sampling, and data congruence." Organisms Diversity & Evolution **5**(1): 25-45.
- Lee, M. S. Y. and J. S. Anderson (2006). "Molecular clocks and the origin(s) of modern amphibians." Molecular Phylogenetics and Evolution **40**(2): 635-639.
- Lequesne, W. J. (1969). "A Method of Selection of Characters in Numerical Taxonomy." Systematic Zoology **18**(2): 201-&.
- Lequesne, W. J. (1972). "Further Studies Based on Uniquely Derived Character Concept." Systematic Zoology **21**(3): 281-&.
- Lieberman, B. S. (2003). "Paleobiogeography: The relevance of fossils to biogeography." Annual Review of Ecology Evolution and Systematics **34**: 51-69.
- Liu, Y. Q., Y. X. Liu, S. A. Ji and Z. Q. Yang (2006). "U-Pb zircon age for the Daohugou Biota at Ningcheng of Inner Mongolia and comments on related issues." Chinese Science Bulletin **51**(21): 2634-2644.
- Lombard, R. and J. Bolt (1979). "Evolution of the tetrapod ear: an analysis and reinterpretation." Biological Journal of the Linnean Society **11**(1): 19.

- Lukoschek, V., Scott, K. J., Avise, J. C. (2011). "Evaluating Fossil Calibrations for Dating Phylogenies in Light of Rates of Molecular Evolution: A Comparison of Three Approaches" *Systematic Biology* **61**: 22-43
- Macey, J. R. (2005). "Plethodontid salamander mitochondrial genomics: A parsimony evaluation of character conflict and implications for historical biogeography." *Cladistics* **21**(2): 194-202.
- Maddin, H. C., F. A. Jenkins and J. S. Anderson (2012). "The Braincase of Eocaecilia micropodia (Lissamphibia, Gymnophiona) and the Origin of Caecilians." *Plos One* **7**(12).
- Maddison, W. P. (2008). "Mesquite: a modular system for evolutionary analysis." *Evolution* **62**(5): 1103.
- Marjanović, D. (2008). "A reevaluation of the evidence supporting an unorthodox hypothesis on the origin of extant amphibians." *Contributions to Zoology* **77**(3): 149.
- Marjanovic, D. and M. Laurin (2007). "Fossils, molecules, divergence times, and the origin of Lissamphibians." *Systematic Biology* **56**(3): 369-388.
- Marjanović, D. and M. Laurin (2007). "Fossils, molecules, divergence times, and the origin of lissamphibians." *Systematic Biology* **56**(3): 369-388.
- Majtánová, K., Choleva, L., Symonová, R., Ráb, P., Kotusz, J., Pekárik, L., and Janko, K. (2016). "Asexual Reproduction Does Not Apparently Increase the Rate of Chromosomal Evolution: Karyotype Stability in Diploid and Triploid Clonal Hybrid Fish (Cobitis, Cypriniformes, Teleostei)". *PLoS ONE* **11**(1): e0146872
- McCracken, K. G., J. Harshman, D. A. McClellan and A. D. Afton (1999). "Data set incongruence and correlated character evolution: An example of functional convergence in the hindlimbs of stifftail diving ducks." *Systematic Biology* **48**(4): 683-714.
- McGowan, G. and S. E. Evans (1995). "Albanerpetontid amphibians from the Cretaceous of Spain." *Nature* **373**(6510): 143-145.
- McGowan, G. J. (2002). "Albanerpetontid amphibians from the Lower Cretaceous of Spain and Italy: a description and reconsideration of their systematics." *Zoological Journal of the Linnean Society* **135**(1): 1-32.
- McKinney, M. L. and K. McNamara (1991). *Heterochrony: the evolution of ontogeny*, Plenum Press, pp.
- Meyer, A. and R. Zardoya (2003). "Recent advances in the (molecular) phylogeny of vertebrates." *Annual Review of Ecology Evolution and Systematics* **34**: 311-338.
- Milner, A. R. (1983). The biogeography of salamanders in the Mesozoic and early Cenozoic: a cladistic vicariance model. *Evolution, time, and space: the emergence of the biosphere*. R. W. Sims, J. H. Price and P. E. S. Whalley (eds), Published for the Systematics Association by Academic Press: 431-468.
- Milner, A. R. (1988). The relationships and the origin of living amphibians. *The Phylogeny and Classification of the Tetrapods: Amphibians, reptiles, birds*. M. J. Benton (eds). Linnean Society of London, Published for the Systematics Association by the Clarendon Press. **2**: 59-102.
- Milner, A. R. (1993). "The Paleozoic Relatives of Lissamphibians." *Herpetological Monographs* **7**(ArticleType: research-article / Full publication date: 1993 / Copyright © 1993 Herpetologists' League): 8-27.
- Milner, A. R. (2000). Mesozoic and Tertiary Caudata and Albanerpetontidae. *Amphibian Biology. Volume 4, Palaeontology: The Evolutionary History of Amphibians*. H. Heatwole and R. L. Carroll (eds). Chipping Norton, Australia, Surrey Beatty & Sons. **4**: 1412-1444.
- Milner, A. R. (2002). Mesozoic and Tertiary Caudata and Albanerpetontidae. *Amphibian Biology, Volume 4: Paleontology*. H. Heatwole and R. L. Carroll (eds), American Society of Ichthyologists and Herpetologists (ASIH). **4**: 1412—1444.
- Min, M. S., S. Y. Yang, R. M. Bonett, D. R. Vieites, R. A. Brandon and D. B. Wake (2005). "Discovery of the first Asian plethodontid salamander." *Nature* **435**(7038): 87-90.

- Mueller, R. L., J. R. Macey, M. Jaekel, D. B. Wake and J. L. Boore (2004). "Morphological homoplasy, life history evolution, and historical biogeography of plethodontid salamanders inferred from complete mitochondrial genomes." Proceedings of the National Academy of Sciences of the United States of America **101**(38): 13820-13825.
- Müller, J. and R. R. Reisz (2005). "Four well-constrained calibration points from the vertebrate fossil record for molecular clock estimates." BioEssays **27**(10): 1069-1075.
- Nadachowska, K., Babik, W., (2009). "Divergence in the face of gene flow: the case of two newts (Amphibia: Salamandridae)". Molecular Biology and Evolution, **26**: 829–841
- Naylor, B. G. (1978). "The Earliest Known Necturus (Amphibia, Urodela), from the Paleocene Ravenscrag Formation of Saskatchewan." Journal of Herpetology **12**(4): 565-569.
- Naylor, B. G. (1979). "The Cretaceous salamander *Prodesmodon* (Amphibia: Caudata)." Herpetologica **35**(1): 11-20.
- Naylor, B. G. (1981). "Cryptobranchid salamanders from the Paleocene and Miocene of Saskatchewan." Copeia **1981**(1): 76-86.
- Naylor, B. G. (1981). "A new salamander of the family Batrachosauroididae from the late Miocene of North America, with notes on other batrachosauroidida." PaleoBios **39**: 1-14.
- Naylor, B. G. and R. C. Fox (1993). "A new Ambystomatid salamander, *Dicamptodon antiquus* n.sp., from the Paleocene of Alberta, Canada." Canadian Journal of Earth Sciences **30**(4): 814-818.
- Naylor, B. G. and D. W. Krause (1981). "Piceoerpeton, a Giant Early Tertiary Salamander from Western North America." Journal of Paleontology **55**(3): 507-523.
- Nesov, L. A. (1981). "Urodele and anuran amphibians from the Cretaceous of Kyzylkum." Trudy Zoologicheskogo Instituta **101**: 57-58.
- Nevo, E. and R. Estes (1969). "*Ramonellus Longispinus*, an Early Cretaceous Salamander from Israel." Copeia(3): 540-&.
- Noble, G. K. (1928). Two New Fossil Amphibia of Zoögeographic Importance from the Miocene of Europe, American Museum of Natural History,pp.
- Noble, G. K. (1931). The Biology of the Amphibia, McGraw-Hill,pp.
- Nussbaum, R. A. (1985). The Evolution of Parental Care in Salamanders, Museum of Zoology, University of Michigan,pp.
- Page, R. D. M. (1991). "Random Dendrograms and Null Hypotheses in Cladistic Biogeography." Systematic Zoology **40**(1): 54-62.
- Page, R. D. M. (1994). "Parallel Phylogenies - Reconstructing the History of Host-Parasite Assemblages." Cladistics-the International Journal of the Willi Hennig Society **10**(2): 155-173.
- Parker, H. W. (1956). "Viviparous Caecilians and Amphibian Phylogeny." Nature **178**(4527): 250-252.
- Parra-Olea, G., M. García-París and D. B. Wake (2004). "Molecular diversification of salamanders of the tropical American genus *Bolitoglossa* (Caudata: Plethodontidae) and its evolutionary and biogeographical implications." Biological Journal of the Linnean Society **81**(3): 325-346.
- Patterson, C., D. M. Williams and C. J. Humphries (1993). "Congruence between Molecular and Morphological Phylogenies." Annual Review of Ecology and Systematics **24**: 153-188.
- Posada, D. and T. R. Buckley (2004). "Model selection and model averaging in phylogenetics: Advantages of akaike information criterion and Bayesian approaches over likelihood ratio tests." Systematic Biology **53**(5): 793-808.
- Prager, E. M. and A. C. Wilson (1988). "Ancient origin of lactalbumin from lysozyme: analysis of DNA and amino acid sequences." Journal of Molecular Evolution **27**(4): 326-335.
- Pyron, R. A. (2011). "Divergence time estimation using fossils as terminal taxa and the origins of Lissamphibia." Systematic Biology **60**(4): 466-481.

- Pyron, R. A. and J. J. Wiens (2011). "A large-scale phylogeny of Amphibia including over 2800 species, and a revised classification of extant frogs, salamanders, and caecilians." Molecular Phylogenetics and Evolution **61**(2): 543-583.
- Rage, J.-C. and D. B. Dutheil (2008). "Amphibians and squamates from the Cretaceous (Cenomanian) of Morocco A preliminary study, with description of a new genus of pipid frog." Palaeontographica Abteilung A **285**(1-3): 1-22.
- Rage, J. C., L. G. Marshall and M. Gayet (1993). "Enigmatic Caudata (Amphibia) from the Upper Cretaceous of Gondwana." Geobios **26**(4): 515-519.
- Ree, R. H. (2005). "A likelihood framework for inferring the evolution of geographic range on phylogenetic trees." Evolution **59**(11): 2299.
- Regal, P. J. (1966). "Feeding Specializations and Classification of Terrestrial Salamanders." Evolution **20**(3): 392-&.
- Ren, D. and J. D. Oswald (2002). A new genus of kalligrammatid lacewings from the Middle Jurassic of China (Neuroptera: Kalligrammatidae), Staatliches Museum für Naturkunde, pp. 1-8.
- Robinson, D. F. and L. R. Foulds (1981). "Comparison of phylogenetic trees." Mathematical Biosciences **53**(1-2): 131-147.
- Roelants, K., D. J. Gower, M. Wilkinson, S. P. Loader, S. D. Biju, K. Guillaume, L. Moriau and F. Bossuyt (2007). "Global patterns of diversification in the history of modern amphibians." Proceedings of the National Academy of Sciences of the United States of America **104**(3): 887-892.
- Rohlf, F. (2004). tpsDig, Digitize Landmarks and Outlines, version 2.0, New York: Department of Ecology and Evolution, State University of New York at Stony Brook.
- Romer, A. S. (1968). "The Origin of Terrestrial Vertebrates. I. I. Schmalhausen. Translated from the Russian edition (Moscow, 1964) by Leon Kelso. Keith Stewart Thomson, Ed. Academic Press, New York, 1968. xii + 314 pp., illus. \$15." Science **162**(3850): 250-251.
- Ronquist, F. (1997). "Dispersal-Vicariance Analysis: A New Approach to the Quantification of Historical Biogeography." Systematic Biology **46**(1): 195-203.
- Ronquist, F. and J. P. Huelsenbeck (2003). "MrBayes 3: Bayesian phylogenetic inference under mixed models." Bioinformatics **19**(12): 1572-1574.
- Ronquist, F. and J. Liljeblad (2001). "Evolution of the gall wasp-host plant association." Evolution **55**(12): 2503-2522.
- Ronquist, F., P. van der Mark and J. P. Huelsenbeck (2009). "Bayesian phylogenetic analysis using MRBAYES." Phylogenetic Handbook: A Practical Approach to Phylogenetic Analysis and Hypothesis Testing, 2nd Edition: 210-266.
- Rosen, D. E. (1975). "A vicariance model of Caribbean biogeography." Systematic Biology **24**(4): 431.
- Rosen, D. E. (1978). "Vicariant Patterns and Historical Explanation in Biogeography." Systematic Biology **27**(2): 159-188.
- Ruta, M. and M. I. Coates (2007). "Dates, nodes and character conflict: Addressing the lissamphibian origin problem." Journal of Systematic Palaeontology **5**(1): 69-122.
- Ruta, M., M. I. Coates and D. L. J. Quicke (2003). "Early tetrapod relationships revisited." Biological Reviews **78**(2): 251-345.
- San Mauro, D. (2010). "A multilocus timescale for the origin of extant amphibians." Molecular Phylogenetics and Evolution **56**(2): 554-561.
- San Mauro, D., D. J. Gower, O. V. Oommen, M. Wilkinson and R. Zardoya (2004). "Phylogeny of caecilian amphibians (Gymnophiona) based on complete mitochondrial genomes and nuclear RAG1." Molecular Phylogenetics and Evolution **33**(2): 413-427.
- San Mauro, D., M. Vences, M. Alcobendas, R. Zardoya and A. Meyer (2005). "Initial diversification of living amphibians predated the breakup of Pangaea." American Naturalist **165**(5): 590-599.
- Sanmartin, I. and F. Ronquist (2004). "Southern Hemisphere biogeography inferred by event-based models: Plant versus animal patterns." Systematic Biology **53**(2): 216-243.

- Sanmartín, I. and F. Ronquist (2004). "Southern Hemisphere Biogeography Inferred by Event-Based Models: Plant versus Animal Patterns." Systematic Biology **53**(2): 216-243.
- Sansom, R. S., S. E. Gabbott and M. A. Purnell (2010). "Non-random decay of chordate characters causes bias in fossil interpretation." Nature **463**(7282): 797-800.
- Sansom, R. S. and M. A. Wills (2013). "Fossilization causes organisms to appear erroneously primitive by distorting evolutionary trees." Sci. Rep. **3**.
- Savage, J. M. (1973). The geographic distribution of frogs: Patterns and predictions, (Publisher) Allan Hancock Foundation, University of Southern California, pp. 445.
- Schoch, R. R. and R. L. Carroll (2003). "Ontogenetic evidence for the Paleozoic ancestry of salamanders." Evolution & Development **5**(3): 314-324.
- Schultze, H. P. and L. Trueb (1991). Origins of the Higher Groups of Tetrapods: Controversy and Consensus, Comstock Pub. Associates, pp.
- Schwarz, G. (1978). "Estimating the Dimension of a Model." (2): 461-464.
- Sessions, S. K. (1982). "Cytogenetics of diploid and triploid salamanders of the *Ambystoma jeffersonianum* complex." Chromosoma **84**(5): 599-621.
- Sever, D. M. (1991). "Comparative Anatomy and Phylogeny of the Cloacae of Salamanders (Amphibia: Caudata). I. Evolution at the Family Level." Herpetologica **47**(2): 165-193.
- Sever, D. M. (1992). "Comparative anatomy and phylogeny of the cloacae of salamanders (Amphibia: Caudata). VI. Ambystomatidae and Dicamptodontidae." Journal of Morphology **212**(3): 305-322.
- Sever, D. M. and S. E. Trauth (1990). "Cloacal Anatomy of Female Salamanders of the Plethodontid Subfamily Desmognathinae (Amphibia, Urodela)." Transactions of the American Microscopical Society **109**(2): 193-204.
- Shaffer, H. B. and S. R. Voss (1996). "Phylogenetic and mechanistic analysis of a developmentally integrated character complex: Alternate life history modes in ambystomatid salamanders." American Zoologist **36**(1): 24-35.
- Shubin, N. H. and K. Q. Gao (2003). "Earliest known crown-group salamanders." Nature **422**(6930): 424-428.
- Sigurdson, T. and J. R. Bolt (2010). "The Lower Permian Amphibamid *Doleserpeton* (Temnospondyli: Dissorophoidea), the Interrelationships of Amphibamids, and the Origin of Modern Amphibians." Journal of Vertebrate Paleontology **30**(5): 1360-1377.
- Skutschas, P. and T. Martin (2011). "Cranial anatomy of the stem salamander *Kokartus honorarius* (Amphibia: Caudata) from the Middle Jurassic of Kyrgyzstan." Zoological Journal of the Linnean Society **161**(4): 816-838.
- Skutschas, P. P. (2009). "Re-evaluation of *Mynbulakia* Nesov, 1981 (Lissamphibia: Caudata) and description of a new salamander genus from the Late Cretaceous of Uzbekistan." Journal of Vertebrate Paleontology **29**(3): 659-664.
- Skutschas, P. P. (2014). "Kiyatriton leshchinskiyi Averianov et Voronkevich, 2001, a crown-group salamander from the Lower Cretaceous of Western Siberia, Russia." Cretaceous Research **51**(0): 88-94.
- Skutschas, P. P. and Y. M. Gubin (2012). "A new salamander from the late Paleocene-early Eocene of Ukraine." Acta Palaeontologica Polonica **57**(1): 135-148.
- Skutschas, P. P. and S. A. Krasnolutskii (2011). "A new genus and species of basal salamanders from the Middle Jurassic of Western Siberia, Russia. ." proceedings of the Zoological Institute of the Russian Academy of Science **315**(2): 167-175.
- Sober, E. (1994). Conceptual Issues in Evolutionary Biology, MIT Press, pp.
- Steinfartz, S., M. Veith and D. Tautz (2000). "Mitochondrial sequence analysis of *Salamandra* taxa suggests old splits of major lineages and postglacial recolonizations of Central Europe from distinct source populations of *Salamandra salamandra*." Molecular Ecology **9**(4): 397-410.
- Sullivan, C., Y. Wang, D. W. E. Hone, Y. Q. Wang, X. Xu and F. C. Zhang (2014). "The Vertebrates of the Jurassic Daohugou Biota of Northeastern China." Journal of Vertebrate Paleontology **34**(2): 243-280.

- Sun, G., D. L. Dilcher, H. Wang and Z. Chen (2011). "A eudicot from the Early Cretaceous of China." Nature **471**(7340): 625-628.
- Sutton, M. D., R. J. Garwood, D. J. Siveter and D. J. Siveter (2012). "SPIERS and VAXML; A software toolkit for tomographic visualisation and a format for virtual specimen interchange." Palaeontologia Electronica **15**(2).
- Sweet, S. S. (1982). "A Distributional Analysis of Epigeal Populations of Eurycea-Neotenes in Central Texas, with Comments on the Origin of Troglotic Populations." Herpetologica **38**(3): 430-444.
- Swofford, D. L. (2003). "Phylogenetic Analysis Using Parsimony (*and Other Methods). Version 4." Sinauer Associates, Sunderland, Massachusetts.
- Taylor, E. H. and C. J. Hesse (1943). "A new salamander from the Upper Miocene beds of San Jacinto County, Texas." American Journal of Science **241**(3): 185-193.
- Teeling, E. C., M. S. Springer, O. Madsen, P. Bates, S. J. O'Brien and W. J. Murphy (2005). "A Molecular Phylogeny for Bats Illuminates Biogeography and the Fossil Record." Science **307**(5709): 580-584.
- Templeton, A. R. (1983). "Phylogenetic inference from restriction endonuclease cleavage site maps with particular reference to the evolution of humans and the apes." Evolution: 221-244.
- Trueb, L. and R. Cloutier (1991). A phylogenetic investigation of the inter- and intrarelationships of the Lissamphibia (Amphibia: Temnospondyli). Origins of the Higher Groups of Tetrapods: Controversy and Consensus. H. P. Schultze and L. Trueb (eds). New York, Comstock Pub. Associates: 223-313.
- Upchurch, P. (2008). "Gondwanan break-up: legacies of a lost world?" Trends in Ecology & Evolution **23**(4): 229-236.
- Upchurch, P., C. A. Hunn and D. B. Norman (2002). "An analysis of dinosaurian biogeography: evidence for the existence of vicariance and dispersal patterns caused by geological events." Proceedings of the Royal Society B-Biological Sciences **269**(1491): 613-621.
- Upchurch, P., P. D. Mannion, R. J. Butler, R. B. J. Benson and M. T. Carrano (2011). Geological and anthropogenic controls on the sampling of the terrestrial fossil record: a case study from the Dinosauria. Geological Society, London, Special Publications. A. J. a. S. McGowan, A. B. (eds). **Comparing the Rock and Fossil Records: Implications for Biodiversity**.
- Vallin, G. and M. Laurin (2004). "Cranial morphology and affinities of *Microbrachis*, and reappraisal of the phylogeny and lifestyle of the first amphibians." Journal of Vertebrate Paleontology **24**(1): 56-72.
- Veith, M., S. Steinfartz, R. Zardoya, A. Seitz and A. Meyer (1998). "A molecular phylogeny of 'true' salamanders (family Salamandridae) and the evolution of terrestriality of reproductive modes." Journal of Zoological Systematics and Evolutionary Research **36**(1-2): 7-16.
- Vieites, D. R., M. S. Min and D. B. Wake (2007). "Rapid diversification and dispersal during periods of global warming by plethodontid salamanders." Proceedings of the National Academy of Sciences of the United States of America **104**(50): 19903-19907.
- Vieites, D. R., S. Nieto-Roman and D. B. Wake (2009). "Reconstruction of the climate envelopes of salamanders and their evolution through time." Proceedings of the National Academy of Sciences of the United States of America **106**: 19715-19722.
- Vieites, D. R., P. Zhang and D. B. Wake (2009). Salamanders (Caudata). The timetree of life. S. B. Hedges and S. Kumar (eds). Oxford, Oxford University Press: 365-368.
- Voss, S. R. (1995). "Genetic Basis of Pedomorphosis in the Axolotl, *Ambystoma mexicanum*: A Test of the Single-Gene Hypothesis." Journal of Heredity **86**(6): 441-447.
- Wake, D. (1966). Comparative osteology and evolution of the lungless salamanders, family Plethodontidae, pp.
- Wake, D. B. (1991). "Homoplasy - The result of natural-selection, or evidence of design limitations." American Naturalist **138**(3): 543-567.

- Wake, D. B. and R. Lawson (1973). "Developmental and adult morphology of the vertebral column in the plethodontid salamander *Eurycea bislineata*, with comments on vertebral evolution in the amphibia." Journal of Morphology **139**(3): 251-299.
- Wang, X., Z. Zhou, H. He, F. Jin, Y. Wang, J. Zhang, Y. Wang, X. Xu and F. Zhang (2005). "Stratigraphy and age of the Daohugou Bed in Ningcheng, Inner Mongolia." Chinese Science Bulletin **50**(20): 2369-2376.
- Wang, Y. (2004). "A new Mesozoic caudate (*Liaoxitriton daohugouensis* sp nov.) from Inner Mongolia, China." Chinese Science Bulletin **49**(8): 858-860.
- Wang, Y. (2004). "Taxonomy and stratigraphy of late Mesozoic anurans and urodeles from China." Acta Geologica Sinica-English Edition **78**(6): 1169-1178.
- Wang, Y. and S. E. Evans (2006). "A new short-bodied salamander from the Upper Jurassic/Lower Cretaceous of China." Acta Palaeontologica Polonica **51**(1): 127-130.
- Wang, Y. and C. S. Rose (2005). "*Jeholotriton Paradoxus* (Amphibia : Caudata) from the Lower Cretaceous of southeastern Inner Mongolia, China." Journal of Vertebrate Paleontology **25**(3): 523-532.
- Weisrock, D. W., L. J. Harmon and A. Larson (2005). "Resolving deep phylogenetic relationships in salamanders: Analyses of mitochondrial and nuclear genomic data." Systematic Biology **54**(5): 758-777.
- Welsh, H. H. and L. M. Ollivier (1998). "Stream amphibians as indicators of ecosystem stress: A case study from California's redwoods." Ecological Applications **8**(4): 1118-1132.
- Whiteman, H. H. (1994). "Evolution of facultative pedomorphosis in salamanders." Quarterly Review of Biology **69**(2): 205-221.
- Wiegmann, B., M. Trautwein, J.-W. Kim, B. Cassel, M. Bertone, S. Winterton and D. Yeates (2009). "Single-copy nuclear genes resolve the phylogeny of the holometabolous insects." BMC Biology **7**(1): 34.
- Wiens, J. J., R. M. Bonett and P. T. Chippindale (2005). "Ontogeny discombobulates phylogeny: Paedomorphosis and higher-level salamander relationships." Systematic Biology **54**(1): 91-110.
- Wiens, J. J., P. T. Chippindale and D. M. Hillis (2003). "When are phylogenetic analyses misled by convergence? A case study in Texas cave salamanders." Systematic Biology **52**(4): 501-514.
- Wiley, E. O. and B. S. Lieberman (2011). Phylogenetics: Theory and Practice of Phylogenetic Systematics, Wiley, pp.
- Wilkinson, M. (1997). "Characters, congruence and quality: A study of neuroanatomical and traditional data in caecilian phylogeny." Biological Reviews of the Cambridge Philosophical Society **72**(3): 423-470.
- Wilkinson, M. (2001). "PICA 4.0: software and documentation. Department of Zoology, The Natural History Museum, London."
- Yanxue, L. I. U., L. I. U. Yongqing and Z. Hong (2006). "LA-ICPMS Zircon U-Pb Dating in the Jurassic Daohugou Beds and Correlative Strata in Ningcheng of Inner Mongolia." Acta Geologica Sinica - English Edition **80**(5): 733-742.
- Zachos, J., M. Pagani, L. Sloan, E. Thomas and K. Billups (2001). "Trends, rhythms, and aberrations in global climate 65 Ma to present." Science **292**(5517): 686-693.
- Zardoya, R. and A. Meyer (2001). "On the origin of and phylogenetic relationships among living amphibians." Proceedings of the National Academy of Sciences of the United States of America **98**(13): 7380-7383.
- Zhang, G. L., Y. Wang, M. E. H. Jones and S. E. Evans (2009). "A new Early Cretaceous salamander (*Regalerpeton weichangensis* gen. et sp nov.) from the Huajiying Formation of northeastern China." Cretaceous Research **30**(3): 551-558.
- Zhang, K., D. Yang and D. Ren (2006). "The first snipe fly (Diptera: Rhagionidae) from the Middle Jurassic of Inner Mongolia, China." Zootaxa **1134**: 51-57.

- Zhang, P., Y.-Q. Chen, H. Zhou, Y.-F. Liu, X.-L. Wang, T. J. Papenfuss, D. B. Wake and L.-H. Qu (2006). "Phylogeny, evolution, and biogeography of Asiatic Salamanders (Hynobiidae)." Proceedings of the National Academy of Sciences **103**(19): 7360-7365.
- Zhang, P. and D. B. Wake (2009). "Higher-level salamander relationships and divergence dates inferred from complete mitochondrial genomes." Molecular Phylogenetics and Evolution **53**(2): 492-508.
- Zhang, P., H. Zhou, Y. Q. Chen, Y. F. Liu and L. H. Qu (2005). "Mitogenomic perspectives on the origin and phylogeny of living amphibians." Systematic Biology **54**(3): 391-400.
- Zug, G. R., L. J. Vitt and J. P. Caldwell (2001). Herpetology: An introductory biology of amphibians and reptiles, Academic Press, pp. 630.

Acknowledgements

First and foremost, I would like to express my deepest gratitude to Professor Paul Upchurch, Professor Susan Evans and Dr Mark Wilkinson, my research supervisors, for their patient guidance, encouragement and many useful critiques of my work.

To the many colleagues and institutions who allowed me to visit and collect data, I would like to offer very sincere thanks. Especially, but not restricted to, Dr Florian Witzmann and Dr Johannes Mueller at the Museum für Naturkunde in Berlin; Dr Pat Holroyd and Dr Kevin Padian at the University of California, Museum of Paleontology in San Francisco; Dr James Gardner at the Royal Tyrrell Museum in Drumheller; Professor Yuan Wang and Ms Liping Dong at the Institute of Vertebrate Paleontology and Paleoanthropology in Beijing; Dr Angela Delgado and the staff at the Museo de las Ciencias de Castilla La Mancha in Cuenca; Dr Jean-Claude Rage at the Muséum National d'Histoire Naturelle in Paris; and finally the friendly staff at the Grant Museum and the Natural History Museum in London especially Peter Foster.

I would also like to offer my gratitude to my (past and present) lab mates, colleagues and fellow PhD candidates. The support and encouragement over the past four years has been very much appreciated and special mention must go to Dr Marc Jones, also Dr Roger Benson, Dr Phil Mannion, and Dr Mark Bell for many conversations and advice about my research; Dave Demar, Dr Graeme Lloyd, Professor David Dobson, and Dr James Gardner for their encouragement and enthusiasm for my work (and generally talking to me like I was a real scientist); Dr Mike Chandler and Dr Marie Pears for being metaphorical shoulders to cry on, and finally to the many wonderful people I work alongside who are too numerous to mention here.

Special thanks also go to my friends who have been supportive and understanding especially during the final stages of my work. Among others, a special mention must go to Dr Nooreen Shaikh, Emily Rowley, Olivia Wood, Stephen Wisbey, Steve Donaghy, Dr James Garvey, and Seye Bolade. Dr Ian Sillitoe deserves special mention for his endless encouragement and feedback on my corrections.

Finally, I wish to thank my brothers, Peter Pearson and Philip Pearson, and their families, also and especially, my parents, Rev David Pearson and Mrs Mary Pearson for their unwavering support, encouragement, and confidence in me throughout my many years of study. There is absolutely no way I would have been able to do this without you. Thank you!

Appendix:

Appendix A – Genetic Species List (on CD attached)

Appendix B - Full morphological character set (also on CD attached)

Colour code: **Red** means it's a modified character

Purple means it's an added character for salamanders

Orange means soft body character

Green means ordered multistate character

Skull:

1. Dentition **in adult teeth** (Zhang *et al.* 2009); (0) pedicellate, **(1) sub-pedicellate**, (2) non-pedicellate
2. Fusion of premaxillae (modified from Zhang *et al.* 2009); (0) paired premaxillae, (1) **fused at base**, (2) fully fused premaxillae (**ordered**)
3. Contact of premaxillae (between themselves), (modified from Wiens *et al.* 2005); (0) contacting medially **throughout their entire length**, (1) separated **towards the frontals or parietals**, (2) **contacting anteriorly and posteriorly, separated medially with fontanelle exposed** (3) **no contact** (**ordered**)
4. Dorsal process of premaxilla (**ratio data with measurements of width of premaxilla vs length of premaxillary extension**) (Zhang *et al.* 2009); (0) absent or poorly defined, (1) short but well-defined, (2) strong posterior extension (**ordered**)
5. Premaxilla in relation to frontals (modified from Wiens *et al.* 2005); (0) not contacting frontals, (1) contacting frontals, **(2) extension of dorsal process intervenes deeply between the frontals** (**ordered**)
6. Premaxillary dentition presence (Hanken and Hall, 1993); (0) present, (1) absent
7. Premaxilla dentition position (Wiens *et al.* 2005); (0) present lateral to pars dorsalis, (1) absent lateral to pars dorsalis
8. **Premaxilla dentition (shape)**; (0) **conical**, (1) **bulbous**
9. Combined width of premaxilla **measured at the premaxilla/maxilla suture** (Wiens *et al.* 2005); (0) less than interorbital width, (1) greater than interorbital width
10. Premaxilla-palatine contact (Wiens *et al.* 2005); (0) absent, (1) present
11. Premaxilla-vomer contact (Wiens *et al.* 2005); (0) absent, (1) present
12. Premaxilla-nasal contact (Wiens *et al.* 2005); (0) absent, (1) present
13. Maxilla (Zhang *et al.* 2009); (0) presence of bilaterally paired maxillae, (1) greatly reduced as a rudimentary element, (2) entirely absent and functionally replaced by modified vomer (**ordered**)
14. Maxillary dentition (Wiens *et al.* 2005); (0) dentate, (1) reduced, edentulous
15. **Dentition shape**; (0) **mono-cuspid**, (1) **bi-cuspid**, (2) **tricuspid**
16. Posterior process of maxilla (Wiens *et al.* 2005); (0) dentate, (1) edentulous
17. Process from pars dentalis of maxilla overlaps premaxilla (Wiens *et al.* 2005); (0) no, (1) yes
18. Anterior margin of pars facialis of maxilla (modified from Wiens *et al.* 2005); (0) posterior to external naris, (1) **Forms lateral part of external naris**

19. Septomaxilla (Larson and Dimmick, 1993; Hanken and Hall, 1993; Duellman and Trueb, 1994; Gao and Shubin, 2001; Wiens *et al.* 2005; Zhang *et al.* 2009); (0) presence of bilaterally paired septomaxillae, (1) absence of bones.
20. Posterior end of septomaxilla (Wiens *et al.* 2005); (0) not contacting other cranial elements, (1) contacting maxilla, (2) contacting prefrontal, (3) contacting nasal (unordered)
21. Nasal (**modified from** Wiens *et al.* 2005); (0) present, (1) absent
22. Nasal ossification (Hanken and Hall, 1993; Larson and Dimmick, 1993; Gao and Shubin, 2001; Zhang *et al.* 2009); (0) paired nasals with sutural midline contact or fused, (1) nasals separate without midline contact
23. Nasal (Wiens *et al.* 2005); (0) not forked posteriorly, (1) forked posteriorly
24. Nasal shape (Wiens *et al.* 2005); (0) squarish, length and width roughly equal, (1) slender and elongate, length greater than width
25. Nasal-prefrontal contact (Gao and Shubin, 2001; Wiens *et al.* 2005; Zhang *et al.* 2009); (0) present, (1) absent
26. Nasal and maxilla (Wiens *et al.* 2005); (0) contacting or abutting, (1) separated
27. Nasal contact with frontal (Gao and Shubin, 2001; Wiens *et al.* 2005; Zhang *et al.* 2009); (0) separate from frontal, (1) partly or completely fused to frontal
28. Nasal-lacrimal duct (Hanken and Hall, 1993; Gao and Shubin, 2001; Zhang *et al.* 2009); (0) present, (1) absent
29. Lacrimal (Hanken and Hall, 1993; Duellman and Trueb, 1994; Gao and Shubin, 2001; Wiens *et al.* 2005; Zhang *et al.* 2009); (0) present, (1) absent
30. Quadratojugal (Hanken and Hall, 1993; Duellman and Trueb, 1994; Gao and Shubin, 2001; Zhang *et al.* 2009); (0) present, (1) absent
31. Prefrontal (Hanken and Hall, 1993; Gao and Shubin, 2001; Wiens *et al.* 2005; Zhang *et al.* 2009); (0) present, (1) absent
32. Prefrontal posterior process projecting into the orbit (**modified from** Hanken and Hall, 1993; Gao and Shubin, 2001; Wiens *et al.* 2005; Zhang *et al.* 2009); (0) present, (1) absent
33. Prefrontal orientation (**modified from** Wiens *et al.* 2005); (0) present and forms part of the margin of the external naris, (1) present but does not form part of the margin of the external naris
34. Frontal (Duellman and Trueb, 1994); (0) paired roofing bones, (1) fused into a single element
35. Frontal/maxillary contact (Gao and Shubin, 2001; Zhang *et al.* 2009, Wiens *et al.* 2005); (0) frontal and maxilla separated by prefrontal, (1) frontal contacts dorsal process of maxilla
36. Dorsolateral shelf on frontal (Wiens *et al.* 2005); (0) absent, (1) present
37. Postfrontal (Gao and Shubin, 2001, Zhang *et al.* 2009); (0) present, (1) absent
38. Palatal dentition (on the palatine) (**modified from** Gao and Shubin, 2001, Zhang *et al.* 2009); (0) present, (1) absent
39. Vomer dentition (**modified from** Gao and Shubin, 2001, Zhang *et al.* 2009); (0) present, (1) absent
40. Parasphenoid dentition (**modified from** Gao and Shubin, 2001, Zhang *et al.* 2009); (0) present, (1) absent
41. Pterygoid dentition (**modified from** Gao and Shubin, 2001, Zhang *et al.* 2009); (0) present, (1) absent
42. Placement of vomerine teeth (Duellman and Trueb, 1994, Hanken and Hall, 1993; Wiens *et al.* 2005, Zhang *et al.* 2009); (0) medial/lateral transverse row, (1) marginal (adjacent and parallel to max. and premaxillary teeth), (2) teeth centrally located on vomer, (3) teeth in large patches, (4) teeth in M-shaped pattern (unordered)
43. Palatal tooth structure (Hanken and Hall, 1993; Duellman and Trueb, 1994); (0) conical, (1) compressed, (2) bulbous

44. Vomerine teeth (Tihen, 1958; Wiens *et al.* 2005); (0) present on postchoanal process, (1) absent on postchoanal process
45. Vomer with postchoanal process (Wiens *et al.* 2005); (0) with postchoanal process, (1) without postchoanal process
46. Vomer with prechoanal process (Wiens *et al.* 2005); (0) with prechoanal process, (1) without prechoanal process
47. Vomer and pterygoid (Wiens *et al.* 2005); (0) not articulating with pterygoid, (1) articulates with pterygoid
48. Vomers (**modified from** Wiens *et al.* 2005); (0) separated anteriorly and medially, (**1**) **separated medially and posteriorly** (2) **separated entirely**, (3) in contact anteromedially, no fontanelle exposed (unordered)
49. Vomer, posterior dorsal process extending onto orbitosphenoid (Wiens *et al.* 2005); (0) absent, (1) present
50. Pterygoid **shape** (**modified from** Zhang *et al.* 2009); (0) triradiate and boomerang-shaped, (1) enlarged with distinct anteromedial process, (2) straight bar with loss of anteromedial process, (3) absent (unordered)
51. Anterior margin of pterygoid (Wiens *et al.* 2005); (0) smooth, (1) serrate, with irregular projections
52. Pterygoid and coronoid process of prearticular (Wiens *et al.* 2005); (0) well separated, (1) articulating or nearly contacting
53. Posterior margin of pterygoid extends posterior to jaw articulation (Wiens *et al.* 2005); (0) no, (1) yes
54. Pterygoid, with dorsomedial process that articulates with orbitosphenoid and forms foramen posterior to optic foramen (Wiens *et al.* 2005); (0) absent, (1) present
55. Internal carotid foramen (Zhang *et al.* 2009; Gao and Shubin, 2001); (0) present, (1) absent
56. Squamosal-frontal (Wiens *et al.* 2005); (0) does not contact frontal, (1) contacts frontal
57. Squamosal (Wiens *et al.* 2005); (0) not expanded ventrally, (1) expanded ventrally, occupies articular region
58. Squamosal, main shaft in lateral view (Gao and Shubin, 2001; Wiens *et al.* 2005; Zhang *et al.* 2009); (0) oriented roughly vertically, (1) oriented diagonally, with dorsoposterior inclination
59. Hook-like (ventrally-directed) process on dorsal head of squamosal (Wiens *et al.* 2005); (0) absent, (1) present
60. Columellar process of squamosal, connecting stapes and squamosal (Wiens *et al.* 2005); (0) absent, (1) present
61. Squamosal contact with the parietal or other roofing elements (**modified from** Gao and Shubin, 2001; Zhang *et al.* 2009); (0) contact present, (1) absent **or virtually absent**
62. Prootic-exoccipital-opisthotic fusion (Hanken and Hall, 1993; Duellman and Trueb, 1994; Gao and Shubin, 2001; Wiens *et al.* 2005; Zhang *et al.* 2009); (0) three separate elements, (1) prootic-exoccipital fused, separate opisthotic, (2) all three elements fused (**ordered**)
63. Exposure of prootic-exoccipital-opisthotic complex in dorsal view (Zhang *et al.* 2009); (0) the complex largely concealed by parietal or exposed posterior to skull table, (1) large exposure extends lateral to parietal table
64. Exoccipitals (Wiens *et al.* 2005); (0) separated medially at tectum synoticum, (1) fused
65. Operculum (Hanken and Hall, 1993; Zhang *et al.* 2009); (0) present and free, (1) absent or fused
66. Stapes (Hanken and Hall, 1993; Zhang *et al.* 2009); (0) present, (1) absent
67. Orbitosphenoid (Wiens *et al.* 2005); (0) present, (1) absent
68. Orbitosphenoid (Wiens *et al.* 2005); (0) not extending lateral to frontals, or extending only slightly anteriorly, (1) extending well lateral to frontals throughout their length

69. *Sagittal crest **formed at the midline between the parietals** of the skull (**modified from** Wiens *et al.* 2005); (0) absent, (1) present
70. Dermal sculpture on skull roof (Zhang *et al.* 2009); (0) present, coarse, (1) present, weak, (2) absent
71. Posterior edge of parietals, extends between exoccipitals to edge of foramen magnum on tectum synoticum (Wiens *et al.* 2005); (0) no, (1) yes
72. Ventrolateral extension of parietal covers orbitosphenoid region anteriorly (in lateral view), (Wiens *et al.* 2005); (0) absent, (1) present
73. *Parietal and exoccipital (Wiens *et al.* 2005); (0) not forming casque around foramen magnum, (1) forming casque around foramen magnum
74. Anterolateral process of parietal (**modified from** Gao and Shubin, 2001; Zhang *et al.* 2009); (0) absent, (1) present
75. Anterolateral process of parietal (**modified from** Gao and Shubin, 2001; Zhang *et al.* 2009); (0) forms less than 50% of the total length of the parietal, (1) makes up more than 50% of total length of the parietal
76. Medial border of orbit (Zhang *et al.* 2009); (0) more than 50% of orbital margin formed by frontal, (1) frontal contributes less than 50% of the orbit margin, (2) frontal fully excluded from entering orbital margin (unordered)
77. Angular/prearticular fusion (Duellman and Trueb, 1986; Larson and Dimmick, 1993; Hanken and Hall, 1993; Duellman and Trueb, 1994; Gao and Shubin, 2001; Wiens *et al.* 2005; Zhang *et al.* 2009); (0) angular distinct from the prearticular, (1) no distinct angular (absent or fused to prearticular in adult).
78. Coronoid (Hanken and Hall, 1993; Gao and Shubin, 2001; Wiens *et al.* 2005); (0) present as a separate element, (1) absent in adult stage
79. Coronoid dentition (Hanken and Hall, 1993; Wiens *et al.* 2005); (0) dentate, (1) edentulous
80. Articular (modified from Gao and Shubin, 2001; Wiens *et al.* 2005; Zhang *et al.* 2009); (0) present as separate element, (1) fused with prearticular, (2) **absent/unossified** (unordered)
81. Meckel's cartilage (Wiens *et al.* 2005); (0) does not extend to mandibular symphysis, (1) extends to mandibular symphysis
82. *Mandible (in anterior view) (Wiens *et al.* 2005); (0) thickens suddenly at symphysis, (1) thins/ stays the same towards the symphysis
83. Mandibular symphysis (Duellman and Trueb, 1994); (0) simple union of the mandibular rami, (1) rami have an interlocking symphysis
84. Dentary (Wiens *et al.* 2005); (0) dentate, (1) edentulous
85. **Dentary teeth shape; (0) conical, (1) bulbous**
86. **Dentary symphyseal teeth; (0) present, (1) absent**
87. **Dentary lateral sensory nerve foramina; (0) absent, (1) present**
88. Retroarticular process (**modified from** Wiens *et al.* 2005); (0) **very small**/absent, (1) present
89. Coronoid process of prearticular (Wiens *et al.* 2005); (0) adjacent to jaw articulation, (1) distinctly anterior to jaw articulation
90. Palatine and pterygoid (Wiens *et al.* 2005); (0) palatine absent (1) palatine present
91. Quadrate ossification (Wiens *et al.* 2005); (0) present, (1) absent
92. Posterior process on pars quadrati of quadrate (Wiens *et al.* 2005); (0) absent, (1) present
93. Jaw articulation (Wiens *et al.* 2005); (0) well ventral to level of ventral margin of braincase, (1) at level of ventral margin of braincase
94. Quadrate-parasphenoid articulation (Wiens *et al.* 2005); (0) absent, (1) present
95. Parasphenoid (Wiens *et al.* 2005); (0) not extending laterally beyond level of orbitosphenoid, (1) extending laterally beyond level of orbitosphenoid

96. Optic foramen (**modified from** Wiens *et al.* 2005); (0) enclosed in **the orbitosphenoid** bone anteriorly or not at all, (1) enclosed entirely in **the orbitosphenoid** bone
97. Posteriormost margin of auditory capsules (Wiens *et al.* 2005); (0) anterior to occipital condyles, (1) posterior to occipital condyles
98. Lateral flange on prootic extending to the squamosal (Wiens *et al.* 2005); (0) absent, (1) present
99. **Second basibranchial (ventral view); (0) bar (horizontal or vertical), (1) Y-shaped (two branches), (2) multiple branches (more than two) (unordered)**

Atlas:

100. Position of atlas posterior cotyle relative to anterior cotyles (J. Gardner, 2000); (0) the posterior cotyle is approximately in line with the anterior cotyles in lateral view, (1) the posterior cotyle is displaced ventrally in relation to the anterior cotyles.
101. Notochordal pit in posterior cotyle of the atlas (modified from J. Gardner, 2000); (0) the notochordal pit is open and has no infilling of calcified or ossified cartilage, **(1) partly in-filled by ossified cartilage**, (2) totally in-filled and bulging beyond the edge of the centrum with ossified cartilage (**ordered**)
102. Relative depth of anterior atlas cotyles (modified from J. Gardner, 2000); (0) deeply concave, (1) nearly flat to shallowly concave, **(2) convex** (although the structure is called a cotyle which means cup-like, they are sometimes convex) (**ordered**)
103. Outline of anterior atlas cotyles (J. Gardner, 2000); (0) compressed dorsoventrally, (1) subcircular, (2) compressed lateromedially (**ordered**)
104. Form of odontoid process (modified from J. Gardner, 2000); **(0) knob-like**, (1) dorsoventrally flattened, **(2) separate (not joined in the middle), (3) highly reduced or absent** (unordered)
105. Position of atlas neural canal relative to the anterior cotyles (J. Gardner, 2000); (0) the neural canal is situated above the anterior cotyles, (1) the neural canal protrudes in between the anterior cotyles, but up to half way or less than the dorsoventral distance of the anterior cotyles, (2) Neural canal intrudes deeply or completely between the anterior cotyles (**ordered**)
106. Size of atlas neural canal relative to the anterior cotyles (J. Gardner, 2000); (0) the anterior circumference of the neural canal is approximately equal to or greater than the circumference of one of the anterior cotyles, (1) the neural canal is smaller than the anterior cotyle
107. Posterior extent of neural arch roof of the atlas (modified from J. Gardner, 2000); (0) extends past the edge of the posterior cotyle, **(1) in line with the posterior cotyle, (2) the posterior edge of the neural arch roof is shorter i.e. does not reach to the edge of the posterior cotyle (ordered)**
108. Dorsal outline of posterior margin of the atlas neural arch roof (modified from J. Gardner, 2000); (0) truncated, (1) forked, **(2) pointed** (unordered)
109. Dorsal outline of the atlas' neural arch crest (modified from J. Gardner, 2000); (0) the outline of the crest broadens posteriorly, (1) it narrows posteriorly, **(2) relatively straight, (3) it is hourglass shaped i.e. narrows then broadens** (unordered)
110. Shape of anterior end of neural arch crest on the atlas (modified from J. Gardner, 2000); (0) not elaborated, **(1) swollen or thickened**, (2) paired anterior processes (unordered)
111. Postzygapophyses prominence on the atlas (modified from J. Gardner, 2000); **(0) prominent, (1) small.**
112. Postzygapophyses articular surface on the atlas (modified from J. Gardner, 2000); **(0) laterally divergent, (1) directed ventro-laterally.**
113. Postzygapophyses; (0) diverge from the end of the neural arch crest on the atlas, **(1) diverge from along the neural arch crest of the atlas.**

114. Condition of the dorsal part of the neural arch crest of the atlas (J. Gardner, 2000); (0) finished in cartilage, (1) finished in bone
115. Condition of the posterior end of the neural arch spine of the atlas; (0) finished in cartilage, (1) finished in bone
116. Four faceted articulation of exoccipital and atlas (Wiens *et al.* 2005; Zhang *et al.* 2009); (0) absent due to reduction in odontoid process, (1) absent due to continuous surface of odontoid and anterior cotyles, (2) present (unordered)
117. Atlantal spinal nerve foramen (Zhang *et al.* 2009); (0) absent, (1) a notch, (2) fully enclosed (ordered)
118. Atlas, transverse process (Wiens *et al.* 2005); (0) absent, (1) present
119. Shape of atlas centrum in ventral view (Zhang *et al.* 2009); (0) shorter than postatlantals, (1) roughly equal in length to postatlantals, (2) longer than postatlantals (unordered)
120. Basapophyses on the atlas; (0) absent, (1) present
121. Neural cord supports, (0) absent, (1) present

Presacral Vertebrae:

122. Centrum of presacral vertebrae (modified from J. Gardner, 2000); (0) amphicoelous, (1) semi-opisthocoelous, (2) fully opisthocoelous, (3) procoelous (unordered)
123. Size of the 4th trunk vertebrae (5th presacral) neural canal relative to its anterior size of the centrum; (0) neural canal is approximately equal in size (radius) to, or greater than, the size of the anterior centrum, (1) neural canal smaller than the anterior centrum
124. Posterior basapophyses of the presacrals (J. Gardner, 2000); (0) absent, (1) present
125. Anterior basapophyses of the presacrals (Wiens *et al.* 2005); (0) absent, (1) present
126. Condition of neural spine (J. Gardner, 2000); (0) finished in cartilage, (1) finished in bone
127. Prominent, v-shaped hypapophyses (J. Gardner, 2000); (0) absent, (1) present
128. Bony lamina between diapophyses and parapophyses (modified from Wiens *et al.* 2005); (0) absent, (1) partial presence, (2) present – full lamina (ordered)
129. Mid-ventral keel on mid-body vertebrae (modified from Wiens *et al.* 2005); (0) absent, (1) present (small), (2) Large – extends below the ventral edge of the centrum cotyles (ordered)
130. Posterolateral flanges on mid-dorsal keel on mid-body vertebrae (Wiens *et al.* 2005); (0) absent, (1) present
131. Anterior keel/flange on transverse process (extending from, and between the transverse process to anterior edge of centrum) (modified from Wiens *et al.* 2005); (0) absent, (1) present
132. Fenestra in anterior keel; (0) present, (1) absent
133. Anterodorsal keel on transverse process (extending from transverse process to anterior zygapophysis) (modified from Wiens *et al.* 2005); (0) absent, (1) present
134. Posterior keel of transverse process (extends from transverse process to posterior centrum edge); (0) absent, (1) present
135. Dermal sculpture on dorsal surface of neural arch; (0) present, (1) absent
136. Shape of the neural spine of mid-body vertebrae (modified from Wiens *et al.* 2005); (0) absent/truncated, (1) single median process (spine-like projection), (2) present (paired process)
137. Posteriorly projecting neural spine(s) (past the posterior centrum edge); (0) shorter than posterior centrum edge, (1) in line with posterior centrum edge, (2) projecting past the posterior centrum edge (ordered)

138. Posterior zygapophyses facet face of presacral vertebrae; (0) latero-medially divergent (facing slightly outwards, away from each other), (1) directed ventrally
139. Transverse process in anterior part of trunk series, excluding first presacral vertebra (J. Gardner, 2000); (0) Unicapitate, (1) bicapitate, (2) absent
140. Mid-dorsal keel (neural arch crest) on presacral vertebra (Wiens *et al.* 2005); (0) absent, (1) present
141. Mid-dorsal keel (neural arch crest) on presacral vertebra length; (0) short (does not run the length of the vertebra), (1) long (runs from at least just behind the anterior zygapophyses to neural spine)

Caudal Vertebrae:

142. Caudal vertebrae, neural spine (Wiens *et al.* 2005); (0) with one process, (1) paired process
143. Mid-dorsal crest on caudal vertebrae (Wiens *et al.* 2005); (0) absent, (1) present
144. Dermal sculpturing on dorsal surface of neural arch on the caudal vertebrae; (0) present, (1) absent
145. Caudal vertebrae (Wiens *et al.* 2005); (0) ventral keels absent, low, and/or rounded, (1) dorsal and ventral keels raised and distinctly rectangular
146. Transverse process of anterior caudal vertebrae (Wiens *et al.* 2005); (0) posteriorly orientated, (1) anteriorly oriented
147. Transverse process of anterior caudal vertebrae; (0) unicapitate, (1) bicapitate
148. Caudal vertebrae, anterior keel on haemal arch (Wiens *et al.* 2005); (0) absent, (1) present
149. Caudal vertebrae, haemal arch (Wiens *et al.* 2005); (0) complete, lateral halves fused to form median process, (1) incomplete, two ventral lamina do not contact or fuse on anterior caudal vertebrae, (2) incomplete for all caudal vertebrae (unordered)
150. Caudal vertebrae, haemal arch spine (Wiens *et al.* 2005); (0) paired process, (1) single process
151. Caudosacral vertebrae (number of caudal vertebrae lacking a haemal arch, plus the sacral vertebra) (Character from Wake, 1966; Wiens *et al.* 2005); (0) 2, (1) 3, (2) 4 (ordered)
152. Zygapophyses connecting caudal vertebrae (Wiens *et al.* 2005); (0) present on all or most vertebrae, (1) absent from posterior caudal vertebrae

Ribs:

153. Number of ribs on anterior caudal vertebrae (Zhang *et al.* 2009); (0) more than 3 pairs, (1) 2-3 pairs, (2) free ribs absent (ordered)
154. Atlantal Ribs (Larson and Dimmick, 1993); (0) absent, (1) present
155. Postatlantal ribs (modified from Zhang *et al.* 2009); (0) bicapitate, (1) unicapitate, (2) absent (unordered)
156. Dorsal process of bicapitate ribs (Wiens *et al.* 2005); (0) articulates with diapophysis, (1) reduced, does not articulate with diapophysis
157. Ribs on mid-body presacral vertebrae (Wiens *et al.* 2005); (0) present, (1) absent
158. Ribs on last presacral vertebra (Wiens *et al.* 2005); (0) present, (1) absent
159. Rib on penultimate presacral vertebra (Wiens *et al.* 2005); (0) present, (1) absent
160. Sacral rib (Wiens *et al.* 2005); (0) free, (1) fused
161. Dorsal process on mid-body of rib of 4th trunk vertebra (4th presacral excluding the atlas) (Wiens *et al.* 2005); (0) absent, (1) present
162. Bony lamina between ventral and dorsal processes of ribs (Wiens *et al.* 2005); (0) absent, (1) present

Spinal nerves:

163. Spinal nerves in posterior trunk vertebrae (data from Edwards, 1976; modified character from character X of Duellman and Trueb, 1986; Wiens *et al.* 2005); (0) exit intervertebrally, (1) exit intravertebrally
164. Spinal nerve exit in caudal vertebrae (data from Edwards, 1976; modified character from character X of Duellman and Trueb, 1986; Wiens *et al.* 2005); (0) intervertebral in all caudal vertebrae, (1) intravertebral in some or all caudal vertebrae
165. Dorsal and ventral roots of spinal nerves in trunk vertebrae (modified from Edwards, 1976; Duellman and Trueb, 1986; Wiens *et al.* 2005 and Thien and Chantell 1963); (0) exit through single foramen, (1) dorsal and ventral roots of presacral vertebrae exit through separate foramina
166. Presacral spinal nerve foramina (modified from Edwards, 1976; Duellman and Trueb, 1986; Wiens *et al.* 2005 and Thien and Chantell 1963); (0) spinal nerve exits intervertebrally, (1) spinal nerve exits intravertebrally in some vertebrae, (2) all spinal nerves exit intravertebrally (ordered)

Pectoral girdle:

167. Scapula-coracoid ossification (modified from Duellman and Trueb, 1986; Larson and Dimmick, 1993; Gao and Shubin, 2001; Wiens *et al.* 2005; Zhang *et al.* 2009); (0) ossified as separate elements, (1) two elements as a single ossification
168. Coracoids (Wiens *et al.* 2005); (0) not contacting medially, (1) contacting/overlapping medially, (2) fused medially (ordered)
169. Procoracoid and coracoid (Wiens *et al.* 2005); (0) not overlapping anteriorly, (1) overlapping anteriorly, enclosing foramen
170. Supracoracoid foramen (modified from Wiens *et al.* 2005); (0) entirely in cartilage/absent, (1) partly in bone, (2) entirely in bone
171. Suprascapula (modified from Wiens *et al.* 2005); (0) expanded in width dorsally, (1) not expanded, about same width as dorsal width of scapula
172. Crista dorsalis of humerus (Wiens *et al.* 2005); (0) present, (1) absent
173. Carpals (Wiens *et al.* 2005); (0) all elements cartilaginous, (1) some (but not all) ossified, (2) all elements at least partly ossified (ordered)
174. Fusion of distal carpal 1+2 (Gao and Shubin, 2001; Zhang *et al.* 2009); (0) fusion absent, (1) fusion present
175. Distal carpal 4 and 5 (Gao and Shubin, 2001; Zhang *et al.* 2009); (0) two elements remain separate, (1) fused
176. Carpals 3 and 4 (Wiens *et al.* 2005); (0) separate, (1) fused
177. Prepollex and radiale (Wiens *et al.* 2005); (0) separate, (1) fused
178. Ulnare (the carpal that articulates with the ulna) and intermedium (the bone or cartilage between the radiale and ulnare in the carpus) (Gao and Shubin, 2001; Wiens *et al.* 2005; Zhang *et al.* 2009); (0) separate, (1) fused
179. Ulnare and carpal 4 (Wiens *et al.* 2005); (0) separate, (1) fused
180. Intermedium and centrale (Wiens *et al.* 2005); (0) separate, (1) fused
181. Number of centralia in manus (or pes) (Gao and Shubin, 2001); (0) more than one Centralia element, (1) one central element
182. Number of manual digits (fingers) on forelimb (Wiens *et al.* 2005); (0) four, (1) three, (2) two, (3) one (unordered)
183. Number of phalanges on digit I of manus (Wiens *et al.* 2005); (0) two, (1) one

Pelvic girdle:

184. Hind limbs (Wiens *et al.* 2005); (0) present, (1) absent

185. Pelvic girdle (structure), (Wiens *et al.* 2005); (0) halves fused medially, (1) halves separate medially
186. Lateral processes of pubis (Wiens *et al.* 2005); (0) present, (1) absent
187. Ossification of ischium (Wiens *et al.* 2005); (0) not extending to anterior margin of pelvic girdle, (1) extending to anterior margin of pelvic girdle
188. Ossification of ischia (Wiens *et al.* 2005); (0) meeting mid-ventrally (separated by thin strip of cartilage), (1) well-separated mid-ventrally
189. Posterior median process on ischium (Wiens *et al.* 2005); (0) absent, (1) present
190. Median processes of pubis (Wiens *et al.* 2005); (0) posterior to or level with lateral processes, (1) anterior to lateral processes
191. Femur trochanter; (0) absent, (1) present
192. Tibial spur (Wiens *et al.* 2005); (0) absent, (1) present, not elongate and pointed, (2) elongate and pointed (unordered)
193. Fusion of tarsals 1 and 2 (Wiens *et al.* 2005; Zhang *et al.* 2009); (0) separate, (1) fused
194. Distal tarsals 4 and 5 (Wiens *et al.* 2005); (0) separate, (1) fused
195. Number of toes on hindlimb (Wiens *et al.* 2005); (0) five, (1) four, (2) three, (3) two, (4) one (**ordered**)
196. Number of phalanges on digit IV of pes (Wiens *et al.* 2005); (0) three, (1) four
197. Phalanges on digit I of pes (Wiens *et al.* 2005); (0) two, (1) one

Soft body coding:

198. Junction of the periotic canal and cistern (Duellman and Trueb 1986); (0) periotic canal joins the periotic cistern dorsally at its posterior aspect, (1) the junction of the canal and the cistern is slightly dorsal and posterior to the festra ovalis, (2) the junction of the cistern and canal is formed through the protrusion of the cistern into the fenestra ovalis
199. Flexures of periotic canal (Duellman and Trueb 1986); (0) the periotic canal curves ventrally and medially from its junction with the periotic cistern, (1) the canal takes a relatively horizontal course, (2) canal with one or more flexures
200. Basilar complex of inner ear (Duellman and Trueb 1986); (0) recessus basilaris and papillae are present in the inner ear, (1) absence of papillae, (2) absence of entire complex
201. First hypobranchial and first ceratobranchial (Duellman and Trueb 1986); (0) separate elements, (1) fusion of the two elements
202. Second ceratobranchial (Duellman and Trueb 1986); (0) present, (1) absent
203. Number of larval gill slits (Duellman and Trueb 1986); (0) four pairs, (1) three pairs, (2) two pairs, (3) one pair
204. Ypsiloid cartilage (Duellman and Trueb 1986); (0) present, (1) absent
205. Levator mandibulae muscle (Duellman and Trueb 1986); (0) originates on the skull roof, (1) origin on the side of the skull, (2) an origin that includes the exoccipital (or cervical vertebrae),
206. Pubotibialis and puboischiotibialis muscles (Duellman and Trueb 1986); (0) separate muscles, (1) fusion of the two muscles
207. Kidney (Duellman and Trueb 1986); (0) presence of well-developed glomeruli in anterior of kidney, (1) reduction of absence of anterior glomeruli
208. Mode of fertilisation (Duellman and Trueb 1986); (0) external fertilisation, (1) internal fertilisation
209. Recessus amphibiorum (Larson and Dimmick 1993) (0) horizontal orientation of the recessus amphibiorum of the inner ear, (1) vertical orientation

210. Otic sac (Larson and Dimmick 1993) (0) multilobate sac which is vascularised and filled with calcium, (1) bulbar, partially vascularised sac, (2) bulbar unvascularised sac
211. Amphibian periotic canal connective tissue (Larson and Dimmick 1993) (0) absence of this tissue, (1) Presence of fibrous connective tissue around amphibian periotic canal
212. Periotic cistern (0) large cistern, (1) small cistern
213. Fenestral relations of the periotic cistern (Larson and Dimmick 1993) (0) absence of protrusion, (1) protrusion of the cistern into the fenestra
214. Palatal dentition (unordered) (Larson and Dimmick 1993) (0) replacement of vomerine teeth proceeds laterally in parallel to the maxillary teeth, (1) from the posterior of the vomer, (2) both laterally and posteriorly, (3) medially
215. Epidermis (Larson and Dimmick 1993) (0) absence in female salamanders of an epidermal lining in the anterior half of the cloacal chamber, (1) presence of the epidermal lining
216. Male anterior ventral glands (Larson and Dimmick 1993)(0) absence, (1) presence
217. CTL/TCL cloacal tube length divided by total cloacal length quotient in females (Sever 1991); (0) present, (1) absent
218. CTL/TCL cloacal tube length divided by total cloacal length quotient in males, (Sever 1991); (0) present, (1) absent
219. Ciliated epithelium in the cloacal tube and/or anterior cloacal chamber of females, (Sever 1991); (0) present, (1) absent
220. Ciliated epithelium in the cloacal tube and/or anterior cloacal chamber of males, (Sever 1991); (0) present, (1) absent
221. Extent of epidermis in the female cloacal chamber, (Sever 1991); (0) the epidermal lining does not extend into the anterior one-half of the cloacal chamber, (1) the epidermal lining does extend into the anterior one-half of the cloacal chamber
222. Cloacal recess in females (Sever 1991); (0) absent, (1) present
223. Number of pairs of rugae in the male cloaca (Sever 1991); (0) < 10, (1) > 10
224. Primary and secondary folds in the male cloacal tube, (Sever 1991); (0) absent, (1) present
225. Middorsal evagination of the male cloacal chamber (Sever 1991); (0) absent, (1) present
226. Dorsolateral recesses in the male cloacal chamber (Sever 1991); (0) absent, (1) present
227. Pseudopenis in the male cloaca (Sever 1991); (0) absent, (1) present
228. Female anterior ventral glands (Sever 1991); (0) absent, (1) present
229. Spermathecae (Sever 1991); (0) absent, (1) present
230. Common tube to the spermathecae (Sever 1991); (0) absent, (1) present
231. Female dorsal glands (Sever 1991); (0) absent, (1) present
232. Other female cloacal glands (Sever 1991); (0) absent, (1) present
233. Male anterior ventral glands (Sever 1991); (0) absent, (1) present
234. Posterior ventral glands (Sever 1991); (0) absent, (1) present
235. Kingsbury's glands (Sever 1991); (0) absent, (1) present
236. Dorsal pelvic glands (Sever 1991); (0) absent, (1) present
237. Lateral pelvic glands (Sever 1991); (0) absent, (1) present
238. Caudal pelvic glands (Sever 1991); (0) absent, (1) present
239. Male dorsal or vent glands (Sever 1991); (0) absent, (1) present
240. Amphiumid pit glands (Sever 1991); (0) absent, (1) present
241. Other male cloacal glands (Sever 1991); (0) absent, (1) present
242. Lateral wall of nasal capsule (Zhang *et al.* 2009); (0) complete, (1) incomplete
243. Lateral narial fenestra (Zhang *et al.* 2009); (0) absent, (1) present

244. Posterior wall of nasal capsule (Zhang *et al.* 2009); (0) complete, (1) incomplete
245. Origin of m. adductor mandibulae internus superficialis (Zhang *et al.* 2009); (0) on dorsolateral surface of parietal, (1) origin extends posteriorly to exoccipital, (2) origin extends to cervical vertebra, (3) origin extends anteriorly towards level of frontal
246. Microchromosome (Zhang *et al.* 2009); (0) present, (1) absent
247. Ectopterygoid (Zhang *et al.* 2009); (0) present, (1) absent
248. Haploid Chromosomes (Gao and Shubin 2001); (0) more than 20, (1) reduced to 19, (2) further reduced to 14 or less
249. Diploid Chromosomes (Gao and Shubin 2001); (0) 56 or more, (1) 40-55, (2) lower than 40

Appendix C – Morphological Datasheet (on CD attached)

Appendix D – Species list (on CD attached)

Appendix E – RI Dataset (on CD attached)

Appendix F – LQ Dataset (on CD attached)

Appendix G – Comparison between RI and Le Quesne datasets (also on CD attached)

Full morphological character set colour coded

NB: (For character numbers for the RI and Le Quesne characters, please see Appendix E and F respectively)

Colour code: **Green** means RI characters (only)

Blue means Le Quesne character (only)

Red means both RI and Le Quesne characters

Black means character removed from both RI and Le Quesne sets

Skeletal characters:

Skull: (RI = 42, LQ = 31, agreed = 24)

1. Dentition in adult teeth (Zhang *et al.* 2009); (0) pedicellate, (1) sub-pedicellate, (2) non-pedicellate
2. Fusion of premaxillae (modified from Zhang *et al.* 2009); (0) paired premaxillae, (1) fused at base, (2) fully fused premaxillae (ordered)
3. Contact of premaxillae (between themselves), (modified from Wiens *et al.* 2005); (0) contacting medially throughout their entire length, (1) separated towards the frontals or parietals, (2) contacting anteriorly and posteriorly, separated medially with fontanelle exposed (3) no contact (ordered)

4. Dorsal process of premaxilla (ratio data with measurements of width of premaxilla vs length of premaxillary extension) (Zhang *et al.* 2009); (0) absent or poorly defined, (1) short but well-defined, (2) strong posterior extension (ordered)
5. Premaxilla in relation to frontals (modified from Wiens *et al.* 2005); (0) not contacting frontals, (1) contacting frontals, (2) extension of dorsal process intervenes deeply between the frontals (ordered)
6. Premaxillary dentition presence (Hanken and Hall, 1993); (0) present, (1) absent
7. Premaxilla dentition position (Wiens *et al.* 2005); (0) present lateral to pars dorsalis, (1) absent lateral to pars dorsalis
8. Premaxilla dentition (shape); (0) conical, (1) bulbous
9. Combined width of premaxilla measured at the premaxilla/maxilla suture (Wiens *et al.* 2005); (0) less than interorbital width, (1) greater than interorbital width
10. Premaxilla-palatine contact (Wiens *et al.* 2005); (0) absent, (1) present
11. Premaxilla-vomer contact (Wiens *et al.* 2005); (0) absent, (1) present
12. Premaxilla-nasal contact (Wiens *et al.* 2005); (0) absent, (1) present
13. Maxilla (Zhang *et al.* 2009); (0) presence of bilaterally paired maxillae, (1) greatly reduced as a rudimentary element, (2) entirely absent and functionally replaced by modified vomer
14. Maxillary dentition (Wiens *et al.* 2005); (0) dentate, (1) reduced, edentulous
15. Dentition shape; (0) mono-cuspid, (1) bi-cuspid, (2) tricuspid
16. Posterior process of maxilla (Wiens *et al.* 2005); (0) dentate, (1) edentulous
17. Process from pars dentalis of maxilla overlaps premaxilla (Wiens *et al.* 2005); (0) no, (1) yes
18. Anterior margin of pars facialis of maxilla (modified from Wiens *et al.* 2005); (0) posterior to external naris, (1) Forms lateral part of external naris
19. Septomaxilla (Larson and Dimmick, 1993; Hanken and Hall, 1993; Duellman and Trueb, 1994; Gao and Shubin, 2001; Wiens *et al.* 2005; Zhang *et al.* 2009); (0) presence of bilaterally paired septomaxillae, (1) absence of bones
20. Posterior end of septomaxilla (Wiens *et al.* 2005); (0) not contacting other cranial elements, (1) contacting maxilla, (2) contacting prefrontal, (3) contacting nasal (unordered)
21. Nasal (modified from Wiens *et al.* 2005); (0) present, (1) absent
22. Nasal ossification (Hanken and Hall, 1993; Larson and Dimmick, 1993; Gao and Shubin, 2001; Zhang *et al.* 2009); (0) paired nasals with sutural midline contact or fused, (1) nasals separate without midline contact
23. Nasal (Wiens *et al.* 2005); (0) not forked posteriorly, (1) forked posteriorly
24. Nasal shape (Wiens *et al.* 2005); (0) squarish, length and width roughly equal, (1) slender and elongate, length greater than width
25. Nasal-prefrontal contact (Gao and Shubin, 2001; Wiens *et al.* 2005; Zhang *et al.* 2009); (0) present, (1) absent
26. Nasal and maxilla (Wiens *et al.* 2005); (0) contacting or abutting, (1) separated
27. Nasal contact with frontal (Gao and Shubin, 2001; Wiens *et al.* 2005; Zhang *et al.* 2009); (0) separate from frontal, (1) partly or completely fused to frontal
28. Nasal-lacrimal duct (Hanken and Hall, 1993; Gao and Shubin, 2001; Zhang *et al.* 2009); (0) present, (1) absent
29. Lacrimal (Hanken and Hall, 1993; Duellman and Trueb, 1994; Gao and Shubin, 2001; Wiens *et al.* 2005; Zhang *et al.* 2009); (0) present, (1) absent
30. Quadratojugal (Hanken and Hall, 1993; Duellman and Trueb, 1994; Gao and Shubin, 2001; Zhang *et al.* 2009); (0) present, (1) absent
31. Prefrontal (Hanken and Hall, 1993; Gao and Shubin, 2001; Wiens *et al.* 2005; Zhang *et al.* 2009); (0) present, (1) absent

32. Prefrontal posterior process projecting into the orbit (modified from Hanken and Hall, 1993; Gao and Shubin, 2001; Wiens *et al.* 2005; Zhang *et al.* 2009); (0) present, (1) absent
33. Prefrontal orientation (modified from Wiens *et al.* 2005); (0) present and forms part of the margin of the external naris, (1) present but does not form part of the margin of the external naris
34. Frontal (Duellman and Trueb, 1994); (0) paired roofing bones, (1) fused into a single element
35. Frontal/maxillary contact (Gao and Shubin, 2001; Zhang *et al.* 2009, Wiens *et al.* 2005); (0) frontal and maxilla separated by prefrontal, (1) frontal contacts dorsal process of maxilla
36. Dorsolateral shelf on frontal (Wiens *et al.* 2005); (0) absent, (1) present
37. Postfrontal (Gao and Shubin, 2001, Zhang *et al.* 2009); (0) present, (1) absent
38. Palatal dentition (on the palatine) (modified from Gao and Shubin, 2001, Zhang *et al.* 2009); (0) present, (1) absent
39. Vomer dentition (modified from Gao and Shubin, 2001, Zhang *et al.* 2009); (0) present, (1) absent
40. Parasphenoid dentition (modified from Gao and Shubin, 2001, Zhang *et al.* 2009); (0) present, (1) absent
41. Pterygoid dentition (modified from Gao and Shubin, 2001, Zhang *et al.* 2009); (0) present, (1) absent
42. Placement of vomerine teeth (Duellman and Trueb, 1994, Hanken and Hall, 1993; Wiens *et al.* 2005, Zhang *et al.* 2009); (0) medial/lateral transverse row, (1) marginal (adjacent and parallel to max. and premaxillary teeth), (2) teeth centrally located on vomer, (3) teeth in large patches, (4) teeth in M-shaped pattern
43. Palatal tooth structure (Hanken and Hall, 1993; Duellman and Trueb, 1994); (0) conical, (1) compressed, (2) bulbous
44. Vomerine teeth (Tihen, 1958; Wiens *et al.* 2005); (0) present on postchoanal process, (1) absent on postchoanal process
45. Vomer with postchoanal process (Wiens *et al.* 2005); (0) with postchoanal process, (1) without postchoanal process
46. Vomer with prechoanal process (Wiens *et al.* 2005); (0) with prechoanal process, (1) without prechoanal process
47. Vomer and pterygoid (Wiens *et al.* 2005); (0) not articulating with pterygoid, (1) articulates with pterygoid
48. Vomeres (modified from Wiens *et al.* 2005); (0) separated anteriorly and medially, (1) separated medially and posteriorly (2) separated entirely, (3) in contact anteromedially, no fontanelle exposed (unordered)
49. Vomer, posterior dorsal process extending onto orbitosphenoid (Wiens *et al.* 2005); (0) absent, (1) present
50. Pterygoid shape (modified from Zhang *et al.* 2009); (0) triradiate and boomerang-shaped, (1) enlarged with distinct anteromedial process, (2) straight bar with loss of anteromedial process, (3) absent
51. Anterior margin of pterygoid (Wiens *et al.* 2005); (0) smooth, (1) serrate, with irregular projections
52. Pterygoid and coronoid process of prearticular (Wiens *et al.* 2005); (0) well separated, (1) articulating or nearly contacting
53. Posterior margin of pterygoid extends posterior to jaw articulation (Wiens *et al.* 2005); (0) no, (1) yes
54. Pterygoid, with dorsomedial process that articulates with orbitosphenoid and forms foramen posterior to optic foramen (Wiens *et al.* 2005); (0) absent, (1) present
55. Internal carotid foramen (Zhang *et al.* 2009; Gao and Shubin, 2001); (0) present, (1) absent

56. Squamosal-frontal (Wiens *et al.* 2005); (0) does not contact frontal, (1) contacts frontal
57. Squamosal (Wiens *et al.* 2005); (0) not expanded ventrally, (1) expanded ventrally, occupies articular region
58. Squamosal, main shaft in lateral view (Gao and Shubin, 2001; Wiens *et al.* 2005; Zhang *et al.* 2009); (0) oriented roughly vertically, (1) oriented diagonally, with dorsoposterior inclination
59. Hook-like (ventrally-directed) process on dorsal head of squamosal (Wiens *et al.* 2005); (0) absent, (1) present
60. Columellar process of squamosal, connecting stapes and squamosal (Wiens *et al.* 2005); (0) absent, (1) present
61. Squamosal contact with the parietal or other roofing elements (modified from Gao and Shubin, 2001; Zhang *et al.* 2009); (0) contact present, (1) absent or virtually absent
62. Prootic-exoccipital-opisthotic fusion (Hanken and Hall, 1993; Duellman and Trueb, 1994; Gao and Shubin, 2001; Wiens *et al.* 2005; Zhang *et al.* 2009); (0) three separate elements, (1) prootic-exoccipital fused, separate opisthotic, (2) all three elements fused
63. Exposure of prootic-exoccipital-opisthotic complex in dorsal view (Zhang *et al.* 2009); (0) the complex largely concealed by parietal or exposed posterior to skull table, (1) large exposure extends lateral to parietal table
64. Exoccipitals (Wiens *et al.* 2005); (0) separated medially at tectum synoticum, (1) fused
65. Operculum (Hanken and Hall, 1993; Zhang *et al.* 2009); (0) present and free, (1) absent or fused
66. Stapes (Hanken and Hall, 1993; Zhang *et al.* 2009); (0) present, (1) absent
67. Orbitosphenoid (Wiens *et al.* 2005); (0) present, (1) absent
68. Orbitosphenoid (Wiens *et al.* 2005); (0) not extending lateral to frontals, or extending only slightly anteriorly, (1) extending well lateral to frontals throughout their length
69. *Sagittal crest formed at the midline between the parietals of the skull (modified from Wiens *et al.* 2005); (0) absent, (1) present
70. Dermal sculpture on skull roof (Zhang *et al.* 2009); (0) present, coarse, (1) present, weak, (2) absent
71. Posterior edge of parietals, extends between exoccipitals to edge of foramen magnum on tectum synoticum (Wiens *et al.* 2005); (0) no, (1) yes
72. Ventrolateral extension of parietal covers orbitosphenoid region anteriorly (in lateral view), (Wiens *et al.* 2005); (0) absent, (1) present
73. *Parietal and exoccipital (Wiens *et al.* 2005); (0) not forming casque around foramen magnum, (1) forming casque around foramen magnum
74. Anterolateral process of parietal (modified from Gao and Shubin, 2001; Zhang *et al.* 2009); (0) absent, (1) present
75. Anterolateral process of parietal (modified from Gao and Shubin, 2001; Zhang *et al.* 2009); (0) forms less than 50% of the total length of the parietal, (1) makes up more than 50% of total length of the parietal
76. Medial border of orbit (Zhang *et al.* 2009); (0) more than 50% of orbital margin formed by frontal, (1) frontal contributes less than 50% of the orbit margin, (2) frontal fully excluded from entering orbital margin
77. Angular/prearticular fusion (Duellman and Trueb, 1986; Larson and Dimmick, 1993; Hanken and Hall, 1993; Duellman and Trueb, 1994; Gao and Shubin, 2001; Wiens *et al.* 2005; Zhang *et al.* 2009); (0) angular distinct from the prearticular, (1) no distinct angular (absent or fused to prearticular in adult)
78. Coronoid (Hanken and Hall, 1993; Gao and Shubin, 2001; Wiens *et al.* 2005); (0) present as a separate element, (1) absent in adult stage
79. Coronoid dentition (Hanken and Hall, 1993; Wiens *et al.* 2005); (0) dentate, (1) edentulous

80. Articular (modified from Gao and Shubin, 2001; Wiens *et al.* 2005; Zhang *et al.* 2009); (0) present as separate element, (1) fused with prearticular, (2) absent/unossified
81. Meckel's cartilage (Wiens *et al.* 2005); (0) does not extend to mandibular symphysis, (1) extends to mandibular symphysis
82. *Mandible (in anterior view) (Wiens *et al.* 2005); (0) thickens suddenly at symphysis, (1) thins/ stays the same towards the symphysis
83. Mandibular symphysis (Duellman and Trueb, 1994); (0) simple union of the mandibular rami, (1) rami have an interlocking symphysis
84. Dentary (Wiens *et al.* 2005); (0) dentate, (1) edentulous
85. *Dentary teeth shape; (0) conical, (1) bulbous
86. Dentary symphyseal teeth; (0) present, (1) absent
87. *Dentary lateral sensory nerve foramina; (0) absent, (1) present
88. Retroarticular process (modified from Wiens *et al.* 2005); (0) very small/absent, (1) present
89. Coronoid process of prearticular (Wiens *et al.* 2005); (0) adjacent to jaw articulation, (1) distinctly anterior to jaw articulation
90. Palatine and pterygoid (Wiens *et al.* 2005); (0) palatine absent (1) palatine present
91. Quadrate ossification (Wiens *et al.* 2005); (0) present, (1) absent
92. Posterior process on pars quadrati of quadrate (Wiens *et al.* 2005); (0) absent, (1) present
93. Jaw articulation (Wiens *et al.* 2005); (0) well ventral to level of ventral margin of braincase, (1) at level of ventral margin of braincase
94. Quadrate-parasphenoid articulation (Wiens *et al.* 2005); (0) absent, (1) present
95. Parasphenoid (Wiens *et al.* 2005); (0) not extending laterally beyond level of orbitosphenoid, (1) extending laterally beyond level of orbitosphenoid
96. Optic foramen (modified from Wiens *et al.* 2005); (0) enclosed in the orbitosphenoid bone anteriorly or not at all, (1) enclosed entirely in the orbitosphenoid bone
97. Posteriormost margin of auditory capsules (Wiens *et al.* 2005); (0) anterior to occipital condyles, (1) posterior to occipital condyles
98. Lateral flange on prootic extending to the squamosal (Wiens *et al.* 2005); (0) absent, (1) present
99. Second basibranchial (ventral view); (0) bar (horizontal or vertical), (1) Y-shaped (two branches), (2) multiple branches (more than two)

Atlas: (RI = 9, LQ = 5, agreed = 5)

100. Position of atlas posterior cotyle relative to anterior cotyles (J. Gardner, 2000); (0) the posterior cotyle is approximately in line with the anterior cotyles in lateral view, (1) the posterior cotyle is displaced ventrally in relation to the anterior cotyles.
101. Notochordal pit in posterior cotyle of the atlas (modified from J. Gardner, 2000); (0) the notochordal pit is open and has no infilling of calcified or ossified cartilage, (1) partly in-filled by ossified cartilage, (2) totally in-filled and bulging beyond the edge of the centrum with ossified cartilage (ordered)
102. Relative depth of anterior atlas cotyles (modified from J. Gardner, 2000); (0) deeply concave, (1) nearly flat to shallowly concave, (2) convex (although the structure is called a cotyle which means cup-like, they are sometimes convex)
103. Outline of anterior atlas cotyles (J. Gardner, 2000); (0) compressed dorsoventrally, (1) subcircular, (2) compressed lateromedially (ordered)
104. Form of odontoid process (modified from J. Gardner, 2000); (0) knob-like, (1) dorsoventrally flattened, (2) separate (not joined in the middle), (3) highly reduced or absent
105. Position of atlas neural canal relative to the anterior cotyles (J. Gardner, 2000); (0) the neural canal is situated above the anterior cotyles, (1) the neural canal protrudes in between the anterior cotyles, but up to half way or less than the dorso-

- ventral distance of the anterior cotyles, (2) Neural canal intrudes deeply or completely between the anterior cotyles (ordered)
106. Size of atlas neural canal relative to the anterior cotyles (J. Gardner, 2000); (0) the anterior circumference of the neural canal is approximately equal to or greater than the circumference of one of the anterior cotyles, (1) the neural canal is smaller than the anterior coyle
 107. Posterior extent of neural arch roof of the atlas (modified from J. Gardner, 2000); (0) extends past the edge of the posterior cotyle, (1) in line with the posterior cotyle, (2) the posterior edge of the neural arch roof is shorter i.e. does not reach to the edge of the posterior cotyle (ordered)
 108. Dorsal outline of posterior margin of the atlas neural arch roof (modified from J. Gardner, 2000); (0) truncated, (1) forked, (2) pointed
 109. Dorsal outline of the atlas' neural arch crest (modified from J. Gardner, 2000); (0) the outline of the crest broadens posteriorly, (1) it narrows posteriorly, (2) relatively straight, (3) it is hourglass shaped i.e. narrows then broadens (unordered)
 110. Shape of anterior end of neural arch crest on the atlas (modified from J. Gardner, 2000); (0) not elaborated, (1) swollen or thickened, (2) paired anterior processes (unordered)
 111. Postzygapophyses prominence on the atlas (modified from J. Gardner, 2000); (0) prominent, (1) small.
 112. Postzygapophyses articular surface on the atlas (modified from J. Gardner, 2000); (0) laterally divergent, (1) directed ventro-laterally
 113. Postzygapophyses; (0) diverge from the end of the neural arch crest on the atlas, (1) diverge from along the neural arch crest of the atlas.
 114. Condition of the dorsal part of the neural arch crest of the atlas (J. Gardner, 2000); (0) finished in cartilage, (1) finished in bone
 115. Condition of the posterior end of the neural arch spine of the atlas; (0) finished in cartilage, (1) finished in bone
 116. Four facetted articulation of exoccipital and atlas (Wiens *et al.* 2005; Zhang *et al.* 2009); (0) absent due to reduction in odontoid process, (1) absent due to continuous surface of odontoid and anterior cotyles, (2) present (unordered)
 117. Atlantal spinal nerve foramen (Zhang *et al.* 2009); (0) absent, (1) a notch, (2) fully enclosed (ordered)
 118. Atlas, transverse process (Wiens *et al.* 2005); (0) absent, (1) present
 119. Shape of atlas centrum in ventral view (Zhang *et al.* 2009); (0) shorter than postatlantals, (1) roughly equal in length to postatlantals, (2) longer than postatlantals (unordered)
 120. Basapophyses on the atlas; (0) absent, (1) present
 121. Neural cord supports, (0) absent, (1) present

Presacral Vertebrae: (RI = 12, LQ = 6, agreed = 5)

122. Centrum of presacral vertebrae (modified from J. Gardner, 2000); (0) amphicoelous, (1) semi-opisthocoelous, (2) fully opisthocoelous, (3) procoelous
123. Size of the 4th trunk vertebrae (5th presacral) neural canal relative to its anterior size of the centrum; (0) neural canal is approximately equal in size (radius) to, or greater than, the size of the anterior centrum, (1) neural canal smaller than the anterior centrum
124. Posterior basapophyses of the presacrals (J. Gardner, 2000); (0) absent, (1) present
125. Anterior basapophyses of the presacrals (Wiens *et al.* 2005); (0) absent, (1) present
126. Condition of neural spine (J. Gardner, 2000); (0) finished in cartilage, (1) finished in bone

127. Prominent, v-shaped hypapophyses (J. Gardner, 2000); (0) absent, (1) present
128. Bony lamina between diapophyses and parapophyses (modified from Wiens *et al.* 2005); (0) absent, (1) partial presence, (2) present – full lamina
129. Mid-ventral keel on mid-body vertebrae (modified from Wiens *et al.* 2005); (0) absent, (1) present (small), (2) Large – extends below the ventral edge of the centrum cotyles (ordered)
130. Posterolateral flanges on mid-dorsal keel on mid-body vertebrae (Wiens *et al.* 2005); (0) absent, (1) present
131. Anterior keel/flange on transverse process (extending from, and between the transverse process to anterior edge of centrum) (modified from Wiens *et al.* 2005); (0) absent, (1) present
132. Fenestra in anterior keel; (0) present, (1) absent
133. Anterodorsal keel on transverse process (extending from transverse process to anterior zygapophysis) (modified from Wiens *et al.* 2005); (0) absent, (1) present
134. Posterior keel of transverse process (extends from transverse process to posterior centrum edge); (0) absent, (1) present
135. Dermal sculpture on dorsal surface of neural arch; (0) present, (1) absent
136. Shape of the neural spine of mid-body vertebrae (modified from Wiens *et al.* 2005); (0) absent/truncated, (1) single median process (spine-like projection), (2) present (paired process)
137. Posteriorly projecting neural spine(s) (past the posterior centrum edge); (0) shorter than posterior centrum edge, (1) in line with posterior centrum edge, (2) projecting past the posterior centrum edge (ordered)
138. Posterior zygapophyses facet face of presacral vertebrae; (0) latero-medially divergent (facing slightly outwards, away from each other), (1) directed ventrally
139. Transverse process in anterior part of trunk series, excluding first presacral vertebra (J. Gardner, 2000); (0) Unicapitate, (1) bicapitate, (2) absent
140. Mid-dorsal keel (neural arch crest) on presacral vertebra (Wiens *et al.* 2005); (0) absent, (1) present
141. Mid-dorsal keel (neural arch crest) on presacral vertebra length; (0) short (does not run the length of the vertebra), (1) long (runs from at least just behind the anterior zygapophyses to neural spine)

Caudal Vertebrae: (RI = 5, LQ = 2, agreed = 2)

142. Caudal vertebrae, neural spine (Wiens *et al.* 2005); (0) with one process, (1) paired process
143. Mid-dorsal crest on caudal vertebrae (Wiens *et al.* 2005); (0) absent, (1) present
144. Dermal sculpturing on dorsal surface of neural arch on the caudal vertebrae; (0) present, (1) absent
145. Caudal vertebrae (Wiens *et al.* 2005); (0) ventral keels absent, low, and/or rounded, (1) dorsal and ventral keels raised and distinctly rectangular
146. Transverse process of anterior caudal vertebrae (Wiens *et al.* 2005); (0) posteriorly orientated, (1) anteriorly oriented
147. Transverse process of anterior caudal vertebrae; (0) unicapitate, (1) bicapitate
148. Caudal vertebrae, anterior keel on haemal arch (Wiens *et al.* 2005); (0) absent, (1) present
149. Caudal vertebrae, haemal arch (Wiens *et al.* 2005); (0) complete, lateral halves fused to form median process, (1) incomplete, two ventral lamina do not contact or fuse on anterior caudal vertebrae, (2) incomplete for all caudal vertebrae
150. Caudal vertebrae, haemal arch spine (Wiens *et al.* 2005); (0) paired process, (1) single process

151. Caudosacral vertebrae (number of caudal vertebrae lacking a haemal arch, plus the sacral vertebra) (Character from Wake, 1966; Wiens *et al.* 2005); (0) 2, (1) 3, (2) 4
152. Zygapophyses connecting caudal vertebrae (Wiens *et al.* 2005); (0) present on all or most vertebrae, (1) absent from posterior caudal vertebrae

Ribs: (RI = 3, LQ = 3, agreed = 3)

153. Number of ribs on anterior caudal vertebrae (Zhang *et al.* 2009); (0) more than 3 pairs, (1) 2-3 pairs, (2) free ribs absent
154. Atlantal Ribs (Larson and Dimmick, 1993); (0) absent, (1) present
155. Postatlantal ribs (modified from Zhang *et al.* 2009); (0) bicapitate, (1) unicapitate, (2) absent
156. Dorsal process of bicapitate ribs (Wiens *et al.* 2005); (0) articulates with diapophysis, (1) reduced, does not articulate with diapophysis
157. Ribs on mid-body presacral vertebrae (Wiens *et al.* 2005); (0) present, (1) absent
158. Ribs on last presacral vertebra (Wiens *et al.* 2005); (0) present, (1) absent
159. Rib on penultimate presacral vertebra (Wiens *et al.* 2005); (0) present, (1) absent
160. Sacral rib (Wiens *et al.* 2005); (0) free, (1) fused
161. Dorsal process on mid-body of rib of 4th trunk vertebra (4th presacral excluding the atlas) (Wiens *et al.* 2005); (0) absent, (1) present
162. Bony lamina between ventral and dorsal processes of ribs (Wiens *et al.* 2005); (0) absent, (1) present

Spinal nerves: (RI = 4, LQ = 4, agreed = 4)

163. Spinal nerves in posterior trunk vertebrae (data from Edwards, 1976; modified character from character X of Duellman and Trueb, 1986; Wiens *et al.* 2005); (0) exit intervertebrally, (1) exit intravertebrally
164. Spinal nerve exit in caudal vertebrae (data from Edwards, 1976; modified character from character X of Duellman and Trueb, 1986; Wiens *et al.* 2005); (0) intervertebral in all caudal vertebrae, (1) intravertebral in some or all caudal vertebrae
165. Dorsal and ventral roots of spinal nerves in trunk vertebrae (modified from Edwards, 1976; Duellman and Trueb, 1986; Wiens *et al.* 2005 and Thien and Chantell 1963); (0) exit through single foramen, (1) dorsal and ventral roots of presacral vertebrae exit through separate foramina
166. Presacral spinal nerve foramina (modified from Edwards, 1976; Duellman and Trueb, 1986; Wiens *et al.* 2005 and Thien and Chantell 1963); (0) spinal nerve exits intervertebrally, (1) spinal nerve exits intravertebrally in some vertebrae, (2) all spinal nerves exit intravertebrally

Pectoral girdle: (RI = 8, LQ = 6, agreed = 6)

167. Scapula-coracoid ossification (modified from Duellman and Trueb, 1986; Larson and Dimmick, 1993; Gao and Shubin, 2001; Wiens *et al.* 2005; Zhang *et al.* 2009); (0) ossified as separate elements, (1) two elements as a single ossification
168. Coracoids (Wiens *et al.* 2005); (0) not contacting medially, (1) contacting/overlapping medially, (2) fused medially (ordered)
169. Procoracoid and coracoid (Wiens *et al.* 2005); (0) not overlapping anteriorly, (1) overlapping anteriorly, enclosing foramen
170. Supracoracoid foramen (modified from Wiens *et al.* 2005); (0) entirely in cartilage/absent, (1) partly in bone, (2) entirely in bone
171. Suprascapula (modified from Wiens *et al.* 2005); (0) expanded in width dorsally, (1) not expanded, about same width as dorsal width of scapula
172. Crista dorsalis of humerus (Wiens *et al.* 2005); (0) present, (1) absent

173. Carpals (Wiens *et al.* 2005); (0) all elements cartilaginous, (1) some (but not all) ossified, (2) all elements at least partly ossified
174. Fusion of distal carpal 1+2 (Gao and Shubin, 2001; Zhang *et al.* 2009); (0) fusion absent, (1) fusion present
175. Distal carpal 4 and 5 (Gao and Shubin, 2001; Zhang *et al.* 2009); (0) two elements remain separate, (1) fused
176. Carpals 3 and 4 (Wiens *et al.* 2005); (0) separate, (1) fused
177. Prepollex and radiale (Wiens *et al.* 2005); (0) separate, (1) fused
178. Ulnare (the carpal that articulates with the ulna) and intermedium (the bone or cartilage between the radiale and ulnare in the carpus) (Gao and Shubin, 2001; Wiens *et al.* 2005; Zhang *et al.* 2009); (0) separate, (1) fused
179. Ulnare and carpal 4 (Wiens *et al.* 2005); (0) separate, (1) fused
180. Intermedium and centrale (Wiens *et al.* 2005); (0) separate, (1) fused
181. Number of centralia in manus (or pes) (Gao and Shubin, 2001); (0) more than one Centralia element, (1) one central element
182. Number of manual digits (fingers) on forelimb (Wiens *et al.* 2005); (0) four, (1) three, (2) two, (3) one (unordered)
183. Number of phalanges on digit I of manus (Wiens *et al.* 2005); (0) two, (1) one

Pelvic girdle: (RI = 1, LQ = 1, agreed = 1)

184. Hind limbs (Wiens *et al.* 2005); (0) present, (1) absent
185. Pelvic girdle (structure), (Wiens *et al.* 2005); (0) halves fused medially, (1) halves separate medially
186. Lateral processes of pubis (Wiens *et al.* 2005); (0) present, (1) absent
187. Ossification of ischium (Wiens *et al.* 2005); (0) not extending to anterior margin of pelvic girdle, (1) extending to anterior margin of pelvic girdle
188. Ossification of ischia (Wiens *et al.* 2005); (0) meeting mid-ventrally (separated by thin strip of cartilage), (1) well-separated mid-ventrally
189. Posterior median process on ischium (Wiens *et al.* 2005); (0) absent, (1) present
190. Median processes of pubis (Wiens *et al.* 2005); (0) posterior to or level with lateral processes, (1) anterior to lateral processes
191. Femur trochanter (0) absent, (1) present
192. Tibial spur (Wiens *et al.* 2005); (0) absent, (1) present, not elongate and pointed, (2) elongate and pointed (unordered)
193. Fusion of tarsals 1 and 2 (Wiens *et al.* 2005; Zhang *et al.* 2009); (0) separate, (1) fused
194. Distal tarsals 4 and 5 (Wiens *et al.* 2005); (0) separate, (1) fused
195. Number of toes on hindlimb (Wiens *et al.* 2005); (0) five, (1) four, (2) three, (3) two, (4) one (ordered)
196. Number of phalanges on digit IV of pes (Wiens *et al.* 2005); (0) three, (1) four
197. Phalanges on digit I of pes (Wiens *et al.* 2005); (0) two, (1) one

Soft body coding: (RI = 38, LQ = 38, agreed = 38)

198. Junction of the periotic canal and cistern (Duellman and Trueb 1986); (0) periotic canal joins the periotic cistern dorsally at its posterior aspect, (1) the junction of the canal and the cistern is slightly dorsal and posterior to the fenestra ovalis, (2) the junction of the cistern and canal is formed through the protrusion of the cistern into the fenestra ovalis
199. Flexures of periotic canal (Duellman and Trueb 1986); (0) the periotic canal curves ventrally and medially from its junction with the periotic cistern, (1) the canal takes a relatively horizontal course, (2) canal with one or more flexures

200. Basilaris complex of inner ear (Duellman and Trueb 1986); (0) recessus basilaris and papillae are present in the inner ear, (1) absence of papillae, (2) absence of entire complex
201. First hypobranchial and first ceratobranchial (Duellman and Trueb 1986); (0) separate elements, (1) fusion of the two elements
202. Second ceratobranchial (Duellman and Trueb 1986); (0) present, (1) absent
203. Number of larval gill slits (Duellman and Trueb 1986); (0) four pairs, (1) three pairs, (2) two pairs, (3) one pair
204. Ypsiloid cartilage (Duellman and Trueb 1986); (0) present, (1) absent
205. Levator mandibulae muscle (Duellman and Trueb 1986); (0) originates on the skull roof, (1) origin on the side of the skull, (2) an origin that includes the exoccipital (or cervical vertebrae),
206. Pubotibialis and puboischiotibialis muscles (Duellman and Trueb 1986); (0) separate muscles, (1) fusion of the two muscles
207. Kidney (Duellman and Trueb 1986); (0) presence of well-developed glomeruli in anterior of kidney, (1) reduction of absence of anterior glomeruli
208. Mode of fertilisation (Duellman and Trueb 1986); (0) external fertilisation, (1) internal fertilisation
209. Recessus amphibiorum (Larson and Dimmick 1993) (0) horizontal orientation of the recessus amphibiorum of the inner ear, (1) vertical orientation
210. Otic sac (Larson and Dimmick 1993) (0) multilobate sac which is vascularised and filled with calcium, (1) bulbar, partially vascularised sac, (2) bulbar unvascularised sac
211. Amphibian periotic canal connective tissue (Larson and Dimmick 1993) (0) absence of this tissue, (1) Presence of fibrous connective tissue around amphibian periotic canal
212. Periotic cistern (0) large cistern, (1) small cistern
213. Fenestral relations of the periotic cistern (Larson and Dimmick 1993) (0) absence of protrusion, (1) protrusion of the cistern into the fenestra
214. Palatal dentition (unordered) (Larson and Dimmick 1993) (0) replacement of vomerine teeth proceeds laterally in parallel to the maxillary teeth, (1) from the posterior of the vomer, (2) both laterally and posteriorly, (3) medially
215. Epidermis (Larson and Dimmick 1993) (0) absence in female salamanders of an epidermal lining in the anterior half of the cloacal chamber, (1) presence of the epidermal lining
216. Male anterior ventral glands (Larson and Dimmick 1993)(0) absence, (1) presence
217. CTL/TCL cloacal tube length divided by total cloacal length quotient in females (Sever 1991); (0) present, (1) absent
218. CTL/TCL cloacal tube length divided by total cloacal length quotient in males, (Sever 1991); (0) present, (1) absent
219. Ciliated epithelium in the cloacal tube and/or anterior cloacal chamber of females, (Sever 1991); (0) present, (1) absent
220. Ciliated epithelium in the cloacal tube and/or anterior cloacal chamber of males, (Sever 1991); (0) present, (1) absent
221. Extent of epidermis in the female cloacal chamber, (Sever 1991); (0) the epidermal lining does not extend into the anterior one-half of the cloacal chamber, (1) the epidermal lining does extend into the anterior one-half of the cloacal chamber
222. Cloacal recess in females (Sever 1991); (0) absent, (1) present
223. Number of pairs of rugae in the male cloaca (Sever 1991); (0) < 10, (1) > 10
224. Primary and secondary folds in the male cloacal tube, (Sever 1991); (0) absent, (1) present

225. Middorsal evagination of the male cloacal chamber (Sever 1991); (0) absent, (1) present
226. Dorsolateral recesses in the male cloacal chamber (Sever 1991); (0) absent, (1) present
227. Pseudopenis in the male cloaca (Sever 1991); (0) absent, (1) present
228. Female anterior ventral glands (Sever 1991); (0) absent, (1) present
229. Spermathecae (Sever 1991); (0) absent, (1) present
230. Common tube to the spermathecae (Sever 1991); (0) absent, (1) present
231. Female dorsal glands (Sever 1991); (0) absent, (1) present
232. Other female cloacal glands (Sever 1991); (0) absent, (1) present
233. Male anterior ventral glands (Sever 1991); (0) absent, (1) present
234. Posterior ventral glands (Sever 1991); (0) absent, (1) present
235. Kingsbury's glands (Sever 1991); (0) absent, (1) present
236. Dorsal pelvic glands (Sever 1991); (0) absent, (1) present
237. Lateral pelvic glands (Sever 1991); (0) absent, (1) present
238. Caudal pelvic glands (Sever 1991); (0) absent, (1) present
239. Male dorsal or vent glands (Sever 1991); (0) absent, (1) present
240. Amphiumid pit glands (Sever 1991); (0) absent, (1) present
241. Other male cloacal glands (Sever 1991); (0) absent, (1) present
242. Lateral wall of nasal capsule (Zhang *et al.* 2009); (0) complete, (1) incomplete
243. Lateral narial fenestra (Zhang *et al.* 2009); (0) absent, (1) present
244. Posterior wall of nasal capsule (Zhang *et al.* 2009); (0) complete, (1) incomplete
245. Origin of m. adductor mandibulae internus superficialis (Zhang *et al.* 2009); (0) on dorsolateral surface of parietal, (1) origin extends posteriorly to exoccipital, (2) origin extends to cervical vertebra, (3) origin extends anteriorly towards level of frontal
246. Microchromosome (Zhang *et al.* 2009); (0) present, (1) absent
247. Ectopterygoid (Zhang *et al.* 2009); (0) present, (1) absent
248. Haploid Chromosomes (Gao and Shubin 2001); (0) more than 20, (1) reduced to 19, (2) further reduced to 14 or less
249. Diploid Chromosomes (Gao and Shubin 2001); (0) 56 or more, (1) 40-55, (2) lower than 40

Appendix A - GenBank accession numbers for sampled amphibian and outgroup taxa.

Species	12S	16S	cytb	CXCR4	H3A	NCX1	POMC	RAG1	RHOD	SIA	SLC8A3
<i>Alligator mississippiensis</i>	NC_001922.1	NC_001922.1	NC_001922.1	JN702314.1	---	---	NM_001287606.2	JN654850.1	---	---	---
<i>Ambystoma mexicanum</i>	DQ283213	Y10947	AY341745	EF107455	DQ284244	EF107230	---	AY323752	DQ283893	---	EF107367
<i>Ambystoma opacum</i>	---	---	EF036638	---	---	---	---	AY650130	---	---	---
<i>Ambystoma tigrinum</i>	DQ283407	DQ283407	EF036667	---	DQ284388	---	---	---	DQ284016	DQ282864	---
<i>Amphiuma means</i>	GQ368656	FJ951270	FJ951335	EF107472	---	EF107248	FJ951366	AY650127	---	---	EF107406
<i>Amphiuma tridactylum</i>	DQ283119	DQ283119	FJ951356	---	DQ284165	FJ951361	FJ951368	FJ951369	---	---	FJ951419
<i>Andrias davidianus</i>	AY915966	AY915966	AF255430	---	---	AY948847	EU275843	AY650142	---	---	AY948911
<i>Andrias japonicus</i>	DQ283274	DQ283274	AB445775	---	DQ284293	---	---	AY583346	---	---	---
<i>Ascaphus montanus</i>	---	AY523779	DQ087512	---	---	---	---	AY650146	---	---	EF107399
<i>Ascaphus truei</i>	X86225	DQ283116	AF277330	---	DQ284162	---	EU275850	AY323754	DQ347404	---	AY948893
<i>Bombina bombina</i>	AY333663	DQ283250	EF212589	---	DQ284275	---	---	---	DQ283920	---	---
<i>Bombina variegata</i>	AY333688	AY333725	EU531284	---	DQ284274	---	---	AY523750	---	---	EF107347
<i>Caiman crocodilus</i>	NC_002744.2	NG_002744.2	NC_002744.2	---	---	---	---	---	---	---	---
<i>Cryptobranchus alleganiensis</i>	DQ283263	DQ283263	AY691719	---	DQ284286	---	---	AY650141	---	---	---
<i>Desmognathus fuscus</i>	AF437402	U71222	EF028653	---	---	---	EU275812	EU275781	---	---	---
<i>Dicamptodon ensatus</i>	DQ283118	DQ283118	AY734622	EF107496	DQ284164	EF107276	---	EF107335	---	---	---
<i>Gallus gallus</i>	JN695761.1	NG_001323.1	NC_001323.1	NM_204617.2	---	DQ267621.1	NM_001287606.2	NM_001031188.1	---	---	NM_001293097.1
<i>Homo sapiens</i>	FJ775667	FJ775667	FJ775667	AF025375	NM_003529	AF108389	J00292	NG_007528	K02281	U63295	X93017
<i>Hydromantes italicus</i>	FJ602131	FJ602187	FJ602300	EF107476	---	EF107253	EU275826	EU275792	---	---	EF107415
<i>Ichthyophis bannanicus</i>	Y10949	Y10949	GQ249909	EF107451	---	EF107225	---	EF107288	---	---	EF107358
<i>Ichthyophis tricolor</i>	AF461138	AF461139	---	---	---	---	---	---	---	---	---
<i>Ichthyosaura alpestris</i>	AY147256	AY147257	EF089334	---	---	---	---	---	---	---	---
<i>Latimeria chalumnae</i>	NC_001804.1	NC_001804.1	NC_001804.1	---	DQ284319.1	---	---	---	---	---	---
<i>Leiopelma hamiltoni</i>	X86241	X86275	FJ950426	---	---	---	---	---	---	---	---
<i>Lissotriton vulgaris</i>	U04704	U04705	U55948	---	---	---	---	---	---	---	---
<i>Necturus maculosus</i>	DQ283412	DQ283412	AY691724	---	---	---	AY141897	AY650137	---	---	---
<i>Onychodactylus japonicus</i>	AY915970	AY915971	AB452892	---	---	---	---	AY583350	---	---	---

<i>Pelobates cultripes</i>	AY364341	AY333689	DQ333373	AY364171	---	---	---	AY323758	AY364386	---	AY948857
<i>Pelobates fuscus</i>	DQ283113	AJ440812	EF133852	---	DQ284159	---	---	---	DQ283826	---	---
<i>Pleurodeles waltl</i>	AY522564	DQ283445	AY222514	---	DQ284420	---	---	AY523736	---	---	AY948856
<i>Proteus anguinus</i>	DQ494769	EF107180	GQ368659	EF107467	---	EF107243	---	AY650138	---	---	EF107402
<i>Protopterus dolloi</i>	NC_001708.1	NC_001708.1	NC_001708.1	---	---	---	---	---	---	---	---
<i>Pseudotriton ruber</i>	AF290190	---	AY528404	---	---	---	EU275854	AY650123	---	---	---
<i>Rhinatrema bivittatum</i>	AY101207	DQ283385	AY101247	EF107478	DQ284370	EF107255	---	AY456257	DQ284002	---	EF107417
<i>Rhyacotriton olympicus</i>	X86251	X86285	EF036689	---	---	---	---	---	---	---	---
<i>Rhyacotriton variegatus</i>	---	EF107179	AY691726	EF107466	---	EF107242	EU275823	AY691693	---	---	EF107401
<i>Salamandra salamandra</i>	DQ283440	DQ283440	EU852738	EF017999	DQ284416	EF018024	---	AY583352	DQ347354	---	EF107368
<i>Salamandrella keyserlingii</i>	AY916003	AY916002	AB363595	---	---	---	---	AY650145	---	---	---
<i>Sphenodon punctatus</i>	---	DQ267621.1	---	JN702443.1	---	---	---	---	---	---	JF804271.1
<i>Takydromus tachydromoides</i>	NC_008773.1	NC_008773.1	NC_008773.1	---	---	---	---	---	---	---	---
<i>Siren lacertina</i>	DQ283181	DQ283181	AY713291	EF107471	DQ284216	EF107247	---	EF107307	---	DQ282729	EF107405
<i>Taricha torosa</i>	---	EF107218	L22701	---	---	EF107281	---	EF107340	---	---	EF107444
<i>Triturus marmoratus</i>	AY147252	EF107162	DQ092231	EF107448	---	EF107222	---	AY583354	---	---	EF107350
<i>Tylotriton verrucosus</i>	---	AY336631	EF627476	---	---	---	---	---	---	---	---
<i>Typhlonectes natans</i>	DQ283085	EU753984	EU753999	---	DQ284136	---	AF369043	EF551566	---	---	---

Appendix B

Skeletal characters:

Colour code: **Red** means it's a modified character

Purple means it's a new character for salamanders

Orange means soft body character

Green means ordered multistate character

Skull:

1. Dentition **in adult teeth** (Zhang et al. 2009); (0) pedicellate, **(1) sub-pedicellate**, (2) non-pedicellate
2. Fusion of premaxillae (modified from Zhang et al. 2009); (0) paired premaxillae, **(1) fused at base**, (2) fully fused premaxillae **(ordered)**
3. Contact of premaxillae (between themselves), (modified from Wiens et al. 2005); (0) contacting medially **throughout their entire length**, **(1) separated towards the frontals or parietals**, **(2) contacting anteriorly and posteriorly, separated medially with fontanelle exposed** **(3) no contact (ordered)**
4. Dorsal process of premaxilla **(ratio data with measurements of width of premaxilla vs length of premaxillary extension)** (Zhang et al. 2009); (0) absent or poorly defined, (1) short but well-defined, (2) strong posterior extension **(ordered)**
5. Premaxilla in relation to frontals (modified from Wiens et al. 2005); (0) not contacting frontals, (1) contacting frontals, **(2) extension of dorsal process intervenes deeply between the frontals (ordered)**

6. Premaxillary dentition presence (Hanken and Hall, 1993); (0) present, (1) absent
7. Premaxilla dentition position (Wiens et al. 2005); (0) present lateral to pars dorsalis, (1) absent lateral to pars dorsalis
8. Premaxilla dentition (shape); (0) conical, (1) bulbous
9. Combined width of premaxilla measured at the premaxilla/maxilla suture (Wiens et al. 2005); (0) less than interorbital width, (1) greater than interorbital width
10. Premaxilla-palatine contact (Wiens et al. 2005); (0) absent, (1) present
11. Premaxilla-vomer contact (Wiens et al. 2005); (0) absent, (1) present
12. Premaxilla-nasal contact (Wiens et al. 2005); (0) absent, (1) present
13. Maxilla (Zhang et al. 2009); (0) presence of bilaterally paired maxillae, (1) greatly reduced as a rudimentary element, (2) entirely absent and functionally replaced by modified vomer (ordered)
14. Maxillary dentition (Wiens et al. 2005); (0) dentate, (1) reduced, edentulous
15. Dentition shape; (0) mono-cuspid, (1) bi-cuspid, (2) tricuspid
16. Posterior process of maxilla (Wiens et al. 2005); (0) dentate, (1) edentulous
17. Process from pars dentalis of maxilla overlaps premaxilla (Wiens et al. 2005); (0) no, (1) yes
18. Anterior margin of pars facialis of maxilla (modified from Wiens et al. 2005); (0) posterior to external naris, (1) Forms lateral part of external naris
19. Septomaxilla (Larson and Dimmick, 1993; Hanken and Hall, 1993; Duellman and Trueb, 1994; Gao and Shubin, 2001; Wiens et al. 2005; Zhang et al. 2009); (0) presence of bilaterally paired septomaxillae, (1) absence of bones.
20. Posterior end of septomaxilla (Wiens et al. 2005); (0) not contacting other cranial elements, (1) contacting maxilla, (2) contacting prefrontal, (3) contacting nasal (unordered)
21. Nasal (modified from Wiens et al. 2005); (0) present, (1) absent

22. Nasal ossification (Hanken and Hall, 1993; Larson and Dimmick, 1993; Gao and Shubin, 2001; Zhang et al. 2009); (0) paired nasals with sutural midline contact or fused, (1) nasals separate without midline contact
23. Nasal (Wiens et al. 2005); (0) not forked posteriorly, (1) forked posteriorly
24. Nasal shape (Wiens et al. 2005); (0) squarish, length and width roughly equal, (1) slender and elongate, length greater than width
25. Nasal-prefrontal contact (Gao and Shubin, 2001; Wiens et al. 2005; Zhang et al. 2009); (0) present, (1) absent
26. Nasal and maxilla (Wiens et al. 2005); (0) contacting or abutting, (1) separated
27. Nasal contact with frontal (Gao and Shubin, 2001; Wiens et al. 2005; Zhang et al. 2009); (0) separate from frontal, (1) partly or completely fused to frontal
28. Nasal-lacrimal duct (Hanken and Hall, 1993; Gao and Shubin, 2001; Zhang et al. 2009); (0) present, (1) absent
29. Lacrimal (Hanken and Hall, 1993; Duellman and Trueb, 1994; Gao and Shubin, 2001; Wiens et al. 2005; Zhang et al. 2009); (0) present, (1) absent
30. Quadratojugal (Hanken and Hall, 1993; Duellman and Trueb, 1994; Gao and Shubin, 2001; Zhang et al. 2009); (0) present, (1) absent
31. Prefrontal (Hanken and Hall, 1993; Gao and Shubin, 2001; Wiens et al. 2005; Zhang et al. 2009); (0) present, (1) absent
32. Prefrontal posterior process projecting into the orbit (modified from Hanken and Hall, 1993; Gao and Shubin, 2001; Wiens et al. 2005; Zhang et al. 2009); (0) present, (1) absent
33. Prefrontal orientation (modified from Wiens et al. 2005); (0) present and forms part of the margin of the external naris, (1) present but does not form part of the margin of the external naris
34. Frontal (Duellman and Trueb, 1994); (0) paired roofing bones, (1) fused into a single element

35. Frontal/maxillary contact (Gao and Shubin, 2001; Zhang et al. 2009, Wiens et al. 2005); (0) frontal and maxilla separated by prefrontal, (1) frontal contacts dorsal process of maxilla
36. Dorsolateral shelf on frontal (Wiens et al. 2005); (0) absent, (1) present
37. Postfrontal (Gao and Shubin, 2001, Zhang et al. 2009); (0) present, (1) absent
38. Palatal dentition (on the palatine) (modified from Gao and Shubin, 2001, Zhang et al. 2009); (0) present, (1) absent
39. Vomer dentition (modified from Gao and Shubin, 2001, Zhang et al. 2009); (0) present, (1) absent
40. Parasphenoid dentition (modified from Gao and Shubin, 2001, Zhang et al. 2009); (0) present, (1) absent
41. Pterygoid dentition (modified from Gao and Shubin, 2001, Zhang et al. 2009); (0) present, (1) absent
42. Placement of vomerine teeth (Duellman and Trueb, 1994, Hanken and Hall, 1993; Wiens et al. 2005, Zhang et al. 2009); (0) medial/lateral transverse row, (1) marginal (adjacent and parallel to max. and premaxillary teeth), (2) teeth centrally located on vomer, (3) teeth in large patches, (4) teeth in M-shaped pattern (unordered)
43. Palatal tooth structure (Hanken and Hall, 1993; Duellman and Trueb, 1994); (0) conical, (1) compressed, (2) bulbous
44. Vomerine teeth (Tihen, 1958; Wiens et al. 2005); (0) present on postchoanal process, (1) absent on postchoanal process
45. Vomer with postchoanal process (Wiens et al. 2005); (0) with postchoanal process, (1) without postchoanal process
46. Vomer with prechoanal process (Wiens et al. 2005); (0) with prechoanal process, (1) without prechoanal process
47. Vomer and pterygoid (Wiens et al. 2005); (0) not articulating with pterygoid, (1) articulates with pterygoid

48. Vomers (**modified from** Wiens et al. 2005); (0) separated anteriorly and medially, (1) **separated medially and posteriorly** (2) **separated entirely**, (3) in contact anteromedially, no fontanelle exposed (unordered)
49. Vomer, posterior dorsal process extending onto orbitosphenoid (Wiens et al. 2005); (0) absent, (1) present
50. Pterygoid **shape** (**modified from** Zhang et al. 2009); (0) triradiate and boomerang-shaped, (1) enlarged with distinct anteromedial process, (2) straight bar with loss of anteromedial process, (3) absent (unordered)
51. Anterior margin of pterygoid (Wiens et al. 2005); (0) smooth, (1) serrate, with irregular projections
52. Pterygoid and coronoid process of prearticular (Wiens et al. 2005); (0) well separated, (1) articulating or nearly contacting
53. Posterior margin of pterygoid extends posterior to jaw articulation (Wiens et al. 2005); (0) no, (1) yes
54. Pterygoid, with dorsomedial process that articulates with orbitosphenoid and forms foramen posterior to optic foramen (Wiens et al. 2005); (0) absent, (1) present
55. Internal carotid foramen (Zhang et al. 2009; Gao and Shubin, 2001); (0) present, (1) absent
56. Squamosal-frontal (Wiens et al. 2005); (0) does not contact frontal, (1) contacts frontal
57. Squamosal (Wiens et al. 2005); (0) not expanded ventrally, (1) expanded ventrally, occupies articular region
58. Squamosal, main shaft in lateral view (Gao and Shubin, 2001; Wiens et al. 2005; Zhang et al. 2009); (0) oriented roughly vertically, (1) oriented diagonally, with dorsoposterior inclination
59. Hook-like (ventrally-directed) process on dorsal head of squamosal (Wiens et al. 2005); (0) absent, (1) present
60. Columellar process of squamosal, connecting stapes and squamosal (Wiens et al. 2005); (0) absent, (1) present

61. Squamosal contact with the parietal or other roofing elements (**modified from** Gao and Shubin, 2001; Zhang et al. 2009); (0) contact present, (1) absent **or virtually absent**
62. Prootic-exoccipital-opisthotic fusion (Hanken and Hall, 1993; Duellman and Trueb, 1994; Gao and Shubin, 2001; Wiens et al. 2005; Zhang et al. 2009); (0) three separate elements, (1) prootic-exoccipital fused, separate opisthotic, (2) all three elements fused (**ordered**)
63. Exposure of prootic-exoccipital-opisthotic complex in dorsal view (Zhang et al. 2009); (0) the complex largely concealed by parietal or exposed posterior to skull table, (1) large exposure extends lateral to parietal table
64. Exoccipitals (Wiens et al. 2005); (0) separated medially at tectum synoticum, (1) fused
65. Operculum (Hanken and Hall, 1993; Zhang et al. 2009); (0) present and free, (1) absent or fused
66. Stapes (Hanken and Hall, 1993; Zhang et al. 2009); (0) present, (1) absent
67. Orbitosphenoid (Wiens et al. 2005); (0) present, (1) absent
68. Orbitosphenoid (Wiens et al. 2005); (0) not extending lateral to frontals, or extending only slightly anteriorly, (1) extending well lateral to frontals throughout their length
69. *Sagittal crest **formed at the midline between the parietals** of the skull (**modified from** Wiens et al. 2005); (0) absent, (1) present
70. Dermal sculpture on skull roof (Zhang et al. 2009); (0) present, coarse, (1) present, weak, (2) absent
71. Posterior edge of parietals, extends between exoccipitals to edge of foramen magnum on tectum synoticum (Wiens et al. 2005); (0) no, (1) yes
72. Ventrolateral extension of parietal covers orbitosphenoid region anteriorly (in lateral view), (Wiens et al. 2005); (0) absent, (1) present
73. *Parietal and exoccipital (Wiens et al. 2005); (0) not forming casque around foramen magnum, (1) forming casque around foramen magnum

74. Anterolateral process of parietal (modified from Gao and Shubin, 2001; Zhang et al. 2009); (0) absent, (1) present
75. Anterolateral process of parietal (modified from Gao and Shubin, 2001; Zhang et al. 2009); (0) forms less than 50% of the total length of the parietal, (1) makes up more than 50% of total length of the parietal
76. Medial border of orbit (Zhang et al. 2009); (0) more than 50% of orbital margin formed by frontal, (1) frontal contributes less than 50% of the orbit margin, (2) frontal fully excluded from entering orbital margin (unordered)
77. Angular/prearticular fusion (Duellman and Trueb, 1986; Larson and Dimmick, 1993; Hanken and Hall, 1993; Duellman and Trueb, 1994; Gao and Shubin, 2001; Wiens et al. 2005; Zhang et al. 2009); (0) angular distinct from the prearticular, (1) no distinct angular (absent or fused to prearticular in adult).
78. Coronoid (Hanken and Hall, 1993; Gao and Shubin, 2001; Wiens et al. 2005); (0) present as a separate element, (1) absent in adult stage
79. Coronoid dentition (Hanken and Hall, 1993; Wiens et al. 2005); (0) dentate, (1) edentulous
80. Articular (modified from Gao and Shubin, 2001; Wiens et al. 2005; Zhang et al. 2009); (0) present as separate element, (1) fused with prearticular, (2) absent/unossified (unordered)
81. Meckel's cartilage (Wiens et al. 2005); (0) does not extend to mandibular symphysis, (1) extends to mandibular symphysis
82. *Mandible (in anterior view) (Wiens et al. 2005); (0) thickens suddenly at symphysis, (1) thins/ stays the same towards the symphysis
83. Mandibular symphysis (Duellman and Trueb, 1994); (0) simple union of the mandibular rami, (1) rami have an interlocking symphysis
84. Dentary (Wiens et al. 2005); (0) dentate, (1) edentulous
85. *Dentary teeth shape; (0) conical, (1) bulbous
86. Dentary symphyseal teeth; (0) present, (1) absent

87. *Dentary lateral sensory nerve foramina; (0) absent, (1) present
88. Retroarticular process (modified from Wiens et al. 2005); (0) very small/absent, (1) present
89. Coronoid process of prearticular (Wiens et al. 2005); (0) adjacent to jaw articulation, (1) distinctly anterior to jaw articulation
90. Palatine and pterygoid (Wiens et al. 2005); (0) palatine absent (1) palatine present
91. Quadrate ossification (Wiens et al. 2005); (0) present, (1) absent
92. Posterior process on pars quadrati of quadrate (Wiens et al. 2005); (0) absent, (1) present
93. Jaw articulation (Wiens et al. 2005); (0) well ventral to level of ventral margin of braincase, (1) at level of ventral margin of braincase
94. Quadrate-parasphenoid articulation (Wiens et al. 2005); (0) absent, (1) present
95. Parasphenoid (Wiens et al. 2005); (0) not extending laterally beyond level of orbitosphenoid, (1) extending laterally beyond level of orbitosphenoid
96. Optic foramen (modified from Wiens et al. 2005); (0) enclosed in the orbitosphenoid bone anteriorly or not at all, (1) enclosed entirely in the orbitosphenoid bone
97. Posterioormost margin of auditory capsules (Wiens et al. 2005); (0) anterior to occipital condyles, (1) posterior to occipital condyles
98. Lateral flange on prootic extending to the squamosal (Wiens et al. 2005); (0) absent, (1) present
99. Second basibranchial (ventral view); (0) bar (horizontal or vertical), (1) Y-shaped (two branches), (2) multiple branches (more than two) (unordered)

Atlas:

100. Position of atlas posterior cotyle relative to anterior cotyles (J. Gardner, 2000); (0) the posterior cotyle is approximately in line with the anterior cotyles in lateral view, (1) the posterior cotyle is displaced ventrally in relation to the anterior cotyles.

101. Notochordal pit in posterior cotyle of the atlas (modified from J. Gardner, 2000); (0) the notochordal pit is open and has no infilling of calcified or ossified cartilage, (1) partly in-filled by ossified cartilage, (2) totally in-filled and bulging beyond the edge of the centrum with ossified cartilage (ordered)
102. Relative depth of anterior atlas cotyles (modified from J. Gardner, 2000); (0) deeply concave, (1) nearly flat to shallowly concave, (2) convex (although the structure is called a cotyle which means cup-like, they are sometimes convex) (ordered)
103. Outline of anterior atlas cotyles (J. Gardner, 2000); (0) compressed dorsoventrally, (1) subcircular, (2) compressed lateromedially (ordered)
104. Form of odontoid process (modified from J. Gardner, 2000); (0) knob-like, (1) dorsoventrally flattened, (2) separate (not joined in the middle), (3) highly reduced or absent (unordered)
105. Position of atlas neural canal relative to the anterior cotyles (J. Gardner, 2000); (0) the neural canal is situated above the anterior cotyles, (1) the neural canal protrudes in between the anterior cotyles, but up to half way or less than the dorso-ventral distance of the anterior cotyles, (2) Neural canal intrudes deeply or completely between the anterior cotyles (ordered)
106. Size of atlas neural canal relative to the anterior cotyles (J. Gardner, 2000); (0) the anterior circumference of the neural canal is approximately equal to or greater than the circumference of one of the anterior cotyles, (1) the neural canal is smaller than the anterior coyle
107. Posterior extent of neural arch roof of the atlas (modified from J. Gardner, 2000); (0) extends past the edge of the posterior cotyle, (1) in line with the posterior cotyle, (2) the posterior edge of the neural arch roof is shorter i.e. does not reach to the edge of the posterior cotyle (ordered)

108. Dorsal outline of posterior margin of the atlas neural arch roof (modified from J. Gardner, 2000); (0) truncated, (1) forked, (2) pointed (unordered)
109. Dorsal outline of the atlas' neural arch crest (modified from J. Gardner, 2000); (0) the outline of the crest broadens posteriorly, (1) it narrows posteriorly, (2) relatively straight, (3) it is hourglass shaped i.e. narrows then broadens (unordered)
110. Shape of anterior end of neural arch crest on the atlas (modified from J. Gardner, 2000); (0) not elaborated, (1) swollen or thickened, (2) paired anterior processes (unordered)
111. Postzygapophyses prominence on the atlas (modified from J. Gardner, 2000); (0) prominent, (1) small.
112. Postzygapophyses articular surface on the atlas (modified from J. Gardner, 2000); (0) laterally divergent, (1) directed ventro-laterally.
113. Postzygapophyses; (0) diverge from the end of the neural arch crest on the atlas, (1) diverge from along the neural arch crest of the atlas.
114. Condition of the dorsal part of the neural arch crest of the atlas (J. Gardner, 2000); (0) finished in cartilage, (1) finished in bone
115. Condition of the posterior end of the neural arch spine of the atlas; (0) finished in cartilage, (1) finished in bone
116. Four faceted articulation of exoccipital and atlas (Wiens et al. 2005; Zhang et al. 2009); (0) absent due to reduction in odontoid process, (1) absent due to continuous surface of odontoid and anterior cotyles, (2) present (unordered)
117. Atlantal spinal nerve foramen (Zhang et al. 2009); (0) absent, (1) a notch, (2) fully enclosed (ordered)
118. Atlas, transverse process (Wiens et al. 2005); (0) absent, (1) present

119. Shape of atlas centrum in ventral view (Zhang et al. 2009); (0) shorter than postatlantals, (1) roughly equal in length to postatlantals, (2) longer than postatlantals (unordered)
120. Basapophyses on the atlas; (0) absent, (1) present
121. Neural cord supports, (0) absent, (1) present

Presacral Vertebrae:

122. Centrum of presacral vertebrae (modified from J. Gardner, 2000); (0) amphicoelous, (1) semi-opisthocoelous, (2) fully opisthocoelous, (3) procoelous (unordered)
123. Size of the 4th trunk vertebrae (5th presacral) neural canal relative to its anterior size of the centrum; (0) neural canal is approximately equal in size (radius) to, or greater than, the size of the anterior centrum, (1) neural canal smaller than the anterior centrum
124. Posterior basapophyses of the presacrals (J. Gardner, 2000); (0) absent, (1) present
125. Anterior basapophyses of the presacrals (Wiens et al. 2005); (0) absent, (1) present
126. Condition of neural spine (J. Gardner, 2000); (0) finished in cartilage, (1) finished in bone
127. Prominent, v-shaped hypapophyses (J. Gardner, 2000); (0) absent, (1) present
128. Bony lamina between diapophyses and parapophyses (modified from Wiens et al. 2005); (0) absent, (1) partial presence, (2) present – full lamina (ordered)
129. Mid-ventral keel on mid-body vertebrae (modified from Wiens et al. 2005); (0) absent, (1) present (small), (2) Large – extends below the ventral edge of the centrum cotyles (ordered)
130. Posterolateral flanges on mid-dorsal keel on mid-body vertebrae (Wiens et al. 2005); (0) absent, (1) present

131. Anterior keel/flange on transverse process (extending from, and between the transverse process to anterior edge of centrum) (modified from Wiens et al. 2005); (0) absent, (1) present
132. Fenestra in anterior keel; (0) present, (1) absent
133. Anterodorsal keel on transverse process (extending from transverse process to anterior zygapophysis) (modified from Wiens et al. 2005); (0) absent, (1) present
134. Posterior keel of transverse process (extends from transverse process to posterior centrum edge); (0) absent, (1) present
135. Dermal sculpture on dorsal surface of neural arch; (0) present, (1) absent
136. Shape of the neural spine of mid-body vertebrae (modified from Wiens et al. 2005); (0) absent/truncated, (1) single median process (spine-like projection), (2) present (paired process)
137. Posteriorly projecting neural spine(s) (past the posterior centrum edge); (0) shorter than posterior centrum edge, (1) in line with posterior centrum edge, (2) projecting past the posterior centrum edge (ordered)
138. Posterior zygapophyses facet face of presacral vertebrae; (0) latero-medially divergent (facing slightly outwards, away from each other), (1) directed ventrally
139. Transverse process in anterior part of trunk series, excluding first presacral vertebra (J. Gardner, 2000); (0) Unicapitate, (1) bicapitate, (2) absent
140. Mid-dorsal keel (neural arch crest) on presacral vertebra (Wiens et al. 2005); (0) absent, (1) present
141. Mid-dorsal keel (neural arch crest) on presacral vertebra length; (0) short (does not run the length of the vertebra), (1) long (runs from at least just behind the anterior zygapophyses to neural spine)

Caudal Vertebrae:

142. Caudal vertebrae, neural spine (Wiens et al. 2005); (0) with one process, (1) paired process
143. Mid-dorsal crest on caudal vertebrae (Wiens et al. 2005); (0) absent, (1) present
144. Dermal sculpturing on dorsal surface of neural arch on the caudal vertebrae; (0) present, (1) absent
145. Caudal vertebrae (Wiens et al. 2005); (0) ventral keels absent, low, and/or rounded, (1) dorsal and ventral keels raised and distinctly rectangular
146. Transverse process of anterior caudal vertebrae (Wiens et al. 2005); (0) posteriorly orientated, (1) anteriorly oriented
147. Transverse process of anterior caudal vertebrae; (0) unicapitate, (1) bicapitate
148. Caudal vertebrae, anterior keel on haemal arch (Wiens et al. 2005); (0) absent, (1) present
149. Caudal vertebrae, haemal arch (Wiens et al. 2005); (0) complete, lateral halves fused to form median process, (1) incomplete, two ventral lamina do not contact or fuse on anterior caudal vertebrae, (2) incomplete for all caudal vertebrae (unordered)
150. Caudal vertebrae, haemal arch spine (Wiens et al. 2005); (0) paired process, (1) single process
151. Caudosacral vertebrae (number of caudal vertebrae lacking a haemal arch, plus the sacral vertebra) (Character from Wake, 1966; Wiens et al. 2005); (0) 2, (1) 3, (2) 4 (ordered)
152. Zygapophyses connecting caudal vertebrae (Wiens et al. 2005); (0) present on all or most vertebrae, (1) absent from posterior caudal vertebrae

Ribs:

153. Number of ribs on anterior caudal vertebrae (Zhang et al. 2009); (0) more than 3 pairs, (1) 2-3 pairs, (2) free ribs absent (**ordered**)
154. Atlantal Ribs (Larson and Dimmick, 1993); (0) absent, (1) present
155. Postatlantal ribs (modified from Zhang et al. 2009); (0) bicapitate, (1) unicapitate, (**2**) **absent** (unordered)
156. Dorsal process of bicapitate ribs (Wiens et al. 2005); (0) articulates with diapophysis, (1) reduced, does not articulate with diapophysis
157. Ribs on mid-body presacral vertebrae (Wiens et al. 2005); (0) present, (1) absent
158. Ribs on last presacral vertebra (Wiens et al. 2005); (0) present, (1) absent
159. Rib on penultimate presacral vertebra (Wiens et al. 2005); (0) present, (1) absent
160. Sacral rib (Wiens et al. 2005); (0) **free**, (1) **fused**
161. Dorsal process on mid-body of rib of 4th trunk vertebra (4th presacral excluding the atlas) (Wiens et al. 2005); (0) absent, (1) present
162. Bony lamina between ventral and dorsal processes of ribs (Wiens et al. 2005); (0) absent, (1) present

Spinal nerves:

163. Spinal nerves in posterior trunk vertebrae (data from Edwards, 1976; modified character from character X of Duellman and Trueb, 1986; Wiens et al. 2005); (0) exit intervertebrally, (1) exit intravertebrally
164. Spinal nerve exit in caudal vertebrae (data from Edwards, 1976; modified character from character X of Duellman and Trueb, 1986; Wiens et al. 2005); (0) intervertebral in all caudal vertebrae, (1) intravertebral in some or all caudal vertebrae

165. Dorsal and ventral roots of spinal nerves in trunk vertebrae (modified from Edwards, 1976; Duellman and Trueb, 1986; Wiens et al. 2005 and Thien and Chantell 1963); (0) exit through single foramen, (1) dorsal and ventral roots of presacral vertebrae exit through separate foramina
166. Presacral spinal nerve foramina (modified from Edwards, 1976; Duellman and Trueb, 1986; Wiens et al. 2005 and Thien and Chantell 1963); (0) spinal nerve exits intervertebrally, (1) spinal nerve exits intravertebrally in some vertebrae, (2) all spinal nerves exit intravertebrally (ordered)

Pectoral girdle:

167. Scapula-coracoid ossification (modified from Duellman and Trueb, 1986; Larson and Dimmick, 1993; Gao and Shubin, 2001; Wiens et al. 2005; Zhang et al. 2009); (0) ossified as separate elements, (1) two elements as a single ossification
168. Coracoids (Wiens et al. 2005); (0) not contacting medially, (1) contacting/overlapping medially, (2) fused medially (ordered)
169. Procoracoid and coracoid (Wiens et al. 2005); (0) not overlapping anteriorly, (1) overlapping anteriorly, enclosing foramen
170. Supracoracoid foramen (modified from Wiens et al. 2005); (0) entirely in cartilage/absent, (1) partly in bone, (2) entirely in bone
171. Suprascapula (modified from Wiens et al. 2005); (0) expanded in width dorsally, (1) not expanded, about same width as dorsal width of scapula
172. Crista dorsalis of humerus (Wiens et al. 2005); (0) present, (1) absent
173. Carpals (Wiens et al. 2005); (0) all elements cartilaginous, (1) some (but not all) ossified, (2) all elements at least partly ossified (ordered)
174. Fusion of distal carpal 1+2 (Gao and Shubin, 2001; Zhang et al. 2009); (0) fusion absent, (1) fusion present

175. Distal carpal 4 and 5 (Gao and Shubin, 2001; Zhang et al. 2009); (0) two elements remain separate, (1) fused
176. Carpals 3 and 4 (Wiens et al. 2005); (0) separate, (1) fused
177. Prepollex and radiale (Wiens et al. 2005); (0) separate, (1) fused
178. Ulnare (the carpal that articulates with the ulna) and intermedium (the bone or cartilage between the radiale and ulnare in the carpus) (Gao and Shubin, 2001; Wiens et al. 2005; Zhang et al. 2009); (0) separate, (1) fused
179. Ulnare and carpal 4 (Wiens et al. 2005); (0) separate, (1) fused
180. Intermedium and centrale (Wiens et al. 2005); (0) separate, (1) fused
181. Number of centralia in manus (or pes) (Gao and Shubin, 2001); (0) more than one Centralia element, (1) one central element
182. Number of manual digits (fingers) on forelimb (Wiens et al. 2005); (0) four, (1) three, (2) two, (3) one (unordered)
183. Number of phalanges on digit I of manus (Wiens et al. 2005); (0) two, (1) one

Pelvic girdle:

184. Hind limbs (Wiens et al. 2005); (0) present, (1) absent
185. Pelvic girdle (structure), (Wiens et al. 2005); (0) halves fused medially, (1) halves separate medially
186. Lateral processes of pubis (Wiens et al. 2005); (0) present, (1) absent
187. Ossification of ischium (Wiens et al. 2005); (0) not extending to anterior margin of pelvic girdle, (1) extending to anterior margin of pelvic girdle
188. Ossification of ischia (Wiens et al. 2005); (0) meeting mid-ventrally (separated by thin strip of cartilage), (1) well-separated mid-ventrally
189. Posterior median process on ischium (Wiens et al. 2005); (0) absent, (1) present

190. Median processes of pubis (Wiens et al. 2005); (0) posterior to or level with lateral processes, (1) anterior to lateral processes
191. Femur “crista dorsalis”; (0) absent, (1) present
192. Tibial spur (Wiens et al. 2005); (0) absent, (1) present, not elongate and pointed, (2) elongate and pointed (unordered)
193. Fusion of tarsals 1 and 2 (Wiens et al. 2005; Zhang et al. 2009); (0) separate, (1) fused
194. Distal tarsals 4 and 5 (Wiens et al. 2005); (0) separate, (1) fused
195. Number of toes on hindlimb (Wiens et al. 2005); (0) five, (1) four, (2) three, (3) two, (4) one (ordered)
196. Number of phalanges on digit IV of pes (Wiens et al. 2005); (0) three, (1) four
197. Phalanges on digit I of pes (Wiens et al. 2005); (0) two, (1) one

Soft body coding:

198. Junction of the periotic canal and cistern (Duellman and Trueb 1986); (0) periotic canal joins the periotic cistern dorsally at its posterior aspect, (1) the junction of the canal and the cistern is slightly dorsal and posterior to the festra ovalis, (2) the junction of the cistern and canal is formed through the protrusion of the cistern into the fenestra ovalis
199. Flexures of periotic canal (Duellman and Trueb 1986); (0) the periotic canal curves ventrally and medially from its junction with the periotic cistern, (1) the canal takes a relatively horizontal course, (2) canal with one or more flexures
200. Basilaris complex of inner ear (Duellman and Trueb 1986); (0) recessus basilaris and papillae are present in the inner ear, (1) absence of papillae, (2) absence of entire complex
201. First hypobranchial and first ceratobranchial (Duellman and Trueb 1986); (0) separate elements, (1) fusion of the two elements
202. Second ceratobranchial (Duellman and Trueb 1986); (0) present, (1) absent

203. Number of larval gill slits (Duellman and Trueb 1986); (0) four pairs, (1) three pairs, (2) two pairs, (3) one pair
204. Ypsiloid cartilage (Duellman and Trueb 1986); (0) present, (1) absent
205. Levator mandibulae muscle (Duellman and Trueb 1986); (0) originates on the skull roof, (1) origin on the side of the skull, (2) an origin that includes the exoccipital (or cervical vertebrae),
206. Pubotibialis and puboischiotibialis muscles (Duellman and Trueb 1986); (0) separate muscles, (1) fusion of the two muscles
207. Kidney (Duellman and Trueb 1986); (0) presence of well-developed glomeruli in anterior of kidney, (1) reduction of absence of anterior glomeruli
208. Mode of fertilisation (Duellman and Trueb 1986); (0) external fertilisation, (1) internal fertilisation
209. Recessus amphibiorum (Larson and Dimmick 1993) (0) horizontal orientation of the recessus amphibiorum of the inner ear, (1) vertical orientation
210. Otic sac (Larson and Dimmick 1993) (0) multilobate sac which is vascularised and filled with calcium, (1) bulbar, partially vascularised sac, (2) bulbar unvascularised sac
211. Amphibian periotic canal connective tissue (Larson and Dimmick 1993) (0) absence of this tissue, (1) Presence of fibrous connective tissue around amphibian periotic canal
212. Periotic cistern (0) large cistern, (1) small cistern
213. Fenestral relations of the periotic cistern (Larson and Dimmick 1993) (0) absence of protrusion, (1) protrusion of the cistern into the fenestra
214. Palatal dentition (unordered) (Larson and Dimmick 1993) (0) replacement of vomerine teeth proceeds laterally in parallel to the maxillary teeth, (1) from the posterior of the vomer, (2) both laterally and posteriorly, (3) medially

215. Epidermis (Larson and Dimmick 1993) (0) absence in female salamanders of an epidermal lining in the anterior half of the cloacal chamber, (1) presence of the epidermal lining
216. Male anterior ventral glands (Larson and Dimmick 1993)(0) absence, (1) presence
217. CTL/TCL cloacal tube length divided by total cloacal length quotient in females (Sever 1991); (0) present, (1) absent
218. CTL/TCL cloacal tube length divided by total cloacal length quotient in males, (Sever 1991); (0) present, (1) absent
219. Ciliated epithelium in the cloacal tube and/or anterior cloacal chamber of females, (Sever 1991); (0) present, (1) absent
220. Ciliated epithelium in the cloacal tube and/or anterior cloacal chamber of males, (Sever 1991); (0) present, (1) absent
221. Extent of epidermis in the female cloacal chamber, (Sever 1991); (0) the epidermal lining does not extend into the anterior one-half of the cloacal chamber, (1) the epidermal lining does extend into the anterior one-half of the cloacal chamber
222. Cloacal recess in females (Sever 1991); (0) absent, (1) present
223. Number of pairs of rugae in the male cloaca (Sever 1991); (0) < 10, (1) > 10
224. Primary and secondary folds in the male cloacal tube, (Sever 1991); (0) absent, (1) present
225. Middorsal evagination of the male cloacal chamber (Sever 1991); (0) absent, (1) present
226. Dorsolateral recesses in the male cloacal chamber (Sever 1991); (0) absent, (1) present
227. Pseudopenis in the male cloaca (Sever 1991); (0) absent, (1) present
228. Female anterior ventral glands (Sever 1991); (0) absent, (1) present
229. Spermathecae (Sever 1991); (0) absent, (1) present

230. Common tube to the spermathecae (Sever 1991); (0) absent, (1) present
231. Female dorsal glands (Sever 1991); (0) absent, (1) present
232. Other female cloacal glands (Sever 1991); (0) absent, (1) present
233. Male anterior ventral glands (Sever 1991); (0) absent, (1) present
234. Posterior ventral glands (Sever 1991); (0) absent, (1) present
235. Kingsbury's glands (Sever 1991); (0) absent, (1) present
236. Dorsal pelvic glands (Sever 1991); (0) absent, (1) present
237. Lateral pelvic glands (Sever 1991); (0) absent, (1) present
238. Caudal pelvic glands (Sever 1991); (0) absent, (1) present
239. Male dorsal or vent glands (Sever 1991); (0) absent, (1) present
240. Amphiumid pit glands (Sever 1991); (0) absent, (1) present
241. Other male cloacal glands (Sever 1991); (0) absent, (1) present
242. Lateral wall of nasal capsule (Zhang *et al.* 2009); (0) complete, (1) incomplete
243. Lateral narial fenestra (Zhang *et al.* 2009); (0) absent, (1) present
244. Posterior wall of nasal capsule (Zhang *et al.* 2009); (0) complete, (1) incomplete
245. Origin of m. adductor mandibulae internus superficialis (Zhang *et al.* 2009); (0) on dorsallateral surface of parietal, (1) origin extends posteriorly to exoccipital, (2) origin extends to cervical vertebra, (3) origin extends anteriorly towards level of frontal
246. Microchromosome (Zhang *et al.* 2009); (0) present, (1) absent
247. Ectopterygoid (Zhang *et al.* 2009); (0) present, (1) absent
248. Haploid Chromosomes (Gao and Shubin 2001); (0) more than 20, (1) reduced to 19, (2) further reduced to 14 or less
249. Diploid Chromosomes (Gao and Shubin 2001); (0) 56 or more, (1) 40-55, (2) lower than 40

References:

- Duellman, W. E. and L. Trueb (1994). Biology of Amphibians, Johns Hopkins University Press, pp. 461-508.
- Edwards, J. L. (1976). "Spinal nerves and their bearing on salamander phylogeny." Journal of Morphology **148**(3): 305-328.
- Gardner, J. D. (2000). Late Cretaceous North America Amphibians. PhD Thesis
- Gao, K. Q. and N. H. Shubin (2001). "Late Jurassic salamanders from northern China." Nature **410**(6828): 574-577.
- Hanken, J. and B. K. Hall (1993). The Skull: Patterns of structural and systematic diversity, University of Chicago Press, pp.
- Larson, A. and W. W. Dimmick (1993). "Phylogenetic relationships of the salamander families: An analysis of congruence among morphological and molecular characters." Herpetological Monographs **7**(ArticleType: research-article / Full publication date: 1993 / Copyright © 1993 Herpetologists' League): 77-93.
- Tihen, J. A. and C. J. Chantell (1963). "Urodele remains from the Valentine Formation of Nebraska." Copeia **1963**(3): 505-510.
- Wang, Y. and S. E. Evans (2006). "A new short-bodied salamander from the Upper Jurassic/Lower Cretaceous of China." Acta Palaeontologica Polonica **51**(1): 127-130.
- Wiens, J. J., R. M. Bonett and P. T. Chippindale (2005). "Ontogeny discombobulates phylogeny: Paedomorphosis and higher-level salamander relationships." Systematic Biology **54**(1): 91-110.
- Zhang, G. L., Y. Wang, M. E. H. Jones and S. E. Evans (2009). "A new Early Cretaceous salamander (*Regalerpeton weichangensis* gen. et sp. nov.) from the Huajiying Formation of northeastern China." Cretaceous Research **30**(3): 551-558.